

SYNTHESIS, CHARACTERIZATION OF CHITOSAN-BASED DERIVATIVES,
THEIR HYDROGELS AND HYBRIDS, AND A NEW FAMILY OF ARGININE
BASED POLYESTER UREA URETHANE

A dissertation submitted to Graduate Faculty of
Cornell University in fulfillment of the requirements
of the Degree of Doctor of Philosophy

by

MINGYU HE

August 2013

© 2013 Mingyu He
ALL RIGHTS RESERVED

SYNTHESIS, CHARACTERIZATION OF CHITOSAN-BASED DERIVATIVES,
THEIR HYDROGELS AND HYBRIDS, AND A NEW FAMILY OF ARGININE
BASED POLYESTER UREA URETHANE

Mingyu He, Ph.D

Cornell University 2013

Two categories of biodegradable polymeric materials which could be photocrosslinked by UV-cure were synthesized. One is water soluble glycidyl methacrylate chitosan (GMA-Chitosan). Unsaturated methacrylate groups were introduced onto the chitosan backbones as side groups to prepare hydrogel precursors for subsequent UV crosslinking to generate a hydrogel having 3D network structure. The effect of reaction conditions on the degree of substitution was studied. A series of hybrid hydrogels with different composition ratios and with positive or negative charge, GMA-chitosan/2-(acryloyloxy) ethyl trimethylammonium (AETA) and GMA-chitosan/vinyl sulfonic acid (VSA) were then prepared by UV photocrosslinking of the methacrylate groups. GMA-chitosan is also used to fabricate hybrid hydrogels with different composition ratios with unsaturated Arginine based polyester amide as the second hydrogel precursor for the study of the wound healing model. The enzymatic degradation, mechanical strength and swelling properties changes of the hybrid hydrogel depended upon the composition ratio of the precursors. When the biodegradable hydrogels were used as protein carriers, the release of bovine serum albumin (BSA) could be controlled by the hydrogel charge density and the rate of degradation of hydrogels.

Another main category of polymer materials is Arginine based polyester urea urethane (Arg-PEUU) which is newly synthesized by a two-step solution polycondensation of three monomers: L-Arg hydrochloride alkylene diester (Arg- x -Cl), hexamethylene diisocyanate (HDI) and glycerol α -monoallyl ether (GAE). Arg-PEUUs

can be photo-crosslinked into elastic gels. The newly synthesized polymers and gels were characterized by standard polymer characterization methods like NMR, FTIR and elemental analysis. By adjusting the composition ratio of three monomers, a wide range of hydrophilicity, degradation, thermal and mechanical properties could be controlled.

BIOGRAPHICAL SKETCH

Mingyu He was born in Tianjin, China on August 6th, 1982. He began his undergraduate studies at Tianjin University in Tianjin, China, where he completed his bachelor's degree in Department of Polymer material science and engineering in 2004. In September of the same year, Mingyu began her graduate studies at Tianjin University in Tianjin. He received his Master of Science degree in Department of Material science and engineering in 2007. In the same year, he started his Ph.D. studies at Cornell University in the fall of 2007. At Cornell University, he specialized in the study of polymeric biomaterials, especially designing biocompatible and biodegradable polymers which could be photo-crosslinked for biomedical application study.

ACKNOWLEDGMENTS

I would like to express my gratitude to my major advisor, Professor Chu, for his guidance throughout the research. I wish also to express my deep and sincere appreciation to the Professor Claudia Fischbach, Professor Martin Jin and Professor Anil Netravali for serving as my graduate study committee members. Their comments and suggestions have largely improved the quality of this research. Also with heartfelt thanks, I would like to acknowledge Alice Woo who generously funded my graduate study for 3 years. Her financial support made me was able to concentrate on my research.

I am grateful to the Dr. Dequn Wu, Dr. Mingxiao Deng, Dr. Xuan Pang, for their valuable advice. I am grateful to Dr Bin Duan who proved cell source in my study and Lin Chen who helped in the GPC test. Finally, I owe much to my parents for always believing in me and encouraging me to achieve my goals. Their compassion, generosity, and steadfast emotional support have been invaluable in helping me to focus on my academic pursuits.

TABLE OF CONTENTS

LIST OF FIGURES	xv
LIST OF TABLES	xix
Chapter 1 Summary of chitosan based hydrogel fabrication methods.....	1
1.1 Introduction of Chitosan and chitosan based hydrogel.....	2
1.2 Physical association chitosan hydrogels.....	3
1.2.1 Ionic complex chitosan hydrogel.....	4
1.2.2 Polyelectrolyte complexes.....	6
1.2.3 Physical mixtures and secondary bonding.....	7
1.2.4 Thermo-reversible hydrogels and hydrophobic associations.....	8
1.3 Chemically crosslinked chitosan hydrogel.....	9
1.3.1 Small molecule cross-linkers.....	10
1.3.2 Polymer-polymer crosslinking.....	11
1.3.3 Photo-crosslinking.....	12
1.3.4 Enzymatic crosslinking.....	14
1.4 Conclusions.....	16
Chapter 2 Synthesis and characterization of glycidyl methacrylate chitosan and photocrosslinked glycidyl methacrylate-chitoan hydrogel.....	21
2.1 Abstract.....	22
2.2 Introduction.....	23
2.2.1 Hydrogel.....	23
2.2.2 Chitosan.....	25
2.2.3 Modification of polysacchride by glycidyl methacrylate.....	26
2.2.4 The attempts to synthesise photo crosslinkable chitosan derivatives in organic solvent.....	28
2.3 Experimental.....	34

2.3.1 Materials.....	34
2.3.2 Synthesis of glycidyl methacrylate chitosan (GMA-chitosan).....	34
2.3.3 Characterization of GMA-chitosan.....	36
2.3.4 Cytotoxicity of GMA-Chitosan.....	36
2.3.4.1 Cell culture.....	36
2.3.4.2 Cytotoxicity of GMA-chitosan.....	36
2.3.4.3 Statistical analysis.....	37
2.3.5 Fabrication of photo-crosslinked GMA-chitosan hydrogel.....	38
2.3.6 Equilibrated swelling ratio (Q_{eq}) of GMA-chitosan hydrogel.....	38
2.3.7 Compressive modulus test of GMA-chitosan hydrogel.....	39
2.3.8 Morphology of GMA-chitosan hydrogel.....	40
2.3.9 Enzymatic biodegradation of GMA-chitosan hydrogels in vitro.....	40
2.3.10 In vitro release of bovine serum albumin (BSA) from GMA-chitosan hydrogel.....	41
2.4 Results and discussion.....	42
2.4.1 Synthesis of GMA-chitosan in DMSO.....	42
2.4.2 Characterization of GMA-chitosan.....	43
2.4.3 Effect of reaction time and molar feed ratio of GMA to chitosan on the DS of GMA-chitosan.....	48
2.4.4 Cytotoxicity of GMA-chitosan in aqueous media.....	50
2.4.5 Photo-crosslinked GMA-chitosan hydrogel Q_{eq} and hydrogel compressive modulus.....	51
2.4.6 Interior morphology (SEM) of GMA-chitosan hydrogel.....	53
2.4.7 Enzymatic biodegradation of GMA-chitosan hydrogel by lysozyme.....	53
2.4.8 Release of BSA from GMA-chitosan hydrogel.....	57
2.5 Conclusions and recommendation for future work.....	60

Chapter 3 Synthesis and characterization of water soluble glycidyl methacrylate chitosan and 2-(acryloyloxy) ethyl trimethylammonium and the fabrication into hybrid hydrogel in aqueous medium.....	67
3.1 Abstract.....	68
3.2 Introduction.....	68
3.2.1 Polysaccharide hydrogels.....	68
3.2.2 Polyelectrolyte complexes hydrogel.....	69
3.2.3 Crosslinked chitosan hydrogel.....	70
3.2.3.1 Small molecule crosslinkers.....	70
3.2.3.2 Polymer-polymer crosslinking.....	71
3.2.4 Photocrosslinking of chitosan based hydrogel.....	72
3.2.5 pH and ionic strength sensitive hydrogel.....	73
3.2.6 Quaternary ammonium group.....	75
3.3 Experimental.....	76
3.3.1 Materials.....	76
3.3.2 Methods.....	77
3.3.2.1 Synthesis of glycidyl methacrylate chitosan (degree of substitution 37)	77
3.3.2.2 Fabrication of GMA-chitosan/2-(Acryloyloxy) ethyl trimethylammonium (AETA) hybrid hydrogel.....	78
3.3.2.3 Fourier Transform Infrared (FTIR) Characterization of dried GMA-chitosan / AETA hybrid hydrogel.....	80
3.3.2.4 Swelling ratio (Q_{eq}) under different ionic strength and pH environment.....	80
3.3.2.5 Morphological study of GMA-chitosan/AETA hybrid hydrogel.....	80
3.3.2.6 Compression mechanical properties of GMA-chitosan / AETA hybrid hydrogel.	81
3.3.2.7 Enzymatic degradation of GMA-chitosan/AETA hybrid hydrogel.....	81

3.3.2.8 Release study of bovine serum albumin (BSA) from GMA-chitosan / AETA hydrogel.....	82
3.4 Results and discussion.....	83
3.4.1 FTIR spectroscopy.....	83
3.4.2 Images of GMA-chitosan/AETA hybrid hydrogel after swelling.....	84
3.4.3 The influence of ionic strength on the swelling ratio of GMA-chitosan / AETA hybrid hydrogel.....	85
3.4.4 The influence of pH on the swelling ratio of GMA-chitosan / AETA hybrid hydrogels.....	88
3.4.5 Morphology of GMA-chitosan/AETA hybrid hydrogel.....	90
3.4.6 Compressive mechanical properties of GMA-chitosan/AETA hybrid hydrogel.....	91
3.4.7 Enzymatic degradation of GMA-chitosan/AETA-67/33 hybrid hydrogels.....	93
3.4.8 BSA release from GMA-chitosan/AETA hybrid hydrogel at pH 3 and pH 7.4.....	95
3.5 Conclusions.....	97
Chapter 4 Synthesis and characterization of water soluble glycidyl methacrylate chitosan and vinyl sulfonic acid and the fabrication into hybrid hydrogel in aqueous medium.....	103
4.1 Abstract.....	104
4.2 Introduction.....	104
4.2.1 Glycosaminoglycans.....	104
4.2.2 The interaction of polysaccharide and protein.....	106
4.3 Experimental.....	108
4.3.1 Materials.....	108
4.3.2 Methods.....	108

4.3.2.1 Synthesis of glycidyl methacrylate chitosan (degree of substitution 37)	108
4.3.2.2 Fabrication of GMA-chitosan/VSA hybrid hydrogel and bovine serum albumin (BSA) loaded hybrid hydrogel fabrication.....	109
4.3.2.3 Fourier Transform Infrared (FTIR) characterization of GMA-chitosan/VSA hybrid hydrogel.....	112
4.3.2.4 Swelling ratio test under different ionic strength.....	113
4.3.2.5 Morphological study of GMA-chitosan/VSA hybrid hydrogel.....	113
4.3.2.6 Compressive mechanical properties of GMA-chitosan/VSA hybrid hydrogel.....	114
4.3.2.7 Release study of bovine serum albumin from GMA-chitosan/VSA hydrogel.....	114
4.4 Results.....	115
4.4.1 FTIR spectroscopy.....	115
4.4.2 Images of GMA-chitosan/VSA hybrid hydrogel after swelling in deionized water.....	116
4.4.3 The influence of ionic strength to the swelling ratio of GMA-chitosan/VSA hybrid hydrogel.....	117
4.4.4 Morphology of GMA-chitosan/VSA hybrid hydrogel.....	122
4.4.5 Mechanical properties of GMA-chitosan/VSA hybrid hydrogel.....	124
4.4.6 BSA release from GMA-chitosan/VSA hybrid hydrogel.....	126
4.5 Conclusions.....	130
Chapter 5 Synthesis, characterization of cationic Arginine based polyester amide/glycidyl methacrylate chitosan hybrid hydrogel and albumin release study.....	135
5.1 Abstract.....	136
5.2 Introduction.....	137

5.2.1 Arginine metabolism.....	137
5.2.2 NO physiological functions.....	139
5.2.3 The role of arginine in wound healing.....	141
5.2.4 The effect of arginine dietary supplement on wound healing, diabetic ulcer and tumor.....	143
5.2.5 The effect of chitosan on arginine metabolism in macrophage.....	147
5.2.6 The rationale of the design of glycidyl methacrylate Arg-UPEA/GMA-chitosan hybrid hydrogel and its possible application in wound healing study and tumor study.....	148
5.3 Experimental.....	150
5.3.1 Materials.....	150
5.3.2 Methods.....	150
5.3.2.1 Synthesis of unsaturated Di-p-nitrophenyl ester of dicarboxylic acid (monomer 1)	151
5.3.2.2 Synthesis of tetra-p-toluene sulfonic acid salt of bis (L-arginine) alkylene diesters (monomer 2).....	151
5.3.2.3 Synthesis of Unsaturated Arg Polyester amide (Arg-UPEA).....	152
5.3.2.4 Cytotoxicity of Arg-UPEA/ GMA-chitosan hybrid hydrogel precursor in the aqueous solution.....	153
5.3.2.5 Fabrication of Arg-UPEA/ GMA-chitosan hybrid hydrogel.....	155
5.3.2.6 Characterization of 2-UArg-4-S PEA and its hybrid hydrogel with GMA-chitosan.....	156
5.3.2.7 Equilibrium swelling ratio (Q_{eq}) test under different pH environment at room temperature.....	156
5.3.2.8 Morphological study of 2-UArg-4-S/GMA-chitosan hydrogels.....	157

5.3.2.9	Compression mechanical properties of 2-UArg-4-S/GMA-chitosan hydrogels.....	157
5.3.2.10	Enzymatic degradation of 2-UArg-4-S/GMA-chitosan-33/67 hybrid hydrogels.....	158
5.3.2.11	Release study of bovine serum albumin from 2-UArg-4-S/GMA-chitosan-33/67 hydrogel.....	158
5.4	Results.....	160
5.4.1	¹ H NMR spectroscopy of Arg-UPEA monomers.....	160
5.4.2	Fabrication of Arg-UPEA/ GMA-chitosan Hybrid Hydrogel.....	161
5.4.3	FTIR spectroscopy.....	161
5.4.4	Elemental analysis of Arg-UPEA/GMA-chitosan hybrid hydrogel.....	164
5.4.5	Cytotoxicity of 2-UArg-4-S/GMA-chitosan-33/67 hybrid hydrogel.....	164
5.4.6	Equilibrium swelling ratio (Q_{eq}) test of Arg-UPEA/GMA-chitosan hybrid hydrogels under different pH environment at room temperature.....	166
5.4.7	Morphology of 2-UArg-4-S/GMA-chitosan hybrid hydrogel.....	170
5.4.8	Mechanical properties of 2-UArg-4-S/GMA-chitosan hybrid hydrogel.....	172
5.4.9	Enzymatic degradation of 2-UArg-4-S/GMA-chitosan hybrid hydrogel.....	174
5.4.10	Cumulative Release of Bovine Serum Albumin (BSA) from 2-UArg-4-S/GMA-chitosan Hybrid Hydrogel at 37 °C, pH 7.4.	178
5.5	Conclusions and recommendation for future work.....	180
Chapter 6 A new family of functional biodegradable Arginine-based polyester urea urethane: synthesis, characterization and biodegradation.....		189
6.1	Abstract.....	190
6.2	Introduction.....	190
6.2.1	Polyurethane.....	190
6.2.2	Degradation of polyurethane.....	192

6.2.3 Enzymatic degradation of polyurethane.....	192
6.2.4 Arginine based polymer.....	194
6.2.5 Design of biodegradable PUs for the in vivo environment.....	195
6.3 Experimental.....	197
6.3.1 Materials.....	197
6.3.2 Methods.....	197
6.3.2.1 Synthesis of di-hydrochloride acid salt of bis (L-Arg) alkylene diester monomers (Arg-x-Cl)	197
6.3.2.2 Synthesis of Arg-PEUU.....	200
6.3.2.3 Characterization of Arg-x-Cl monomer and Arg-PEUU.....	206
6.3.2.4 Molecular weight determination of Arg-PEUU.....	206
6.3.2.5 Thermal properties of Arg-PEUU.....	206
6.3.2.6 Water contact angle test of Arg-PEUU.....	207
6.3.2.7 Cytotoxicity test of 6-Arg-2 PEUU suspension (MTT assay)	207
6.3.2.8 Fabrication of Arg-PEUU gel via UV-crosslinking.....	209
6.3.2.9 Compressive mechanical property of Arg-PEUU gels.....	209
6.3.2.10 Enzymatic biodegradation of Arg-PEUU films <i>in vitro</i>	210
6.4 Results and discussion.....	211
6.4.1 ¹ H NMR spectroscopy of of Arg-x-Cl monomers.....	211
6.4.2 Arg-PEUU synthesis and characterization.....	216
6.4.3 Structure difference of Arg-PEUU with other published polyurethane materials with amino acids building blocks.....	220
6.4.4 Thermal properties of Arg-PEUU.....	224
6.4.5 Water contact angle of Arg-PEUU.....	229
6.4.6 Solubility of Arg-PEUU in common solvents at room temperature.....	230
6.4.7 Cytotoxicity of 6-Arg-2 PEUU A/G-1/1 and 6-Arg-2 PEUU A/G-4/1.....	232

6.4.8 Photo-crosslinked Arg-PEUU and the interior morphology.....	234
6.4.9 Compressive mechanical properties of photo-crosslinked Arg-PEUU gels.....	237
6.4.10 In vitro enzymatic biodegradation of Arg-PEUU and photo-crosslinked Arg-PEUU films.....	239
6.5 Conclusion and recommendation for future work.....	242
Chapter 7 A new family of functional biodegradable Arginine-based polyether ester urea urethane: synthesis, characterization, biodegradation and gel or microsphere fabrication	250
7.1 Abstract.....	251
7.2 Introduction.....	252
7.3 Materials and methods.....	254
7.3.1 Materials.....	254
7.3.2 Synthesis of di-hydrochloride acid salt of bis (L-Arg) oligoethylene glycol diester monomers (Arg-xEG-Cl)	254
7.3.3 Synthesis of Arg based poly(ether ester urea urethane)s (Arg-PEEUU)	255
7.3.4 Characterization of Arg-xEG-Cl monomer and Arg-PEEUU.....	255
7.3.5 Molecular weight determination of Arg-PEEUU.....	259
7.3.6 Thermal properties of Arg-PEEUU.....	259
7.3.7 Water contact angle test of Arg-PEEUU.....	259
7.3.8 The water solubility change of Arg-PEEUU at different temperature.....	260
7.3.9 Cytotoxicity test of 6-Arg-2EG PEEUU A/G-4/1 and 6-Arg-4EG PEEUU A/G-4/1 (MTT assay)	260
7.3.10 Fabrication, size and ζ -potential characterization of Arg-PEEUU microsphere in deionized water.....	262
7.3.11 Fabrication of Arg-PEEUU gel via UV-crosslinking.....	263

7.3.12 Compressive mechanical property of Arg-PEEUU gels.....	263
7.3.13 Enzymatic biodegradation of Arg-PEEUU films <i>in vitro</i>	264
7.4 Results and discussion.....	265
7.4.1 Synthesis of Arg-xEG-Cl monomers.....	265
7.4.2 Arg-PEEUU synthesis and characterization.....	266
7.4.3 Thermo property of Arg-PEEUU.....	269
7.4.4 Water contact angle of Arg-PEEUU.....	273
7.4.5 Water solubility of Arg-PEEUU at different temperature.....	274
7.4 .6 Cytotoxicity of 6-Arg-2EG PEEUU A/G-4/1 and 6-Arg-4EG PEEUU A/G-4/1 (MTT assay)	276
7.4 .7 Characterization of Arg-PEEUU microsphere.....	277
7.4 .8 Photo-crosslinked Arg-PEEUU gel.....	280
7.4 .9 Compressive mechanical property of photo-crosslinked Arg-PEEUU gels.....	281
7.4.10 <i>In vitro</i> enzymatic biodegradation of Arg-PEEUU and photo-crosslinked Arg- PEEUU films.....	284
7.5 Conclusions and recommendation for future work.....	288

LIST OF FIGURES

Figure 1.1 Chemical structure of chitosan.....	2
Figure 1.2 Schematic representation of chitosan based hydrogels derived from different physical associations.....	4
Figure 1.3 pH-sensitive swelling of an ionically crosslinked chitosan hydrogel.....	5
Figure 1.4 Hydrogels prepared by blending solutions of chitosan (CS) and PEI.....	7
Figure 1.5 Schematic diagram of the multi-membrane onion-like chitosan hydrogel....	8
Figure 1.6 Genipin-chitosan crosslinking.....	11
Figure 1.7 Illustration of the chitosan hydrogel network linked by alkyl chains.....	13
Figure 1.8 Scheme of preparation of chitosan/NIPAAm hybrid hydrogels.....	14
Figure 1.9 Chit-Ph hydrogel formation.....	15
Figure 2.1 GMA-chitosan synthesis.....	35
Figure 2.2 Photo-crosslinked network structures of GMA-chitosan hydrogel.....	39
Figure 2.3 ¹ H-NMR spectrum of GMA-chitosan (DS 13) dissolved in DMSO- <i>d</i> ₆	45
Figure 2.4 FT-IR of GMA-chitosan.....	46
Figure 2.5 Effects of molar feed ratio of GMA to chitosan and reaction time on the GMA degree of substitution.....	49
Figure 2.6 MTT assay (porcine aortic valve smooth muscle cell) of GMA-chitosan...50	
Figure 2.7 Image of photo-crosslinked GMA-chitosan (DS 37) hydrogel.....	52
Figure 2.8 SEM images of swollen GMA-chitosan (DS 37) hydrogel.....	54
Figure 2.9 Enzymatic biodegradation of photo-crosslinked GMA-chitosan (DS 37) hydrogel.....	55
Figure 2.10 SEM images of morphologic changes of GMA-chitosan hydrogel <i>in vitro</i>	57
Figure 2.11 Cumulative BSA release from GMA-chitosan (DS 37) hydrogel.....	58

Figure 2.12 Square-root of time relationship for release of BSA from GMA-chitosan.....	60
Figure 3.1 Illustration of the chitosan hydrogel network.....	73
Figure 3.2 One representative GMA-chitosan / AETA hybrid hydrogel.....	79
Figure 3.3 FTIR of GMA-chitosan/AETA-67/33 hybrid hydrogel.....	84
Figure 3.4 Images of GMA-chitosan/AETA-67/33 hydrogel.....	85
Figure 3.5 The influence of ionic strength of the immersion media to the swelling ratio of GMA-chitosan/AETA hybrid hydrogel.....	86
Figure 3.6 The influence of pH environment to the swelling ratio of GMA-chitosan / AETA hybrid hydrogels.....	89
Figure 3.7 SEM images of GMA-chitosan hydrogel and GMA-chitosan/ AETA hybrid hydrogels.....	91
Figure 3.8 <i>In vitro</i> enzymatic degradation of GMA-chitosan hydrogel and GMA-chitosan/AETA-67/33 hybrid hydrogel.....	94
Figure 3.9 Cumulative BSA release profile from GMA-chitosan/AETA-67/33 hybrid hydrogels and GMA-chitosan hydrogel.....	96
Figure 4.1 Fabrication of GMA-chitosan / VSA hybrid hydrogel.....	112
Figure 4.2 FTIR of GMA-chitosan hydrogel and GMA-Chitosan/VSA-67/33 hybrid hydrogel.....	116
Figure 4.3 Images of GMA-chitosan/VSA hybrid hydrogel or GMA-chitosan hydrogel.....	117
Figure 4.4 The influence of ionic strength environment to the swelling ratio of GMA-chitosan or GMA-chitosan/VSA hybrid hydrogel.....	118
Figure 4.5 SEM images of GMA-chitosan/VSA hybrid hydrogels.....	123
Figure 4.6 The initial compression modulus of GMA-chitosan hydrogel, GMA-chitosan/VSA hybrid hydrogel.....	125

Figure 4.7 Cumulative BSA release of GMA-chitosan hydrogel, GMA-chitosan/VSA - 80/20 hybrid hydrogel.....	127
Figure 5.1 Metabolic fates of arginine in mammalian cells.....	138
Figure 5.2 Phases of wound healing and the generation of wound NO.....	140
Figure 5.3 Synthesis of Arg-PEA monomers.....	152
Figure 5.4 H-NMR of bis (L-Arginine) alkylene diester.....	160
Figure 5.5 Images of 2-UArg-4-S/GMA-chitosan-33/67 hybrid hydrogel.....	161
Figure 5.6 FTIR spectra of 2-UArg-4-S, GMA-chitosan and 2-UArg-4-S/GMA-chitosan-33/67 hybrid hydrogel.....	163
Figure 5.7 Porcine aortic valve smooth muscle cell viability test by MTT assay of 2-UArg-4-S/GMA-chitosan-33/67 mixed solution.....	165
Figure 5.8 The influence of pH environment to the equilibrium swelling ratio Q_{eq} of Arg-UPEA/GMA-chitosan hybrid hydrogels.....	169
Figure 5.9 SEM images of the interior morphology of 2-UArg-4-S/GMA-chitosan hybrid hydrogels.....	171
Figure 5.10 <i>In vitro</i> enzymatic degradation of GMA-chitosan hydrogel and 2-UArg-4-S /GMA-chitosan-33/67 hybrid hydrogel.....	176
Figure 5.11 Cumulative BSA release profile from 2-UArg-4-S /GMA-chitosan hybrid hydrogels.....	179
Figure 6.1 Representation of the catalytic site of depolymerase and the mechanism of action.....	194
Figure 6.2 Synthesis of di-hydrochloride acid salt of bis(L-Arg) alkylene diester monomers.....	202
Figure 6.3 Synthetic pathway for the preparation of Arg-PEUU.....	205
Figure 6.4 ^1H NMR spectroscopy of Arg diester monomers.....	213
Figure 6.5 ^1H NMR spectroscopy of Arg-PEUU.....	215

Figure 6.6 FTIR of 6-Arg-2 PEUU synthesized with different monomer feed ratio and allyl PU.....	217
Figure 6.7 DSC of Arg-PEUU.....	226
Figure 6.8 MTT Assay of 6-Arg-2 PEUU.....	233
Figure 6.9 Images of photo-crosslinked Arg-PEUU gels.....	235
Figure 6.10 SEM images of cross section of photocrosslinked Arg-PEUU.....	237
Figure 6.11 Effect of lipase concentration on the biodegradation rate of the 6-Arg-2 PEUU film.....	241
Figure 7.1 Synthesis of di-hydrochloride acid salt of bis(L-Arg) oligoethylene glycol diesters.....	256
Figure 7.2 Synthetic pathway for the preparation of Arg-PEEUU.....	257
Figure 7.3 ¹ H NMR spectroscopy of Arg oligoethylene glycol diester monomers....	268
Figure 7.4 FTIR of 6-Arg-2EG PEEUU synthesized with different monomer feed ratio and allyl PU.....	269
Figure 7.5 MTT Assay of Arg-PEEUU.....	277
Figure 7.6 6-Arg-2EG PEEUU A/G-1/1 microsphere.....	279
Figure 7.7 Images of photo-crosslinked 6-Arg-4EG PEEUU A/G-1/1 gel.....	281
Figure 7.8 Effect of lipase concentration on the biodegradation rate of the 6-Arg-4EG PEEUU film.....	286

LIST OF TABLES

Table 2.1 Comparison of GMA-chitosan to other reported chitosan derivatives with unsaturated groups.....	33
Table 2.2 Relative carbon and nitrogen contents of raw chitosan and GMA-chitosan.....	47
Table 2.3 Solubility of GMA-chitosan in several common solvents.....	47
Table 2.4 Zeta potential of GMA-chitosan.....	48
Table 3.1 The compression initial modulus of swollen GMA-chitosan hydrogel and GMA-chitosan/AETA hybrid hydrogel.....	92
Table 4.1 Compositions of GMA-chitosan in GMA-chitosan / VSA hybrid hydrogel precursor.....	111
Table 5.1 Carbon and nitrogen content analysis of GMA-chitosan and Arg-UPEA hybrid hydrogel.....	168
Table 5.2 Mechanical property of Arg-UPEA/GMA-chitosan hybrid hydrogel.....	173
Table 6.1 The chemical structures of raw materials of Arg-PEUU.....	198
Table 6.2 List of L-Arg alkylene diester monomers used in the synthesis of Arg-PEUU.....	201
Table 6.3 Arg-PEUU series synthesized.....	204
Table 6.4 Carbon and Nitrogen contents of Arg-PEUU.....	219
Table 6.5 Molecular weight and molecular weight distribution of Arg-PEUU.....	221
Table 6.6 Comparison of Arg-PEUU with published amino acid contained polyurethane.....	223
Table 6.7 T_g and T_m of Arg-PEUU.....	229
Table 6.8 Water contact angle of Arg-PEUU.....	230
Table 6.9 Solubility of Arg-PEUU in common solvents at room temperature.....	231

Table 6.10 Compression mechanical data of allyl PU gel and Arg-PEUU gels.....	236
Table 7.1 Arg-PEEUU series synthesized.....	258
Table 7.2 C% and N% of Arg-PEEUU.....	270
Table 7.3 Molecular weight of Arg-PEEUU.....	271
Table 7.4 T_g and water contact angle of Arg-PEEUU.....	272
Table 7.5 Water solubility of Arg-PEEUU at different temperature.....	275
Table 7.6 ζ -potential and the average hydrodynamic diameter of Arg-PEEUU microsphere.....	280
Table 7.7 Compression mechanical data of Arg-PEEUU gels.....	282

CHAPTER ONE:
SUMMARY OF CHITOSAN BASED HYDROGEL FABRICATION METHODS

1.1 Introduction of Chitosan and chitosan based hydrogel

Natural polymers (polysaccharides and proteins) are used in the development of hydrogels as structural materials. Compared with other natural polymers, polysaccharides have excellent biocompatibility, low immunogenicity, low toxicity, and enzymatic degradation property. Chitosan is one linear polysaccharide composed of randomly distributed β -(1-4)-linked D-glucosamine and N-acetyl-D-glucosamine units. It is commercially produced by the deacetylation of chitin which is extracted from crustaceans and insects. The chemical structure of chitosan is shown in Figure 1.1. Due to these characteristics and abundant source to produce, chitosan has attracted a wide range of medical and pharmaceutical applications^{1,3}. At pH below its pKa (pH 6.2), chitosan is water-soluble and positively charged due to protonation of amine groups present on the polymer chain. When the pH exceeds 6.2, chitosan aqueous solution forms a gel precipitation forms due to the neutralization of chitosan amine groups, leading to the balance of repulsion between chitosan molecules breaks in the stable water solution. By using this property of chitosan, the neutralization of chitosan solution by counter-ionic salt is applied as one method to fabricate chitosan hydrogels⁴.

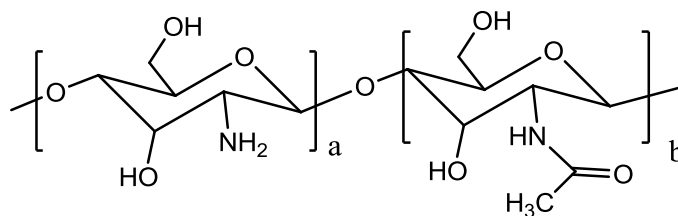


Figure 1.1 Chemical structure of chitosan

High water content crosslinked chitosan hydrogels are able to be used as intelligent carrier which provides sustained, local delivery of therapeutic agents. Many chitosan hydrogel preparation methods have been developed. In each method, chitosan

is either physically associated or chemically cross-linked to form 3D network structures. To form stabilizing linkage, chitosan must have functional moieties that all binding between the chains to prevent gel dissolution. The bonding can be accomplished by non-covalent physical association, such as hydrogen bonding or ionic bonding, physical entanglement, or by chemically covalent crosslinking. The physical associations are reversible bonds, whereas the covalent crosslinkages of chitosan are not. These methods were summarized below as physical association of chitosan hydrogel and chemical crosslinked chitosan two approaches.

1.2 Physical association chitosan hydrogels

In order to fabricate physical chitosan hydrogels, chitosan polymer which is used as precursor must have strong enough inter-chain interactions to form semi-permanent junction points in the hydrogels. Another condition is this network should promote the access and residence of water. There are four major physical interactions that lead to the gelation of a chitosan solution, ionic, polyelectrolyte, interpolymer complex, and hydrophobic associations⁵. Figure 1.2 schematically shows these interactions between the secondary chemical in the hydrogel formation and chitosan. The gel formation by all of these interactions can be reversed. Chitosan-based physical gel can often be obtained by simply mixing the components which make up the gel under the appropriate conditions.

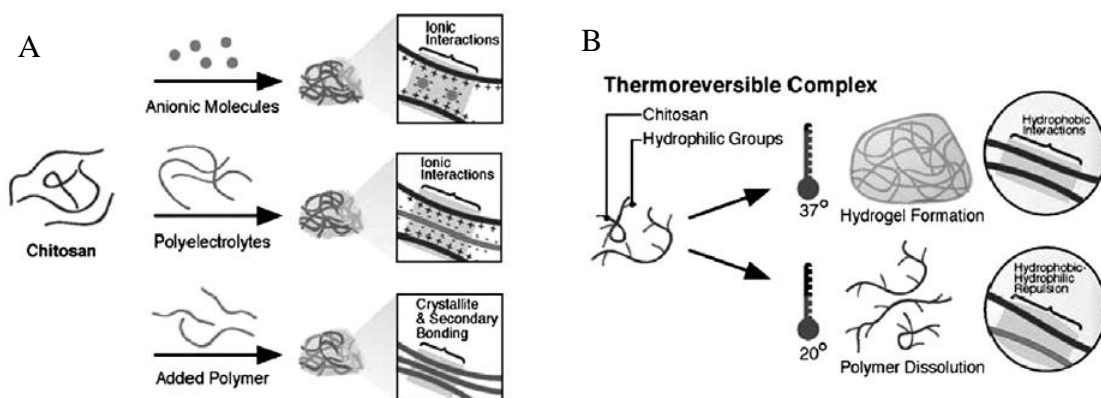


Figure 1.2 Schematic representation of chitosan based hydrogels derived from different physical associations: (A) network of chitosan formed with counter-ionic molecules, polyelectrolyte polymer and neutral polymers; (B) thermo-reversible networks of chitosan graft copolymer ⁵.

1.2.1. Ionic complex chitosan hydrogel

Ionic complexation of chitosan and small anionic molecules can be formed by the interaction of cationic amino groups and negatively charged molecules. In former studies, small anionic molecules, such as sulfates, citrates and phosphates or anions of metals like Pt (II), Pd (II) and Mo (VI) ^{6, 7}. The material properties vary with the charge density and the size of the anionic agents. In the study of Chenite et al, β -glycerol phosphate neutralized the chitosan solution without immediate gel-like precipitation. Furthermore, this precursor forms hydrogel after subsequent heating ⁴. The sol/gel transition temperature was pH-sensitive and gelling time was shown to be temperature-dependent. Both of anions and metal ions bind chitosan via its protonated amino group, but metal ion works through coordinate-covalent bonds instead of electrostatic interactions. Chitosan has interesting metal ion uptake property which has been extensively studied ⁵. In the study of Dambies et al, molybdate was used as the gelling agent to prepare chitosan gel beads ⁸. This gelation technique leads to a different structure compared with simple alkaline coagulation of chitosan solution.

Under optimum conditions, chitosan forms a double layer structure in a molybdate solution, a nonporous thick external layer and an internal structure of small pores. Another ionic complexation can be formed by other secondary interchain interactions including hydrogen bonding between chitosan's hydroxyl groups and the ionic molecules or by using the interactions of chitosan after neutralization of cationic amine groups. For instance, in the research of Mi et al, iron (III) forms crosslinked hydrogel microsphere with carboxymethylchitin. It demonstrates iron (III) is able to crosslink the hydroxyl groups of chitosan ⁹.

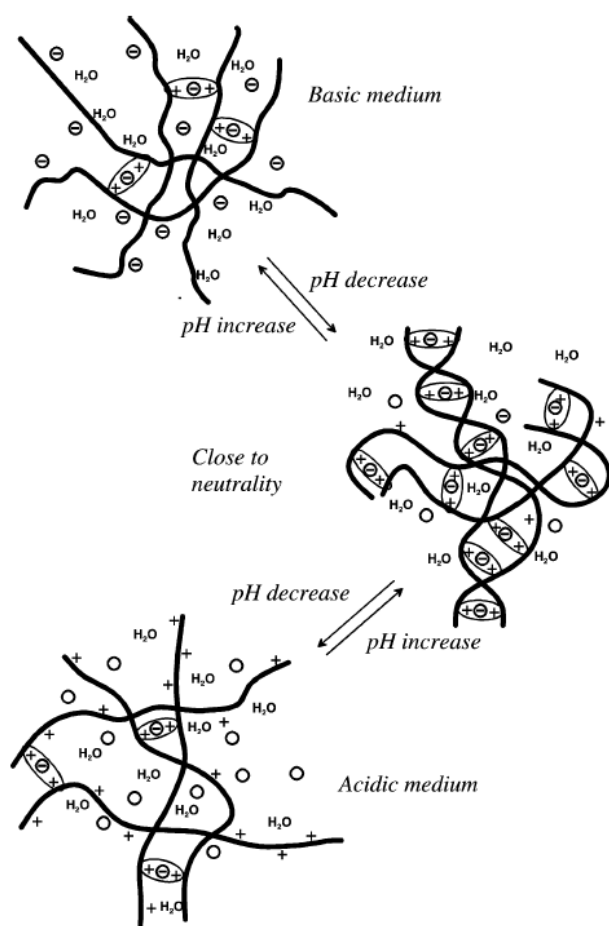


Figure 1.3 pH-sensitive swelling of an ionically crosslinked chitosan hydrogel containing an ionic molecule as crosslinker ¹⁰

One advantage of this category chitosan hydrogels is, compared with covalently crosslinked hydrogels, ionically crosslinked hydrogel cannot only swell in acidic but also in alkaline conditions, as shown in Figure 1.3¹⁰. This property extends their potential application in drug delivery.

1.2.2. Polyelectrolyte complexes

Polysaccharides, proteins and synthetic polyelectrolytes also form electrostatic interactions with chitosan. The associations between the chitosan polymer and polyelectrolytes are stronger than other secondary binding interactions like hydrogen bonding or van der Waals interactions. Chitosan-based polyelectrolyte complex networks have been produced by water-soluble anionic macromolecules like DNA, alginate, GAGs (e.g. chondroitin sulfate, hyaluronic acid, or heparin), proteins (e.g. gelatin, albumin), and anionic synthetic polymers (e.g. polyacrylic acid). The formation of chitosan-based polyelectrolyte hydrogel can be a one-stage process or a two stage procedure. Saether et al. used the one-stage process¹¹. A sodium alginate solution was added to a chitosan chloride solution under high shearing conditions, or chitosan chloride was added to sodium alginate. The polyelectrolyte complex was very stable at pH above 7 over a temperature range of 4-37 °C¹¹. In a two stage procedure, the first step in this process is the preparation of Ca-alginate gel beads¹². Then the beads are then transferred into a chitosan solution, and a polyelectrolyte complex membrane is formed on the surface of the beads. The alginate/chitosan ratio in the preparation was found to affect nanoparticle formation, as did polymer molecular weight and pH. The smallest nanoparticles have a mean diameter of 314 nm, and are prepared using low viscosity alginate and low molecular weight chitosan in a ratio of 2 : 3. The alginate/chitosan ratio in the preparation was found to affect particle size to a greater degree than any other parameter¹². Polyelectrolyte complexes which consist of

chitosan and the polyelectrolyte are reversible. The stability of these compounds is dependent on charge density, solvent, ionic strength, pH and temperature.

1.2.3. Physical mixtures and secondary bonding

Hydrogels can be formed by chitosan and other water-soluble nonionic polymer through physical interactions. After lyophilization or after several freeze-thaw cycles, nonionic polymer and chitosan formed junction points in the form of crystallites or interpolymer complexation.

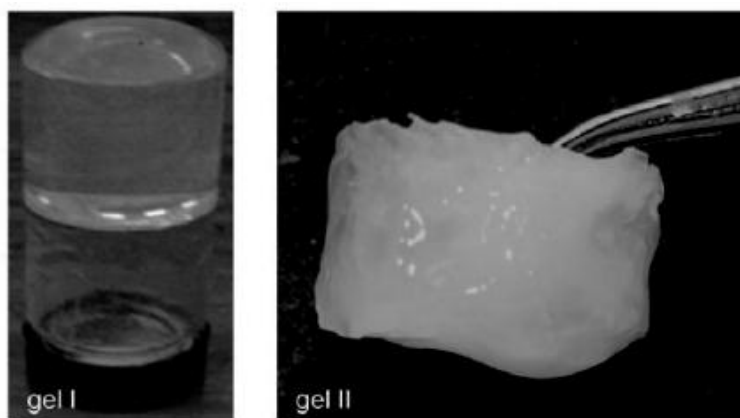


Figure 1.4 Hydrogels prepared by blending solutions of chitosan (CS) and PEI: gel I (chitosan/PEI 10:90) and gel II (chitosan/PEI 40:60) ¹³

By mixing polyethylenimine with chitosan, a 3D hydrogel was formed within 5min that was stable under cell culture conditions and could support the growth of primary human fetal skeletal cells. It is posited that the gel structure is held together by chitosan–chitosan interactions. When the polymer mixture is prepared at pH 7.5, chitosan is insoluble, possibly leading to crystallite formation between its chains ¹³.

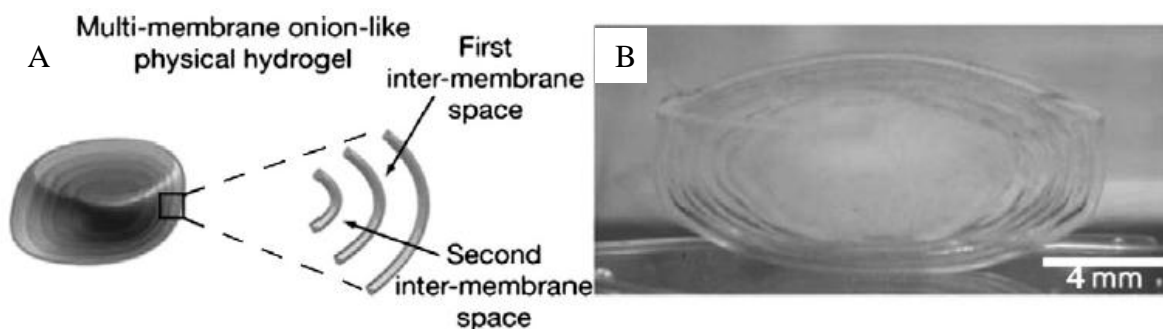


Figure 1.5 (A) Schematic diagram of the multi-membrane onion-like structures; (B) multi-membrane biomaterial with ‘onion-like’ structure based on chitosan hydrogel ¹⁴.

Ladet et al used a sodium hydroxide solution neutralized chitosan’s amino groups. One interesting multilayered “onion-like” hydrogel could be prepared without the addition of any other polymer or complexing molecule ¹⁴. This approach prevented ionic repulsion between the polymer chains, allowing for the formation of hydrogen bonds, hydrophobic interactions, and chitosan crystallites.

1.2.4. Thermo-reversible hydrogels and hydrophobic associations

Thermo-reversible polymer hydrogels that undergo a sol-to-gel transition in response to temperature changes are of great interest in therapeutic delivery and tissue engineering as injectable depot systems. The mechanism of thermo-reversible hydrogel is that the hydrophobic interactions or secondary bonding of the polymer form junctions between chains. These polymers undergo a hydrophilic-hydrophobic transition when the solution temperature reaches a lower critical solution temperature (LCST). The hydrophobic interaction made the system forms a semi-rigid gel. Some ionic complex chitosan hydrogel has the thermo-reversible property. Glycerol phosphate disodium salt has the temperature-sensitive behavior and can be used to neutralize the amine groups of chitosan. The chitosan/glycerol phosphate mixture remains a clear liquid at room temperature and gelation happens at 37 °C ⁴.

Polyethylene glycol (PEG), poly (ethylene oxide) / poly (propylene oxide) block copolymers or Poly N-isopropylacrylamide (PNIPAAm) modified chitosan systems are another several main categories of thermo-reversible hydrogels. In the Bhattarai et al. study, monohydroxyl PEG was chemically grafted on the chitosan backbone. At the optimum feed ratio of chitosan and PEG, the modified chitosan polymer forms an injectable solution at room temperature whereas it forms a gel at body temperature ¹⁵. Poly (ethylene oxide) / poly (propylene oxide) block copolymers is usually made as amphiphilic triblock copolymer PEO-PPO-PEO. Traditional view considers this triblock polymer has a center hydrophobic segment with two hydrophilic regions. When the concentration of this polymer is above a critical value, polymer solution undergoes a sol-gel transition. Park et al. grafted the terminal groups of PEO-PPO-PEO on chitosan ¹⁶. The aqueous chitosan-PEO-PPO-PEO solution had a solution-gel transition at about 25 °C which can be used as injectable hydrogel for cartilage regeneration. Similarly, an aqueous PNIPAAm solution precipitates above 32 °C (LCST). Below the LCST, the enthalpy term, which is mostly contributed by the hydrogen bonding between polymer polar groups and water molecules, leads to dissolution of the polymer. Gel formation at higher temperatures is caused by dehydration of the hydrophobic isopropyl groups during the coil-to-globule transition. In the study of Chen et al., PNIPAAm-COOH was synthesized and was conjugated on the amine group of chitosan ¹⁷. Chitosan-PNIPAAm hydrogels exhibit reversible soluble-insoluble characteristics, fast phase transition kinetics, excellent phase transition repeatability, and significant improvement in mechanical strength over PNIPAAm hydrogels. The major advantage of thermo-reversible chitosan hydrogels is it can be introduced in the body without big surgery and very suitable for irregular shape of tissue cavity in clinic application.

1.3 Chemically crosslinked chitosan hydrogel

The limitation of physically bonded hydrogels is their inconsistent performance, due to the lack of stable network structure formed by covalent crosslinking sites. Moreover, to precisely control the physical gel shape and pore size are very hard. More robust chitosan hydrogels is able to be fabricated by using small molecules crosslinkers, secondary polymerization or irradiation chemistry. The primary amines and hydroxyl groups of chitosan chain are able to react with many kinds of crosslinkers. Chemical cross-linked network can be formed by using small molecule cross-linkers, polymer-polymer reactions between activated functional groups.

1.3.1 Small molecule cross-linkers.

Many bifunctional small molecules could be used to crosslink chitosan. Crosslinkers are molecules with at least two reactive functional groups that all the formation of bridges between chitosan chains. One kind of commonly used crosslinkers is dialdehydes, such as glutaraldehyde or glyoxal. The aldehyde groups for covalent imine bonds with the amino groups of chitosan via a Schiff base reaction. Dialdehydes react with amino groups in aqueous media without the addition of auxiliary molecules such as reducer. For example, Yamada et al. produced a water-resistant adhesive by using glutaraldehyde as crosslinker of chitosan¹⁸.

However, dialdehydes are generally considered to be toxic. The residue dialdehydes which are not completely reacted may induce toxic effect. Besides dialdehydes, diglycidyl ether, diisocyanate, diacrylate were used to crosslink chitosan hydrogel¹⁹⁻²¹. Recently, genipin, which is a naturally occurring material and used in herbal medicine and food dye are used as an alternative of chitosan crosslinker²². Figure 1.6 shows the reaction between chitosan and genipin. Genipin has been reported to bind biological tissues and biopolymers, such as chitosan and gelatin. In addition, genipin cross-linked chitosan membranes exhibit a slower degradation rate that induces extended drug release²³.

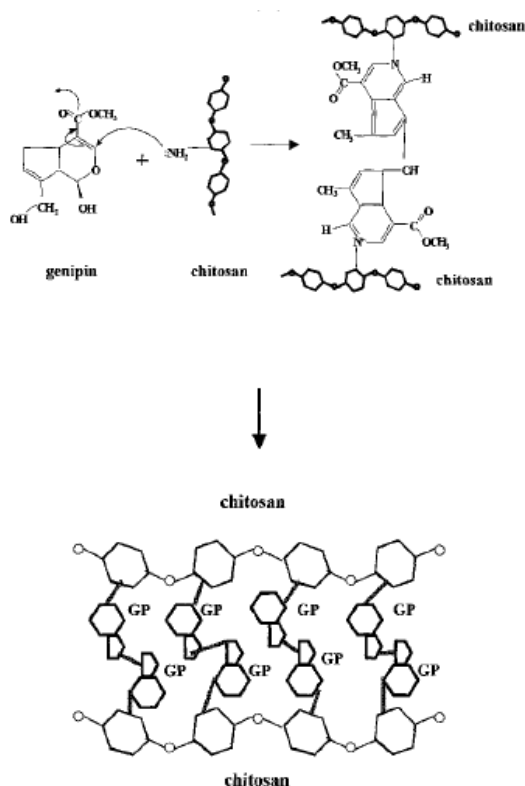


Figure 1.6 Genipin-chitosan crosslinking ²³

1.3.2 Polymer-polymer crosslinking

Even though small molecules are able to provide desirable properties, but many cross-linkers are considered to be toxic. In order to eliminate the use of crosslinker molecules during gelation, functionalized polymer chains with reactive groups were used in chitosan hydrogel fabrication. In Tan et al. study, chitosan and hyaluronic acid hydrogel was produced by schiff bases reaction in situ ²⁴. A water soluble chitosan derivative, N-Succinyl-chitosan and oxidized hylauronic acid were mixed with various volume ratios to form chitosan / hyaluronic acid hybrid hydrogels. Schiff base was formed with in 4 mins after N-Succinyl-chitosan and hylauronic acid with aldehyde group. Chondrocytes culture test demonstrates the composite hydrogel supports

chondrocyte adhesion and encapsulation. Schiff bases reaction were also used in the preparation of oxidized dextran and chitosan²⁵. Ono et al. reported Chitosan hydrogels which have also been made by using Michael addition reactions²⁶. In this study, thiol modified chitosan was synthesized and mixed with PEG diacrylate. Hydrogel was rapidly formed in situ under physiological conditions. Chitosan's primary amino groups react with the vinyl group on another polymer. The advantage of this approach is its rapid reaction time and different choices of bonds. The disadvantage of polymer-polymer system is it requires multi-step preparation and purification processes. Moreover, the reactive groups some times are cytotoxic.

1.3.3 Photo-crosslinking

Chitosan hydrogels can be formed in situ using photo-sensitive functional groups. Chitosan with reactive moieties forms crosslinkage upon irradiation with UV light. This technique offers considerable advantages (ease to control shape, safety, etc). Functionalized chitosan with azide groups (-N₃) has been developed by Ono et al²⁶. The azide is converted into a reactive nitrene group which reacts with chitosan's free amine group. The gelation happens within 60 seconds. Another type thermo-sensitive, chitosan-pluronic hybrid hydrogel precursor which is functionalized with acrylate groups was also made through UV photocrosslinking. After UV radiation, the precursor could form a physical network at the temperature above its LCST²⁷. Some researchers tried to introduce unsaturated double bond on the chitosan main chain. Figure 1.7 shows the scheme of chitosan derivative with the pendant double bonds. Hong et al. developed one water soluble and crosslinkable chitosan derivative via the condensation reaction between amino groups and carboxyl groups under the catalysis of carbodiimide²⁸. This chitosan hydrogel is soluble in neutral water and does not precipitate till pH 9. The chitosan hydrogel was formed in the mold at a temperature of 37 °C under the initiation of a redox system, ammonium persulfate (APS) / N, N, N,

N- tetramethylethylenediamine (TMEDA). The same reaction and gelation method was used by Hong et al. again to synthesis another water-soluble chitosan derivative having double bonds. Methacrylic acid (MA) and lactic acid (LA) was grafted via the reaction between amino groups and carboxyl groups under the catalysis of carbodiimide ²⁹.

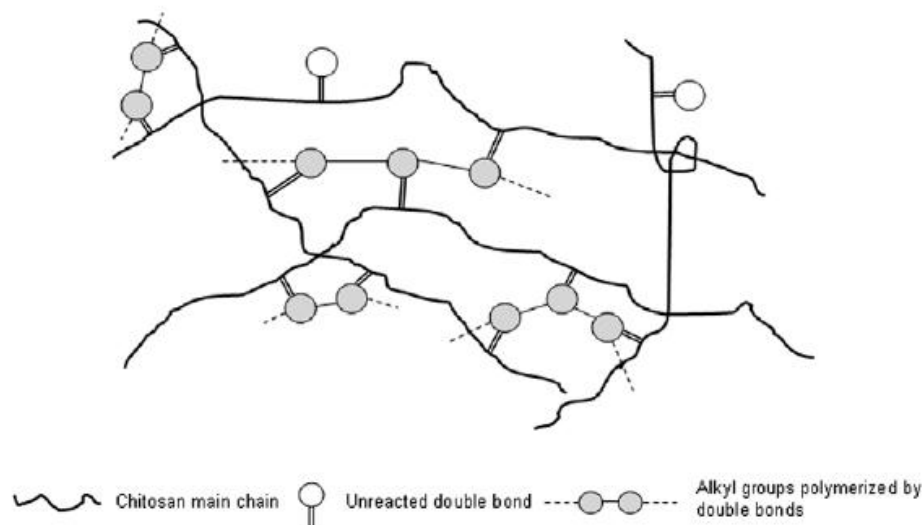


Figure 1.7 Illustration of the chitosan hydrogel network linked by alkyl chains which are formed via carbon-carbon double bond polymerization.

Ramirez et al. took advantage of the rapid reaction between epoxy groups of glycidyl methacrylate and the amine groups of chitosan to develop one chitosan derivative with double bonds. The synthesis process is in acidic water solution ³⁰. Pure chitosan-glycidyl methacrylate derivative hydrogel has not been reported. Han et al. used very similar method to produce a series of hybrid hydrogels based on glycidyl methacrylated chitosan (CS-GMA)/ N-isopropylacrylamide (NIPAAm) UV photopolymerization technology chitosan hydrogel with small molecule crosslinker, N, N-methylene bisacrylamide (MBAA) ³¹ (Shown in Figure 1.8).

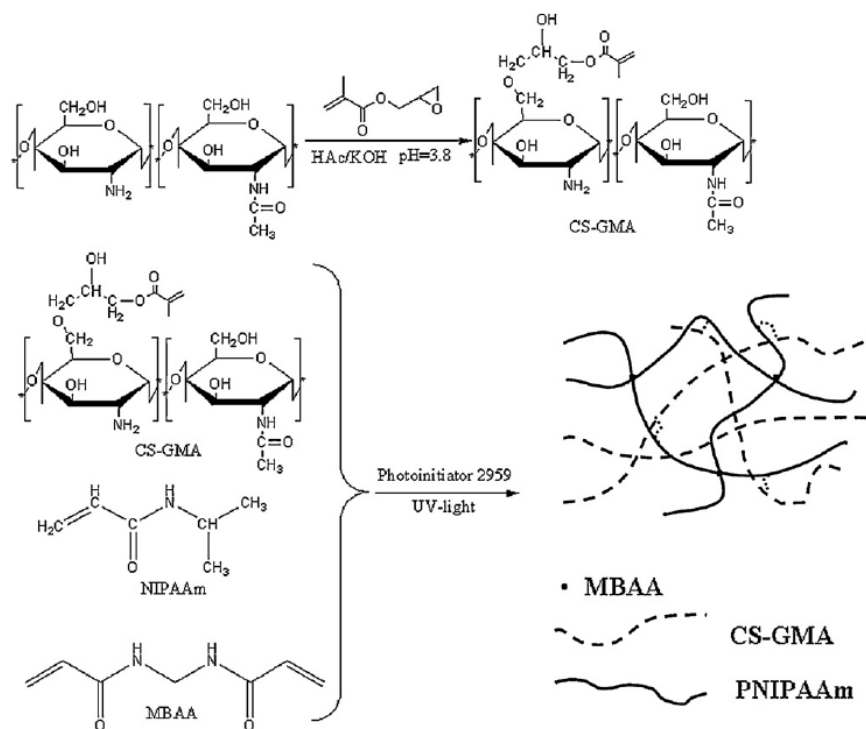


Figure 1.8 Scheme of preparation of Chitosan/NIPAAm hybrid hydrogels ³¹

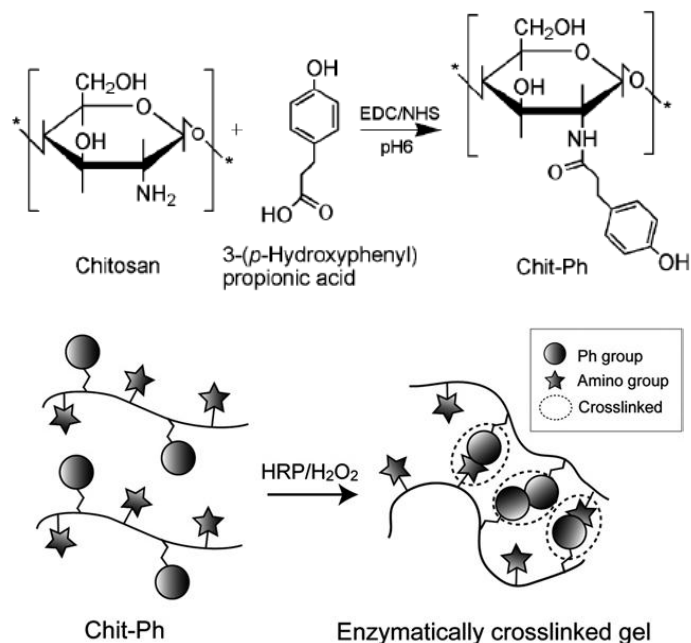
This hydrogel system has temperature sensitivity which is contributed by NIPAAm component. Due to the residue cationic amine groups of chitosan component, this hybrid hydrogel also shows pH sensitivity in aqueous environment.

1.3.4 Enzymatic crosslinking

Even though photocrosslinking technology forms hydrogels in situ and represent a promising class of chitosan hydrogels. But it usually requires photosensitizer and UV radiation, which may damage neighboring cells and tissue in situ formation. A mild and new approach, enzyme-catalyzed cross-linking reaction is employed to fabricate chitosan hydrogel.

Tyrosinase (polyphenol oxidase, a copper-containing monooxygenation enzyme) was used as catalyst for the modification of natural polymers. Phenol moiety-incorporated chitosan derivatives were subjected to tyrosinase-catalyzed cross-linking, yielding

stable and self-sustaining gels³². The inspiration of this tyrosinase cross-linking idea is from crosslinking of structural protein of animals. Protein cross-linking in biological systems includes addition of amino groups of lysine to quinone. When the addition reaction is followed by the rearrangement of hydrolysis of the azomethine, an aldehyde is generated in a Streicker-type reaction. The aldehyde is itself reactive as both an electrophilic amino group acceptor and a component in aldol condensation. Chitosan is considered, because of the large availability of primary aliphatic amino groups for carrying out selective reactions with phenols mediated by tyrosinase. Another case of enzymatic chitosan hydrogel preparation is tyrosinase oxidizes the tyrosyl residues of gelatin, forming quinone residues which then react with chitosan's amino groups and form crosslinked structure. The gelation time of chitosan and gelatin is about 30 mins³³.



Another enzyme used is called horseradish peroxidase (HRP), a single-chain β -type hemoprotein that catalyzes the coupling of phenol or aniline derivatives via the decomposition of hydrogen peroxide, has been used to catalyze cross-linking reaction. Sakai et al conjugated chitosan with HRP via carbodiimidemediated 3-(p-hydroxyphenyl) propionic acid condensation reaction (Figure 1.9 A). The resultant chitosan derivative is water-soluble at neutral pH. The hydrogel was obtained via HRP catalyzed crosslinking reaction by consuming H_2O_2 (Figure 1.9 B) ³⁴. Another injectable chitosan-based hydrogel from water-soluble chitosan-graft-glycolic acid and phloretic acid through enzymatic cross-linking with horseradish peroxidase and H_2O_2 was developed by Jin et al ³⁵. Gelation time could be from 4min to 10s depends the concentration of polymer.

1.4 Conclusions

With the development of new molecular agents, variety of chitosan hydrogels can be produced with tailored porosities, mechanical properties and stabilities in terms of different applications. All of these engineering approaches are promising to be used in the localizing drug delivery or 3D tissue engineering. The flexibility of chitosan as a major material in biomedical use is compounded by its biocompatibility and biodegradability.

References:

- 1 Oungbho, K., Muller, B.W., Chitosan sponges as sustained release drug carriers. *Int. J. Pharm.* 1997, 156, 229–237.
- 2 Dodane, V., Vilivalam, V.D., Pharmaceutical applications of chitosan. *Pharm. Sci. Technol. Today* 1998, 1, 246–253.
- 3 Bernkop-Schnurch, A., Chitosan and its derivatives: potential excipients for peroral peptide delivery systems. *Int. J. Pharm.*, 2000, 194, 1–13.

- 4 Chenite,A., Buschmann, M.,Wang, D., Chaput, C., Kandani, N., Rheological characterization of thermogelling chitosan/glycerol-phosphate solutions. *Carbohydr. Polym.* 2001, 46, 39–47.
- 5 Narayan Bhattarai, Jonathan Gunn, Miqin Zhang, Chitosan-based hydrogels for controlled, localized drug delivery, *Advanced Drug Delivery Reviews*, 2010, 62, 83-99
- 6 H.P. Brack, S.A. Tirmizi,W.M. Risen, Aspectroscopic and viscometric study of the metal ion-induced gelation of the biopolymer chitosan, *Polymer*, 1997, 38, 2351–2362.
- 7 L. Dambies, T. Vincent, A. Domard, E. Guibal, Preparation of chitosan gel beads by ionotropic molybdate gelation, *Biomacromolecules*, 2001, 2, 1198–1205.
- 8 Laurent Dambies, Thierry Vincent, Alain Domard, Eric Guibal, Iron(III)-carboxymethylchitin microsphere for the pH-sensitive release of 6-mercaptopurine, *Biomacromolecules*, 2001, 1198-1205
- 9 Fwu-Long Mi, Chin-Ta Chen et al, Iron (III)-carboxymethylchitin microsphere for the pH-sensitive release of 6-mercaptopurine, *Journal of Controlled Release*, 1997, 19-32
- 10 J. Berger, M. Reist, J.M. Mayer, O. Felt, N.A. Peppas, R.Gury, Structure and interactions in covalently and ionically crosslinked chitosan hydrogels for biomedical applications, *European Journal of Pharmaceutics and Biopharmaceutics*, 2004, 57, 19-34
- 11 Heidi Vogt Saether, Hilde K. Holme et al, Polyelectrolyte complex formation using alginate and chitosan, *Carbohydrate Polymers*, 2008, 74, 813-821
- 12 Douglas, K. L., & Tabrizian, M. Effect of experimental parameters on the formation of alginate–chitosan nanoparticles and evaluation of their potential

application as DNA carrier. *Journal of Biomaterials Science, Polymer Edition*, 2005, 16, 43-56.

13 Ferdous Khan, Rahul S. Tare, Richard. O. C. Oreffo, Mark Bradley, Versatile Biocompatible Polymer Hydrogels: Scaffolds for Cell Growth, *Angew. Chem. Int. Ed.* 2009, 48, 978 -982

14 S. Ladet, L. David, A. Domard, Multi-membrane hydrogels, *Nature*, 2008, 452, 76-79.

15 N. Bhattarai, H.R. Ramay, J. Gunn, F.A. Matsen, M.Q. Zhang, PEG-grafted chitosan as an injectable thermosensitive hydrogel for sustained protein release, *J. Control. Release*, 2005, 103, 609-624.

16 K.M. Park, Y.K. Joung, S.J.Na, M.C. Lee, K.D. Park, Thermosensitive chitosan Pluronic hydrogel as an injectable cell delivery carrier for cartilage regeneration, *Acta Biomaterialia* 5, 2009, 1956-1965.

17 Jyh-Ping, Tai-Hong Cheng, 2006, Thermo-Responsive Chitosan-graft-poly(N-isopropylacrylamide) Injectable Hydrogel for Cultivation of Chondrocytes and Meniscus Cells, *Macromol. Biosci.* 2006, 6, 1026-1039

18 Kazunori Yamada et al, Chitosan Based Water-Resistant Adhesive. Analogy to Mussel Glue, *Biomacromolecules*, 2000, 1, 252-258

19 J. Berger, M. Reist, J.M. Mayer, O. Felt, N.A. Peppas, R. Gurny, Structure and interactions in covalently and ionically crosslinked chitosan hydrogels for biomedical applications, *Eur. J. Pharm. Biopharm*, 2004, 57, 19-34

20 W.E. Hennink, C.F. van Nostrum, Novel crosslinking methods to design hydrogels, *Adv. Drug Deliv. Rev.*, 2002, 54, 13-36.

21 A.R. Kulkarni, V.I. Hukkeri, H.W. Sung, H.F. Liang, A novel method for the synthesis of the PEG-crosslinked chitosan with a pH-independent swelling behavior, *Macromol. Biosci.* 2005, 5, 925-928.

- 22 F.L. Mi, Y.C. Tan, H.F. Liang, H.W. Sung, In vivo biocompatibility and degradability of a novel injectable-chitosan-based implant, *Biomaterials*, 2002, 23, 181-191.
- 23 F.L. Mi, Y.C. Tan, H.C. Liang, R.N. Huang, H.W. Sung, In vitro evaluation of a chitosan membrane cross-linked with genipin, *J. Biomater. Sci. Polym. Ed.* 2001, 12 835-850.
- 24 H. Tan, C.R. Chu, K.A. Payne, K.G. Marra, Injectable in situ forming biodegradable chitosan-hyaluronic acid based hydrogels for cartilage tissue engineering, *Biomaterials*, 2009 30, 2499-2506.
- 25 Lihui Weng, Alexander Romanov, Jean Rooney, Weiliam Chen, Non-cytotoxic, in situ gelable hydrogels composed of N-carboxyethyl chitosan and oxidized dextran, *Biomaterials*, 2008, 29, 3905-3913
- 26 K. Ono, Y. Saito, H. Yura, K. Ishikawa, A. Kurita, T. Akaike, M. Ishihara, Photocrosslinkable chitosan as a biological adhesive, *J. Biomed. Mater. Res.*, 2000, 49, 289-295.
- 27 H.S. Yoo, Photo-cross-linkable and thermo-responsive hydrogels containing chitosan and pluronic for sustained release of human growth hormone (hGH), *J. Biomater. Sci. Polym. Ed.* 2007, 18, 1429-1441.
- 28 Yi Hong, Haiqing Song, Yihong Gong, Zhengwei Mao, Changyou Gao, Jiacong Shen, Covalently crosslinked chitosan hydrogel: Properties of in vitro degradation and chondrocyte encapsulation, *Acta Biomaterialia*, 2007, 3, 23-31
- 29 Yi Hong, Zhengwei Mao, Hualin Wang, Changyou Gao, Jiacong Shen, Covalently crosslinked chitosan hydrogel formed at neutral pH and body temperature, *Journal of Biomedical Materials Research Part A*, 2006, 913-922
- 30 Flores-Ramirez et al, Characterization and degradation of functionalized chitosan with glycidyl methacrylate, *J Biomater Sci Polym Ed*, 2005, 16 (4): 473-88.

- 31 Jing Han, Kemin Wang, Dongzhi Yang, Jun Nie, Photopolymerization of methacrylated chitosan/PNIPAAm hybrid dual-sensitive hydrogels as carrier for drug delivery, *International Journal of Biological Macromolecules*, 2009, 44, 229-235
- 32 Muzzarelli, R. A. A.; Ilari, P.; Xia, W.; Pinotti, M.; Tomasetti, M. *Carbohydr. Polym.* 1994, 24, 295.
- 33 Tianhong Chen, Heather D. Embree, Eleanor M. Brown, Maryann M. Taylor, Gregory F. Payne, Enzyme-catalyzed gel formation of gelatin and chitosan: potential for in situ applications, *Biomaterials*, 2003, 24, 2831-2841
- 34 Shinji Sakai, Yusuke Yamada, Takashi Zenke and Koei Kawakami, Novel chitosan derivative soluble at neutral pH and in-situ gellable via peroxidase-catalyzed enzymatic reaction, *J. Mater. Chem.*, 2008, 19, 230-235.
- 35 R. Jin, L.S. Moreira Teixeira, P.J. Dijkstra, M. Karperien, C.A. van Blitterswijk, Z.Y. Zhong, J. Feijen, Injectable chitosan-based hydrogels for cartilage tissue engineering, *Biomaterials*, 2009, 30, 2544-2551

CHAPTER TWO
SYNTHESIS AND CHARACTERIZATION OF GLYCIDYL METHACRYLATE
CHITOSAN AND PHOTOCROSSLINKED GLYCIDYL METHACRYLATE-
CHITOSAN HYDROGEL

2.1 Abstract

A new method to synthesize water soluble, enzymatic biodegradable and photo-crosslinkable glycidyl methacrylate chitosan (GMA-chitosan) was developed for providing a multifunctional precursor to efficiently fabricate cationic chitosan-based hydrogels with improved swelling and protein release property. Unsaturated methacrylate groups from glycidyl methacrylate (GMA) were introduced into chitosan as the pendant functional groups, and the level of GMA incorporation was significantly higher than other reported studies. The effects of feed ratio of reactants and reaction time on the incorporation of glycidyl methacrylate onto the chitosan were examined. The chemical structure of the resulting GMA-chitosan was characterized by nuclear magnetic resonance (NMR), Fourier transform infrared spectroscopy (FTIR), and carbon and nitrogen elemental analysis. GMA-chitosan is a new type of cationic polyelectrolyte with zeta potential from +14.15 to +18.04 mV, depending on the degree of GMA substitution. MTT assay shows virtually non-cytotoxicity of GMA-chitosan toward porcine aortic valve smooth muscle cells.

Optical transparent GMA-chitosan hydrogels were synthesized from the GMA-chitosan aqueous precursor using UV-photo-crosslinking. GMA-chitosan hydrogels showed very high swelling ($6,768 \pm 456\%$) in deionized water. The GMA-chitosan hydrogel has an average initial compressive modulus 17.640 ± 0.75 KPa. The morphology of the GMA-chitosan hydrogels was examined by scanning electron microscopy (SEM). The *in vitro* enzymatic biodegradation property of the GMA-chitosan hydrogels was studied. Bovine serum albumin was used as a model protein to examine the release profiles of the protein up to 12 days, and the data show sustained BSA release from GMA-chitosan hydrogels. The cationic character, hydrophilicity, biodegradability, cell biocompatibility, and photo-crosslinkable in an aqueous medium

make this GMA-chitosan a promising biomaterial in drug delivery and tissue engineering applications.

2.2 Introduction

2.2.1 Hydrogel

Hydrogels are networks of synthetic or natural polymer chains that are hydrophilic. Hydrogels can be hydrated in an aqueous environment and retain large amounts of water (generally more than 50% of the total weight) due to the presence of hydrophilic groups or hydrophilic domains in the polymeric network¹. Crosslinks of polymer chains prevent the dissolution of the hydrophilic polymer chains into an aqueous phase. On the macroscopic scale hydrogels are solid: they are in definite shapes without flowability. However, they also behave like solutions on the molecular scale; water soluble molecules can diffuse into hydrogels with a wide range of diffusivity that reflects the diffusant size, shape, and chemical nature². Due to their high water contents as human tissues as well as their 3D porous morphology, hydrogels have been extensively studied as scaffolds in tissue engineering or sustained-release drug delivery systems. For the controlled release of bioactive molecules, in particular pharmaceutical proteins, hydrogels with biodegradability under physiological condition and good biocompatibility are promising drug carriers as biodegradation of hydrogels could permit the complete release of the impregnated proteins. In a hydrogel, crosslinks must be present in order to prevent dissolution of the hydrophilic polymer chains in an aqueous environment. Many different methods were developed to establish crosslinking of hydrogels which could be categorized mainly into physically crosslinking and chemically crosslinking³.

Physically crosslinked hydrogels were prepared by a non-covalent strategy that takes advantage of electrostatic, hydrophobic, and hydrogen bonding forces between polymer chains. Chitosan and poly (ethylenimine) hybrid hydrogel form by physically

blent is one example ⁴. The advantage of physically crosslinked hydrogels is to eliminate the use of chemical crosslinking agents to prepare such hydrogels. Physically crosslinked hydrogels can often be fabricated by simply mixing the components that make up the hydrogels under appropriate conditions. These hydrogels have a short life time in physiological media, ranging from a few days to a month. Therefore, physical gels are good for short-term drug release applications. Whereas physically bonded hydrogels also have their limitations, weak mechanical properties, instability in a changing environment (e.g., pH, electrolytes, temperature), uncontrolled dissolution ^{4,5}. Moreover, it is difficult to precisely control the physical hydrogel pore size, chemical functionalization, and degradation or dissolution, leading to inconsistent performance *in vivo*.

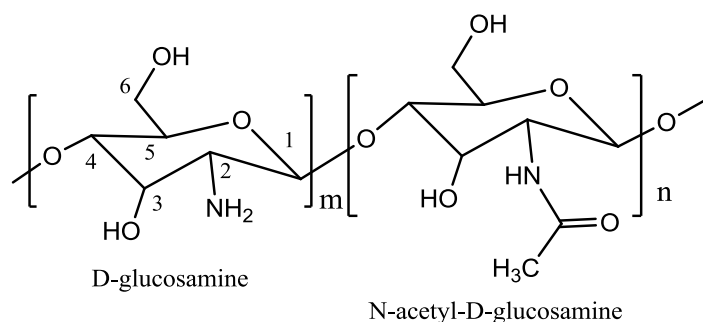
Chemically crosslinking is a better alternative to fabricate irreversible hydrogels. Polymeric chains of hydrogels are covalently bonded together either by using small crosslinker molecules, secondary polymerization, irradiation chemistry, even enzymatic crosslinking ^{6, 7}. Among the chemically crosslinking methods of hydrogel fabrication, photocrosslinking has many advantages: short reaction time at room temperature or physiological temperature, minimal heat production and the possibility to form hydrogels in situ from aqueous precursor. In the photocrosslinking process, visible or UV light in a range of specific wavelength interact with light-sensitive compound called photo-initiators to create free radicals that can initiate chemical reactions to form crosslinked hydrogels. In some biomedical applications, such as tissue engineering, the polymerization of small molecule monomers is not preferable because most photocrosslinkable vinyl-monomers and crosslinking agents are cytotoxic ⁸. Thus, most photocrosslinked hydrogels for biomedical applications are generally been formed from water soluble macromolecular hydrogel precursors which have two or more reactive groups. Moreover, the biodegradability of these

photocrosslinked hydrogels is usually required when they are used as tissue engineering scaffolds or drug carriers.

2.2.2 Chitosan

Chitosan is the partially deacetylated derivative of chitin, which is the second most abundant natural polysaccharides existing in nature⁴. Chitin is a structural biopolymer of most crustaceans and cell walls of fungi, and it has the similar role as that of collagen to higher animals and cellulose to terrestrial plants. The primary unit of chitin is N-acetyl-D-glucosamine while that of chitosan is D-glucosamine linked by β , 1-4 glucosidic linkage⁹. Chitosan is a nonphysiological glycosaminoglycan (GAG) that has antimicrobial properties^{10, 11}, biocompatibility^{12, 13} and accelerates wound healing capability^{14, 15}. Moreover, chitosan and its derivatives are intrinsically enzymatic biodegradable: the hydrolysis of chitosan could be accelerated by enzymes, such as chitosanase and lysozyme¹⁶. Lysozyme is the primary enzyme responsible for *in vivo* degradation of chitosan, which appears to target acetylated residues. The final degradation products of chitosan are biocompatible chitosan oligosaccharides of variable length¹⁷. Therefore, chitosan is an ideal biopolymer with a wide variety of biomedical applications, such as tissue engineering scaffold and drug delivery matrix. Chitosan is insoluble in water, alkali and many organic solvents but is soluble in many dilute aqueous solutions of organic acids, of which the most commonly used are formic and acetic acid. In dilute acids (pH < 6.2), the protonated free amine groups on the D-glucosamine units of chitosan facilitate solubility of the biopolymer¹⁸.

Generally, there are three types of reactive functional groups on chitosan: one amine group on D-glucosamine unit and both primary and secondary hydroxyl groups at C (3) and C (6) positions (shown in Scheme 2.1). These groups allow modification of chitosan for specific applications.



Scheme 2.1 Chemical structure of chitosan

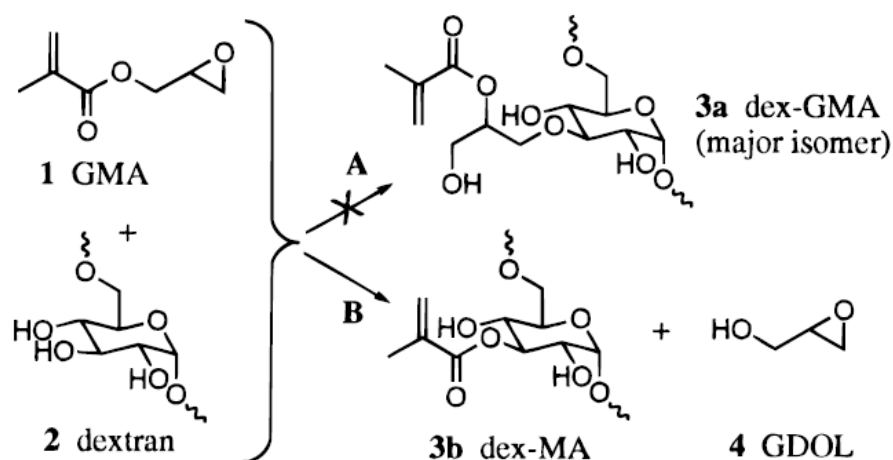
2.2.3 Modification of Polysaccharide by glycidyl methacrylate GMA

Glycidyl methacrylate (GMA) was used to modify many natural polysaccharides, including dextran, galactomannan, cashew gum, hyaluronic acid^{17, 19-22}. The GMA-polysaccharide derivatives were demonstrated to have good biocompatibility, little inflammatory response, similar levels of vascularization at the edge of GMA-polysaccharide derivative hydrogel compared with fibrin positive controls²¹. GMA is a small molecule with one epoxy group at one end and methacrylate group at the other end (Shown in Scheme 2.2). The epoxy group of GMA can react with the hydroxyl groups of polysaccharide in the presence of 4-(*N,N*-dimethylamino) pyridine (DMAP) catalyst^{19, 23, 24}. Prior published studies demonstrated that the methacrylate derivatives of natural polysaccharide: GMA-dextran, GMA-hyaluronic acid are water-soluble and could be radically crosslinked to form hydrogels by using water-soluble initiation systems^{21, 25}.

In the synthesis of GMA-polysaccharide derivatives, choice of a proper solvent in reaction is crucial for controlling the degree of substitution of methacrylate groups. An acidic aqueous reaction condition usually require a longer reaction time²⁶ (~5 days), high feed ratio of glycidyl methacrylate to polysaccharide^{21, 27} (6-fold or 20-fold excess of GMA) and always lead to products of low degree of substitution product (DS, number of methacrylate groups per 100 glucose unit)²⁹. The GMA-

chitosan synthesized in aqueous media usually need other water soluble photocrosslinkable macromolecules, for example, Poly (*N*-isopropylacrylamide) or water soluble polymer (Polyethylene glycol diacrylate), even small molecule crosslinker (*N,N*-methylene bisacrylamide) to form hydrogels to have proper mechanical property and structural integrity^{27,29}. The reason is that the epoxy group of GMA can react with water, yielding glyceryl acrylate which does not react with polysaccharides like dextran further under an alkaline aqueous reaction condition²⁵.

Hennink et al. developed an alternative method of incorporating GMA into polysaccharide by dissolving dextran in a suitable aprotic solvent, dimethyl sulfoxide (DMSO) before reacting with GMA with the presence of basic catalyst including triethylamine, DMAP, pyridine²⁵. The quantitative incorporation of GMA was found and the degree of substitution can be controlled. The reaction of GMA and dextran was a transesterification resulting in a dextran derivative with methacrylate group directly attached to the dextran chain (product 3b in Scheme 2.2)³⁰.



Scheme 2.2 Reaction of dextran with GMA in DMSO³⁰

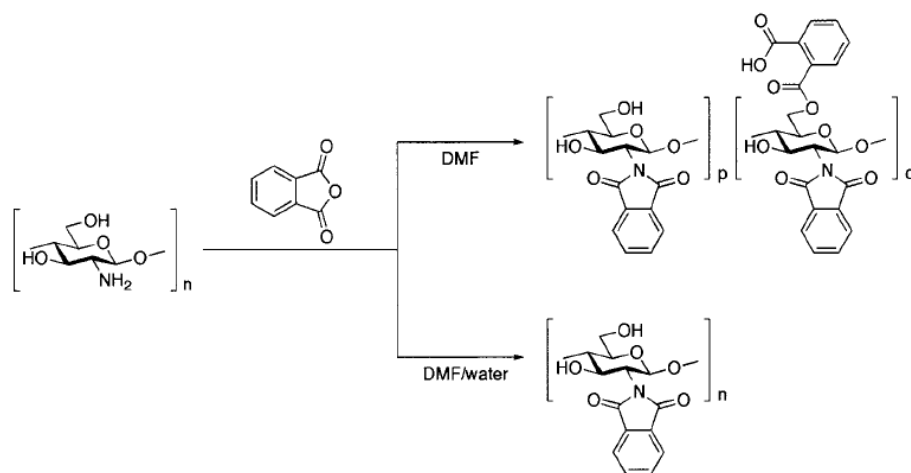
Based on the study of Hennink et al, the absence of a catalyst lead to no incorporation of GMA onto dextran at 50 °C after 70 h reaction²⁵ as the presence of a basic catalyst is necessary to help the reaction of epoxy group of GMA. The possible

mechanism is the hydroxyl groups of dextran could be polarized by the alkaline catalyst which could help the transesterification reaction^{24, 31}. Based on their investigation, the methacrylation of dextran by GMA indeed occurs via a transesterification reaction, yielding dex-MA with the methacryloyl group directly attached to dextran. Triethylamine, pyridine and 4-(*N,N*-dimethylamino) pyridine (DMAP) could be used as effective alkaline catalysts. However, triethylamine and pyridine required a significantly longer reaction time to achieve a substantial degree of substitution compared to DMAP²⁵.

2.2.4 The attempts to synthesize photo crosslinkable chitosan derivatives in organic solvent

Compared with dextran, chitosan has more structure similarity to GAG, cationic property, accelerating wound healing, enzymatic biodegradable by lysozyme which is one enzyme existing in human body. Photocrosslinkable chitosan derivatives based hydrogel for the biomedical applications have attracted significant interests, however, due to the difficulty of chitosan dissolution in organic solvents, the attempts to introduce photocrosslinkable vinyl-groups onto the hydroxyl or amine groups of chitosan have been challenging and less successful³². To design chitosan derivatives which could be dissolved in common organic solvents has been one of the strategies adopted by researchers before their attempt to perform further chemical modification of the hydroxyl groups of chitosan. Harata and Kurita studied synthesized phthaloylated chitosan as an organosoluble precursor^{34, 35} (shown in Scheme 2.3). *N*-phthaloylation reaction was performed between chitosan with phthalic anhydride in *N,N*-dimethylformamide (DMF) at 130 °C. At this reaction condition, the final product usually involves partial *O*-phthaloylation in addition to the expected *N*-phthaloylation. By adding 5% water into the DMF solvent, *O*-phthaloylation was completely suppressed to give regiospecifically substituted 2-*N*-phthaloyl-chitosan³⁴ (shown in

Scheme 2.3) . The resulting phthaloyl-chitosan exhibits much improved solubility in common organic solvents such DMF, N, N-dimethylacetamide, DMSO, and pyridine. With the phthaloylated chitosan, either N, O-phthaloylated or N-phthaloylated chitosan, as a key intermediate, various chemical modification reactions could take place regioselectively in organic solvents ³⁵. The hydroxyl groups of phthaloylated chitosan can be connected with acrylate groups or even another oligosaccharide such as α -Mannoside ³⁵. However, N-phthaloylation reaction consumes large amounts of free amine group of chitosan. Another drawback of these resulting phthaloyl-chitosan derivatives is its insolubility in water. After further modification reaction of phthaloylated chitosan, if the amine group is required to be recovered, hydrazine is the most effective way to deprotect the amine group of chitosan. But hydrazine can also destroy unsaturated vinyl groups or methacrylate groups. Therefore, poor water solubility and the need of using a strong reducing agent in the deprotection of amine groups limit the use of phthaloylated chitosan in the fabrication of chitosan derivative having photo-reactive unsaturated double bonds.



Scheme 2.3 Phthaloylation of chitosan in DMF and DMF/water ³⁴

Prior studies attempted to perform the reaction between chitosan and GMA in an acidic aqueous solution^{29, 36, 37, 38}. Because of the side reaction of GMA with water and the lack of proper basic environment to promote the reaction between the epoxy groups of GMA and hydroxyl groups of chitosan, the degree of substitution of methacrylate group on chitosan derivative is low³⁸ (no higher than 10%). This low degree of GMA substitution in chitosan derivatives synthesized from an aqueous medium may be attributed to the lack of successful fabrication of a pure GMA-chitosan hydrogel, as no such effort has been reported in the literatures. In the published studies, GMA-chitosan synthesized in aqueous solutions is used to fabricate hybrid hydrogels with PMMA or *N*-isopropylacrylamide and even small molecule photocrosslinker^{29, 38} (*N,N*-methylene bisacrylamide). In the several published studies referred GMA-chitosan based hybrid hydrogels, the addition of the second precursor largely limits the application of GMA-chitosan and eliminate the special cell-benign functions of chitosan. For example, in the Elizalde-Pena et al. study²⁹, the final crosslinked product of GMA-chitosan and methyl methacrylate (MMA) is mainly hydrophobic and non-biodegradable. By using the other chemical modification to introduce vinyl groups onto chitosan to fabricate photocrosslinkable chitosan derivatives is much more difficult than the modification method of dextran²⁵ as well due to the acidic aqueous reaction environment required for chitosan solubility. Most photocrosslinked chitosan hydrogel systems usually require the formulation that needs one chitosan derivative precursor and another water soluble non-chitosan-based precursor with a large feed ratio of chitosan derivative precursor to the non-chitosan-based precursor. The non-chitosan-based precursor could be macromolecules which have two or more than two photocrosslinkable groups, such as polyethylene glycol diacrylate (PEGDA) or small molecule photocrosslinker^{37, 38}. The disadvantage of PEGDA-contained hydrogels in the applications of tissue engineering and drug

delivery is their lack of affinity towards proteins and hence cells^{39, 40}. The incorporation of PEGDA does not promote the biocompatibility and cell attachment of chitosan-based hydrogels which are designed to use the cell-benign features of chitosan. Moreover, PEGDA does not contain degradable segments on its polymer backbone. The use of large molecular weight of PEGDA in chitosan based hydrogels may lead to the presence of high molecular weight fragmented products. Hence, two component chitosan-based hydrogels having non-biodegradable precursors is not the optimal system in many specific biomedical applications. Actually, the poor chitosan dissolution in organic solvent problem could be solved into DMSO by adding proper amounts of *p*-toluenesulfonic acid (TsOH) (one solid organic and non-oxidizing acid) to protonate the free amine group of chitosan. Chitosan is able to form a 1.5 wt% homogenous clear solution in DMSO with the presence of 1 wt% *p*-toluenesulfonic in the solution. Then, the addition of DMAP, an alkaline catalyst, could neutralize the acidity of *p*-toluenesulfonic acid and provide a mild basic reaction environment for the reaction between chitosan and GMA. Because DMSO is not ionized as easily as water, chitosan does not precipitate out from DMSO when the pH of the solution is lower than 9. So, this DMSO with *p*-toluenesulfonic acid and excessive DMAP solution system (aprotic solvent, basic pH) appeared suitable for the reaction of GMA and chitosan. The GMA-chitosan synthesized by using the new method could be photocrosslinked without the addition of another non-chitosan-based precursor.

Table 2.1 compared the difference of the synthesis method and property difference of GMA-chitosan with others reported chitosan derivatives having photo-reactive unsaturated double bonds. In this chapter, this novel GMA-chitosan synthesis method will be given; and the effect of reaction time and molar feed ratio of the reactants on the finished products were studied. These newly synthesized GMA-chitosan was characterized by nuclear magnetic resonance (NMR), Fourier transform

infrared spectroscopy (FTIR), carbon and nitrogen elemental analysis. The resulting GMA-chitosan precursor show good water solubility, high degree of GMA substitution, low cytotoxicity to porcine aortic valve smooth muscle cells and the ability to be used as hydrogel precursor to fabricate a pure chitosan-based hydrogels. The transparent GMA-chitosan hydrogel could be fabricated in an aqueous medium by using a simple photocrosslinking technique. The interior morphology of GMA-chitosan hydrogels was examined by using scanning electron microscopy (SEM). The enzymatic degradation of GMA-chitosan hydrogel by lysozyme *in vitro* was studied.

Table 2.1 Comparison of GMA-chitosan to other reported chitosan derivatives with unsaturated groups

Author	Published year	Final product	Reaction media	Catalyst, temperature, time	Water solubility of chitosan derivatives	Degree of substitution
E.A. Elizalde-Pena	2007	GMA-chitosan and MMA copolymer (no hydrogel)	Acetic acid aqueous solution	No catalyst, 70 °C, 3h	No	N/A
Nelly Flores-Ramirzes	2005	GMA-chitosan (no hydrogel)	Acetic acid aqueous solution	No catalyst, 60 °C, >2h	Yes	N/A
Jing Han	2009	Methacrylated chitosan / PNIPAAm hybrid hydrogel	Acetic acid aqueous solution	No catalyst, 60 °C, 6h	Yes	10.4
M. Chellapandian	1998	Chitosan-poly (glycidyl methacrylate) Copolymer (no hydrogel)	Acetic acid aqueous solution	No catalyst, 60 °C, 2h	No	N/A
Chao Zhong	2010	Maleic chitosan (Maleic chitosan/PEGDA hybrid hydrogel)	Formamide	No catalyst 50 °C, 48h	Yes	33
Our approach	2009	GMA-chitosan hydrogel	DMSO/Toluene sulfonic acid	DMAP, 35 °C, 48h	Yes	10~37

2.3. Experimental

2.3.1 Materials

Chitosan (75- 85% deacetylated) of molecular weight (MW) 50,000 -190,000 and Bovine serum albumin (BSA) of molecular weight ~66,000 Da were purchased from Sigma Chemical Co., USA. Glycidyl methacrylate (GMA, 97%), 4-(*N*, *N*-dimethylamino) pyridine (DMAP, 99%), *p*-toluene sulfonic acid monohydrate (TsOH H₂O), dimethyl sulfoxide (DMSO), Triton-X 100, hydrochloric acid (HCl, 33 wt %), lysozyme (from Chicken egg), Thiazolyl blue tetrazolium bromide (MTT reagent), minimal essential medium (MEM) were purchased from VWR Scientific (West Chester, PA). FBS was purchased from Gemini (Woodland, CA). Ethyl acetate, acetone, isopropyl alcohol were purchased from Mallinckrodt incorporation (St.Louis, MO) and used without further purification. Micro BCA protein assay kit was purchased from Thermo Scientific Co., USA. Irgacure 2959 was donated by Ciba Specialty Chemicals Corp. Porcine aortic valve smooth muscle cells (PAVSMC) that used for cytotoxicity study were from Dr. Butcher's lab at Cornell University.

2.3.2 Synthesis of glycidyl methacrylate chitosan (GMA-chitosan)

The reaction scheme of synthesizing GMA-chitosan is depicted in Figure 2.1. Chitosan (3.0 g, about 0.0126 mol -NH₂) was dissolved in 200 mL DMSO with TsOH (2.4 g, 0.0126 mol) at 50 °C for 3 h under dry nitrogen with magnetic stirring to form a viscous clear solution. Then, 1 g DMAP was dissolved in 10 mL DMSO and then added dropwise into the chitosan solution. The addition of DMAP significantly increased the viscosity of the chitosan/DMSO solution. After the total solution was cooled down to room temperature in about 1 h, GMA (2.4 g, 4.8 g or 7.2 g) was added to chitosan at different molar feed ratios of GMA to the repeat units of chitosan ranging from 1/1, 2/1, to 3/1. The reaction was continued at 35 °C for 48 h under stirring. GMA-chitosan samples (20 mL) were taken periodically from the reaction mixture to test the GMA degree of substitution, and the reaction was stopped by adding 0.5 g TsOH to neutralize

the DMAP and to reduce the viscosity of the reaction solution for an easier extraction of the GMA-chitosan product. Then, the sample solution was precipitated out from the solution by adding 200 mL ethyl acetate and dried in vacuum oven at room temperature for 2 h. The resulting crude gel-like GMA- chitosan was cut into 1.5~2 mm cubic pieces

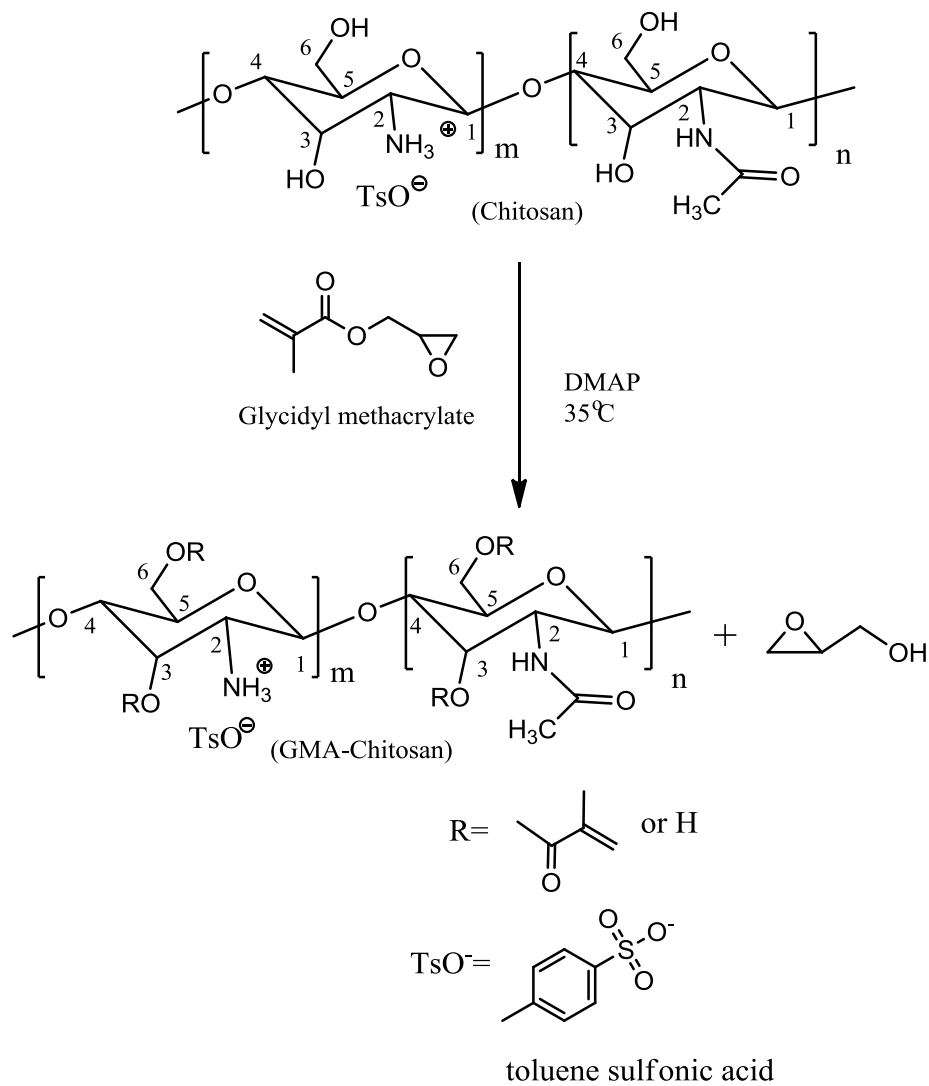


Figure 2.1 Schematic description of functionalization of chitosan by glycidyl methacrylate in DMSO solution with DMAP as catalyst

and were completely washed by Soxhlet's extraction with acetone for 8 h to remove TsOH, DMAP and unreacted GMA and then drying under vacuum. The degree of substitution (DS; the amounts of methacrylate groups per 100 chitosan repeat unit) of GMA-chitosan was determined by ^1H NMR spectroscopy.

2.3.3 Characterization of GMA-chitosan

^1H NMR spectra of GMA-chitosan were recorded on a Varian Unity spectrometer operating at 400 MHz. Samples of GMA-chitosan (15 mg) were dissolved in 800 μL of DMSO-*d*₆ (Cambridge Isotope laboratories, USA). Chemical shifts were reported in parts per million (ppm). For FTIR spectroscopic characterization, dried GMA-chitosan was grinded to powders. FTIR spectra were then obtained with a Perkin-Elmer Nicolet Magna 560 FTIR spectrometer with Omnic software for data acquisition and analysis. The spectra of both raw chitosan and GMA were recorded as the controls. Carbon and nitrogen contents of GMA-chitosan and raw chitosan (as control) were performed on a Thermo Scientific ConFlo III elemental analyzer by stable isotope laboratory of Cornell University. Zeta potentials of GMA-chitosan were tested by using Zetasizer Nano-ZS (Malvern, USA).

2.3.4 Cytotoxicity of GMA-Chitosan

2.3.4.1 Cell culture

Porcine aortic valve smooth muscle cells (PAVSMC) were maintained in minimum essential medium (MEM) supplemented with 10% fetal bovine serum (FBS) and 1% each of penicillin-streptomycin. The cells were incubated in CO₂ incubator at 37 $^{\circ}\text{C}$ with 5% CO₂. After reaching confluence, the cells were detached from the flask with Trypsin-EDTA (Invitrogen, Carlsbad, CA). The cell suspension was centrifuged at 3,000 rpm for 3 min and then re-suspended in the growth medium for a further study. PAVSMCs were used between passages 4 and 7.

2.3.4.2 Cytotoxicity of GMA-chitosan

Evaluation of the cytotoxicity of GMA-chitosan (DS 37) was performed using the MTT assay. GMA-chitosan (DS 37) sample solution (6 wt %) was obtained by dissolving GMA-chitosan in PBS (0.05M, pH 7.4). 6 different concentrations of GMA-chitosan (0.1, 0.3, 0.6, 1, 2 and 4 mg/mL) were prepared by diluting 6 wt % GMA-chitosan solution with MEM media. PAVSMCs at cell density 2,000 cells well⁻¹ were seeded onto 96-well plates and incubated overnight. After 24 h, the cells were treated with 100 µL freshly prepared GMA-chitosan / MEM media at 6 different GMA-chitosan concentrations. The cells treated only with normal cell culture media were used as the control. After 24 h treatment, 10 µL of MTT solution (5 mg/mL thiazolyl blue tetrazolium bromide in deionized water after filtration by 0.22 µm filter) was added into each wells and incubated for another 4 h at 37 °C under a 5 % CO₂ atmosphere to allow the formation of formazan crystals by mitochondrial dehydrogenases. After that, the cell culture medium including GMA-chitosan solution was then carefully removed and 100 µL of acidic isopropyl alcohol (contains 10% Triton-X 100 with 0.1M HCl) was added into each well and gently shaken at room temperature for 1 h to ensure that the purple crystals were completely dissolved. The optical density of the solution was measured at a wavelength of 570 nm and 690 nm (Spectramax plus 384, Molecular Devices, USA). The cell viability (%) was calculated according to the following equation:

$$\text{Viability (\%)} = \frac{[\text{OD}_{570} (\text{sample}) - \text{OD}_{690} (\text{sample})]}{[\text{OD}_{570} (\text{control}) - \text{OD}_{690} (\text{control})]} \times 100\%$$

where the OD₅₇₀ (control) represents the measurement from the wells treated with medium only, and the OD₅₇₀ (sample) from the wells treated with various polymers. 8 samples were analyzed for each experiment.

2.3.4.3 Statistical analysis

Differences between group means were assessed using one-way ANOVA followed by parametric multiple comparison tests. A value of $p < 0.05$ was considered statistically significant.

2.3.5 Fabrication of photo-crosslinked GMA-chitosan hydrogel

GMA-chitosan hydrogel can be obtained by using GMA-chitosan (DS 37) as precursor in an aqueous medium under UV radiation. 300 mg GMA-chitosan (DS 37) was dissolved in 4 mL deionized water with magnetic stirring for at least 3 h to reach a clear viscous solution. 10 mg Irgacure 2959 photo-initiator was dissolved in 100 μ L deionized water and then added to the GMA-chitosan aqueous solution prepared. Every 400 μ L of the mixed GMA-chitosan aqueous solution with Irgacure 2959 was then transferred onto a custom-made 20 well Teflon[®] mold (11 mm diameter, 6 mm depth) and then irradiated by a long wavelength UV light (100 watts, 365nm, Blak-ray[®] lamp) at room temperature for about 30 min until disk-shaped hydrogel was obtained. The resultant hydrogels were immersed into deionized water for 16 h at room temperature to leach residues and reach the swelling equilibrium. The GMA-chitosan hydrogels were then dehydrated in the ambient air at room temperature until the dry weight was constant for further swelling study. The weights of the initial dry hydrogel samples were measured and used for determining equilibrium swelling later. A representative hydrogel network structure is shown in Figure 2.2

2.3.6 Equilibrated swelling ratio (Q_{eq}) of GMA-chitosan hydrogel

The equilibrium swelling of GMA-chitosan hydrogel was performed at room temperature (25 °C) by immersing the purified dehydrated GMA-chitosan hydrogels individually in glass vials containing 15 mL deionized water. After 16 h, the GMA-chitosan hydrogels reached their swelling equilibrium. The swollen hydrogels in the deionized water were then removed, the excess surface water was wiped and the hydrogels were weighed until a constant weight was obtained. The swelling ratios of the hydrogels were calculated from the swollen and dry weights of the hydrogels according to the following equation.

$$\text{Swelling ratio } (Q_{eq}, \%) = (W_i - W_0) / W_0 \times 100$$

W_i is the weight of the hydrogel at swelling equilibrium

W_0 is the initial dry weight of the hydrogel before immersion.

The reproducibility of the swelling profiles of a hydrogel was determined in triplicate.

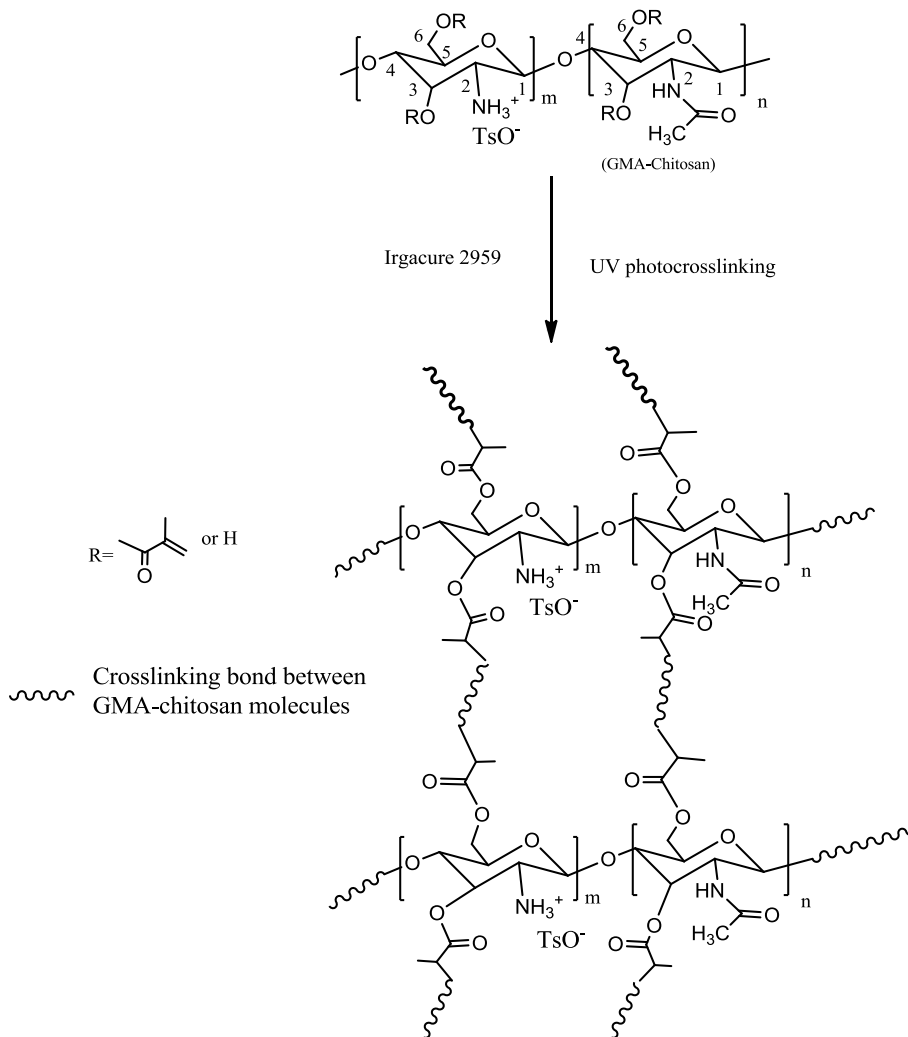


Figure 2.2 A representative possible photo-crosslinked network structures of GMA-chitosan hydrogel

2.3.7 Compressive modulus test of GMA-chitosan hydrogel

The compressive modulus testing of the GMA-chitosan hydrogel was performed on a DMA Q800 Dynamic Mechanical Analyzer (TA Instrument Inc., New Castle, DE) in a “controlled force” compression mode. The compressive modulus of dehydrated

GMA-chitosan hydrogels in circular disc shape after reaching their equilibrium swelling in deionized water were measured at room temperature (25 °C). The swollen hydrogels were mounted between the movable compression probe (diameter 15 mm) and the fluid cup without any liquid media. A compression force from 0.01 to 4 N at a rate of 0.5 N/min was applied on the hydrogel samples at room temperature until fragment of the hydrogel was produced. The initial compressive modulus was calculated from the slope of the initial linear portion of the curve. For each type of hydrogel, five samples were used for the compression test, and their mean value was calculated with a standard deviation.

2.3.8 Morphology of GMA-chitosan hydrogel

The interior morphology of GMA-chitosan (DS 37) hydrogel was probed by scanning electron microscopy (SEM). The equilibrium swollen hydrogel samples were quickly frozen in liquid nitrogen and then freeze dried in a Freezone 2.5 Freeze-drying system (Labconco, USA) under vacuum at -50 °C for 3 days until all water was sublimed. The freeze-dried hydrogel specimens were cut and fixed on aluminum stubs and then coated with gold for 30 s for SEM observation by Leica Microsystems GmbH (Wetzlar, Germany) 440.

2.3.9 Enzymatic biodegradation of GMA-chitosan hydrogels in vitro

The enzymatic biodegradation of the disk shaped GMA-chitosan hydrogels (11 mm diameter, 5 mm thickness) was evaluated by its weight loss at 37 °C in 20 volume glass vials with a constant reciprocal shaking (100 rpm). In the enzymatic biodegradation group, 15mL 0.05M pH 7.4 PBS with 1mg/mL lysozyme was added into the vials which contain GMA-chitosan hydrogels. The incubation media were refreshed daily in order to maintain enzymatic activity. In the control group, the same GMA-chitosan hydrogel samples were incubated in 15 mL PBS (pH 7.4, 0.05M) at 37 °C without any enzyme. The course of enzymatic biodegradation of GMA-chitosan hydrogels was followed gravimetrically until the loss of structural integrity of the hydrogels.

Weight change of the hydrogels was measured at predetermined intervals. For each measurement, three replicated samples were used. Weight loss measurement: The weight of each dry GMA-chitosan hydrogels was measured before immersion. At various immersion intervals, GMA-chitosan hydrogel samples were removed from the immersion medium, washed gently with deionized water and dried under vacuum at room temperature for about 12 h till the weight reached constant. The weight loss was calculated according to the following equation

$$\% \text{ Weight loss} = (W_o - W_t) / W_o \times 100,$$

where W_o was the initial ($t=0$) dry hydrogel weight, and W_t was the dry weight of the hydrogel after t incubation time. Mean value of experimental data was calculated at time t with a standard deviation.

2.3.10 In vitro release of bovine serum albumin (BSA) from GMA-chitosan hydrogel

75 mg BSA was dissolved in 5 mL deionized water to obtain BSA stock solution of 15 mg/mL concentration. GMA-chitosan precursor solution was prepared by dissolving 300 mg of GMA-chitosan dissolved in 4.8 mL deionized water in a 20 mL volume glass vial. A 200 μ L BSA stock solution and 2 mg Irgacure 2959 were then added into the GMA-chitosan precursor aqueous solution and mixed well with GMA-chitosan precursor after 10 min stirring. The 400 μ L BSA-preloaded GMA-chitosan aqueous solution was transferred to a 20-well Teflon[®] mold and photo-crosslinked by using a long wavelength UV light (100 watts, 365nm) for about 30 min. After gelation, each BSA-preloaded GMA-chitosan hydrogel sample (11 mm diameter, 4~5 mm thickness disk-like hydrogel with 240 μ g BSA loaded) was removed from Teflon[®] mold carefully and placed in glass vials individually filled with 5 mL 0.05 M PBS of pH 7.4. At each predetermined time, 100 μ L PBS solution was removed from the vial and diluted to 1mL by deionized water. 100 μ L fresh PBS was added back into the glass vial to keep the PBS medium constant during the immersion.

MicroBCA kit (Thermo Scientific, USA) was used to determine the BSA

concentration. The protocol in the MicroBCA kit was followed. PerkinElmer Lambda 35 UV-Vis spectrophotometer was used to determine the absorbance of the samples at 562 nm wavelength. The standard BSA calibration curve was prepared by plotting the average Blank-corrected 562nm reading for each BSA standard vs. its concentration in $\mu\text{g/mL}$. This BSA standard calibration curve was used to determine the BSA concentration released from the GMA-chitosan hydrogel at a particular time. The amounts of BSA released from GMA-chitosan hydrogel was then calculated from the calibration curve. Samples in triplicate were averaged for each experiment.

2.4. Results and discussion

2.4.1. Synthesis of GMA-chitosan in DMSO

In our proposed new synthesis scheme for GMA-chitosan, chitosan is first dissolved in DMSO as a polar aprotic solvent by adding proper amounts of TsOH to protonize the amine groups of chitosan which is crucial to improve the solubility of chitosan in DMSO. In Dijk-Wolthuis et al. study²⁵ about GMA-dextran, they found a basic catalyst like triethylamine, pyridine or DMAP is necessary to improve the incorporation of GMA. DMAP was used as the catalyst in our new synthesis method. This catalyst could lead to the shortest reaction time in order to obtain a substantial degree of substitution. The pH of the reaction system was tuned to a mild basic environment (pH 8.5-9) by adding DMAP that didn't make chitosan precipitate out from the DMSO solution, and also accelerated the reaction between GMA and chitosan. The role of DMAP is either to work as a Bronsted base to polarize the hydroxyl groups of chitosan that makes hydroxyl groups react with less hindered methylene carbon of the epoxy group of GMA or as a nucleophilic agent promoting the formation of the metacryloyl pyridinium salt^{20,25,30}.

Flores et al.³⁶ reported the use of 0.4 M acetic acid solution for the synthesis of GMA-chitosan. The disadvantage of this method is the reaction between GMA and water leads to a low reaction efficiency and lower incorporation of acrylate groups onto the

GMA-chitosan product when compared with our proposed new method. The Flores et al.³⁶ GMA-chitosan synthesis method was subsequently used by Elizalde-Pena et al.²⁹ and Han et al.³⁸. In those studies, the aqueous medium used led to GMA-chitosan having significantly lower levels of incorporating methacrylate groups, i.e. 10.4%³⁸ than our new synthesis method reported here.

There are two different pathways that could be considered for the chemicals modifications involving polysaccharides when GMA is used as the modifier^{20,24,25,30}. Using an aqueous environment, the dextran could react with GMA by opening the epoxy ring of GMA. In DMSO, the GMA was introduced into the dextran through transesterification reaction yielding glycidol as a by-product³⁰. In our new approach as shown in Figure 2.1, the reaction between chitosan and GMA in DMSO resulted in a direct attachment of methacrylate esters to chitosan and the glycidol byproduct was removed in the purification process.

The major benefit of having higher DS of GMA in GMA-chitosan is that the new GMA-chitosan can be used as a water soluble hydrogel precursor for fabricating single component pure chitosan hydrogel without the need of another polymer precursor and crosslinkers for biomedical applications, such as drug control delivery or tissue engineering scaffolds. Low DS GMA-chitosan synthesized in water media by Han et al,³⁸ required the help of another synthetic polymer [poly(*N*-isopropylacrylamide)] as a co-precursor at a substantial feed ratio to chitosan component (i.e., very low chitosan component in the resulting hybrid hydrogels, 6-30%) as well as the need of low molecular weight crosslinker (*N,N*-methylene bisacrylamide). The pure GMA-chitosan hydrogel obtained in our current approach can retain the biological advantages of chitosan, such as good biocompatibility and biodegradability far better than those reported hybrid hydrogels because of the pure chitosan.

2.4.2 Characterization of GMA-chitosan

The ¹H-NMR spectrum of GMA-chitosan (DS 13) is displayed in Figure 2.3. The

incorporation of double bonds into the chitosan backbone was confirmed by $^1\text{H-NMR}$, as indicated by the appearance of proton signals from the double bond of methacrylate group at δ 5.74 and δ 6.2 ppm²⁵. The methyl groups from GMA and from undeacetylated chitosan unit were observed at δ 1.95 ppm. The signal of the anomeric proton (position 1 in Figure 2.1) shows a shoulder at δ 5.05 ppm. The 6 protons at position 2~6 merge into a peak which is observed at δ 3.1-3.5 ppm. Based on the assignment of the $^1\text{H-NMR}$ spectrum, the degree of substitution of the GMA-chitosan is calculated as $(600x)/y$, in which x is the average integral of the protons at the double bond at δ 5.74 and δ 6.2 ppm and y is the integral of the 6 protons of chitosan repeat unit at δ 3.1-3.5 ppm except the proton at position 1. The calculated DS of methacrylate groups on GMA-chitosan ranged from 13 to 37. Han et al.³⁸ reported the DS of GMA-chitosan synthesized in acidic aqueous environment is about 10.4%, which is lower than the GMA-chitosan synthesized by using the new developed method. As we predicted, the new GMA-chitosan synthesis route significantly improved the GMA DS on chitosan.

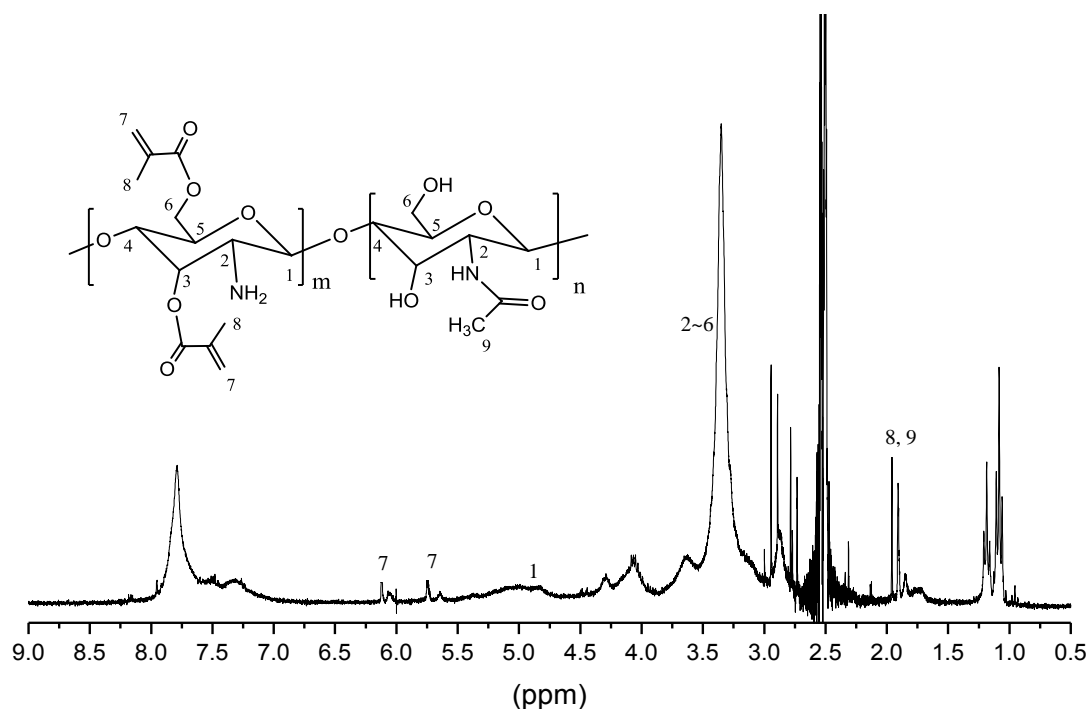


Figure 2.3 ¹H-NMR spectrum of GMA-chitosan (DS 13) dissolved in DMSO-*d*₆

Figure 2.4 shows the FT-IR spectra of chitosan (A) and GMA-chitosan of two different DS (Fig.4 B for DS 37, and Fig.4 C for DS 13) and GMA (D). Both a broad band around 3430 cm⁻¹ (attributed to -NH and -OH stretching vibration) and a weak band at 2930 cm⁻¹ (from -CH stretching) were shown on both chitosan and GMA-chitosan FT-IR spectra (Figure 2.4 B, C). The characteristic peaks at 1650, 1590 cm⁻¹ were assigned to the amide I, amide II absorption bands of chitosan. The absorption band at 1150 cm⁻¹ was assigned to the asymmetric stretching of the C-O-C of chitosan (Figure 2.4 A, B, C). In the spectra of GMA and GMA-chitosan, the absorptions at 1720 cm⁻¹ and at 815 cm⁻¹ are indicative of the carbonyl group and the double bond of methacrylate group²⁵, respectively, which were not presented on the spectra of chitosan (Figure 2.4 A).

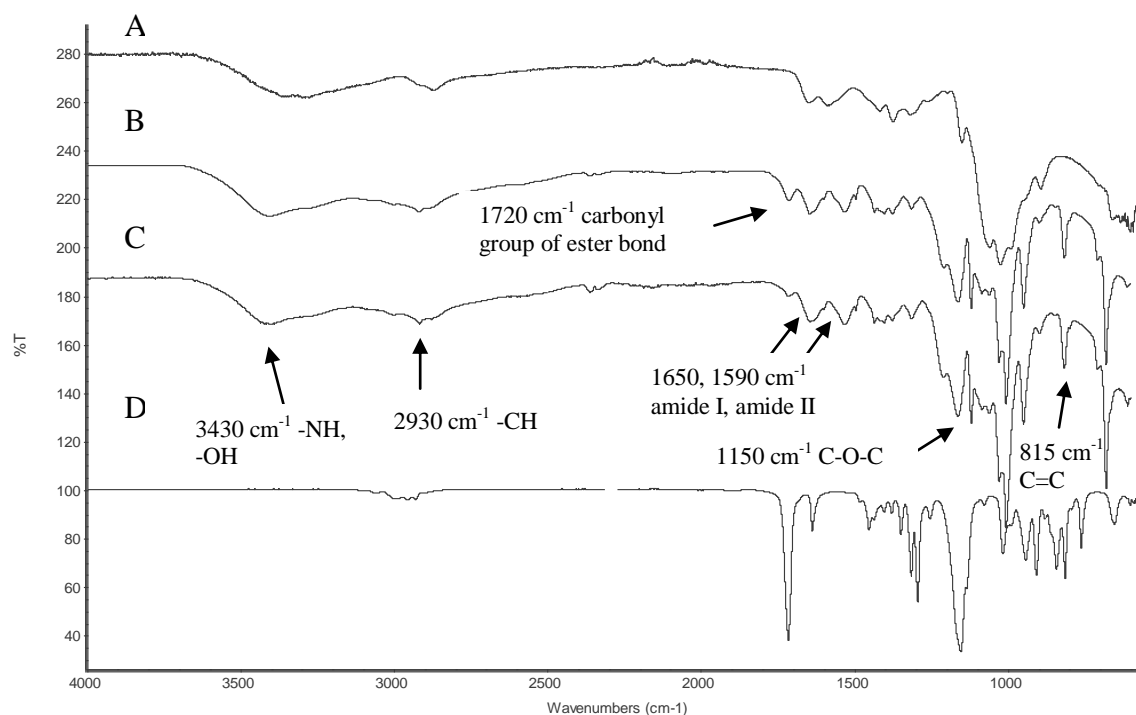


Figure 2.4 FT-IR of GMA-chitosan which is synthesized from different GMA to Chitosan repeat unit molar feed ratio and two raw materials: Chitosan and GMA. (A) Chitosan; (B) GMA-chitosan (DS 37); (C) GMA-chitosan (DS 13); (D) GMA

The elemental analysis data (Table 2.2) shows the relative nitrogen contents decreased when DS of GMA-chitosan increased which means more methacrylate (MA) groups have been grafted onto chitosan. While the carbon contents of the sample increased as the DS of GMA group increased. This is because the GMA group doesn't contain nitrogen element, the relative nitrogen contents of GMA-chitosan would obviously be decreased from chitosan after the substitution reaction. Due to the difference of the relative carbon contents of GMA and chitosan, the carbon content of GMA-chitosan slightly increased, while the relative nitrogen content slightly decreased when DS of GMA to chitosan increased (Table 2.2). The data from elemental analysis was consistent with the composition calculated.

Table 2.2 Relative carbon and nitrogen contents of raw chitosan and GMA-chitosan of different GMA degree of substitutions (DS)

Sample	Carbon content (%)	Nitrogen content (%)	Calculated carbon content (%)	Calculated nitrogen content (%)
Chitosan	40.3	7.5	40.9	7.5
GMA-chitosan (DS 13)	42.1	6.8	42.6	7.05
GMA-chitosan (DS 28)	43.6	6.4	44.3	6.6
GMA-chitosan (DS 37)	44.4	6.1	45.3	6.4

GMA-chitosan was only soluble in water or DMSO at room temperature (Table 2.3). Due to the protonation of amine groups of chitosan in water, GMA-chitosan solutions (0.5 mg/mL) of different DS showed positive zeta potentials ranging from +14.15 to +18.04 mV, depending on DS (Table 2.4) in deionized water. The zeta potential of GMA-chitosan slightly decreased with an increasing degree of GMA substitution. This might be attributed to the partial shielding effect of the incorporated neutral methacrylate group on the positive charge of amine groups on the chitosan backbone.

Table 2.3 Solubility of GMA-chitosan in several common solvents at room temperature

	H ₂ O	DMF	DMSO	DMAc	THF	Ethanol	Chloroform	Benzene
Chitosan	-	-	-	-	-	-	-	-
GMA-chitosan (DS 37)	+	-	+	-	-	-	-	-

+, soluble (solubility \geq 5mg/mL); -, insoluble

Before chitosan react with GMA, TsOH was used to help chitosan dissolve in DMSO. The amine groups of chitosan and TsOH would form the salt that caused the difficulty of the reaction between the amine groups of chitosan and epoxy groups of GMA, i.e., directing the GMA to the -OH sites of chitosan. After the reaction with GMA-

chitosan, a substantial amount of primary amine groups was in TsOH salt form that attributes the GMA-chitosan water solubility and its cationic property in aqueous media.

Table 2.4 Zeta potential[@] of GMA-chitosan of different glycidyl methacrylate (GMA) degree of substitution (DS).

Sample	GMA-chitosan (DS 13)	GMA-chitosan (DS 28)	GMA-chitosan (DS 37)
Zeta potential (mV)	+18.04 ±0.35	+15.86 ±0.63	+ 14.15 ±0.64

@ GMA at 0.5 mg/mL concentration in deionized water at room temperature

2.4.3 Effect of reaction time and molar feed ratio of GMA to chitosan on the DS of GMA-chitosan

Figure 2.5 shows the relationship between the DS of methacrylate group on GMA-chitosan (as determined by ¹H-NMR data) and reaction conditions (i.e., the molar feed ratio of GMA to chitosan glucosamine unit, and reaction time). Increasing the reaction time and feed ratio of GMA to chitosan can effectively improve the DS of GMA-chitosan. For example, the DS of GMA-chitosan synthesized after 16 h at the GMA to chitosan repeat unit 3/1 molar feed ratio is about 28, while the same reaction continued to 48 h could improve DS to 37. At the same reaction time (16 h), the DS of GMA-chitosan synthesized with GMA to chitosan 1/1 molar feed ratio is only about 13.3. The DS of GMA-chitosan up to 37 can be achieved and DS can also be controlled by tuning the reaction time and feed ratio. Although DS greater than 37 was reachable by increasing the reaction time and feed ratio, the resulting GMA-chitosan solubility in both water and DMSO is unsuitable for many applications, such as hydrogel fabrication in an aqueous medium. Due to the hydrophobic nature of GMA group, a higher DS of GMA would make GMA-chitosan difficult to dissolve in water and as we preferred to use an aqueous medium for fabricating hydrogels to minimize adverse

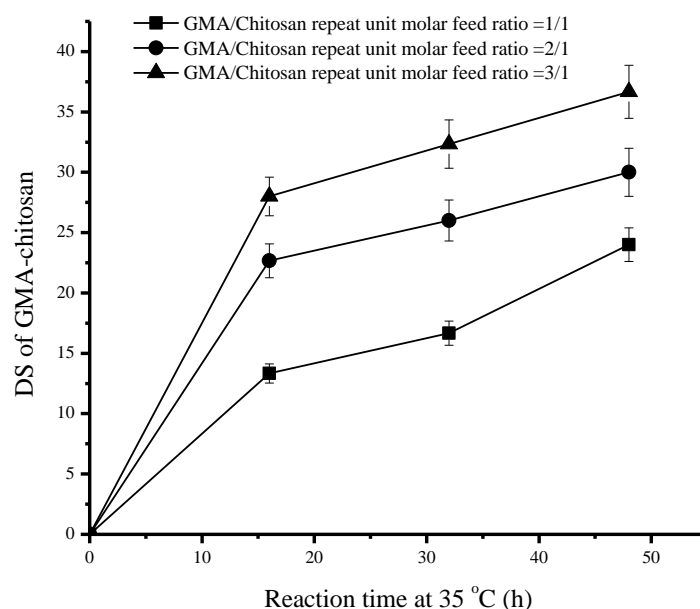


Figure 2.5 Effects of molar feed ratio of GMA to chitosan glucosamine unit and reaction time on the GMA degree of substitution (DS) on GMA-chitosan reacted at 35 °C with DMAP as the catalyst (DS; the amount of methacrylate groups per 100 chitosan repeat unit)

organic solvent effect in biomedical applications. The decreasing solubility in deionized water with the increasing GMA DS was also reported in other study of GMA-galactomannan ²⁰. Moreover, the ¹H-NMR data are hard to obtain from GMA-chitosan with DS higher than 37 due to the poor solubility in DMSO-*d*₆. GMA-chitosan having DS lower than 37 is also not suitable because the hydrogel fabricated from GMA-chitosan precursor with DS lower than 37 usually had low mechanical strength, premature loss of structural integrity, and inconsistent performance which is not proper for further degradation and protein release studies as well as impractical for eventual biomedical uses. Therefore, GMA-chitosan (DS 37) precursor was chosen to fabricate hydrogel samples for all subsequent studies, and this optimized fabrication conditions were: a reaction time of 48 h, and GMA/chitosan repeat unit feed ratio of 3/1 (weight feed ratio of GMA/ chitosan is about 2.4 /1).

2.4.4 Cytotoxicity of GMA-chitosan in aqueous media

MTT assay was done for the six different concentrations of GMA-chitosan: 0.1, 0.3, 0.6, 1, 2 and 4 mg/mL (Figure 2.6). The data in Figure 2.6 indicates no significant difference in cytotoxicity toward porcine aortic valve smooth muscle cells (PAVSMC) in all of the concentration of GMA-chitosan aqueous solution after 24 hr incubation when compared with a blank control. These results indicated that the prepared GMA-chitosan solutions up to 4 mg/mL have virtually no cytotoxicity to

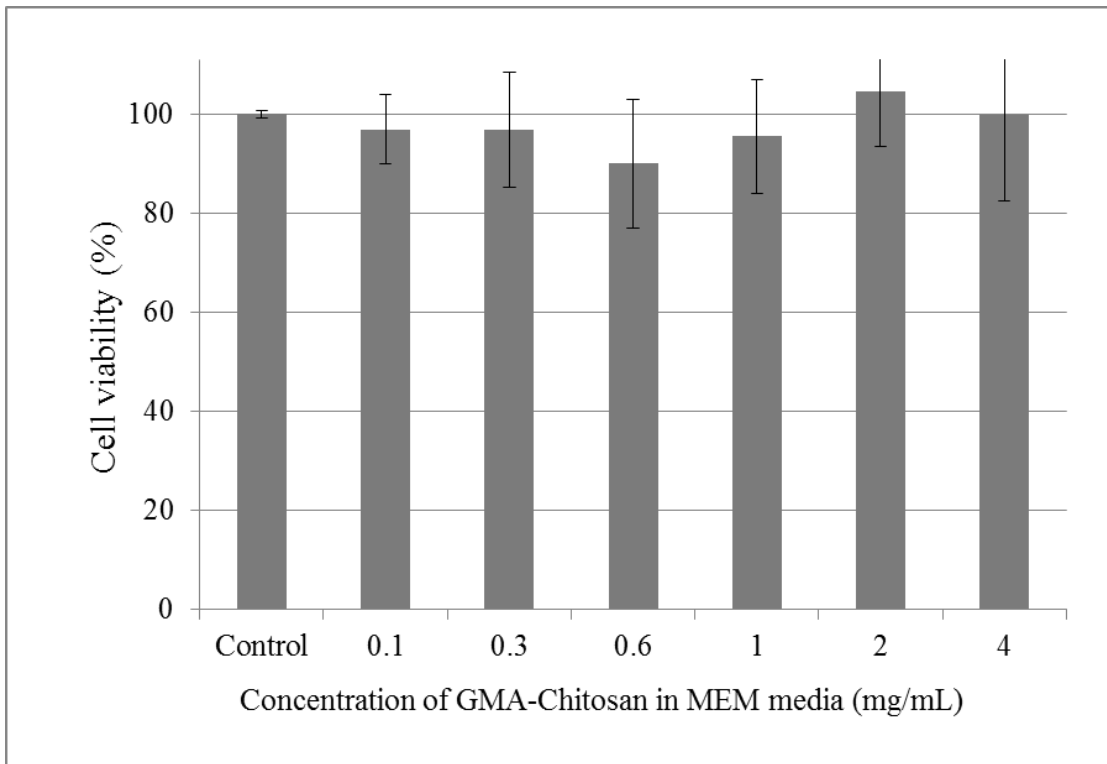


Figure 2.6 MTT assay (porcine aortic valve smooth muscle cell) of GMA-chitosan 0.05M PBS solution at 0.1 mg/mL, 0.3 mg/mL, 0.6 mg/mL, 1 mg/mL, 2 mg/mL, 4 mg/mL concentration (after cultured for 24 h, tissue culture plate as control) PAVSMC cells.

Although there is no GMA-chitosan cell culture study had been reported before, Zhong et al. ³⁶ reported the cytotoxicity study of an anionic chitosan derivative (i.e., maleic chitosan) which can also be used to fabricate photo-crosslinked hybrid hydrogel,

and maleic chitosan aqueous solutions showed little cytotoxicity to bovine aortic endothelial cells (BAEC). More than 80% of cells treated with 3mg maleic chitosan /well for 4 h were viable; however, the viability of BAEC reduced to about 65% after 48 h incubation. Groot et al. ⁴¹ and Moller et al ¹⁹ reported the biocompatibility of methacrylated dextran (GMA-dextran) and methacrylated hyaluronan (MA-HA)/methacrylated aminoethyl carbamidomethyl dextran (MA-ACMD) hybrid hydrogel. The cell proliferation inhibition index (CPII) of human fibroblast cultured with 100 mg/mL GMA-dextran (DS 5, DS 30) showed a relative inhibition of $41 \pm 13\%$ and $35 \pm 8\%$ after 72 h and no statistically significant difference from the CPII of dextran control which can be considered as low cytotoxicity ⁴¹. In summary, the synthesized GMA-polysacchride derivative like GMA-chitosan, GMA-dextran does not change the cell benign characteristics of polysaccharides.

2.4.5 Photo-crosslinked GMA-chitosan hydrogel Q_{eq} and hydrogel compressive modulus

A representative crosslinked chemical structure of GMA-chitosan (DS 37) hydrogel is shown in Figure 2.2. After swelling in deionized water, GMA-chitosan hydrogel is elastic and transparent. The freshly made disc-shaped GMA-chitosan hydrogels were dehydrated at room temperature in air for 2 days, their size was reduced to about 5 mm diameter and 1.5~2 mm thickness (Figure 2.7A).

The equilibrium swelling ratio of GMA-chitosan hydrogel could reach as high as $6,768 \pm 456\%$ after immersed in deionized water for about 16 h. (Figure 2.7B). GMA-chitosan hydrogel could absorb more than 60 folds of its own weight of water which is probably due to the loosely crosslinked polymer network and good hydrophilicity of GMA-chitosan. This very high level of equilibrium swelling of GMA-chitosan is far greater than all reported GMA-polysaccharide-based hydrogels. For example, Chen et al. ²³ reported that GMA derivatized dextran hydrogels had an equilibrium water content

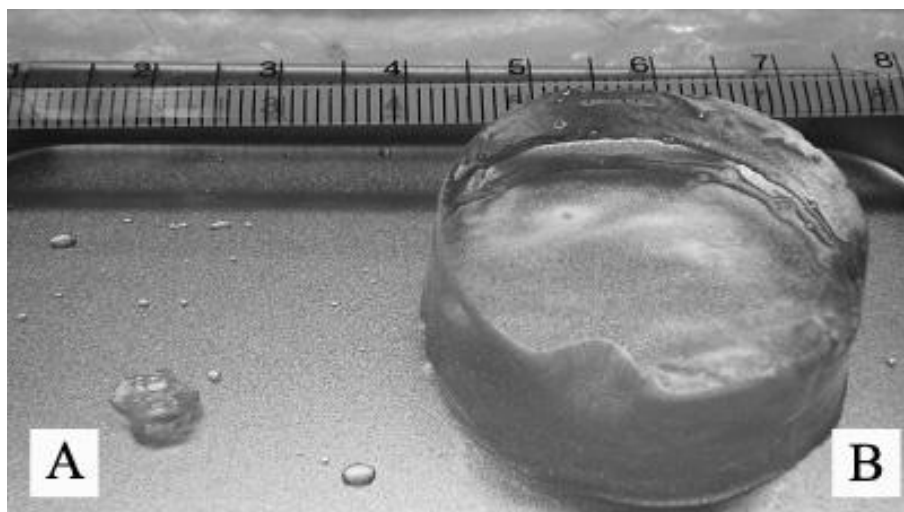


Figure 2.7 Image of photo-crosslinked GMA-chitosan (DS 37) hydrogel. (Gel sample A: dehydrated at room temperature in the air for 2 days on left; gel sample B: swollen GMA-chitosan hydrogel in deionized water after 16 h swelling on right). The swell ratio of GMA-chitosan hydrogel in deionized water is about $6,768 \pm 456\%$. The compressive modulus of swollen GMA-chitosan hydrogel in deionized water was 17.640 ± 0.75 KPa.

about 42.6% that is much lower than the current GMA-chitosan. The possible reason is the difference of hydrophilicity between chitosan and dextran. GMA-chitosan polymer chain is more hydrophilic than that of GMA-dextran after the free amine group on each D-glucosamine forms salt with TsOH which could be protonated in water²³. Whereas, GMA-dextran only has hydroxyl groups which is not easily to be protonated in water.

The calculated compressive modulus for the GMA-chitosan hydrogel was 17.640 ± 0.75 KPa. The mechanical properties of polysaccharide-based hydrogels were rarely reported in the literatures. Zhong et al.³⁶ recently reported a new family of maleic chitosan/polyethylene glycol diacrylate (PEGDA) hybrid hydrogels fabricated in the similar manner as the current UV-crosslinking GMA-chitosan hydrogels. The initial compressive modulus of the maleic chitosan / PEGDA (MW 8,000) hybrid hydrogels was

61±1.9 KPa which was significantly higher than our GMA-chitosan hydrogel. This is because the high composition of PEGDA in maleic chitosan / PEGDA hybrid hydrogel (2 : 1 ratio) can lead to higher crosslinking density than that of our current GMA-chitosan hydrogel which didn't have any co-precursor for gelation as Zhong et al. hybrid hydrogel did (PEGDA co-precursor).

2.4.6 Interior morphology (SEM) of GMA-chitosan hydrogel

The porous interior morphology of a swollen GMA-chitosan hydrogel (swollen in deionized water and then freeze-dried) was shown in Figure 2.8. GMA-chitosan (DS 37) hydrogel shows irregular shaped pores with diameter size ranging from 10~50 μm . The GMA-chitosan (DS 37) hydrogel interior structure is similar to that of the GMA-dextran (DS 4.7, synthesized by the reaction of GMA and dextran) / gelatin hybrid hydrogel that Chen et al.²³ reported which has pore size ranging from 17 μm -50 μm diameter. The porous structure of GMA-chitosan hydrogel provides a great opportunity to be used as tissue engineering scaffold²³.

2.4.7 Enzymatic biodegradation of GMA-chitosan hydrogel by lysozyme

The *in vitro* enzymatic biodegradation property of GMA-chitosan hydrogel (DS 37) was investigated in terms of weight loss in 18 days in both PBS and 1mg/mL lysozyme solutions of pH 7.4 at 37 $^{\circ}\text{C}$. The weight loss rate of GMA-chitosan hydrogel in the lysozyme solution (Figure 2.9) was faster than that in a pure PBS buffer. For example the weight loss of GMA-chitosan hydrogel in the presence of 1mg/mL lysozyme is about 42% after 14 days degradation, whereas the same hydrogel in the PBS control group showed only about 34% weight loss at the same time. In the

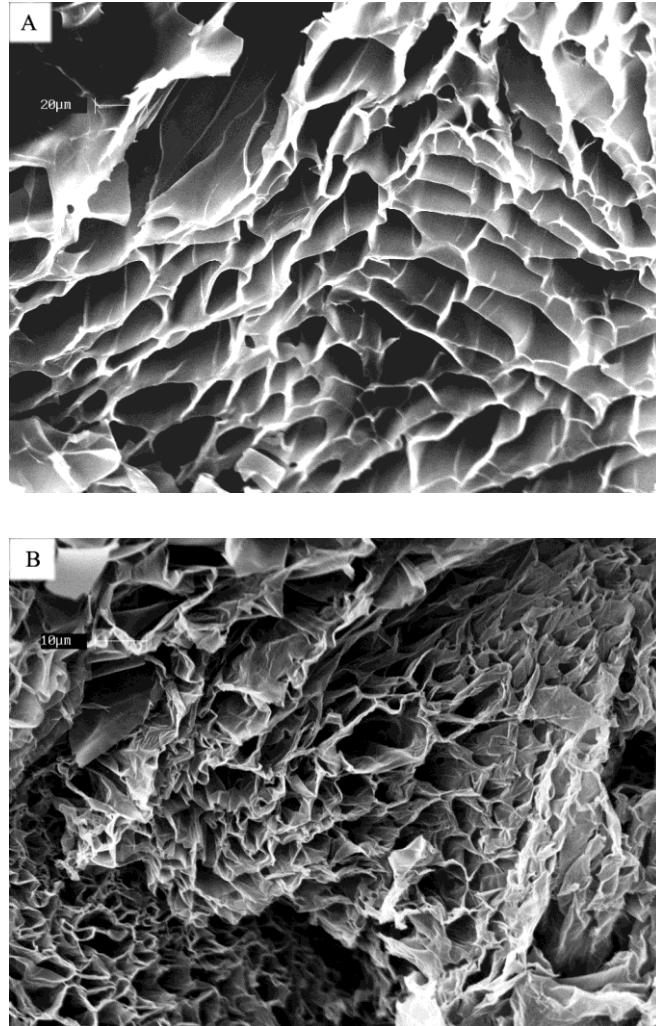


Figure 2.8 SEM images of swollen GMA-chitosan (DS 37) hydrogel in deionized water after 3 days lyophilization (A) 1,000 \times ; (B) 2,000 \times

presence of lysozyme medium, however, GMA-chitosan hydrogels became visibly smaller in size and lose their structure integrity much faster than in the PBS medium. After 5 days incubation, the weight losses of GMA-chitosan hydrogels in the presence of lysozyme were 5% ~ 10% greater than the same hydrogels samples in the PBS only.

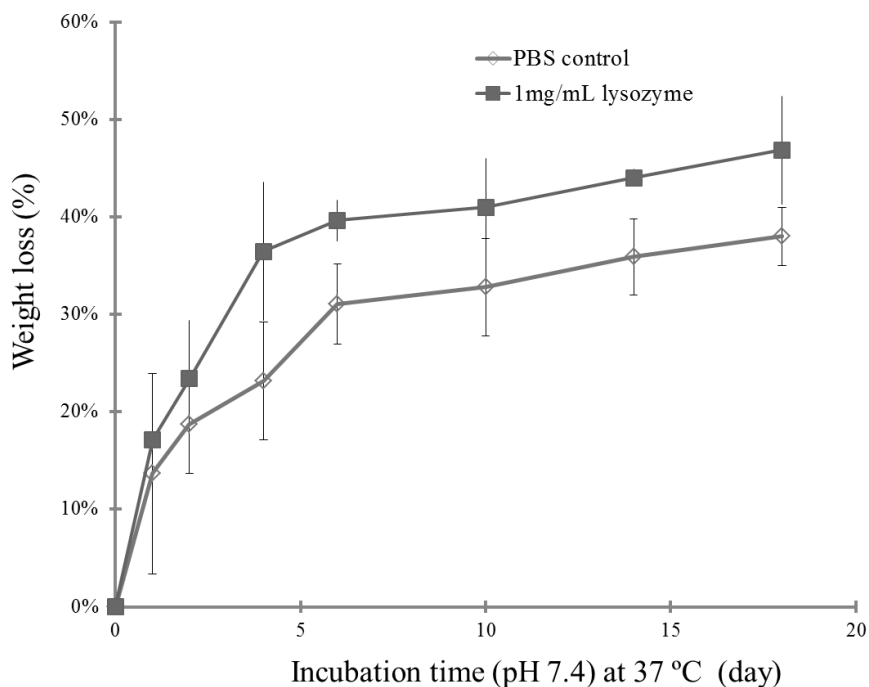


Figure 2.9 Weight loss of photo-crosslinked GMA-chitosan (DS 37) hydrogel as a function of time in 1mg/mL lysozyme 0.05M PBS solution and in 0.05M PBS as the control (pH 7.4) at 37 °C.

The degradation of GMA-chitosan hydrogel can be attributed to two different paths: the hydrolytic degradation of the ester bond of the methacrylate group in GMA, and lysozyme-catalyzed fragmentation of the GMA-chitosan backbones at the β (1, 4) linked glucosamine unit and N-acetyl-D-glucosamine unit¹³. The degradation of GMA-chitosan hydrogel in a pure PBS and by lysozyme are mainly followed a bulk erosion model: the degradation happened both at the surface and interior simultaneously⁴⁸. Because GMA-chitosan has good hydrophilicity and porous structure after swelling, it is able to absorb water and lysozyme into the hydrogel network structure, the degradation of methacrylate linkage and chitosan polymer chain is also happened at the interior of the hydrogel.

After 8 days degradation, the weight loss of GMA-chitosan hydrogel in the next 8 days is about 10%. The possible reason of degradation rate change of chitosan based

hydrogel in lysozyme solution is the result of partial degradation⁴². During the initial stage of enzymatic degradation of GMA-chitosan by lysozyme, breakage of a small number of glycosidic bonds of GMA-chitosan makes part of hydrogel which doesn't contain too much crosslinked methacrylate groups separated from the hydrogel network and diffused in water. This results in the fast weight loss of GMA-chitosan hydrogel in the initial stage. The remained crosslinked region of GMA-chitosan hydrogel takes longer time to be completely degraded, since lysozyme must targets acetylated residues of chitosan before it cleaves the polymer backbone⁴³.

Figure 2.10 shows the morphological structure of the GMA-chitosan upon degradation. When compared with the undegraded GMA-chitosan morphology (16 h in PBS medium, Figure 2.8), the morphological structure of GMA-chitosan hydrogels after 2 days enzymatic biodegradation (Figure 2.10 B) showed less distinctive high profile pores as the control (Figure 2.8 B), and the distinctive pore structure of the GMA-chitosan hydrogels disappeared via the collapsing and merging of pores after 14 days in lysozyme medium (Figure 2.10 D). In the presence of a pure PBS, the porous structure of GMA-chitosan hydrogel was largely filled (Figure 2.10. A, C). The possible reason is the degradation product of GMA-chitosan at the end of 14 days could still be high molecular weight chitosan derivative because hydrolytic scissions only cleave the ester bonds of the pendant methacrylate groups that act as a crosslinker to tie chitosan macromolecules together, i.e., no chitosan backbone fragmentation in a pure PBS environment. The high molecular weight degradation product aggregated on the pore walls and eventually filled up the pores (Figure 2.10 C), whereas the enzymatic biodegradation produces oligosaccharides from chitosan backbone with much lower MW than chitosan. These low MW oligosaccharides degradation products can be easily dissolved away from chitosan hydrogel. So, GMA-chitosan can still keep the porous structure during the process of enzymatic biodegradation, but could not in a PBS medium.

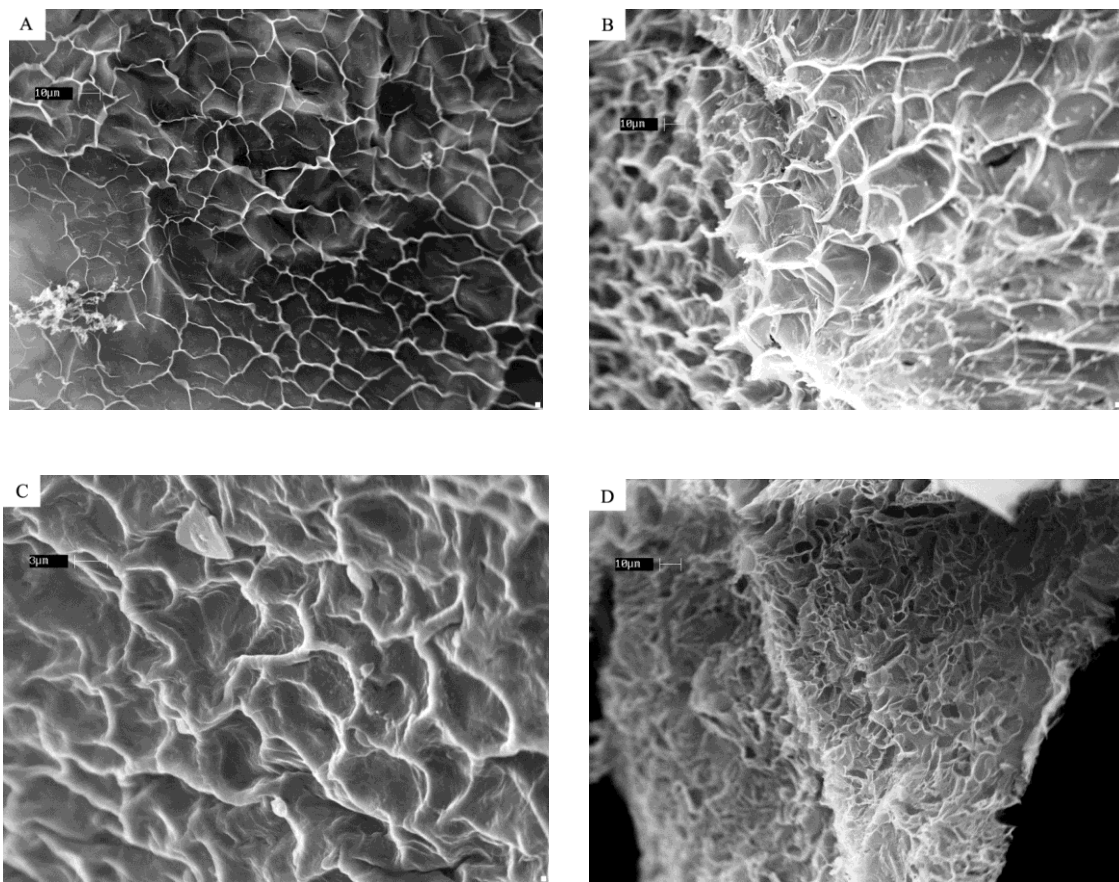


Figure 2.10. SEM images of morphologic changes of GMA-chitosan hydrogel *in vitro* at pH 7.4 and 37 °C. (A) GMA-chitosan hydrogel after 2 days incubation in 0.05M PBS, 1,000 X; (B) GMA-chitosan hydrogel after 2 days incubation in 1mg/mL lysozyme 0.05M PBS solution, 1,000 X; (C) GMA-chitosan hydrogel after 14 days incubation in 0.05M PBS, 2,500 X; (D) GMA-chitosan hydrogel after 14 days incubation in 1mg/mL lysozyme 0.05M PBS solution, 1,000 X

A similar collapse of the pore structure of other types of chitosan-based hydrogels was also reported by Hong et al.⁴² as they observed the pores of the chemically crosslinked CML hydrogel upon lysozyme biodegradation collapsed together with many rumples on the coarse pore walls.

2.4.8 Release of BSA from GMA-chitosan hydrogel

GMA-chitosan hydrogel has been evaluated as the delivery vehicle for controlled release of BSA protein. The advantage of the current GMA-chitosan hydrogel and UV-crosslinking technology in protein drug delivery is that the protein drug can be pre-loaded into the hydrogel precursor aqueous solutions before gelation, and hence provides a more homogeneous and uniform loading without the adverse effect of organic solvents. Release profiles of BSA (MW ~66,000) from GMA-chitosan as a function of incubation time in PBS media are shown in Figure 2.11. At the end of 11 days, more than 80% of

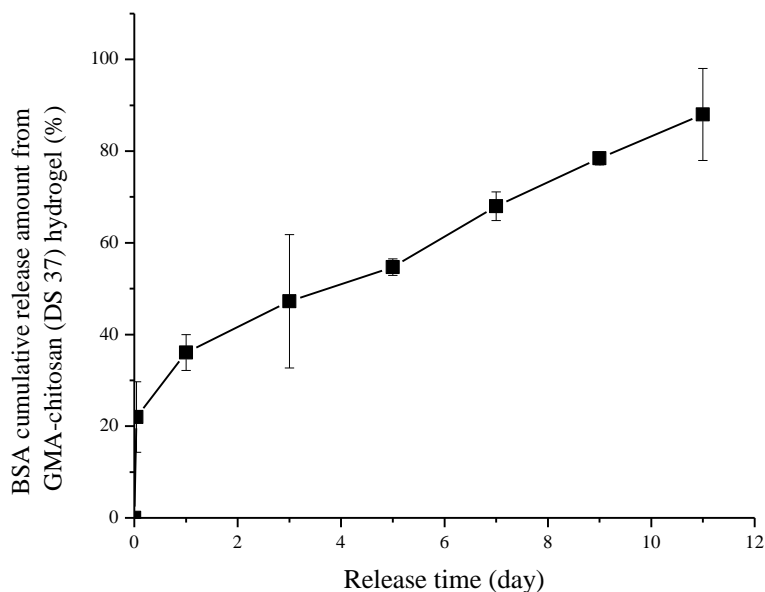


Figure 2.11 Cumulative BSA release from GMA-chitosan (DS 37) hydrogel in PBS (pH 7.4) at 37 °C.

BSA was released from GMA-chitosan hydrogels at 37 °C. Burst release of BSA happened in the first h of incubation which is due to dissolution of BSA near GMA-chitosan hydrogel surface.

The BSA release data from GMA-chitosan hydrogels were further analyzed as a function of the square root of time for assessing whether such a BSA release from the

GMA-chitosan hydrogel would follow a Fickian diffusion mechanism. As shown in Figure 2.12, a close to linear relationship was observed after the initial burst release and before 12 days. In the case of diffusion-controlled system, the release behavior follows the Higuchi square-root of time relationship: $\frac{M_t}{M_\infty} = 4 \left(\frac{Dt}{\pi l^2} \right)^{0.5}$

for $0 \leq M_t / M_\infty \leq 0.6$ where M_t and M_∞ are the fraction of drug released at time t and at equilibrium, D is the diffusion coefficient of the drug in the matrix and l is the sample thickness⁴⁵. The diffusion coefficient (D) of BSA from the GMA-chitosan can be calculated from the linear fitted slope value from Figure 2.12. and hydrogel sample shape and size parameter. Between 2nd and 7th days (excluding the initial burst release), the D of BSA from GMA-chitosan hydrogel is about 0.786×10^{-7} cm²/s. In the last 3 days release (after 7th day), the diffusion coefficient (D) of BSA is about 1.522×10^{-7} cm²/s. These D data suggested that the BSA release kinetics in the GMA-chitosan hydrogel in a PBS is mainly a diffusion-controlled mechanism before the hydrogel lost its microstructure due to degradation. After 7th day, the release rate of BSA was accelerated (i.e., a higher slope in Figure 2.12.) by the degradation of the GMA-chitosan as shown in the weight loss data in Figure 2.9.

When comparing with the Hennink et al.⁴⁶ diffusion coefficient study of BSA release from GMA-dextran hydrogel ($D 5.9 \times 10^{-7}$ cm²/s), the D of BSA from our GMA-chitosan hydrogel was significantly smaller than that of the Hennink et al. methacrylated dextran. Release of a protein through a hydrogel matrix can be influenced by ionic interactions between the protein and the hydrogel⁴⁴. Zeta potential data have demonstrated that GMA-chitosan shows positive charge in its aqueous solution (Table 2.4). The protonized residual amine groups of GMA-chitosan in an aqueous media are able to hold the negatively charged BSA (isoelectric point is about 4.7⁴⁴) by electrostatic interaction. The electrostatic interaction between anionic BSA and the cationic GMA-chitosan could slow down the BSA release, while the GMA-dextran hydrogels didn't

have any positively charged groups to interact with BSA. Compared to GMA-dextran, GMA-chitosan is able to achieve a more sustained protein release in vitro. A slower and more sustained drug release at local sites can prevent the systemic toxicity of many therapeutic agents. GMA-chitosan fabricated as a cationic polyelectrolyte hydrogel is a promising protein controlled delivery device for biomedical applications.

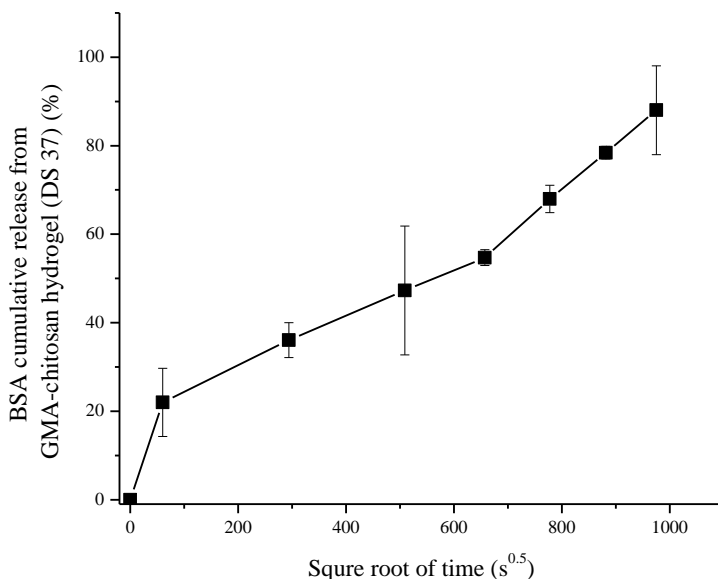


Figure 2.12. Square-root of time relationship for release of BSA from GMA-chitosan in PBS (pH 7.4) buffer at 37 °C

2.5 Conclusions and recommendation for future work

An efficient method has been developed for the synthesis of glycidyl methacrylate derivatized chitosan (GMA-chitosan) having significantly higher degree of GMA substitution than prior others' reported studies. The degree of substitution (DS) ranged from 13 to 37 and can be controlled by the molar feed ratio of GMA to chitosan and reaction time. The GMA-chitosan with DS lower than 37 can dissolve in water or DMSO. The GMA-chitosan is a cationic polymer with positive zeta potentials from +14.15 to +18.04, depending on the degree of GMA substitution. MTT assay showed GMA-

chitosan solution shows no significant cytotoxicity to porcine aortic valve smooth muscle cell. GMA-chitosan (DS 37) can be used as the precursor to fabricate photo-crosslinked cationic hydrogel in an aqueous solution. The GMA-chitosan hydrogel has porous structure and high capacity of water absorption ($6,768 \pm 456\%$ equilibrium swelling ratio in deionized water). The GMA-chitosan hydrogel has an average initial compressive modulus 17.640 ± 0.75 KPa. The enzymatic biodegradation study also demonstrated the biodegradability of the GMA-chitosan hydrogel in the presence of lysozyme. GMA-chitosan hydrogels were under investigation as a protein controlled delivery device and showed 12 days sustained release of BSA at room temperature *in vitro*. The biocompatibility of the GMA-chitosan hydrogel toward 3T3 fibroblast needs to be characterized for the further study by live/dead assay and F-actin staining. The GMA-chitosan hydrogel encapsulation with 3T3 fibroblast needs to be determined by UV-crosslinking the GMA-chitosan hydrogel precursor which mixed with cell suspension.

Acknowledgement

The authors would like to thank the support of Vincent V.C. Woo Fellowship to this study. The authors also wish to thank to Cornell Nanobiotechnology Center (NBTC) who provided cell culture facility and Dr. Duan who provided the PAVSMC cells in our study.

Reference:

- 1 Kuen Yong Lee, Soon Hong Yuk, Polymeric protein delivery systems, Progress in polymer science, 2007, 32, 669-697
- 2 Yoshimi Tanaka, Jain Ping Gong, Yoshihito Osada, Novel hydrogels with excellent mechanical performance, Progress in polymer science, 2005, 30, 1-9
- 3 W.E. Hennink, C.F. van Nostrum, Novel crosslinking methods to design hydrogels, Advanced drug delivery reviews, 2002, 54, 13-36
- 4 J. Berger, M. Reist, J.M. Mayer, O. Felt, R. Gurny, Structure and interactions in chitosan hydrogels formed by complexation or aggregation for biomedical applications, Eur. J. Pharm. Biopharm, 2004, 57, 35-52.

- 5 N. Boucard, C. Viton, A. Domard, Newspects of the formation of physical hydrogels of chitosan in a hydroalcoholic medium, *Biomacromolecules*, 2005, 6, 3227–3237.
- 6 S. Kobayashi, H. Uyama, S. Kimura, Enzymatic polymerization, *Chem. Rev.* 2001, 101, 3793–3818.
- 7 S. Sakai, Y. Yamada, T. Zenke, K. Kawakami, Novel chitosan derivative soluble at neutral pH and in-situ gellable via peroxidase-catalyzed enzymatic reaction, *J. Mater. Chem.* 2009, 19, 230–235.
- 8 Kytai Truong Nguyen, Jennifer L. West, Photopolymerizable hydrogels for tissue engineering applications, *Biomaterials*, 2002, 23, 4307-4314
- 9 C.K.S. Pillai, Willi Paul, Chandra P. Sharma, Chitin and chitosan polymers: Chemistry, solubility and fiber formation, *Progress in polymer science*, 2009, 34, 641-678
- 10 Fwu-Long Mi, Shu-Huei Yu, Chih-Kang Peng, Hsing-Wen Sung, Shin-Shing Shyu, Hsiang-Fa Liang, Mei-Feng Huang, Chee-Chan Wang, Synthesis and characterization of a novel glycoconjugated macromolecule, *Polymer*, 2006, 47 (12), 4348-4358
- 11 Zhilong Shi, K.G. Neoh, E.T. Kang, W. Wang, Antibacterial and mechanical properties of bone cement impregnated with chitosan nanoparticles, *Biomaterials*, 2006, 27 (11), 2440-2449
- 12 Lee, K. Y.; Ha, W. S.; Park, W.H., Blood compatibility and biodegradability of partially N-acylated chitosan derivatives, *Biomaterials* 1995, 16 (16), 1211-1216
- 13 Rao S.B, Sharma CP, Use of chitosan as a biomaterial: Studies on its safety and hemostatic potential, *Biomed. Mater. Res.* 1997, 34 (1): 21-28
- 14 Hiroshi Ueno, Haruo Yamada, Ichiro Tanaka, Naoki Kaba, Mitsunobu Matsuura, Masahiro Okumura et al., Accelerating effects of chitosan for healing at early phase of experimental open wound in dogs, *Biomaterials*, 1999, 20 (15): 1407-1414
- 15 Yong-Woo Cho, Yong-Nam Cho, Sang-Hun Chung, Gyeol Yoo, Sohk-Won Ko, Water-soluble chitin as a wound healing accelerator, *Biomaterials*, 1999, 20 (22), 2139-2145

- 16 Singh DK, Ray AR, Biomedical applications of chitin, chitosan, and their derivatives, *J Macromol Sci Rev, Macromol Chem Phys*, 2000; C40:69–83.
- 17 Shigehiro Hirano, Hisaya Tsuchida, Norio Nagao, N-acetylation in chitosan and the rate of its enzymic hydrolysis, 1989, 10 (8), 574-576
- 18 Madihally SV, Flake AW, Matthew HW. Maintenance of CD34 expression during proliferation of CD34+ cord blood cells on glycosaminoglycan surfaces, *Stem Cells*, 1999, 17(5), 295–305.
- 19 Stephanie Moller, Jurgen Weisser, Sabine Bischoff, Matthias Schnabelrauch, Dextran and hyaluronan methacrylate based hydrogels as matrices for soft tissue reconstruction, *Biomolecular Engineering*, 2007, 24, 496-504
- 20 Adriano V. Reis, Osvaldo A. Cavalcanti, Adley F. Rubira, Edvani C. Muniz, Synthesis and characterization of hydrogels formed from a glycidyl methacrylate derivative of galactomannan, *International Journal of Pharmaceutics*, 2003, 267, 13-25
- 21 Jennie Baier Leach, Kathryn A. Bivens, Charles W. Patrick, Jr., Christine E. Schmidt, Photocrosslinked hyaluronic acid hydrogels: Natural, biodegradable tissue engineering scaffolds, *Biotechnology and Bioengineering*, 2002, 82, (5), 578-589
- 22 Marcos R. Guilherme, Adriano V. Reis, Sue Ien H. Takahashi, Adley F. Rubira, Judith P.A. Feitosab, Edvani C. Muniz, Synthesis of a novel superabsorbent hydrogel by copolymerization of acrylamide and cashew gum modified with glycidyl methacrylate, *Carbohydrate Polymers*, 2005, 61, 464-471
- 23 Fa-Ming Chen, Yi-Min Zhao, Hai-Hua Sun, Tao Jin, Qin-Tao Wang, Wei Zhou, Zhi-Fen Wu, Yan Jin, Novel glycidyl methacrylated dextran (Dex-GMA)/gelatin hydrogel scaffolds containing microspheres loaded with bone morphogenetic proteins: Formulation and characteristics, *Journal of Controlled Release*, 2007, 118, 65–77
- 24 L. Ferreira, M.M. Vidal, C.F.G.C. Geraldes, M.H. Gil, Preparation and characterisation of gels based on sucrose modified with glycidyl methacrylate, *Carbohydrate Polymers*, 2000, 41, 15-24

- 25 W. N. E. van Dijk-Wolthuis, O. Franssen, H. Talsma, M. J. van Steenbergen, J. J. Kettenes-van den Bosch, W. E. Hennink, Synthesis, Characterization, and Polymerization of Glycidyl Methacrylate Derivatized Dextran, *Macromolecules*, 1995, 28, (18), 6317–6322
- 26 P. Edman, B. Ekman and I. Sjöholm, Immobilization of proteins in microspheres of biodegradable polyacyldextran. *Journal of Pharmaceutical Sciences*, 1980, 69, (7), 838–842
- 27 Lihui Weng, Andrew Gouldstone, Yuhong Wu, Weiliam Chen, Mechanically strong double network photocrosslinked hydrogels from N, N-dimethylacrylamide and glycidyl methacrylated hyaluronan, *Biomaterials*, 2008, 29, 2153-2163
- 28 O. Franssen, R.D. van Ooijen, D. de Boer, R.A.A. Maes, J.N. Herron, W.E. Hennink, Enzymatic degradation of methacrylates dextrans, *Macromolecules*, 1997, 30, 7408–7413.
- 29 E.A. Elizalde-Pena, N. Flores-Ramirez, G. Luna-Barcenas, S.R. Vasquez-Garcia, G. Ara'mbula-Villa, B. Garcia-Gaitan, J.G. Rutiaga-Quinones, J. Gonzalez-Hernandez, Synthesis and characterization of chitosan-g-glycidyl methacrylate with methyl methacrylate, *European Polymer Journal*, 2007, 43, 3963–3969
- 30 W. N. E. van Dijk-Wolthuis, J. J. Kettenes-van den Bosch, A. van der Kerk-van Hoof, W. E. Hennink, Reaction of Dextran with Glycidyl Methacrylate: An Unexpected Transesterification, *Macromolecules*, 1997, 30, 3411-3413
- 31 Xin De Feng, Xin Qiu Guo, Kun Yuan Qiu, Study of the initiation mechanism of the vinyl polymerization with the system persulfate / N,N,N',N'-tetramethylethylenediamine, *Die Makromolekulare Chemie*, 1988, 189, (1), 77-83
- 32 Narayan Bhattarai , Jonathan Gunn, Miqin Zhang, Chitosan-based hydrogels for controlled, localized drug delivery, *Advanced Drug Delivery Reviews*, 2010, 62, 83-99
- 33 Shin-ichiro Nishimura, Osamu Kohgo, Keisuke Kurita, Chemospecific manipulations of a rigid polysaccharide: syntheses of novel chitosan derivatives with excellent solubility

in common organic solvents by regioselective Chemical Modifications, *Macromolecules* 1991, 24, 4745-4748

34 Keisuke Kurita, Hiroyuki Ikeda, Yuya Yoshida, Manabu Shimojoh, Manabu Harata, Chemoselective protection of the amino groups of chitosan by controlled phthaloylation: facile preparation of a precursor useful for chemical modifications, *Biomacromolecules*, 2002, 3, (1), 1-4

35 Kurita K, Shimada K, Nishiyama Y, Shimojoh M, Nishimura S, Nonnatural branched polysaccharides: synthesis and properties of chitin and chitosan having α -mannoside branches. *Macromolecules*, 1998, 31, 4764–4769

36 Nelly Flores Ramirez, Eduardo A. Elizalde-Pena, Salomon R. Vasquez-Garcia, Jesus Gonzalez-Hernandez, Agustin Martinez-Ruvalcaba, Isaac C. Sanchez, Gabriel Luna-Barcenas, Ram B. Gupta, Characterization and degradation of functionalized chitosan with glycidyl methacrylate, *J. Biomater. Sci. Polymer Edn* 2005, 16 (4): 473-488

37 Chao Zhong, Jun Wu, C.A. Reinhart-King, C.C. Chu, Synthesis, characterization and cytotoxicity of photo-crosslinked maleic chitosan–polyethylene glycol diacrylate hybrid hydrogels, *Acta Biomaterialia*, 2010, 6, 3908-3918

38 Jing Han, Kemin Wang, Dongzhi Yang, Jun Nie, Photopolymerization of methacrylated chitosan/PNIPAAm hybrid dual-sensitive hydrogels as carrier for drug delivery, *International Journal of Biological Macromolecules*, 2009, 44, 229-235

39 Hern, D., and Hubbell, J. Incorporation of adhesion peptides into nonadhesive hydrogels useful for tissue resurfacing. *J. Biomed. Mater. Res*, 1998, 39, (2), 266-276

40 Mann, B.K., Gobin, A.S., Tsai, A.T., Schmedlen, R.H., and West, J.L. Synthetic ECM analogs: New materials for use as tissue engineering scaffolds. *Biomaterials*, 2001, 22, 3045-3051

41 Cees J. De Groot et al., In vitro biocompatibility of biodegradable dextran-based hydrogels tested with human fibroblasts, *Biomaterials*, 2001, 22, 1197-1203

- 42 Yi Hong, et al., Covalently crosslinked chitosan hydrogel: Properties of in vitro degradation and chondrocyte encapsulation, *Acta Biomaterialia*, 2007, 3, 23-31
- 43 Hiroaki Tanuma, Takashi Saito, Kenichi Nishikawa, Tungalag Dong, Koji Yazawa, Yoshio Inoue, Preparation and characterization of PEG-cross-linked chitosan hydrogel films with controllable swelling and enzymatic degradation behavior, *Carbohydrate Polymers*, 2010, 80, 260-265
- 44 Michael B. Mellott, Katherine Searcy, Michael V. Pishko, Release of protein from highly cross-linked hydrogels of poly(ethylene glycol) diacrylate fabricated by UV polymerization, *Biomaterials*, 2001, 22, 929-941
- 45 Mukesh C. Gohel, Maulik K. Panchal, and Viral V. Jogani, Novel Mathematical Method for Quantitative Expression of Deviation from the Higuchi Model, *AAPS PharmSciTech*, 2000, 1, 43-48
- 46 W.E. Hennink, H. Talsma, J.C.H. Borchert, S.C. De Smedt, J.Demeester, Controlled release of proteins from dextran hydrogels, *Journal of control release*, 1996, 39, 47-55

CHAPTER THREE:
SYNTHESIS AND CHARACTERIZATION OF WATER SOLUBLE GLYCIDYL
METHACRYLATE CHITOSAN AND 2-(ACRLOYLOXY) ETHYL
TRIMETHYLAMMONIUM AND THE FABRICATION INTO HYBRID HYDROGEL
IN AQUEOUS MEDIUM

3.1 Abstract

A new family of cationic hybrid hydrogels from two new positively charged aqueous soluble precursors, glycidyl methacrylate-chitosan (GMA-chitosan) and 2-(acryloyloxy) ethyl trimethylammonium (AETA), was developed via a simple photocrosslinking fabrication method. These hybrid hydrogels have pendant quaternary ammonium functional groups on the AETA segments. The chemical composition of GMA-chitosan / AETA hybrid hydrogels were characterized by fourier transform infrared spectroscopy (FTIR) and their mechanical, swelling and morphological properties were examined as a function of the composition of the hybrids as well as the effect of pH and ionic strength of the surrounding medium. GMA-chitosan/AETA hybrid hydrogels show a porous network structure with average pore diameter 20-50 μm . The compression moduli of these hybrid hydrogels ranged from 27.24 to 28.94 KPa which are significantly higher than a pure GMA-chitosan (17.64 KPa). GMA-chitosan / AETA hybrid hydrogel shows pH / ionic strength responsive swelling behavior due to the presence of the positive charge pendant groups. These hybrid hydrogels showed a sustain BSA protein release and a significantly lower initial burst release than a pure GMA-chitosan hydrogel. The two aqueous soluble precursors and the cationic charge characteristics of the resulting GMA-chitosan / AETA hybrid hydrogels may suggest that this new family of biomaterials may have promising applications as the pH responsive protein drug delivery vehicles.

3.2 Introduction

3.2.1 Polysaccharide hydrogels

Natural polymers which are used in the development of hydrogels, including polysaccharides and proteins have been used as structural material. Compared with other natural polymers, polysaccharides have excellent biocompatibility, low immunogenicity, low toxicity, and enzymatic degradation property. Chitosan is one linear polysaccharide composed of randomly distributed β -(1-4)-linked D-glucosamine and N-acetyl-D-

glucosamine units. It is commercially produced by the deacetylation of chitin which is extracted from crustaceans and insects. Due to these characteristics and abundant source to produce, chitosan has attracted a wide range of medical and pharmaceutical applications^{1,2}. At pH below the pKa of amine groups of chitosan (pKa 6.2), chitosan is water-soluble and positively charged due to protonation of amine groups present on the polymer chain. When the pH exceeds 6.2, chitosan aqueous solution forms a gel precipitation forms due to the neutralization of chitosan amine groups, leading to the balance of repulsion between chitosan molecules breaks in the stable water solution.

High water content crosslinked chitosan hydrogels are able to be used as intelligent drug carrier which provides sustained, local delivery of therapeutic agents. Many chitosan hydrogel preparation methods have been developed^{1, 2-5, 7}. In each method, chitosan is either physically associated or chemically crosslinked to form 3D network structures. To form stabilizing linkage, chitosan must have functional moieties that all binding between the chains to prevent gel dissolution. The bonding can be accomplished by non-covalent physical association, such as hydrogen bonding or ionic bonding, physical entanglement, or by chemically covalent crosslinking. The physical associations are reversible bonds, whereas the covalent crosslinkages are not. These methods were summarized below as physical association of chitosan hydrogel and chemically crosslinked chitosan two approaches.

3.2.2 Polyelectrolyte complexes hydrogel

Polysaccharides, proteins and synthetic polyelectrolytes also form electrostatic interactions with chitosan. The associations between the chitosan polymer and polyelectrolytes are stronger than other secondary binding interactions like hydrogen bonding or van der Waals interactions. Chitosan-based polyelectrolyte complex networks have been produced by water-soluble anionic macromolecules like DNA, alginate, GAGs (e.g. chondroitin sulfate, hyaluronic acid, or heparin), proteins (e.g. gelatin, albumin), and anionic synthetic polymers (e.g. polyacrylic acid). The formation of chitosan-based

polyelectrolyte hydrogel can be a one-stage process or a two stage procedure. H.V. Saether et al. used the one-stage process³. A sodium alginate solution was added to a chitosan chloride solution under high shearing conditions, or chitosan chloride was added to sodium alginate. The polyelectrolyte complex was very stable at pH above 7 over a temperature range of 4-37 °C³. In a two stage procedure reported by Douglas et al., the first step in this process is the preparation of Ca-alginate gel beads⁴. Then the beads are then transferred into a chitosan solution, and a polyelectrolyte complex membrane is formed on the surface of the beads. The alginate / chitosan nanoparticles ratio in the preparation was found to affect nanoparticle formation, as did polymer molecular weight and pH. The smallest nanoparticles have a mean diameter of 314 nm, and are prepared using low viscosity alginate and low molecular weight chitosan in a ratio of 1: 1.5. The alginate / chitosan ratio in the preparation was found to affect particle size to a greater degree than any other parameters⁴. Polyelectrolyte complexes which consist of chitosan and the polyelectrolyte are reversible. The stability of these compounds is dependent on charge density, solvent, ionic strength, pH and temperature.

3.2.3 Crosslinked chitosan hydrogel

The limitation of physically bonded hydrogels is their inconsistent performance, due to the lack of stable network structure formed by covalent crosslinking sites. Moreover, to precisely control the physical gel shape and pore size are very hard. More robust chitosan hydrogels is able to be fabricated by using small molecules crosslinkers, secondary polymerization or irradiation chemistry. The primary amines and hydroxyl groups of chitosan chain are able to react with many kinds of crosslinkers. Chemical crosslinked network can be formed by using small molecule crosslinkers, polymer-polymer reactions between activated functional groups.

3.2.3.1 Small molecule crosslinkers.

Many bifunctional small molecules could be used to crosslink chitosan. Crosslinkers are molecules with at least two reactive functional groups that all the formation of bridges

between chitosan chains. One kind of commonly used crosslinkers is dialdehydes, such as glutaraldehyde or glyoxal. The aldehyde groups form covalent imine bonds with the amino groups of chitosan via a Schiff base reaction. Dialdehydes react with amino groups in aqueous media without the addition of auxiliary molecules such as reducer. For example, Yamada et al. produced a water-resistant adhesive by using glutaraldehyde as crosslinker of chitosan⁵. However, dialdehydes are generally considered to be toxic. The residue dialdehydes which are not completely reacted may induce toxic effect. Besides dialdehydes, diglycidyl ether, diisocyanate, diacrylate were used to crosslink chitosan hydrogel. Recently, genipin, which is a naturally occurring material and used in herbal medicine and food dye are used as an alternative of chitosan crosslinker⁶.

3.2.3.2 Polymer-polymer crosslinking

Even though small molecules are able to provide desirable properties, but many crosslinkers are considered to be toxic. In order to eliminate the use of crosslinker molecules during gelation, functionalized polymer chains with reactive groups were used in chitosan hydrogel fabrication. In Tan et al. study, chitosan and hyaluronic acid hydrogel was produced by schiff bases reaction in situ⁷. A water soluble chitosan derivative, N-Succinyl-chitosan and oxidized hylauronic acid were mixed at various volume ratios to form chitosan/hyaluronic acid hybrid hydrogels. Schiff base was formed with in 4 mins after N-Succinyl-chitosan and hylauronic acid with aldehyde group. Chondrocytes culture test demonstrates the composite hydrogel supports chondrocyte adhesion and encapsulation⁷.

Schiff bases reaction were also used in the preparation of oxidized dextran and chitosan⁸. Chitosan hydrogels have also been made by using Michael addition reaction⁹. In Ono et al. study, thiol modified chitosan was synthesized and mixed with Polyethylene glycol diacrylate (PEGDA). Hydrogel was rapidly formed in situ under physiological conditions. Chitosan's primary amino group reacts with the vinyl group on PEGDA. The advantage of this approach is its rapid reaction time and different choices of bonds. The

disadvantage of polymer-polymer system is it requires multi-step preparation and purification processes. Moreover, the reactive groups some times are cytotoxic.

3.2.4 Photocrosslinking of chitosan based hydrogel

Chitosan hydrogels can be formed in situ using photo-sensitive functional groups. Chitosan with reactive moieties forms crosslinkages upon irradiation with UV light. This technique offers considerable advantages (ease to control shape, safety, etc). Functionalized chitosan with azide groups (-N₃) has been developed by Ono et al. The azide is converted into a reactive nitrene group which reacts with chitosan's free amine group. The gelation happens within 60 seconds⁹.

Another type thermo-sensitive, chitosan-pluronic hybrid hydrogel precursor which is functionalized with acrylate groups was also made through UV photocrosslinking. After UV radiation, the precursor could form a physical network at the temperature above its LCST¹⁰. Some researchers tried to introduce unsaturated double bond on the chitosan main chain. Figure 3.1 shows the scheme of chitosan derivative with the pendant double bonds.

Hong et al. developed one water soluble and crosslinkable chitosan derivative via the condensation reaction between amino groups and carboxyl groups under the catalysis of carbodiimide. This chitosan hydrogel is soluble in neutral water and does not precipitate till pH 9. The chitosan hydrogel was formed in the mold at a temperature of 37 °C under the initiation of a redox system, Irgacure 2959 / N, N, N, N- tetramethyl ethylenediamine (TMEDA)¹¹. The same reaction and gelation method was used by Hong et al. again to synthesize another water-soluble chitosan derivative having double bonds. Methacrylic acid (MA) and lactic acid (LA) was grafted via the reaction between amino groups and carboxyl groups under the catalysis of carbodiimide¹².

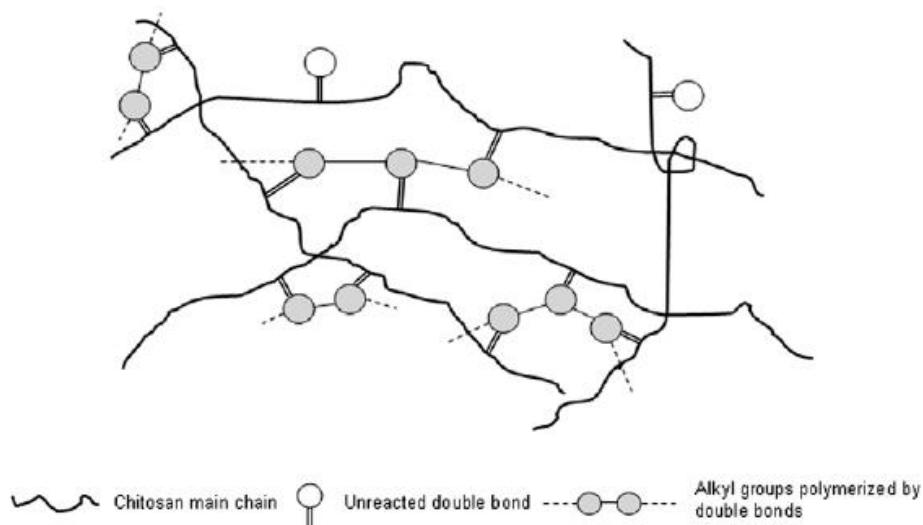


Figure 3.1 Illustration of the chitosan hydrogel network linked by alkyl chains which are formed via carbon-carbon double bond polymerization.

Nelly Flores-Ramirez et al. took advantage of the rapid reaction between epoxy groups of glycidyl methacrylate and the amine groups of chitosan to develop one chitosan derivative with double bonds. The synthesis process is in the acidic water solution¹³. Pure chitosan-glycidyl methacrylate derivative hydrogel has not been reported. This hydrogel system has temperature sensitivity which is contributed by *N*-isopropylarylamide (NIPAAm) component. Due to the residue cationic amine groups of chitosan component, this hybrid hydrogel also shows pH sensitivity in aqueous environment¹⁴.

3.2.5 pH and ionic strength sensitive hydrogel

Stimuli-responsive hydrogels have been produced that exhibit dramatic changes in their swelling behavior, network structure, permeability and mechanical strength in response to a number of external stimuli, including pH, ionic strength of the surrounding fluid, temperature, presence of specific solute and applied electrical or magnetic fields¹⁵. Stimuli-responsive hydrogels can be used in a wide variety of applications, including tissue engineering, biosensors and drug delivery devices. Hydrogels exhibiting pH-

dependent swelling behavior can be swollen from ionic networks. Polyelectrolyte gels change their conformation with the degree of dissociation which is the function of quantities such as pH value, ionic strength, polarity of the solvent and temperature of the external solution. These ionic networks contain either acidic or basic pendant groups. In aqueous media of appropriate pH and ionic strength, the pendant groups can ionize, developing fixed charges on the gel. In these gels, ionization occurs when the pH of the environment is above the pKa of the ionizable group. As the degree of ionization increases (increased system pH), the number of fixed charges increases, resulting in increased electrostatic repulsions between the chains and resulting in an increased hydrophilicity of the hydrogel structure, and greater swelling ratios. Conversely, cationic materials contain pendant groups such as amines. These groups ionize in media which are at a pH below the pK_b of the ionizable species. Thus, in a low pH environment, ionization increases, causing increased electrostatic repulsions. The hydrogel becomes increasingly hydrophilic and will swell to an increased level. One polysaccharide, hyaluronic acid (HA) which is also one kind of linear natural polyelectrolyte with a high molecular weight has a disaccharide repeat unit consisting of 2-acetamide-2-deoxy-β-D-glucose and β-D-glucuronic acid linked by alternating (1-3) and (1-4) glycoside bonding. HA is a weak polyelectrolyte with a low negative charge density. HA-PVA hybrid hydrogel was reported that it has pH-dependent swelling behavior and responsive swelling behavior to the electric field ¹⁶.

In the study of drug delivery, stimuli-responsive hydrogels have been produced that exhibit dramatic changes in their swelling behavior, network structure, permeability and mechanical strength in response to a number of external stimuli, including pH, ionic strength of the surrounding fluid, temperature, presence of specific solute and applied electrical or magnetic fields ^{15,17}. Stimuli-responsive hydrogels can be used in a wide variety of applications, including tissue engineering, biosensors and drug delivery devices. Polyelectrolyte hydrogels exhibit pH-dependent swelling behavior that is the

function of ionic strength, polarity of the solvent and temperature. These ionic networks contain either acidic or basic pendant groups. In aqueous media of appropriate pH and ionic strength, the pendant groups can ionize, developing charges on the hydrogel. Depending on the type of ionizable pendant groups, ionization can occur when the pH of the environment is either above or below the pKa of the ionizable group. As the degree of ionization changes due to the change of pH, the number of charges can increase or decrease, resulting in increased or decreased electrostatic repulsions between the chains and resulting in greater or lower swelling ratios. pH-sensitive hydrogel have been most frequently used to develop controlled release formulation; for example, polycationic hydrogels in the form of semi-IPN have been used for antibiotics drug delivery in the stomach for the treatment of *Helicobacter pylori*.¹⁸

3.2.6 Quaternary ammonium group

Quaternary ammonium cations are permanently positively charged, independent of the pH of their solution. Quaternary ammonium compounds are well-known antiseptics with a favorable safety profile, and have been added to a variety of personal hygiene products¹⁹. Moreover, in the drug release applications, introduction of cationic property in nanoparticles has been considered as an effective approach to increase the permeability of the nanoparticles across the blood-brain barrier. The cationic charge of primary amine usually has high toxicity, but quaternary ammonium cations on polymers which were derived from poly (glycidyl methacrylate) shows significantly reduced cytotoxicity¹⁸. Permeability of quarternization of β -cyclodextrin polymer nanoparticles through blood-brain barrier was investigated as drug carrier by et al²⁰. In their study, quaternary ammonium β -cyclodextrin (QA β CD) nanoparticles showed permeability coefficients about twice higher than that of fluorescein thiocarbamoyl-dextran (FITC-dextran). Moreover, QA β CD significantly enhanced the viability of bovine brain microvessel endothelial cells by protecting cells from the cytotoxicity effects of

doxorubicin. The possible mechanism for the permeability of QA β CD nanoparticles across the blood-brain barrier is endocytosis.

One commercial source of quaternary ammonium cation is 2-(Acryloyloxy) ethyl trimethylammonium (AETA) which is a water-soluble chemical with quaternary ammonium group and unsaturated double bond that is photo-reactive. The unsaturated vinyl end group can be used as the reactive site for chemically incorporating quaternary ammonium cation onto polymers having unsaturated double bonds. In the study of this chapter, GMA-chitosan was used as such a polymer for incorporating quaternary ammonium cation. The aqueous solution of GMA-chitosan which is synthesized by using the new method could be photocrosslinked to form hydrogel. By adding AETA into the GMA-chitosan aqueous solution, cationic hydrogel with quaternary ammonium group could be easily fabricated by using the similar photocrosslinking method.

3.3 Experimental

3.3.1 Materials

Chitosan (75-85% deacetylated) of molecular weight (MW) 50,000-190,000 Da, 2-(Acryloyloxy) ethyl trimethylammonium (AETA) (80 wt% in aqueous solution), bovine serum albumin (BSA) of molecular weight ~66,000 Da were purchased from Sigma Chemical Company (St.Louis, MO). Glycidyl methacrylate (GMA, 97%), 4-(N,N-dimethylamino) pyridine (DMAP, 99%), toluene sulfonic acid monohydrate (TsOH·H₂O) dimethyl sulfoxide (DMSO) were purchased from VWR Scientific (West Chester, PA). Ethyl acetate, acetone were purchased from Mallinckrodt incorporation (St.Louis, MO) and used without further purification. The DMSO, toluene, isopropyl alcohol, ethyl acetate, and acetone were ACS grade. Potassium hydrogen phthalate, hydrochloric acid (10%,v/v), disodium hydrogen phosphate, sodium hydroxide, sodium dihydrogen phosphate monohydrate were purchased from VWR Scientific (West Chester, PA) to prepare buffer solutions of different pH (i.e. 3, 7.4, 10) and different ionic strength

(i.e. 0.05, 0.1, 0.2 M). MicroBCA kit was purchased from Thermo Fisher Scientific (Waltham, MA). Irgacure 2959 was donated by Ciba Specialty Chemicals Corp.

3.3.2 Methods

3.3.2.1 Synthesis of glycidyl methacrylate chitosan (degree of substitution 37)

In order to prepare glycidyl methacrylate chitosan (GMA-chitosan), chitosan was first dissolved in DMSO to achieve 1.5wt%~2wt% solution at a comparatively mild acidic pH (pH 3.5). Then, glycidyl methacrylate and DMAP were added into the chitosan DMSO solution. The epoxy groups of GMA reacted with hydroxyl groups in chitosan. Through this reaction, the unsaturated double bond of the methacrylate group was introduced onto the chitosan backbone which could then be used for a further photocrosslinking reaction. According to published studies of the methacrylation of polysaccharides (dextran, galactomannan or even disaccharide sucrose) by GMA, the reaction did not take place at the epoxide ring^{18,20-22}. The only reaction mechanism between GMA and polysaccharides is transesterification, yielding polysaccharide-MA derivative with methacryloyl group attached to hydroxyl groups and glycidol. DMAP worked as a catalyst to help the transesterification reaction between the epoxy groups of GMA and hydroxyl groups of chitosan.

In a typical synthesis, 1.5 g chitosan and 1.2 g TsOH·H₂O were dissolved in 150 mL DMSO at 50 °C under magnetic stirring for 6 h. The dissolution is preceded by the protonation of the NH₂ groups in chitosan by the TsOH to give a toluene sulfonic acid salt adduct. After chitosan formed a clear solution, 0.5 g DMAP was dissolved in 5 mL DMSO and then added into the chitosan DMSO solution with rapid stirring. The mixture solution was then cooled down to room temperature, 3.6 g of glycidyl methacrylate was then added. The reaction was continued at 35 °C for 48 hours with magnetic stirring. Afterwards, the reaction was stopped by adding 2 molar ratio amounts of toluene sulfonic acid to neutralize the DMAP. GMA-chitosan was precipitated in 600mL ethyl acetate and dried in vacuum oven at room temperature for 2 hours. The crude gel-like GMA-chitosan

was cut into 1.5~2 mm cubic pieces and was completely washed by Soxhlet's extraction with acetone for 8h. The residue toluene sulfonic acid, DMAP, GMA are all have very high solubility in acetone and could be removed in this purification step. Finally, the GMA-chitosan was dried in vacuum oven at room temperature overnight. According to the H-NMR data, the degree of substitution of GMA-chitosan synthesized as described is about 37 (DS is defined as the amount of methacrylate groups per 100 polysaccharide repeat unit). This GMA-chitosan with degree of substitution 37 had good aqueous solubility and is used for all the subsequent GMA-chitosan / AETA hybrid hydrogel study to achieve good mechanical properties of the fabricated hydrogels.

3.3.2.2 Fabrication of GMA-chitosan/2-(Acryloyloxy) ethyl trimethylammonium (AETA) hybrid hydrogel

To fabricate GMA-chitosan/AETA hybrid hydrogels, 0.3g GMA-chitosan (degree of substitution 37) was dissolved in 2 mL water and mixed well with predetermined amounts of AETA aqueous solution. The weight ratio of GMA-chitosan to AETA could be any ratio with GMA-chitosan contents no less than 67/33 to achieve good structural integrity and proper mechanical strength of hybrid hydrogels; in this study, the weight feed ratio of GMA-chitosan to AETA used are 80/20 and 67/33. 5 mg Irgacure 2959 photoinitiator was added into the solution and mixed well at room temperature. Every 400 μ L mixture aqueous solution was transferred onto a Teflon[®] mold (12 mm diameter, 6 mm thickness) and irradiated by a long wavelength UV light (100 watts, 365nm) at room temperature for about 30 min until a disk-shaped hydrogel was obtained. The hydrogels were soaked in deionized water for 16 h at room temperature to remove the unreacted GMA-chitosan and AETA residues. The swollen GMA-chitosan/AETA hybrid hydrogel samples were then dehydrated on a Teflon plate in the ambient air at room temperature until the dry weight was constant for further studies, such as FTIR, equilibrium swelling ratio.

A representative chemical structure of GMA-chitosan/AETA hydrogels is shown in Figure 3.2. Pure GMA-chitosan hydrogels as a control were fabricated by photocrosslinking 6% GMA-chitosan aqueous solution without the presence of AETA.

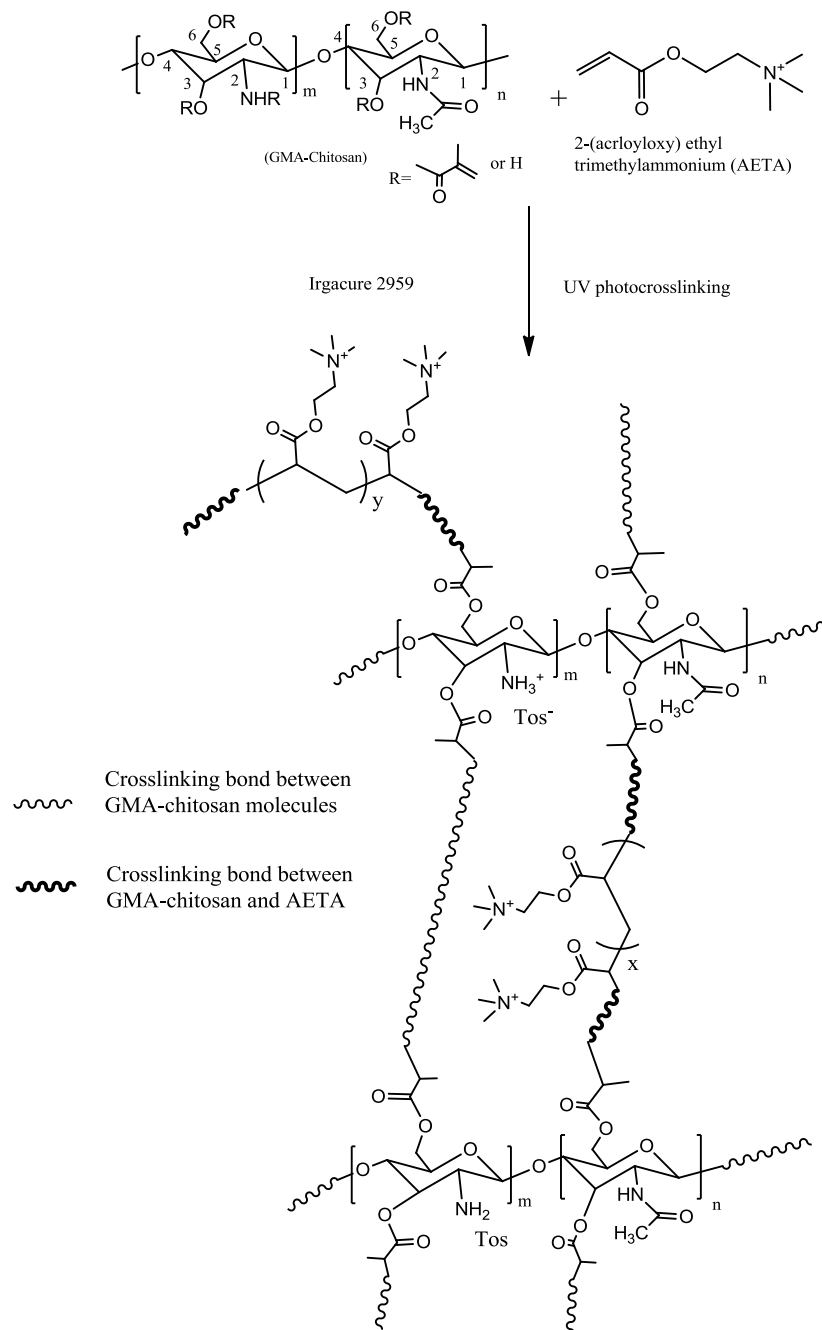


Figure 3.2 One representative GMA-chitosan / AETA hybrid hydrogel

3.3.2.3 Fourier Transform Infrared (FTIR) Characterization of dried GMA-chitosan / AETA hybrid hydrogel

Dehydrated GMA-chitosan/AETA hybrid hydrogel (dehydrated in ambient air at room temperature) were analyzed by Fourier Transform Infrared (FTIR) using a PerkinElmer (Madison, WI) Nicolet Magna 560 FTIR spectrophotometer with Omnic software for data acquisition and analysis. The spectra of dry GMA-chitosan / AETA hybrid hydrogel were recorded and compared with a pure GMA-chitosan FTIR spectra.

3.3.2.4 Swelling ratio (Q_{eq}) under different ionic strength and pH environment

The Q_{eq} of dehydrated GMA-chitosan/AETA hybrid hydrogel and the pure GMA-chitosan hydrogel (as control) were performed at room temperature (25 °C) by immersing dehydrated hydrogels individually in glass vials containing 15 mL 0.05M buffers (pH 3, 7.4, 10) or 15 mL pH 7.4 (0.05 M, 0.1 M, 0.2M). After 16 h, the GMA-chitosan/AETA hybrid hydrogels reached their swelling equilibrium. The swollen hydrogels were then removed, the excess surface water was wiped and the hydrogels were weighed until a constant weight was obtained. The swelling ratios of the hydrogels were calculated from the swollen and dry weights of the hydrogels according to the following equation.

$$Q_{eq} (\%) = (W_t - W_0) / W_0 \times 100$$

W_t is the weight of the hydrogel at swelling equilibrium

W_0 is the initial dry weight of the hydrogel before immersion.

The swelling profiles of a hydrogel were determined in triplicate.

3.3.2.5 Morphological study of GMA-chitosan/AETA hybrid hydrogel

Scanning electron microscope (SEM) was employed to analyze the interior microstructure of GMA-chitosan/AETA-67/33 hybrid hydrogel. A pure GMA-chitosan hydrogel was examined for comparison. Individual hydrogels were soaked in deionized water at room temperature to reach their swelling equilibrium. Then, the hydrogels were transferred into liquid nitrogen immediately to freeze and retain the swollen structure.

The samples were subsequently freeze-dried for 72 h in a Labconco (Kansas City, MO) Freezone 2.5 Freeze drier under vacuum at -50 °C, and finally glued onto aluminum stubs and coated with gold for 30s for SEM observation by Leica Microsystems GmbH (Wetzlar, Germany) 440 SEM.

3.3.2.6 Compression mechanical properties of GMA-chitosan / AETA hybrid hydrogel

The mechanical testing of the GMA-chitosan/AETA hybrid hydrogel and GMA-chitosan hydrogel was performed on a DMA Q800 Dynamic Mechanical Analyzer (TA Instrument Inc., New Castle, DE) in a “controlled force” compression mode. The compressive mechanical property of GMA-chitosan/AETA hybrid hydrogels and GMA-chitosan hydrogel in circular disc shape after reached their equilibrium swelling in deionized water were measured at room temperature (25 °C). The hydrogels were mounted between the movable compression probe (diameter 15mm) and the fluid cup without any liquid media. A compression force from 0.01 to 4 N at a rate of 0.5 N/min was applied on the swollen hydrogel samples at room temperature until fragment of the hydrogels was produced. TA Universal Analysis software was used for mechanical data analysis. Initial compressive modulus and compressive strain at break were used to examine the hydrogel mechanical property. The initial compressive modulus was calculated from the slope of the initial linear portion of the curve. For each type of hydrogel, five samples were used, and their mean value was calculated with a standard deviation.

3.3.2.7 Enzymatic degradation of GMA-chitosan/AETA hybrid hydrogel

The enzymatic biodegradation of the circular disk shaped GMA-chitosan/AETA-67/33 hybrid hydrogel and GMA-chitosan hydrogel was evaluated by their weight loss at 37 °C in 15mL lysozyme (1mg/mL) in 0.05M pH 7.4 phosphate buffered saline (PBS) over a period of 10 days. A 15 mL PBS of pH 7.4 served as the control.

The weight of each dry GMA-chitosan/AETA-67/33 hybrid hydrogel or GMA-chitosan hydrogels was measured before immersion. At various immersion intervals,

three GMA-chitosan/AETA-67/33 hybrid hydrogels (or GMA-chitosan hydrogels) samples were removed from the immersion solution and dried under vacuum at room temperature till constant weights. The weight loss was calculated according to the following equation: $\% \text{ Weight loss} = (W_o - W_t) / W_o \times 100\%$, where W_o was the initial ($t=0$) dry weight of hydrogel, and W_t was the dry weight of the hydrogel after incubation at time t . Mean value of was calculated as the weight loss at time t with a standard deviation.

3.3.2.8 Release study of bovine serum albumin (BSA) from GMA-chitosan / AETA hydrogel.

75 mg BSA was dissolved in 5 mL deionized water to obtain BSA stock solution of 15 mg/mL concentration. GMA-chitosan/AETA-67/33 precursor solution was prepared in a 20 mL glass vial wherein 300 mg of GMA-chitosan and 187 mg AETA aqueous solution (80 wt%) dissolved in 4.6 mL deionized water. 200 μ L BSA stock solution and 10 mg Irgacure 2959 were then added into the GMA-chitosan/AETA-67/33 aqueous solution and mixed well after 10 min magnetic stirring. The 400 μ L BSA-preloaded GMA-chitosan/AETA-67/33 aqueous solution was transferred to a 20-well Teflon[®] mold with a micropipette and photo-crosslinked by using a long wavelength UV light (100 watts, 365nm) for about 30 min. After gelation, each BSA-preloaded GMA-chitosan/AETA-67/33 hydrogel sample (with 240 μ g BSA loaded) was removed from Teflon[®] mold carefully and placed in glass vials individually filled with 5 mL 0.05M pH 3 buffer or 0.05 M PBS of pH 7.4 supplemented with 0.02 w/v% sodium azide, and then incubated at 37°C (Julabo, waterbath). At each predetermined time interval, 100 μ L buffer solution was removed from the vial and diluted to 1mL by deionized water. 100 μ L fresh buffer solution (0.05M pH 3 buffer or 0.05 M PBS of pH 7.4) was added back into the glass vial to keep the PBS medium constant during the immersion.

MicroBCA kit (Thermo Scientific, USA) was used to determine the BSA concentration. The protocol in the MicroBCA receipt was followed when using the

MicroBCA kit. PerkinElmer (Madison, WI) Lambda 35 UV-Vis spectrophotometer was used to determine the absorption of the samples at 562nm wavelength. The standard BSA calibration curve was prepared by plotting the average Blank-corrected 562nm reading for each BSA standard which is provided in the kit vs. its concentration in $\mu\text{g/mL}$. This BSA standard calibration curve was used to determine the BSA concentration released from the testing hydrogels at a particular time interval. The amounts of BSA released from the testing hydrogels were then calculated from the calibration curve. Samples in triplicate were averaged for each experiment.

3.4 Results and discussion

3.4.1 FTIR spectroscopy

Figure 3.3 shows the FTIR spectra of GMA-chitosan / AETA- 67 / 33 hybrid hydrogel. The sharp carbonyl bands of ester bonds at $1745\text{-}1749\text{ cm}^{-1}$ was shown on AETA spectra. The ester bond of methacrylate in GMA-chitosan is about 1725 cm^{-1} . The peak at 1475 cm^{-1} is ascribed to the symmetrical bending vibration of $-\text{CH}_3$ of quaternary ammonium group. GMA-chitosan also shows amide (I) band and amide (II) band at $1648\text{-}1650\text{ cm}^{-1}$ and $1538\text{-}1542\text{ cm}^{-1}$, respectively due to the incomplete deacetylated N-acetyl-D- glucosamine units. The GMA-chitosan/AETA hybrid hydrogel also showed the amide (I) and amide (II) bands which are absent in the AETA spectrum. The amide groups were from the N-acetyl-D-glucosamine repeat unit of chitosan. On the spectrum of the chitosan / AETA hybrid hydrogel, the peak at 1475 cm^{-1} of quaternary ammonium group was shown but absent in a pure GMA-chitosan. The FTIR data demonstrated that AETA was successfully incorporated into the GMA-chitosan hydrogel network upon the UV-crosslinking process. The absorption of ester bond at 1745 cm^{-1} of GMA-chitosan/AETA hybrid hydrogel is strengthened when comparing with a pure GMA-chitosan hydrogel due to the presence of the ester unit in AETA.

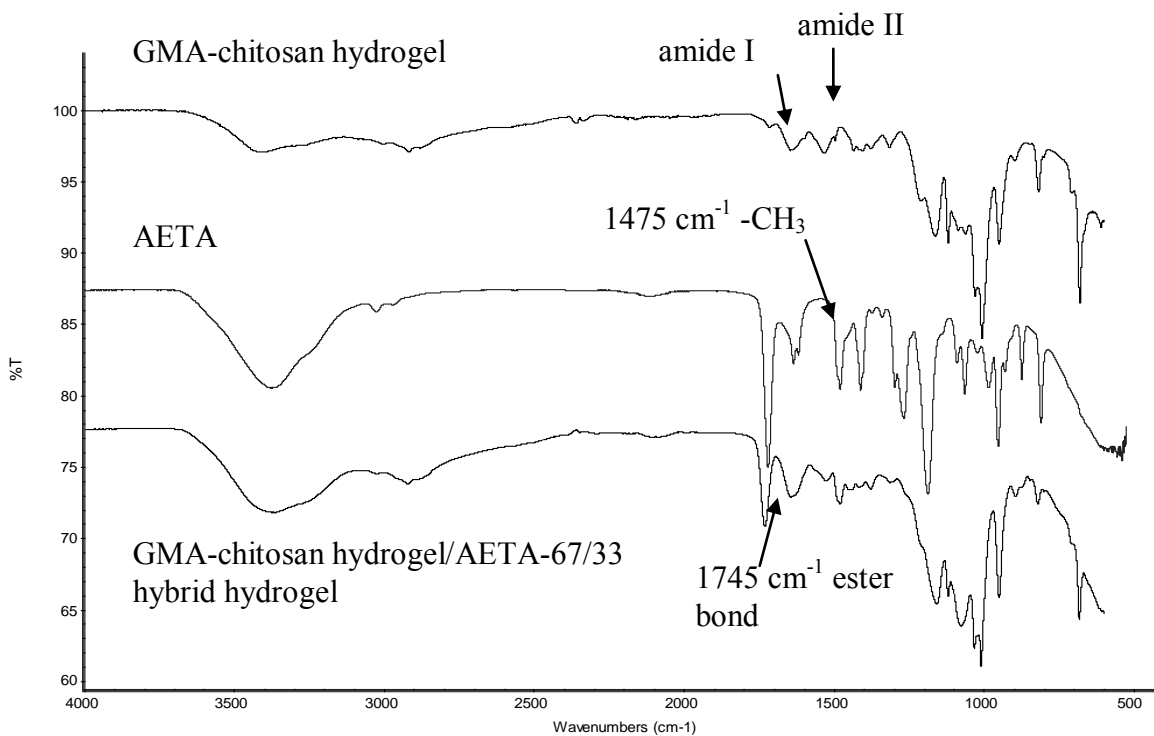


Figure 3.3 FTIR of GMA-chitosan/AETA-67/33 hybrid hydrogel and its corresponding pure precursors.

3.4.2 Images of GMA-chitosan/AETA hybrid hydrogel after swelling

Figure 3.4 A shows the image of a dehydrated GMA-chitosan/AETA hydrogel in an ambient environment after 48 h. Figure 3.4 B shows the optical image of a GMA-chitosan / AETA hydrogel after 16 hours swelling in deionized water. The GMA-chitosan/AETA hybrid hydrogel shows high swelling in water and good transparency with no color.

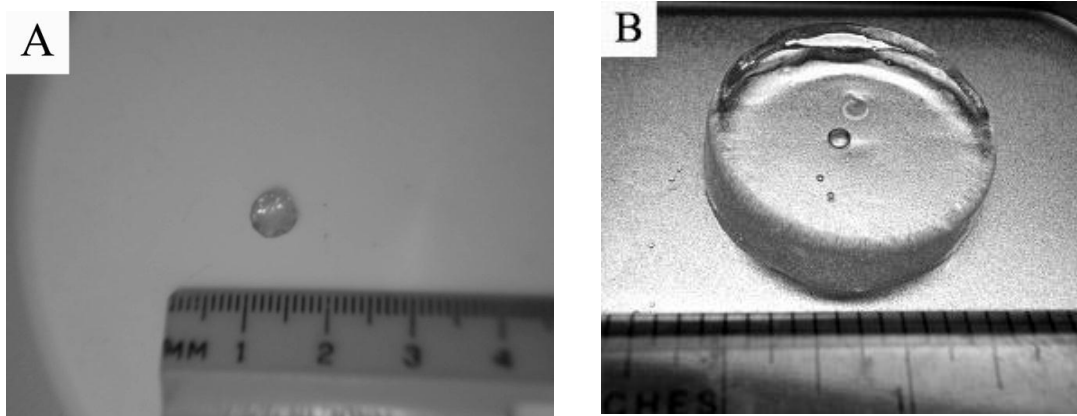


Figure 3.4 Images of GMA-chitosan/AETA-67/33 hydrogel. (A) dehydrated GMA-chitosan/AETA-67/33 hydrogel; (B) after swelling in deionized water for 16 hours immersion

3.4.3 The influence of ionic strength on the swelling ratio of GMA-chitosan / AETA hybrid hydrogel

All of the GMA-chitosan / AETA hybrid hydrogels and the pure GMA-chitosan hydrogel control reached their largest swelling ratio after 16 hours immersion in deionized water as shown in Figure 3.5. The swelling ratio of GMA-chitosan / AETA hybrid hydrogel in pH 7.4 buffers at different salt concentrations ranged from 2,994% to 1,035%, depending on the GMA-chitosan to AETA feed ratio. As the concentration of the salt in buffer increased, i.e., stronger ionic strength, the swelling ratio of the hybrid hydrogel and the GMA-chitosan based hydrogels decreased. For example, GMA-chitosan / AETA-67/33 hybrid hydrogel achieved 2,109% 1,887% and 1,332% swelling ratio in 0.05M, 0.1 M and 0.2M pH 7.4 buffer, respectively, but they were all smaller than the same hybrid hydrogels in deionized water (2,675%).

Moreover, GMA-chitosan / AETA hybrid hydrogels having higher AETA contents showed smaller swelling ratios than those hybrids having smaller AETA contents in deionized water and the 0.05M ionic strength aqueous environment. For example, the swelling ratio of GMA-chitosan/AETA-80/20 hydrogel is about 2,994% in

0.05 M pH 7.4 buffer, while the data of GMA-chitosan/AETA-67/33 in 0.05 M pH 7.4 buffer is 2,109%. However, higher AETA contents in hybrid hydrogel led to larger swelling ratios in 0.1M and 0.2 M pH 7.4 buffer.

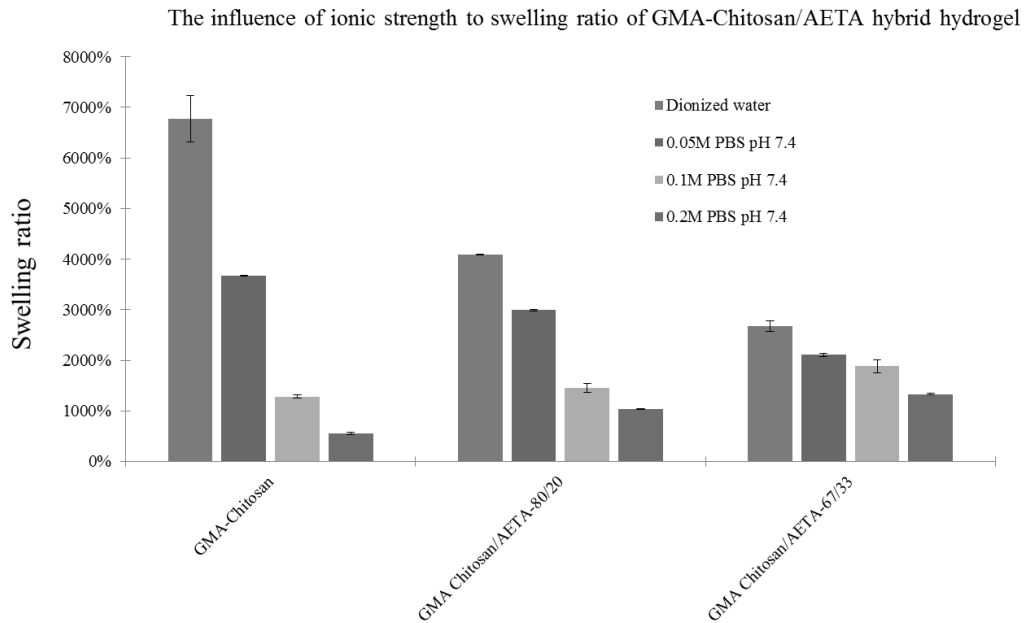


Figure 3.5 The influence of ionic strength of the immersion media to the swelling ratio of GMA-chitosan/AETA hybrid hydrogel of different GMA-chitosan to AETA contents in deionized water and pH 7.4 at room temperature

Many polyelectrolyte hydrogels have the ionic strength responsive swelling behavior²²⁻²⁴. For example, in the study of Poly(L-glutamic acid) (PLG) / Polyethylene glycol (PEG) hybrid hydrogels which have secondary amine groups, Markland et al.²¹ reported that an increase in ionic strength of medium resulted in a reduction in the swelling ratio of the PLG/PEG hydrogels at several different pH (2.5-7). Generally, the extent to which a polyelectrolyte hydrogel swells at equilibrium in a buffer solution depends on the amounts of the ionizable groups of the polyelectrolyte and the ionic strength of the immersion medium. An increase in ionic strength of the medium generally

decreases the difference in concentration of mobile ions between a hydrogel and surrounding medium, which subsequently reduce the osmotic swelling pressure inside a hydrogel, i.e., reduced swelling ratio.

In 0.1M or 0.2M buffer medium, the hybrid hydrogels with higher AETA content achieve higher swelling, i.e. GMA-chitosan/AETA-67/33. Consequently, there are more cationic moieties dispersed in the GMA-chitosan / AETA hybrid hydrogels with higher AETA content. Those cationic quaternary ammonium moiety of AETA is still positively charged (pKa ~10), and the electrostatic repulsion among the quaternary ammonium groups in those hybrids having high AETA contents could result in a higher swelling ratio of the hybrid hydrogel than a pure GMA-chitosan hydrogel. Another factor which could influence the swelling ratio of GMA-chitosan / AETA hybrid hydrogels is their level of the crosslinking density. Because the molecular weight of the chitosan raw material is 50,000-190,000 Da, the GMA grafted onto the chitosan backbone could be relatively “invisible” in the mass of chitosan space due to the shorter spacer between the chitosan backbone and the photo-reactive vinyl end group in GMA pendant group, i.e., lesser level of photocrosslinking. The presence of unsaturated small molecules like AETA in the GMA-chitosan precursor, however, could promote the crosslinking between the methacrylate groups on the GMA-chitosan molecules and AETA. Several published studies have demonstrated that the two component hybrid hydrogel system that contains both water soluble small moiety having vinyl groups and polysaccharide derivative having unsaturated groups is able to achieve a higher crosslinking density than those hydrogels formed by a single component and hence influence the swelling.²¹⁻²³ In Markland et al. study²¹ about Poly(L-glutamic acid)/PEG hybrid hydrogel, the formation of a higher intermolecular crosslinking density resulted in a reduced degree of swelling. An increase in the AETA contents in the GMA-chitosan / AETA hybrid hydrogels could led to higher crosslinking level in a 0.05M buffer or deionized water, i.e, smaller swelling ratio of the hybrid hydrogel (2,994% swelling in 0.05 M pH 7.4 buffer) than a pure

GMA-chitosan hydrogel (3,668% swelling in 0.05M pH 7.4 buffer). This higher crosslinking in the GMA-chitosan / AETA hybrid hydrogels was also reflected in their higher mechanical property as described later.

3.4.4 The influence of pH on the swelling ratio of GMA-chitosan / AETA hybrid hydrogels

Figure 3.6 shows the effect of pH of the medium on the swelling behavior of GMA-chitosan / AETA hybrid hydrogels of different GMA-chitosan to AETA feed ratio at the same ionic strength (0.1M). All GMA-chitosan / AETA hybrid hydrogels and the pure GMA-chitosan hydrogels changed their ability to swell when the environmental pH was altered, i.e., lower swelling at a higher pH. For example, GMA-chitosan/AETA-80/20 hybrid hydrogels achieved 2,187%, 1,732% and 587% swelling ratios in pH 3, 7.4 and 10 buffers, respectively. In an acidic medium (pH 3), both hybrid hydrogels exhibited similar swelling ratios (2,187% for 80/20 and 2,253% for 67/33), but a pure GMA-chitosan hydrogels had the highest swelling ratio (2,592%). However this trend disappeared in a basic medium. In a slightly basic medium (pH 7.4), there was no significant difference in swelling among the 2 types of hybrid hydrogels and the control pure GMA-chitosan hydrogel. In a more basic medium (pH 10), both hybrids showed higher swelling than the pure GMA-chitosan control, particularly the hybrid having higher AETA content, i.e., GMA-chitosan / AETA - 67/33 hybrid hydrogel shows the largest swelling (1,177%) while the swelling data of GMA-chitosan / AETA -80/20 and pure GMA-chitosan are 587% and 317%, respectively.

The swelling ratio of the hydrogels increases only when the amine groups of chitosan and quaternary ammonium groups of AETA are ionized under the condition of low or acidic pH, i.e., protonation. And the pKa of quaternary amine in the GMA-chitosan/AETA is about 10, while the pKa of amine groups of GMA-chitosan is about 7.3-7.6.²⁴ The primary amine groups of GMA-chitosan in these hydrogels deprotonized and the quaternary ammonium groups are partially deprotonized with the increasing

environmental pH from 3 to 10. So, the osmotic pressure inside the hydrogels decreases as the pH increasing. As a consequence, the decrease in swelling with increasing pH from 3 to 10 can be explained in that a dissociation process of amine groups and quaternary ammonium groups in these hydrogels.

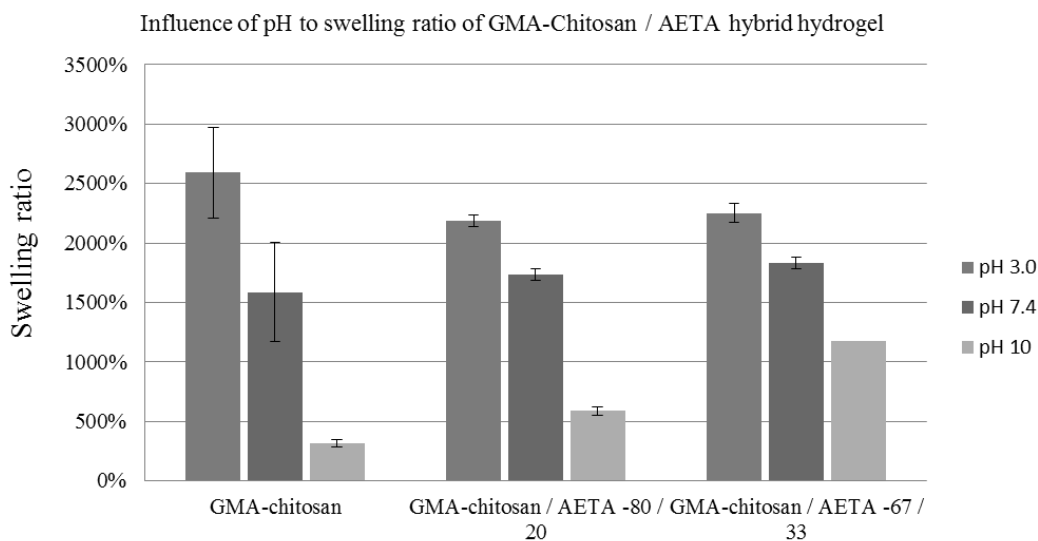


Figure 3.6 The influence of pH environment to the swelling ratio of GMA-chitosan / AETA hybrid hydrogels of different GMA-chitosan to AETA contents in an ionic strength 0.1M aqueous buffer at room temperature.

In the same basic environment (pH 10), the swelling of hybrid hydrogels with more AETA contents (1,177%) is significantly higher than that hybrid hydrogels having lower AETA contents (587%), and much higher than a pure GMA-chitosan hydrogel (317%). The reason is because the primary amine groups of GMA-chitosan hydrogel is deprotonated at pH 10, while the quaternary ammonium groups in AETA can remain partially ionized at pH 10. So, the GMA-chitosan/AETA hydrogel interior is able to keep part of positively charge character at this high pH. The osmotic pressure generated by the

ionized quaternary ammonium groups led to the higher AETA content hybrid hydrogel achieved higher swelling than a lower AETA content hybrid hydrogel.

The pH effect on the swelling property of other polysaccharide-based hydrogels has also been reported^{25,26}. The direction and magnitude of pH effect depend on the type of polysaccharides, particularly their charge characteristic of the ionizable groups. In the Zhong et al.²⁵ study of anionic maleic-chitosan /PEGDA hybrid hydrogels, they also discovered pH-dependent swelling; but the anionic maleic-chitosan/ PEGDA hybrid hydrogel achieved a higher swelling ratio at an alkaline pH than at an acidic condition, opposite to what we observed in the current cationic GMA-chitosan/AETA hybrids. This is because the ionizable groups in maleic-chitosan / PEGDA hybrids is mainly carboxyl group (pKa 1.8-2.4), the osmotic pressure inside the maleic-chitosan/ PEGDA hybrid hydrogels is higher at an alkaline condition as carboxyl groups in maleic chitosan are easier to be ionized (deprotonized) in such an alkaline condition.

3.4.5 Morphology of GMA-chitosan/AETA hybrid hydrogel

GMA-chitosan/AETA hybrid hydrogels also have 3D porous network structure upon swelling. Based on the SEM images in Figure 3.7, the GMA-chitosan/AETA hybrid hydrogel network has pores that exhibit irregular shape and thin wall (Figure 3.7 A & B), and the diameter of the most pores ranges from 20 μm to 50 μm . The micro-structure of GMA-chitosan/AETA hybrid hydrogel shows no apparent difference from a pure GMA-chitosan hydrogel (Figure 3.7 C, pore size ranging from 10 μm to 50 μm).

In the Bhattarai et al. study of the PEG grafted chitosan (PEG-g-chitosan), they reported that an increase in the genipin treatment time to PEG-g-chitosan (i.e., increasing crosslinking density) decreased the porosity of the hydrogel²⁷. But the PEG-g-chitosan shows very irregular pores (about 30 μm diameter) and drastic morphology change after increasing genipin treatment time. When comparing with dextran-based hydrogels^{28, 29}, GMA-chitosan/AETA hybrid hydrogels show more interconnected network structure and larger pore size which could lead to faster drug release rate. In the Sinhee et al. study of

dextran methacrylate hydrogels, the pore size varied from the hydrogel surface to its interior because the dextran methacrylate precursor is not completely transparent and the level of UV radiation strength decreased with increasing depth from the surface. The pores of the hydrogel surface were mainly smaller pores from 2 μm to 25 μm , while the pore size of interior ranged from 10 to 40 μm ²⁹.

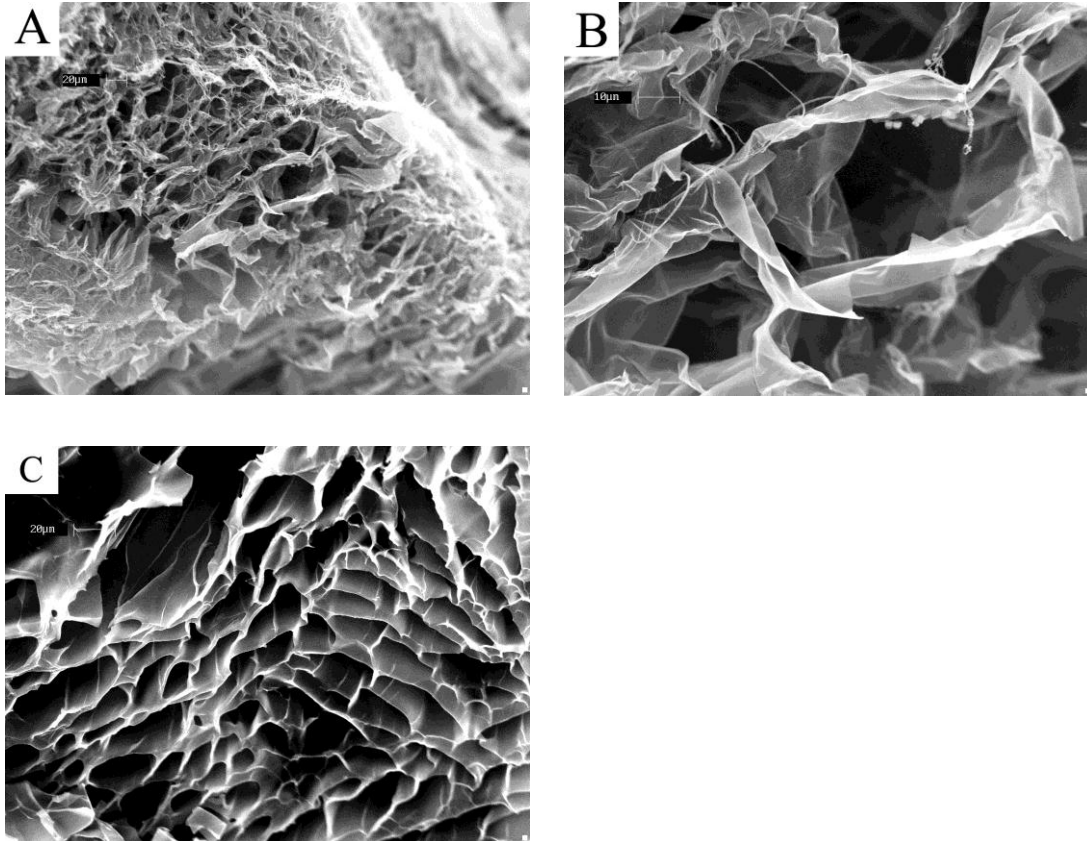


Figure 3.7 SEM images of GMA-chitosan hydrogel and GMA-chitosan/ AETA hybrid hydrogels (A, GMA-chitosan/AETA -67/33 hybrid hydrogel at 500 \times ; B, GMA-chitosan/AETA -67/33 hybrid hydrogel at 2,000 \times ; C, GMA-chitosan hydrogel at 1,000 \times

3.4.6 Compressive mechanical properties of GMA-chitosan/AETA hybrid hydrogel

The compression mechanical data of the GMA-chitosan/ AETA hybrid hydrogels are shown in Table 3.1. In general, the compression moduli of the hybrid hydrogels are significantly higher than the pure GMA-chitosan control, and no significant different

moduli due to different feed ratios of GMA-chitosan to AETA (27.24 ± 3.22 vs. 28.94 ± 4.44 KPa). The compression moduli of the crosslinked GMA-chitosan/ AETA hybrid hydrogels were about 59%-63% higher than that of a pure GMA-chitosan hydrogel (17.64 ± 5.52 KPa). The addition of AETA co-precursor apparently increased the stiffness of the hybrid hydrogel. The reason might also be attributed to a higher level of crosslinking density of the GMA-chitosan/AETA hybrid hydrogels than a pure GMA-chitosan hydrogel due to the presence of the much smaller AETA co-precursor that could facilitate crosslinking reactions. The effect of feed ratio of the 2 precursors on the compression modulus of the GMA-chitosan/AETA hybrid hydrogels appears not apparent, i.e., 28.94 ± 4.44 KPa (GMA-chitosan/AETA at 80/ 20) vs. 27.24 ± 3.22 KPa (GMA-chitosan/AETA at 67/ 33).

Table 3.1 The compression initial modulus of swollen GMA-chitosan hydrogel and GMA-chitosan/AETA hybrid hydrogel at room temperature

Hydrogel samples	Compressive modulus (KPa)
GMA-chitosan	17.64 ± 5.52
GMA-chitosan/AETA-80/20	28.94 ± 4.44
GMA-chitosan/AETA-67/33	27.24 ± 3.22

The compression moduli of the GMA-chitosan/AETA hybrid hydrogels are lower than the Zhong et al.²⁵ recently reported a new family of anionic maleic chitosan/polyethylene glycol diacrylate (PEGDA) hybrid hydrogels fabricated in the similar manner as the current UV-crosslinking method. The initial modulus of anionic maleic chitosan / PEGDA (MW 8,000) hybrid hydrogel at 1:2 feed ratio is 61 ± 1.9 KPa. This value is about 1~2 times higher than the current GMA-chitosan / AETA hybrid hydrogel, probably due to the fact that the high composition of PEGDA in maleic chitosan / PEGDA hybrid hydrogel can lead to a higher crosslinking density than that of the GMA-chitosan / AETA hybrid hydrogels. Different from GMA-chitosan /AETA

hybrid hydrogel, the mechanical property of the maleic chitosan/PEGDA hybrid hydrogels largely depended on the molecular weight of the PEGDA co-precursor and the content of PEGDA in the hybrid hydrogel. The composition of PEGDA in the Zhong et al. maleic chitosan hybrid hydrogel is higher than 50%, while the AETA co-precursor composition in the current GMA-chitosan/AETA hybrids are no more than 33% for the purpose of retaining more physiochemical characteristics of chitosan in the hybrids through a higher GMA-chitosan composition.

3.4.7 Enzymatic degradation of GMA-chitosan/AETA-67/33 hybrid hydrogels.

The biodegradation behavior of GMA-chitosan/AETA-67/33 hybrid hydrogels was evaluated in terms of their weight loss in both pure PBS control and lysozyme solution of pH 7.4 at 37 °C over a period of 18 days. The total weight loss of these hydrogels ranged from as high as 45% to as low as 35% over the period of 18 days, depending on the hybrid vs. pure hydrogels and enzymes vs. PBS medium. Figure 3.8 shows that GMA-chitosan/AETA-67/33 hybrid hydrogels in the presence of 1 mg/mL lysozyme were degraded faster than the same hybrid hydrogel in the PBS. GMA-chitosan/AETA-67/33 hybrid hydrogels lost 40.7% of original weight in 1 mg/mL lysozyme solution, but 34.2% in PBS after 10 days incubation at 37°C. Compared to the biodegradation profiles of a pure GMA-chitosan hydrogel, GMA-chitosan/AETA-67/33 hybrid hydrogel was degraded slightly slower in PBS (i.e. 1.5~4% less weight loss) and in 1mg/mL lysozyme solution (i.e. 1.9~4% less weight loss) at the same incubation time.

Lysozyme naturally presents in wound fluid and secretions. Chitosan derivatives are hydrolyzed in vivo by lysozyme to oligomers.³⁰ Lysozyme is able to cleave GMA-chitosan backbone structure at the β (1, 4) linked glucosamine unit and N-acetyl-D-glucosamine unit.³² The biodegradation of GMA-chitosan based hydrogel has two mechanisms simultaneously happened in the presence of lysozyme: (1) the chitosan polymer backbone was cleaved by lysozyme and (2) the ester bonds of methacrylate group on GMA-chitosan was degraded by hydrolysis. The accessibility of the enzyme to

polysaccharide-based hydrogel is one key factor to influence the biodegradation rate because lysozyme needs to target N-acetyl-D-glucosamine unit of chitosan to proceed the degradation³¹. Lysozyme is a 14.4 KDa protein with an isoelectric point 11.2 which is mainly positively charged in water solution.³² The presence of electrostatic repulsion between lysozyme and GMA-chitosan/AETA may led to a slower biodegradation of GMA-chitosan/AETA-67/33 hybrid hydrogel than a pure GMA-chitosan hydrogel because the strong positively charged AETA moiety increased the difficulty of lysozyme to target the specific N-acetyl-D-glucosamine site of chitosan. The higher crosslinking density of GMA-chitosan/AETA hybrid hydrogel than a pure GMA-chitosan which is also reflected in the lower Q_{eq} is another factor also contributed to a slower degradation

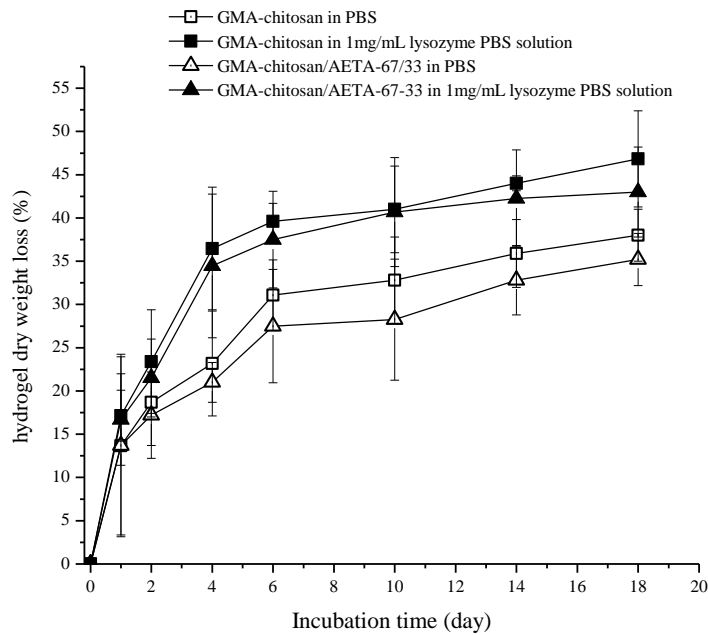


Figure 3.8 *In vitro* enzymatic degradation of GMA-chitosan hydrogel and GMA-chitosan/AETA-67/33 hybrid hydrogel at 37°C, pH 7.4, 0.05M PBS. The solid symbol: degradation of hydrogels with the presence of 1mg/mL lysozyme; open symbol: degradation of hydrogel control samples in PBS. The DS of GMA-chitosan composition is 37.)

rate in the GMA-chitosan/AETA hybrid hydrogels than a pure GMA-chitosan hydrogel in 1 mg/mL lysozyme PBS solution.

The enzymatic biodegradability of GMA-chitosan/AETA hybrid hydrogels could overcome the poor biodegradability of synthetic pH-sensitive polymers for implantable drug delivery agents or implantable biosensors.¹⁷ The combination of pH-sensitivity and biodegradability of GMA-chitosan/AETA hybrid hydrogel can provide an alternative biomaterial for these applications.

3.4.8 BSA release from GMA-chitosan/AETA hybrid hydrogel at pH 3 and pH 7.4

The BSA release profiles from the GMA-chitosan/AETA-67/33 hybrid hydrogels are shown in Figure 3.9. Both GMA-chitosan/AETA hybrid hydrogels and GMA-chitosan hydrogel show burst releases in the first hour of immersion in a pH 3 and 7.4 media, but the hybrid hydrogels showed significantly lower BSA burst release amounts than a pure GMA-chitosan hydrogel at pH 7.4, i.e., 12.0% BSA release from GMA-chitosan/AETA hybrid vs. 32.8 % release from a pure GMA-chitosan hydrogel in the first hour. This significantly lower BSA release rate from the GMA-chitosan/AETA hybrid hydrogels persisted over the entire period of study (11 days). At the end of 11 day, 56% BSA released from the hybrids vs. 88% BSA released from a pure GMA-chitosan hydrogel at pH 7.4. However, the BSA release profiles between GMA-chitosan/AETA-67/33 hybrid hydrogels and pure GMA-chitosan hydrogels are very close at pH 3.

This difference in BSA release profiles at pH 3 and 7.4 is related to pH-responsive property of the hybrid hydrogels and the electrostatic interaction between anionic BSA and cationic hybrid hydrogel structure. The isoelectric point of BSA is about 4.7, and in pH 7.4 PBS, BSA is a negative charge protein of 60,000-70,000 molecule weight.³³ The quaternary ammonium group in the AETA segment of the hybrid hydrogels has pKa ~10, i.e., exhibiting strong positive charge in pH 7.4 PBS, i.e., the GMA-chitosan/AETA-67/33 hybrid hydrogel shows positively charge in a pH 7.4 buffer which could provide stronger electrostatic attraction to the anionic BSA than a pure GMA-

chitosan alone i.e., resulting in a slower and more sustained BSA release from the hybrid hydrogels in this pH level, even though some weak attractions may exist between anionic BSA and cationic GMA-chitosan macromolecules. The cationic nature of GMA-chitosan depends on the amounts of primary amine groups (deacetylation level of chitosan) on the deacetylated chitosan repeat unit, and this primary amine has pKa 7.3-7.6, i.e., a weak cationic in a pH 7.4 medium.

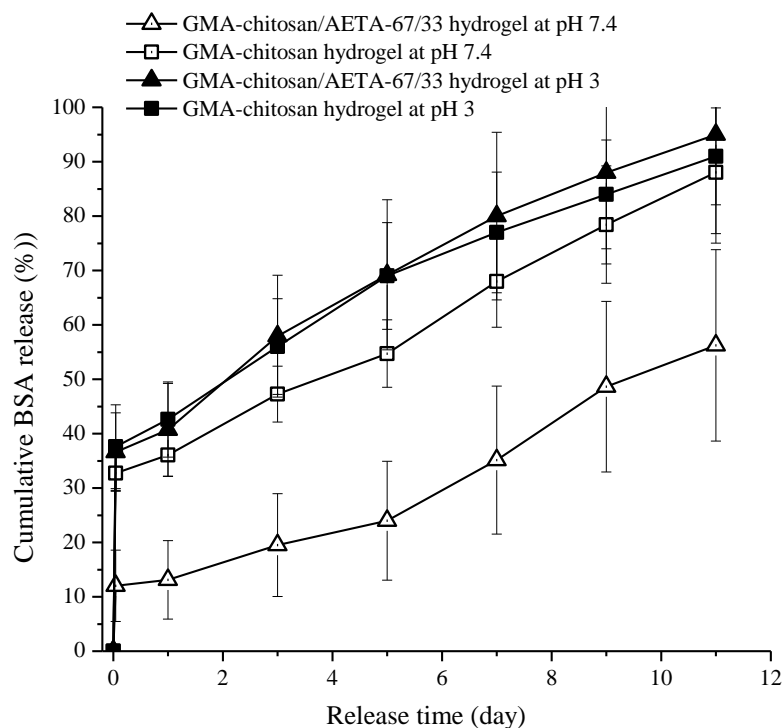


Figure 3.9 Cumulative BSA release profile from GMA-chitosan/AETA-67/33 hybrid hydrogels and GMA-chitosan hydrogel in buffer solutions at 37°C. The solid symbol: BSA release at pH 3, 0.05 M; open symbol: BSA release at pH 7.4, 0.05 M.

At pH 3, the negative charge character of BSA is largely decreased, hence the electrostatic attraction between BSA and cationic GMA-chitosan/AETA-67/33 hybrid hydrogel also decreased, i.e., the advantage of AETA for electrostatic attraction for BSA disappeared. Hence, the BSA release profile of the GMA-chitosan/AETA-67/33 hybrid

hydrogel became similar to that of the pure GMA-chitosan hydrogel at pH 3. The loss of the advantage of electrostatic attraction between BSA and GMA-chitosan/AETA hybrid hydrogels at pH 3 also resulted in a faster BSA release from the hybrid than that of pH 7.4.

pH-sensitive hydrogels have been most frequently used to develop controlled released formulation for oral administration. For example, the pH in the stomach (< 3) is quite different from the neutral pH in the intestine and such a difference is able to elicit pH-dependent drug release behavior from GMA-chitosan/AETA hybrid hydrogels. Another advantage of the current photo-crosslinking fabrication method of protein-impregnated GMA-chitosan/AETA hybrid hydrogels is that water soluble protein drug can be pre-loaded into the hydrogel precursor aqueous solutions before gelation, and hence provides a more homogeneous and uniform loading without the adverse effect of organic solvents. Many other chemically crosslinking methods must follow a post-loading method to prevent the undesirable side reactions between hydrogel precursors, crosslinkers and drugs.^{34, 35}

For example, the dextran hydrogel crosslinked by epichlorohydrin, phosphorus oxychloride and *N, N'*-methylenebisacrylamide is only suitable for protein post-loading method, because the epoxy group of epichlorohydrin is also able to react with the amine or hydroxyl groups of protein which can change the protein chemistry structure and lead to a unpredictable release dynamics.³⁶ A post-loading method can also lead to non-homogeneous and non-uniform drug distribution within the hydrogel matrix as most of the post-loaded drugs stay near the surface of the hydrogels. It usually leads to lower drug loading efficiency and shorter drug release period. In our study, GMA-chitosan /AETA hybrid hydrogels and GMA-chitosan hydrogels achieved at least 11 days sustained release of BSA, whereas, the reported release of post-protein loaded dextran-based hydrogels could only last several hours.²⁰

3.5 Conclusions

A new family of cationic biodegradable GMA-chitosan/AETA hybrid hydrogels was successfully designed and fabricated in an aqueous medium via UV photocrosslinking. The cationic GMA-chitosan/AETA hybrid hydrogels have 3D porous microstructure and a high capacity of water absorption. By varying the feed ratio of GMA-chitosan to AETA, the swelling (from 297.8% to 3318.2%, depending on pH and ionic strength) and mechanical (compressive modulus, $17.649 \pm 0.78 \sim 18.103 \pm 1.30$ KPa) properties of this hybrid hydrogel system could be adjusted. GMA-chitosan/AETA hybrid hydrogels and GMA-chitosan hydrogels achieve their largest swelling ratio in a lower pH PBS solution and lower ionic strength environment due to the balance of osmotic pressure of the hydrogel interior and exterior solution environment. Lysozyme was able to effectively accelerate the GMA-chitosan/AETA hybrid hydrogel biodegradation in aqueous media. A sustained and pH responsive release of BSA can be achieved from GMA-chitosan/AETA hybrid hydrogels in 11 days in vitro. This newly developed cationic GMA-chitosan/AETA hybrid hydrogel system offers the advantage in terms of water soluble precursors for pre-loading therapeutic protein, flexible mechanical property, pH responsive release behavior and biodegradability.

Acknowledgements

The authors would like to thank the support of Vincent V.C. Woo Fellowship to Mingyu He that made this study possible.

References:

- 1 Oungbho, K., Muller, B.W., 1997. Chitosan sponges as sustained release drug carriers. *Int. J. Pharm.* 156, 229–237.
- 2 Bernkop-Schnurch, A., 2000. Chitosan and its derivatives: potential excipients for peroral peptide delivery systems. *Int. J. Pharm.* 194, 1–13.
- 3 Chenite, A., Buschmann, M., Wang, D., Chaput, C., Kandani, N., 2001. Rheological characterization of thermogelling chitosan/glycerol-phosphate solutions. *Carbohydr. Polym.* 46, 39–47.

- 4 Douglas, K. L., Tabrizian, M. (2005). Effect of experimental parameters on the formation of alginate–chitosan nanoparticles and evaluation of their potential application as DNA carrier. *Journal of Biomaterials Science, Polymer Edition*, 16, 43–56.
- 5 Kazunori Yamada et al, 2000, Chitosan Based Water-Resistant Adhesive. Analogy to Mussel Glue, *Biomacromolecules*, 1, 252-258
- 6 F.L. Mi, Y.C. Tan, H.F. Liang, H.W. Sung, 2002, In vivo biocompatibility and degradability of a novel injectable-chitosan-based implant, *Biomaterials* 23, 181-191.
- 7 H. Tan, C.R. Chu, K.A. Payne, K.G. Marra, Injectable in situ forming biodegradable chitosan-hyaluronic acid based hydrogels for cartilage tissue engineering, *Biomaterials* 30, 2009, 2499–2506.
- 8 Lihui Weng, Alexander Romanov, Jean Rooney, Weiliam Chen, 2008, Non-cytotoxic, in situ gelable hydrogels composed of N-carboxyethyl chitosan and oxidized dextran, *Biomaterials* 29, 3905–3913
- 9 K. Ono, Y. Saito, H. Yura, K. Ishikawa, A. Kurita, T. Akaike, M. Ishihara, Photocrosslinkable chitosan as a biological adhesive, *J. Biomed. Mater. Res.* 2000, 49, 289–295.
- 10 H.S. Yoo, 2007, Photo-cross-linkable and thermo-responsive hydrogels containing chitosan and pluronic for sustained release of human growth hormone (hGH), *J. Biomater. Sci. Polym. Ed.* 18 1429–1441.
- 11 Yi Hong, Haiqing Song, Yihong Gong, Zhengwei Mao, Changyou Gao, Jiacong Shen, Covalently crosslinked chitosan hydrogel: Properties of in vitro degradation and chondrocyte encapsulation, 2007, *Acta Biomaterialia*, 3, 23–31
- 12 Yi Hong, Zhengwei Mao, Hualin Wang, Zhengwei Mao, Changyou Gao, Jiacong Shen, Covalently crosslinked chitosan hydrogel formed at neutral pH and body temperature, 2006, *Journal of Biomaterials Research Part A*, 79A, 4, 913-922
- 13 Flores-Ramirez et al, 2005, Characterization and degradation of functionalized chitosan with glycidyl methacrylate, *J Biomater Sci Polym Ed*, 16(4):473-88.

- 14 Jing Han, Kemin Wang, Dongzhi Yang, Jun Nie, 2009, Photopolymerization of methacrylated chitosan/PNIPAAm hybrid dual-sensitive hydrogels as carrier for drug delivery, *International Journal of Biological Macromolecules*, 44, 229–235
- 15 Rhongsheng Zhang, Mingguo Tang, Adrian Bowyer, Robert Eisenhals, John Hubble, A novel pH- and ionic-strength-sensitive carboxy methyl dextran hydrogel, *Biomaterials*, 2005, 26, 4677-4683
- 16 Seon Jeong Kim, Chang Kee Lee, Young Moo Lee, In Young Kim, Sun I. Kim, Electrical / pH-sensitive swelling behavior of polyelectrolyte hydrogels prepared with hyaluronic acid–poly(vinyl alcohol) interpenetrating polymer networks, *Reactive & Functional Polymers*, 2003, 55, 291-298
- 17 Yong Qiu, Kinam Park, Environment-sensitive hydrogels for drug delivery, *Advanced Drug Delivery Reviews*, 2001, 53, 321-329
- 18 El-Refaie Kenawy, Fouad I. Abdel-Hay, Abd El-Raheem R. El-Shanshoury, Mohamed H. El-Newehy, Biologically active polymers: synthesis and antimicrobial activity of modified glycidyl methacrylate polymers having a quaternary ammonium and phosphonium groups, *Journal of Controlled Release*, 1998, 50, 145-152
- 19 V.R. Patel, M.M. Amiji, Preparation and characterization of site-specific antibiotic delivery in the stomach, *Pharm. Res.* 1996, 13, 588–593.
- 20 Eun Seok Gil, Jianshu Li, Huining Xiao, Tao Lu Lowe, Quaternary ammonium β -cyclodextrin nanoparticles for enhancing doxorubicin permeability across the in vitro blood-brain barrier, *Biomacromolecules*, 2009, 10, 3, 505-516
- 21 Markland P, Zhang Y, Amidon GL, Yang VC, A pH- and ionic strength-responsive polypeptide hydrogel: synthesis, characterization, and preliminary protein release studies, *J Biomed Mater Res*, 1999, 15, 47, 595-602
- 22 Sinan Oren, Tuncer Caykara, Omer Kantoglu, Olgun Guven, Effect of pH, Ionic Strength, and Temperature on Uranyl Ion Adsorption by Poly(N-vinyl 2-pyrrolidone-g-tartaric Acid) Hydrogels, *Journal of applied polymer science*, 78, 12, 2219-2216

- 23 Sun Namkung, Chih-Chang Chu, Effect of solvent mixture on the properties of temperature and pH sensitive polysaccharide –based hydrogel, *J Biomater Sci Polymer Edn*, 2006, 17, 5, 519-546
- 24 Qi Zhao Wang, Xi Guang Chen, Nan Liu, Shi Xi Wang, Cheng Sheng Liu, Xiang Hong Meng, Chen Guang Liu, Protonation constants of chitosan with different molecular weight and degree of deacetylation, *Carbohydrate polymers*, 2006, 65, 194-201
- 25 Chao Zhong, Jun Wu, C.A. Reinhart-King, C.C. Chu, Synthesis, characterization and cytotoxicity of photo-crosslinked maleic chitosan–polyethylene glycol diacrylate hybrid hydrogels, *Acta Biomaterialia*, 2010, 6, 3908-3918
- 26 G. M. Sun, X. Z. Zhang, C. C. Chu, Formation and Characterization of Chitosan-Based Hydrogel Films with both Temperature and pH Sensitivity, *J. Mater. Sci. Mater. in Medicine*, 2007, 18, 1563-1577
- 27 Narayan Bhattarai, Hassna R. Ramay, Jonathan Gunn, Frederick A. Matsen, Miqin Zhang, PEG-grafted chitosan as an injectable thermosensitive hydrogel for sustained protein release, 2005, 103, 3 609-624
- 28 S.H. Kim, C.Y. Won, C.C.Chu, Synthesis and characterization of dextran-based hydrogel prepared by photocrosslinking, *Carbohydrate Polymer*, 1999, 40, 183-190
- 29 Sin-hee Kim, Chih-Chang Chu, Fabrication of a Biodegradable Polysaccharide Hydrogel With Riboflavin, Vitamin B₂, as a Photo-Initiator and L-Arginine as Coinitiator Upon UV Irradiation, *Journal of Biomedical Materials Research Part B: Applied Biomaterials*, 2009, 91B, 1, 390-400
- 30 Dinesh K Singh, Alok R Ray, Biomedical Applications of Chitin, Chitosan, and Their Derivatives, *Journal of Macromolecular Science, Part C: Polymer Reviews*, 2000, 40:1, 69-83
- 31 Shigehiro Hirano, Hisaya Tsuchida, Norio Nagao. N-acetylation in chitosan and the rate of its enzymic hydrolysis. *Biomaterials*. 1989; 10 (8) : 574-576.

- 32 Daniel E. Kuehner, Jan Engmann, Florian Fergg, Meredith Wernick, Harvey W. Blanch, and John M. Prausnitz, Lysozyme Net Charge and Ion Binding in Concentrated Aqueous Electrolyte Solutions, *J. Phys. Chem. B* 1999, 103, 1368-1374
- 33 Z.G. Peng, K. Hidajat, M. S. Uddin, Adsorption of bovine serum albumin on nanosized magnetic particles, *Journal of Colloid and Interface Science*, 2004, 271, 277-283
- 34 Xianzheng Zhang, Da-qing Wu, Chih-Chang Chu, Synthesis, characterization and controlled drug release of thermosensitive IPN-PNIPAAm hydrogels, *Biomaterials*, 2004, 25, 3793-3805
- 35 Bradley K. Wacker, Evan A. Scott, Megan M. Kaneda, Shannon K. Alford, and Donald L. Elbert, Delivery of Sphingosine 1-Phosphate from Poly(ethylene glycol) Hydrogels, *Biomacromolecules* 2006, 7, 1335-1343
- 36 Dilek Imren, Menemse Gumusderelioglu, Ali Guner, In Vitro Release Kinetics of Bovine Serum Albumin from Highly Swellable Dextran Hydrogels, *Journal of Applied Polymer Science*, 2009, 115, 740-747

CHAPTER FOUR:
SYNTHESIS AND CHARACTERIZATION OF WATER SOLUBLE GLYCIDYL
METHACRYLATE CHITOSAN AND VINYL SULFONIC ACID AND THE
FABRICATION INTO HYBRID HYDROGEL IN AQUEOUS MEDIUM

4.1 Abstract

A new family of cationic hybrid hydrogels from positively charged glycidyl methacrylate-chitosan (GMA-chitosan) and vinyl sulfonic acid (VSA) was developed via a photocrosslinking fabrication method. The chemical composition and mechanical property of GMA-chitosan / VSA hybrid hydrogels were characterized by fourier transform infrared spectroscopy (FTIR) and dynamic mechanical thermal analysis (DMA). Optical transparent GMA-chitosan / VSA hydrogel with high water absorbent capacity was synthesized from GMA-chitosan / VSA aqueous precursor with tunable feed ratio by using photo-crosslinking technique. The compression modulus of GMA-chitosan / VSA hybrid hydrogel is lower than that of pure GMA-chitosan hydrogel.

The morphology of GMA-chitosan / VSA hybrid hydrogel was examined by scanning electron microscopy (SEM). GMA-chitosan / VSA hybrid hydrogel shows ionic strength responsible swelling behavior due to the presence of the negative charge in the interior. The incorporation of negatively charged sulfonic group makes GMA-chitosan / VSA hybrid hydrogel sustained protein release rate and thoroughly release at low protein concentration. GMA-chitosan / VSA hybrid hydrogel has promising application in the protein drug delivery.

4.2 Introduction

4.2.1 Glycosaminoglycans

Glycosaminoglycans (GAGs) are linear polysaccharides that can be divided into two main types, non-sulphated GAGs such as hyaluronic acid (HA), sulphated GAGs including chondroitin sulphate (CS), dermatan sulphate (DS), keratan sulphate (KS), heparin and heparan sulphate (HS). GAGs differ according to the type of hexosamine, hexos and hexuronic acid unit that they contain, as well as the geometry of the glycosidic linkage between the units. CS and DS which contain galactosamine are called galactosaminoglycans, whereas heparin and HS, which contain glucosamine, are called

glucosaminoglycans. The amino sugar may be sulphated on carbon 4 or 6 or on the non-acetylated nitrogen. As a result, the sugar backbone of GAGs can be sulphated at various positions and have numerous sulphation sequences. At physiological pH, all carboxylic acid and sulphate groups are deprotonated, giving GAGs very high negative charge densities¹. GAGs play a major role in cell signaling and development, angiogenesis, axonal growth, tumor progression, metastasis and anti-coagulation because they act as co-receptors for growth factors of the fibroblast growth factor (FGF) family. Anti-coagulation was the first described function for sulphated GAGs. Moreover, sulphated GAGs are a common constituent in many different types of amyloid, playing an important role in the pathology of amyloid diseases such as amyloid A-amyloidosis, Alzheimer's disease, type-2 diabetes, Parkinson's disease and prion diseases which are characterized by the deposition in tissues of fibrillar aggregates of polypeptides². Diseases such as rheumatoid arthritis, inflammatory bowel disease and microbial infections are associated with inflammatory responses. Glycosaminoglycans such as heparin have important roles in these processes, as adhesion ligands in leukocyte extravasation and carriers/presenters of chemokines and growth factors.

In nature, all GAG chains with the exception of HA are covalently linked to a core protein to give a Proteoglycans (PG). These saccharide residues are coupled to the protein core through an O-glycosidic bond to a serine residue. Some forms of KSs are linked to the protein core through an N-asparaginyl bond. The highly sulphated analogues heparin and HS have been studied extensively due to their functions in anticoagulation. Heparin is a linear, unbranched polysaccharide that tends to have an extended conformation in solution because of its highly hydrophilic nature arising from its extensive degree of sulphation. Heparan sulphate contains a higher level of acetylated glucosamine and is less sulphated than heparin.

On the cell surface, the O-sulphonate and N-sulphonate groups are deprotonated in HS and attract positively charged counter ions to form a salt under physiological

condition. Structure and sequence-based statistical analyses indicate that Asp, Glu, Gln, Arg, His and Trp are more likely to make up the binding sites for non-sulphated carbohydrates than other amino acids. The aromatic residue Trp has a significantly higher mean solvent accessibility in carbohydrate binding locations, whereas aliphatic residues Ala, Gly, Ile and Leu, hydrophobic residues which are usually buried inside proteins, do not appear to participate in sugar binding. The aromatic ring in Trp can pack against the hydrophobic face of a sugar molecule. Strong ionic interactions are expected between GAGs and proteins. Clusters of positively charged basic amino acids on proteins form ion pairs with spatially defined negatively charged sulphate or carboxylate groups on heparin chains. Glycosaminoglycans interact with residues that are prominently exposed on the surface of proteins. The main contribution to binding affinity comes from ionic interactions between the highly acidic sulphate groups and the basic side chains of arginine, lysine and, to a less extent, histidine³. The relative strength of heparin binding by basic amino acid residues has been compared and arginine has been shown to bind 2.5 times more tightly than lysine. The guanidino group in arginine forms more stable hydrogen bonds as well as stronger electrostatic interactions with sulphate groups. The ratio of these two residues is said to define, in part, the affinity of a binding site in a protein for GAGs⁴. The periodicity of sulphate group cluster in an oligosaccharide chain can play a key role in determining the structure of the GAG binding site on the surface of either α -helical or β -sheet proteins. The relative proportion of N- and O-linked sulphate groups and N-linked acetyl groups in heparin / HS can influence their interaction with proteins too.

4.2.2 The interaction of polysaccharide and protein

Protein adsorption on material's surface is generally regarded as a primary event that occurs when the material comes into contact with biological surroundings. In some cases, this type of biofouling is detrimental to technologies that require precise manipulation of

proteins, such as controlling cell organization, screening of DNA and protein libraries and blood contacting devices. On the other hand, it is beneficial to wound healing application which demands plasma protein absorption and platelet adhesion and activation⁵.

The carbohydrate-protein interactions may be mimicked by designing small molecule drugs with appropriate binding affinity and selectivity. The binding affinity of carbohydrate-protein interactions are in the mili- to micromolar range. Consequently, synthetic compounds have been specifically designed to mimic the structure and interactions of carbohydrates. The design of GAG mimetics requires an understanding of the mechanism and specificity of a given GAG-protein interaction. The specificity of GAG-protein interactions is governed by the ionic interactions of the sulfate and carboxylate groups with the basic amino acids on the protein as well as the optimal structural fit of a GAG chain into the binding site of the protein^{6,7}.

The development of chemical modification strategies lead to material's surface having desirable biofouling characteristics. Researchers have reported that the incorporation of sulfonate groups into hydrogel reduced protein absorption or platelet adhesion due to their negative charge in aqueous solutions⁷. Chitosan is a partially deacetylated form of chitin, a natural substrate found abundantly in the exoskeletons of insects, shell of crustaceans and fungal cell walls. The repeat units of chitosan are β -(1, 4)-linked glucosamines that constitute a large number of hydroxyl and amino groups which offer several possibilities for derivatization and immobilization of biological active species. Under acidic conditions, chitosan in its original form adopts a positive charge which can attract negatively charged plasma proteins leading to platelet adhesion and activation followed by thrombus formation and blood coagulation^{8,9}. It was revealed that blood compatibility of a chitosan surface can be improved by complexation-interpenetration methods using sulfonate derivative of poly (ethylene glycol)¹⁰. Taking advantage of functional group availability in the formation of chitosan based hydrogel,

this research aims to tailor protein adsorption and release of the hydrogel in aqueous media by introducing sulphate groups.

In this study, we developed a chitosan based hydrogel with sulfonic groups and investigate the properties change brought by adding VSA component in the hydrogel and the possibility to use the hybrid hydrogel as protein drug release material.

4.3 Experimental

4.3.1 Materials

Chitosan (75-85% deacetylated) of molecular weight (MW) 50,000-190,000 Da, vinyl sulfonic acid (VSA) sodium salt solution (25 wt% in aqueous solution) and Bovine serum albumin (BSA) of molecular weight ~66,000 Da and Irgacure 2959 (ACS reagent) were purchased from Sigma Chemical Company (St.Louis, MO). Glycidyl methacrylate (GMA, 97%), 4-(N, N-dimethylamino) pyridine (DMAP, 99%), toluene sulfonic acid monohydrate (TsOH·H₂O), dimethyl sulfoxide (DMSO) were purchased from VWR Scientific (West Chester, PA). Ethyl acetate, acetone were purchased from Mallinckrodt incorporation (St.Louis, MO) and used without further purification. The DMSO, DMAc, toluene, isopropyl alcohol, ethyl acetate and acetone were ACS grade. Disodium hydrogen phosphate, sodium chloride, Sodium dihydrogen phosphate monohydrate were purchased from VWR Scientific (West Chester, PA) to prepare buffer solutions with different ionic strength (i.e. 0.05M, 0.1M, 0.2M). MicroBCA kit was purchased from Thermo Fisher Scientific (Waltham, MA). Irgacure 2959 was donated by Ciba Specialty Chemicals Corp.

4.3.2 Methods

4.3.2.1 Synthesis of glycidyl methacrylate chitosan (degree of substitution 37)

In order to prepare glycidyl methacrylate chitosan (GMA-chitosan), chitosan was first dissolved in DMSO to acquire 1.5wt%~2wt% solution at a comparatively mild

acidic pH (pH 3.5). Then, glycidyl methacrylate and DMAP was added into the chitosan DMSO solution. The epoxy groups of GMA reacted with hydroxyl groups in chitosan. Through this reaction, the unsaturated double bond of the methacrylate group was introduced onto the chitosan backbone which could be used for a further photocrosslinking reaction.

In a typical synthesis, 1.5 g chitosan and 1.2 g TsOH·H₂O were dissolved in 150 mL DMSO at 50 °C under magnetic stirring for 6 h. The dissolution is preceded by protonation of NH₂ groups to give a toluene sulfonic acid salt adduct. After chitosan formed a clear solution, 0.5 g DMAP was dissolved in 5 mL DMSO and then added into the chitosan DMSO solution with rapid stirring. The mixture solution was then cooled down to room temperature, 3.6 g of glycidyl methacrylate was added in. The reaction was continued at 35 °C for 48 hours with magnetic stirring. Afterwards, the reaction was stopped by adding 2 molar ratio amounts of TsOH·H₂O to neutralize the DMAP. GMA-chitosan was precipitated in 600mL ethyl acetate and dried in vacuum oven at room temperature for 2 hours. The raw gel-like GMA-chitosan was cut into 1.5~2 mm cubic pieces and was completely washed by Soxhlet's extraction with acetone for 8h. The residue TsOH, DMAP and GMA are all have very large solubility in acetone and could be removed in this purification step. Finally, the GMA-chitosan was dried in vacuum oven at room temperature overnight.

According to the H-NMR data, the degree of substitution of GMA-chitosan synthesized as described is about 37. (The degree of substitution, DS; the amount of methacrylate groups per 100 chitosan repeat unit). The GMA-chitosan with degree of substitution 37 is used for all the GMA-chitosan / VSA study to achieve good solubility in the aqueous precursor and good mechanical properties of formed hydrogel.

4.3.2.2 Fabrication of GMA-chitosan/VSA hybrid hydrogel and bovine serum albumin (BSA) loaded hybrid hydrogel fabrication

To fabricate GMA-chitosan hydrogel, GMA-chitosan was dissolved in deionized water at room temperature to obtain a final homogenous solution with 7% w/v concentration. To this solution, Irgacure 2959 was added as a photo-initiator at room temperature and mixed well. The mixture aqueous solution was transferred onto a Teflon® mold and irradiated by a long wavelength UV light (100 watts, 365nm) for about 30 mins at room temperature until a solid hydrogel was formed (12 mm diameter, 6 mm thickness). To fabricate GMA-chitosan hybrid hydrogel with VSA, 0.3g GMA-chitosan (synthesized as described before, degree of substitution 37) was dissolved in about 2 mL water and mixed well with desired amount of vinyl sulfonic acid (VSA) aqueous solution (The weight ratio of GMA-chitosan could be any ratio with GMA-chitosan content no less than 67/33 to achieve good integrity of hybrid hydrogel and proper mechanical strength, the feed ratio used in further hybrid hydrogel studies of GMA-chitosan/VSA are 80/20, 67/33). The detailed composition of GMA-chitosan/VSA hybrid hydrogel precursor is shown in Table 4.1. 5 mg Irgacure 2959 was added into the solution as photo-initiator and mixed well at room temperature. Every 250µL mixture aqueous solution was transferred onto a Teflon® mold and irradiated by a long wavelength (100 watts, 365nm) UV light at room temperature until a disk-shaped hydrogel was obtained (12 mm diameter, 6 mm thickness). The chemical structures of GMA-chitosan/VSA hydrogels are presented in Figure 4.1. The hydrogels were soaked in deionized water for 16 hours at room temperature to remove the unreacted GMA-chitosan and residue of VSA.

BSA loading method: calculated volume of 15 mg/mL BSA aqueous solution was added in 2 mL GMA-chitosan hydrogel precursor or 2 mL GMA-chitosan/VSA hydrogel precursor. (The weight ratio of GMA-chitosan/VSA is no less than 67/33) and mixed well after 10 mins magnetic stirring. Then, the precursor with BSA loaded was UV-crosslinked by using long wavelength (100 watts, 365nm) UV light for 30 mins with 5mg Irgacure 2959.

Table 4.1 Compositions of GMA-chitosan in GMA-chitosan / VSA hybrid hydrogel precursor

	Weight of GMA-chitosan (g)	Deionized water used to dissolve GMA-chitosan (g)	Weight of VSA in hybrid hydrogel precursor (g)	Weight of VSA aqueous solutions added in hybrid hydrogel precursor (g)
GMA-chitosan /VSA-80/20	0.4	6.2	0.1	0.4
GMA-chitosan /VSA-67/33	0.4	5.7	0.2	0.8
GMA-chitosan	0.4	6.5	0	0

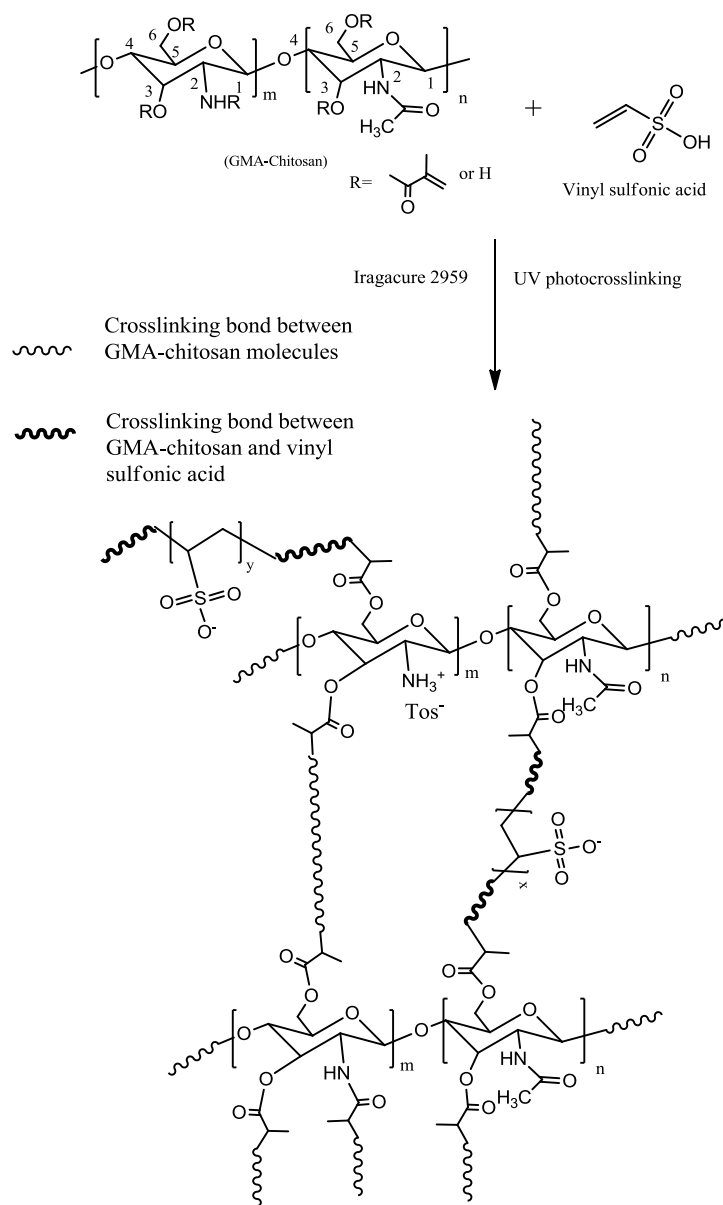


Figure 4.1 Fabrication of GMA-chitosan / VSA hybrid hydrogel

4.3.2.3 Fourier Transform Infrared (FTIR) characterization of GMA-chitosan/VSA hybrid hydrogel

Freeze-dried GMA-chitosan hydrogel, GMA-chitosan/VSA hybrid hydrogel were analyzed by fourier transform infrared (FTIR). Individual GMA-chitosan/VSA hybrid hydrogel were soaked in deionized water at room temperature to reach its

swelling equilibrium and freeze-dried for 24 hours. The spectra of dry GMA-chitosan/VSA hybrid hydrogel were recorded and compared with the GMA-chitosan hydrogel FTIR. All of FTIR spectra were recorded on a PerkinElmer (Madison, WI) Nicolet Magna 560 FTIR spectrophotometer with Omnic software for data acquisition and analysis.

4.3.2.4 Swelling ratio test under different ionic strength

The swelling study of GMA-chitosan hydrogel and GMA-chitosan/VSA hybrid hydrogels were performed at room temperature (25 °C) immersing hydrogels individually in glass vials containing 15 ml buffer solution of different buffer concentration (0.05M, 0.1M, 0.2M). After 16 hours, GMA-chitosan based hydrogels reach their swelling equilibrium. The swollen hydrogels were removed, the excess surface water was wiped and the hydrogels were weighed until equilibrium was attained. The swelling ratios of the hydrogels were calculated from the swollen and dry weights of the hydrogels. The reproducibility of the swelling profiles of a hydrogel was determined in triplicate. Each hydrogel samples after swelling in the buffer solutions was then individually soaked in 50 ml deionized water to remove the absorbed inorganic salt in the swelling hydrogels. The weight of the dry hydrogel samples was measured after vacuum dried for 24 hours at room temperature.

$$\text{Swelling ratio (\%)} = (W_t - W_0) / W_0 \times 100$$

W_t is the weight of the hydrogel after swelling equilibrium

W_0 is the weight of the dry hydrogel

4.3.2.5 Morphological study of GMA-chitosan/VSA hybrid hydrogel

Scanning electron microscope (SEM) was employed to analyze the interior microstructure of GMA-chitosan/VSA hybrid hydrogels. Cryofixation technique was

used to observe the swollen hydrogel structure with minimal artifacts. Individual GMA-chitosan/VSA hybrid hydrogels were soaked in deionized water at room temperature to reach its swelling equilibrium. Then, the hydrogels were transferred into liquid nitrogen immediately to freeze and retain the swollen structure. The sample was subsequent freeze-dried for 72 hours in a Labconco (Kansas City, MO) Freezone 2.5 Freeze drier under vacuum at $-50\text{ }^{\circ}\text{C}$, and finally stuck on aluminum stubs and coated with gold for 30s for SEM observation by Leica Microsystems GmbH (Wetzlar, Germany) 440 SEM.

4.3.2.6 Compressive mechanical properties of GMA-chitosan/VSA hybrid hydrogel

The compressive mechanical properties of GMA-chitosan/VSA hybrid hydrogels were measured by a TA Dynamic Mechanical Thermal Analysis Q800 (TA instruments) at room temperature ($25\text{ }^{\circ}\text{C}$) and submersion compression load clamp. The hydrogels swollen in deionized water were placed on the top plate of a submersion compression load plate without any liquid media and compressed between the plate and a parallel disk (diameter 14mm) at a constant increasing load rate of 0.5 N/min until fragment of the hydrogel was produced. Initial compression modulus, was used to represent the hydrogel strength. For each type of hydrogel, three samples were used for the compression test. Mean value was calculated with a standard deviation. The initial compression modulus was calculated from the stress-strain curve.

4.3.2.7 Release study of bovine serum albumin from GMA-chitosan/VSA hydrogel.

Each GMA-chitosan/VSA hydrogel sample (11 mm diameter, 6 mm thickness disk-like hydrogel with 240 μg BSA loaded) was put in 20ml volume glass vials individually with 5mL PBS. At each time point, 100 μL solution was taken out from the vial and was diluted to 1 mL. 100 μL fresh PBS was added in the PBS bath of

hydrogel to compensate the amount extracted for the test. MicroBCA kit was used to acquire the BSA concentration data in the PBS bath solutions. The test was followed the protocol in the MicroBCA manual. PerkinElmer (Madison, WI) Lambda 35 UV-Vis spectrophotometer was used to test the absorption of samples at 562nm wavelength. The standard curve was prepared by plotting the average Blank-corrected 562nm reading for each BSA standard which is provided in the kit vs. its concentration in $\mu\text{g/mL}$. The standard curve was used to determine the protein concentration of each unknown sample.

4.4 Results

4.4.1 FTIR spectroscopy

Figure 4.2 shows the FT-IR spectra of the GMA-chitosan/VSA-67/33 hybrid hydrogel UV-crosslinked for 30 min. The absorption band of ester ($-\text{COO}-$) appeared at $1725\text{--}1730\text{ cm}^{-1}$ was evident on both of the GMA-chitosan and GMA-chitosan/VSA-67/33 hybrid hydrogel, but not in VSA since VSA does not contain ester bond in its chemical structure. Moreover, the appearance of amide (I) band and amide (II) band at $1648\text{--}1650\text{ cm}^{-1}$ and $1538\text{--}1542\text{ cm}^{-1}$ on GMA-chitosan and GMA-chitosan/VSA-67/33 hybrid hydrogel demonstrate that GMA-chitosan is one main component in the hybrid hydrogel.

According to Chansaia et al. and Rhim et al. studies about hydrogels with sulfate groups^{11, 12}, the absorption bands at 1088 cm^{-1} and 1255 cm^{-1} on the GMA-chitosan/VSA-67/33 hybrid hydrogel indicate the presence of sulfonic acid group from VSA, and hence the crosslinking reaction occurs mainly between the vinyl groups of VSA and the methacrylate groups of GMA-Chitosan^{11, 12}. From the results in Figure 4.2, the spectral change are evidence of crosslinking occurred between GMA-chitosan and VSA.

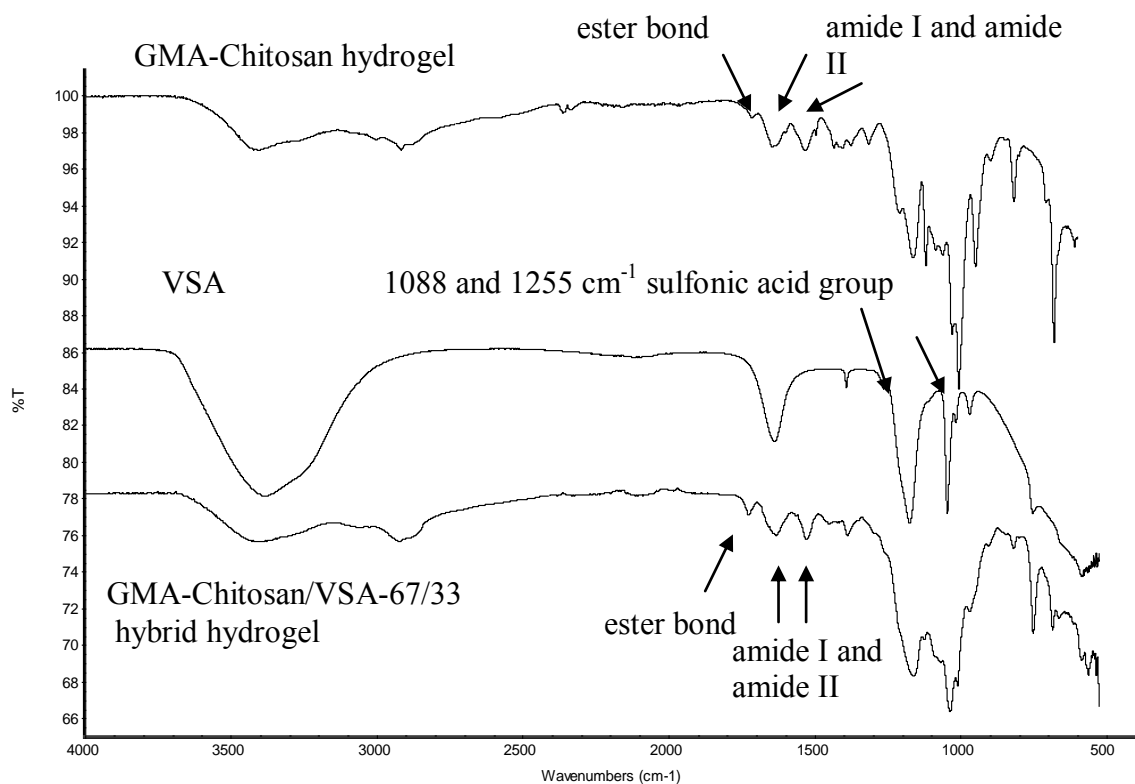


Figure 4.2 FTIR of GMA-chitosan hydrogel and GMA-Chitosan/VSA-67/33 hybrid hydrogel

4.4.2 Images of GMA-chitosan/VSA hybrid hydrogel after swelling in deionized water

One advantage of GMA-chitosan is its hydrogels (shown in Figure 4.3 A) and hybrid hydrogels are usually hydrophilic and transparent with well-defined shape. While the films or hydrogels made by chemically crosslinked chitosan material usually failed forming a transparent appearance. And the material is mainly hydrophobic similar to the raw chitosan material too^{5,9}.

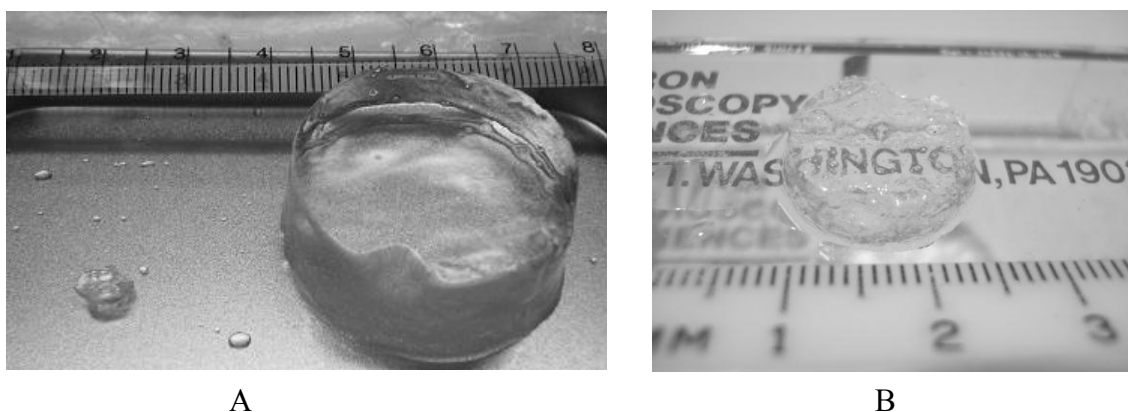


Figure 4.3 Images of GMA-chitosan/VSA hybrid hydrogel or GMA-chitosan hydrogel
 (A) GMA-chitosan hydrogel swollen in deionized water for 16 hours,
 (B) GMA-chitosan/VSA – 67/33 hydrogel swollen in deionized water for 16 hours

Figure 4.3 B shows the optical images of the GMA-chitosan/VSA hybrid hydrogel after 16 hours swelling in deionized water. The negatively charged VSA are able to be covalently bonded in the hydrogel matrix and the hybrid hydrogel is still transparent.

4.4.3 The influence of ionic strength to the swelling ratio of GMA-chitosan/VSA hybrid hydrogel

The effect of ionic strength of the medium and the effect of VSA contents on the swelling behavior of GMA-chitosan/VSA hybrid hydrogels are shown in Figure 4.4. All of the GMA-chitosan/VSA hybrid hydrogel and pure GMA-chitosan hydrogel reach their largest swelling ratio at the lowest ionic strength environment (i.e., deionized water). The swelling ratio of GMA-chitosan/VSA hybrid hydrogel and GMA-chitosan hydrogel in PBS buffer (pH 7.4) of different salt concentration varied from 6,768% to 554%. The swelling ratio of GMA-Chitosan/VSA 80/20 is 6,625±45% in deionized water, whereas the same hydrogel only achieved 1,154±44%

in 0.2M PBS. As the concentration of saline increase which means stronger ionic strength, the swelling ratio of GMA-Chitosan and GMA-Chitosan/VSA hydrogels decrease. GMA-chitosan/VSA hybrid hydrogel with higher VSA composition shows smaller swelling behavior in the same ionic strength aqueous environment. For example, in 0.05M PBS, GMA Chitosan/VSA-80/20 achieved 3,574±33% which is higher than that of GMA Chitosan/VSA-67/33 (3,185±152%). When ionic strength increased to 0.2M, the swelling ratio of both of these two types of hybrid hydrogels decreased to 1,154±44% and 1,274±22%, respectively, and the swelling ratio of GMA Chitosan/VSA-80/20 is still higher than that of GMA Chitosan/VSA-67/33. In the study of hydrogel swelling theory, if the polymer chains making up the network contain ionizable groups, the forces influencing swelling may be increased greatly

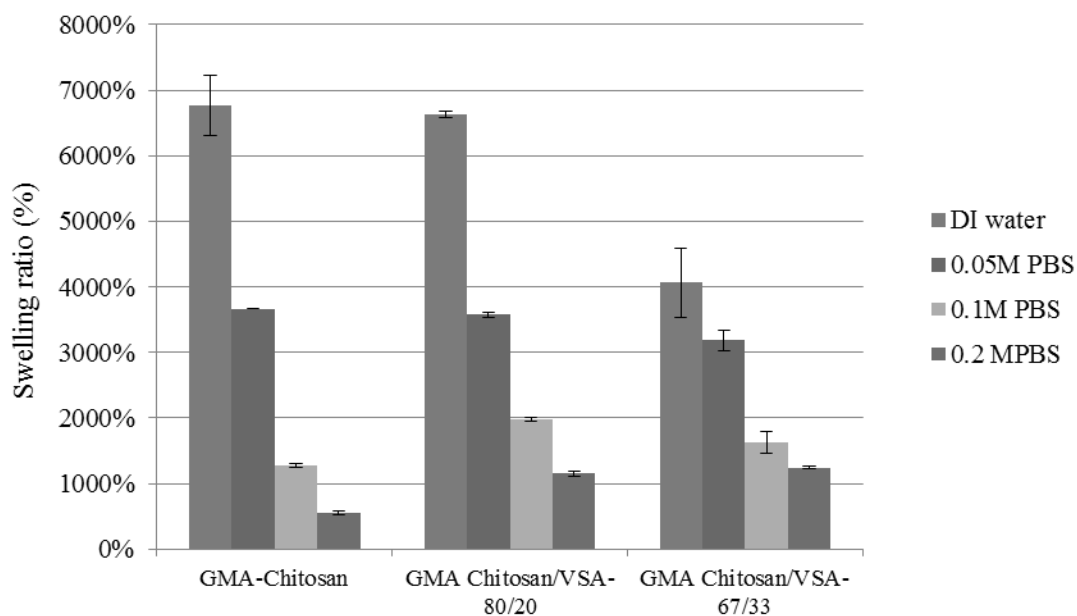


Figure 4.4 The influence of ionic strength environment to the swelling ratio of GMA-chitosan or GMA-chitosan/VSA hybrid hydrogel of different GMA-chitosan to VSA contents at neutral pH (deionized water, pH 7.4)

because of the localization of charges within the hydrogel¹³. GMA-chitosan/VSA hybrid hydrogel and GMA-Chitosan are ionized hydrogel that their swelling behavior depends on the ionic strength of the medium. The swelling of electrolyte hydrogel was influenced by the force of localized charges within the hydrogel, and the osmotic pressure difference between the interior ionic strength of the hydrogel and external ionic strength of the external solution. Polyelectrolyte behavior is governed by the ratio of the electrostatic energy between two neighboring charges on the chain to the thermal energy. As the density of charges on the polymer molecules increased, the relative importance of van der Waals force and repulsive electrostatic interactions changes. The relevant characteristic length scale is defined by the Bjerrum length¹⁴

$$\lambda = e^2 / \epsilon kT$$

Where e is the electron charge, ϵ is the permittivity of water, and k is the Boltzmann constant. (At $\lambda=1$, attractive to repulsive interactions are equal.) When the distance, d , between neighboring charges is much larger than the λ ($d/\lambda \gg 1$), counterions are uniformly distributed throughout the gel. Consequently, swelling is driven by their osmotic pressure. When ($d/\lambda < 1$), the charge density exceeds a critical threshold value, and counterions are closely bound to the chain¹⁵.

In deionized water, the polyelectrolyte hydrogel will absorb solvent and expand in volume due to the osmotic pressure difference caused by the presence of ionizable groups within the hydrogel¹⁵. One driving force of the swelling process of GMA-chitosan / VSA hydrogel in saline solution is the presence of mobile osmotically active counterions in PBS. When the salt concentration increases, ions diffuse from the solution into the network. Consequently, the driving force (congeneric localized charge repulsion) of swelling decreases with increasing salt concentration due to the charge shielding effect. For the GMA-chitosan / VSA hydrogel, the negative charged sulfate group is dominant in the localized charges within the interior of hybrid

hydrogel. The counterions are Na^+ , K^+ ions. Whereas the swelling decreases too, due to the reduced charge repulsion.

For pure GMA-chitosan hydrogel, the swelling ratio value at equilibrium depends on the positively charged $-\text{NH}_3^+$ ions. The local electrostatic repulsion of the congeneric charge in the hydrogel network becomes weaker when the saline concentration increasing. Meanwhile, the osmotic pressure between the interior of GMA-chitosan and saline solution is decreased when the exterior saline concentration increasing. As a result, the decrease of swelling driving force leads the decrease of swelling ratio in saline solution. For GMA-chitosan/VSA hybrid hydrogels, the increasing ionic strength shielding and decreased the repulsion interaction of the bonded sulfonic groups in the hydrogels and the osmotic pressure change lead to the lower swelling ratio of hybrid hydrogel in the saline solution with higher ionic strength as well.

In low ionic strength environment (deionized water, 0.05M PBS), pure GMA-chitosan always shows larger swelling than GMA-chitosan / VSA hybrid hydrogel. One possible reason is when two water soluble precursors with opposite charges mixed together. The ionic interaction makes them form polyelectrolyte complex which creates more hinderance to prevent hydrogel expansion¹⁶. However, in high ionic strength environment, the GMA-chitosan / VSA hybrid hydrogel has larger swelling ratio than that of pure GMA-chitosan hydrogel. In the 0.2M saline solution, the equilibrium swelling ratio of GMA Chitosan/VSA-80/20 is $1,154 \pm 44\%$, and the swelling ratio of pure GMA-chitosan hydrogel is $554 \pm 30\%$. This is attribute to the presence of strong negative charge sulfonic groups (pK_a -2.8) makes the crosslinked network structure still keep anion-anion repulsion in some extent due to the repulsion between sulfonic groups¹⁸. While the pK_b of amine groups of GMA-chitosan hydrogel is 6.5-6.7 (pK_a 7.3-7.5 at room temperature), in pH 7.4 PBS, part of the amine groups

are not ionized ¹⁹. As a result, GMA-chitosan hydrogel has less ionized groups in 0.2 M PBS which leads to lower swelling driving force after the ionic groups was screened by 0.2M saline solution.

In the Sun et al. study about the dextran based hydrogel which has amine groups, the dextran-allyl isocyanate ethylamine (Dex-AE) / PEGDA hybrid hydrogel achieved about 800% swelling in deionized water, about 700% swelling in 1.0 M ionic strength aqueous solution and about 570% swelling in 2.5 M ionic strength aqueous solution after 16 hours swelling ²⁰. The increased ionic strength of the surrounding medium reduced the mobility of ions due to the electrostatic interaction. Thus, the reduction in ion mobility in the surrounding medium could give rise to a higher osmotic pressure, in turn could facilitate the diffusion of pure water molecules from interior of Dex-AE/PEGDA hydrogel into saline solution, i.e., lower swelling ratio in a high ionic strength medium. In the study of Namkung et al. about the dextran-maleic acid (Dex-MA) / *N*-isopropylacrylamide (NIPAAm) hybrid hydrogel, ionic strength sensitivity is observed too ²¹. The swelling ratio of Dex-MA / NIPAAm hybrid hydrogel with certain two precursor feed ratio in deionized water is about 650% and about 50% in 2.5M saline solution after 4 hours swelling. As the ionic strength increased, the swelling ratios of all hybrid hydrogels with different Dex-MA / NIPAAm content decreased due to the shielding effect caused by the counter ions in high ionic strength solutions and osmotic pressure change. Moreover, similar to GMA-chitosan/ VSA hybrid hydrogel, in this system, Dex-MA / NIPAAm hybrid hydrogels both have carboxylic anions from Dex-MA and secondary amine groups from NIPAAm. They suggested that the expansion of ionized hydrogels was hindered by the formation of the polyelectrolyte complex between two components with positive and negative charge. As a result, the swelling ratios of the hybrid hydrogels which are made from

two opposite charged components are lower than that of the pure single component hydrogel in low ionic strength medium^{16,21}.

4.4.4 Morphology of GMA-chitosan/VSA hybrid hydrogel

GMA-chitosan/VSA hybrid hydrogel has porous structure after freeze-drying. Based on the SEM images in Figure 4.5 A, B, C, the size of the most pores of GMA-chitosan/VSA hybrid hydrogel with 67/33 and 80 /20 feed ratio is from 15 μ m to 35 μ m (Figure 4.5 B). The GMA-chitosan/VSA hybrid hydrogel showed more compact structure, thinner wall and bigger pore size than pure GMA-chitosan hydrogel (shown in Figure 4.5 D). In general, the GMA-chitosan / VSA hydrogel has more homogenous and slightly larger porosity than that of pure GMA-chitosan. This was probably due to the addition of VSA into GMA-chitosan hydrogel increased uniformity of crosslinked chitosan molecules, because the high molecular weight of chitosan creates hindrance for unsaturated methacrylate groups covalently bonded to each other. When the viscous GMA-chitosan aqueous solution forms hydrogel, it usually has uneven spot which has lower or higher crosslinking density than other parts of the hydrogel. The addition of VSA increased the reactive double bond amount in the precursor and makes the reactive double bonds distributed more even in the hydrogel precursor. The morphology of hydrogel microstructure reflected the distribution of the pore and pore size of hybrid hydrogel is more uniform by adding VSA.

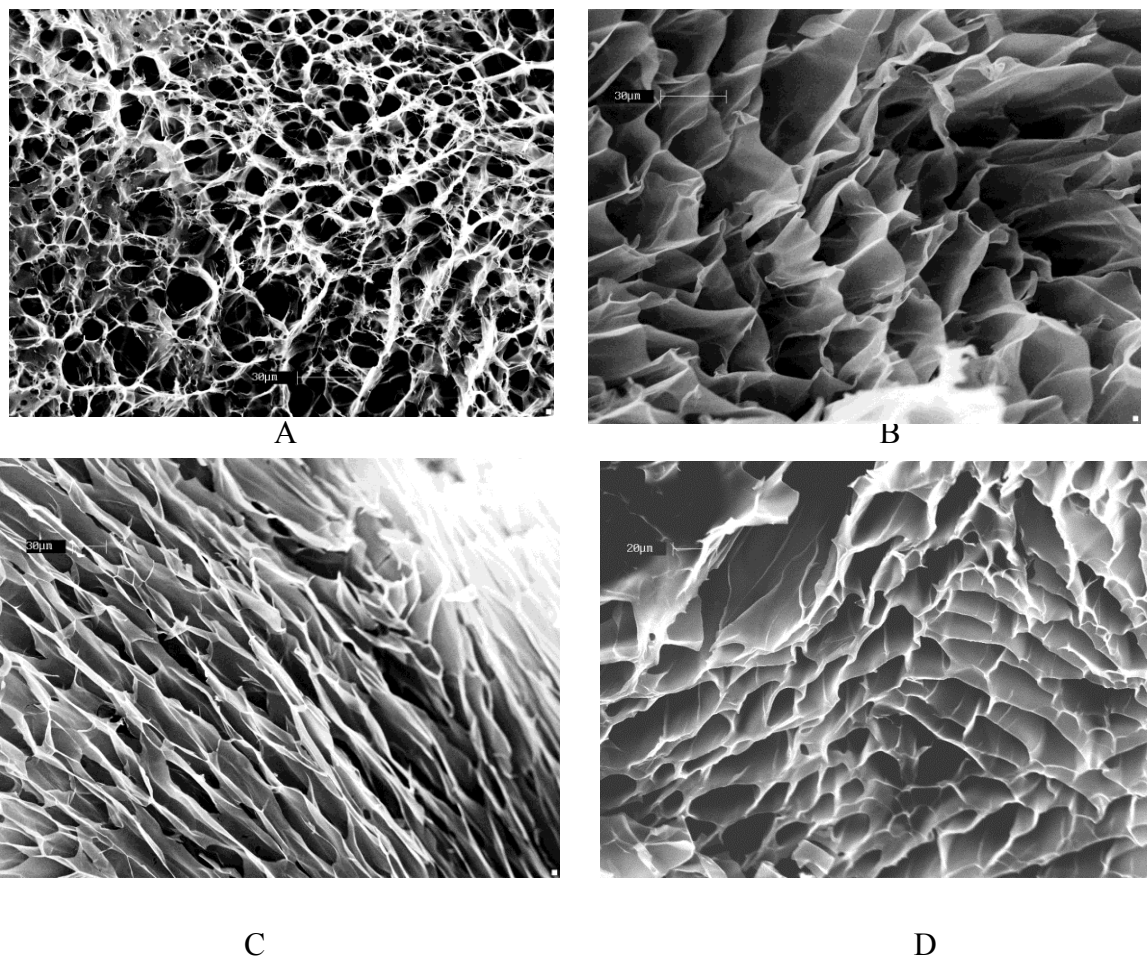


Figure 4.5 SEM images of GMA-chitosan/VSA hybrid hydrogels (A, GMA-Chitosan/VSA -67/33 hybrid hydrogel at 500 \times ; B, GMA-Chitosan/VSA -67/33 hybrid hydrogel at 1,500 \times ; C, GMA-Chitosan/VSA -80/20 hybrid hydrogel at 1,500 \times ; D, GMA-Chitosan hydrogel at 1,000 \times)

Forming porous structures for use in cell transplantation is one of chitosan's most promising features. Freezing and lyophilizing chitosan based hydrogel is the most common method in suitable molds to prepare porous structure. During the freezing process, ice crystals nucleate from solution and grow along the lines of thermal gradients²². In Zhong et al. study, maleic chitosan / PEGDA hydrogels show honeycomb-like porous structures and the pore size could be adjusted from 5 μm to 20

μm by changing the feed ratio of maleic chitosan /PEGDA ²³. And the change of morphology represents the variation of crosslinking density of hybrid hydrogel. In their result, higher crosslinking density leads to lower swelling ratio, tighter network structure.

4.4.5 Mechanical properties of GMA-chitosan/VSA hybrid hydrogel

The compressive mechanical properties of the GMA-chitosan/VSA hybrid hydrogel scaffolds were next evaluated (Figure. 4.6). In general, the compression modulus of GMA-chitosan hydrogel/VSA hybrid hydrogels with different ratio of VSA is between 7~18 kPa. The initial compression modulus of the crosslinked GMA-chitosan/VSA hybrid hydrogel (7.83~8.59 kPa) was lower than GMA-chitosan hydrogel (17.64 ± 7.52 kPa), indicating that the stiffness of the GMA-chitosan/VSA hydrogel decreased with the addition of VSA. Pore size and the interaction between the crosslinked molecule chains are the two main factors which can influence the mechanical properties of the hydrogel ^{22, 24}. The tensile testing of hydrated chitosan samples shows porous structure have greatly reduced elastic moduli compared to non-porous chitosan samples. Higher porosity usually leads to lower mechanical strength ²². Comparing Figure 4.5 B. C., the porous structure of GMA-chitosan / VSA hydrogel has thinner wall and higher porosity than that of pure GMA-chitosan hydrogel. So, the morphology difference is one possible reason that GMA-chitosan / VSA has lower compression modulus than that of hydrogels without VSA. Zhong et al.²³ recently reported the compressive mechanical properties of maleic chitosan/polyethylene glycol diacrylate (PEGDA) that was fabricated by using similar UV-crosslinking technology. Different with GMA-chitosan /VSA hybrid hydrogel, the mechanical property of the maleic chitosan/PEGDA hybrid hydrogels largely depended on the molecular weight of the PEGDA co-precursor. Because the major composition

PEGDA (PEGDA in the maleic chitosan / PEGDA hybrid hydrogel is no less than 67%) determines the crosslinking density of the hydrogel. Low molecular weight PEGDA as co-precursor means more crosslinkable unsaturated acrylate end groups was added. Thus, the hydrogel could achieve higher crosslinking density and further higher mechanical strength. The compression modulus of maleic chitosan / PEGDA (MW 8,000)= 1/ 2 hybrid hydrogels is 61 ± 1.9 KPa.

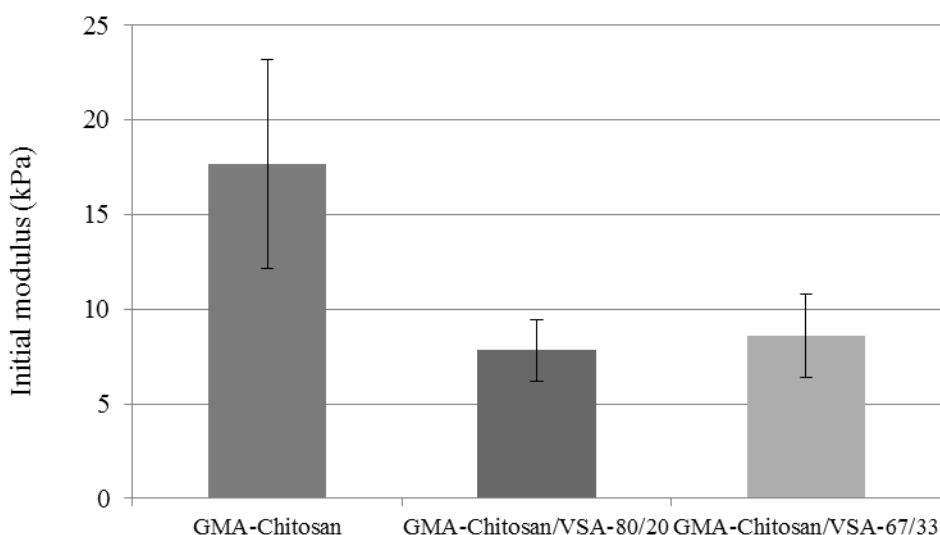


Figure 4.6 The initial compression modulus of GMA-chitosan hydrogel, GMA-chitosan/VSA hybrid hydrogel swollen in deionized water at room temperature

The feed ratio change of GMA-chitosan/VSA in the hydrogel precursor doesn't show big difference on the compressive initial modulus. The compression modulus of the GMA-chitosan/VSA -80/ 20 is 7.83 ± 1.62 KPa and the compression modulus of the GMA-chitosan/VSA- 67/ 33 is 8.59 ± 2.20 KPa. The incorporation of VSA in the precursor solution helped GMA-chitosan to form more homogenous hydrogel. In GMA-chitosan hybrid hydrogel precursor solution, increased amount of VSA

molecules was also be mixed and well distributed among GMA-chitosan as low VSA content hybrid hydrogel precursor because VSA is a much smaller molecular which has good water solubility compared to GMA-chitosan. From the SEM image, higher composition of VSA didn't change the porosity (Figure 4.5 B, C) and crosslinking density of GMA-chitosan hybrid hydrogels in a very large extent.

4.4.6 BSA release from GMA-chitosan/VSA hybrid hydrogel

The BSA release profile was shown in Figure 4.7, GMA-chitosan hydrogel and GMA-chitosan/VSA hybrid hydrogel show burst release in the first hour after be immersed in PBS. GMA-Chitosan and GMA-chitosan/VSA-80/20 hybrid hydrogels released about 30% of total loaded BSA in the first 2 hours. The burst release of BSA is due to part of loaded BSA is on the hydrogel surface or close to the hydrogel surface which could be easily diffused into aqueous media. In the first 7 days, the release profile of GMA-Chitosan and GMA-chitosan/VSA -80/20 hybrid hydrogels did not show too much difference. Only after 9 days, the BSA release rate from GMA-chitosan/VSA hybrid hydrogels is higher than that of GMA-chitosan hydrogel and GMA-chitosan/VSA hybrid hydrogels BSA achieved more complete BSA release. After 12 days, 96% of the pre-loaded BSA was released into PBS from GMA-chitosan/VSA hybrid hydrogel. While the amount of BSA release from GMA-chitosan is 88% at the same time.

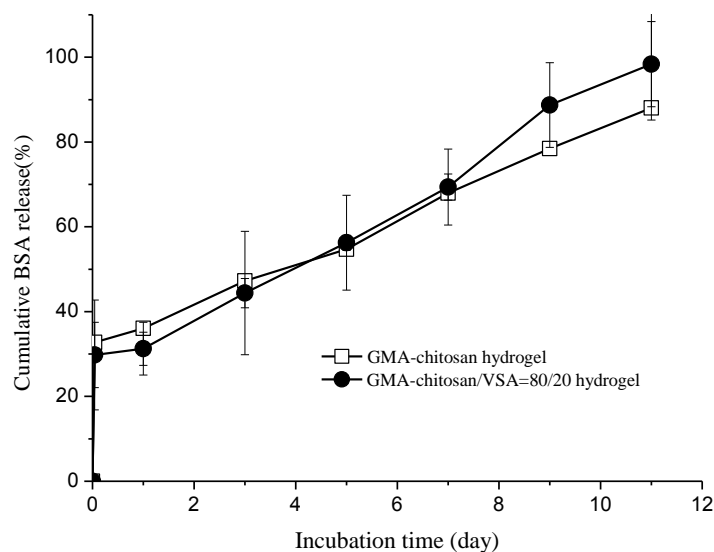


Figure 4.7 Cumulative BSA release of GMA-chitosan hydrogel, GMA-chitosan/VSA - 80/20 hybrid hydrogel in 0.05M PBS (pH 7.4) at 37 °C

Albumin is the major constituent of blood plasma and is one of the smallest proteins in the plasma. The shape of this protein is a prolate ellipsoid with a size of about $15 \times 3.8 \times 3.8 \text{ nm}$ ¹⁷. It contains a comparatively large number of polar and charged residues and thus it is highly soluble in water. The isoelectric point of bovine serum albumin is about 4.7. In pH 7.4 PBS buffer, BSA is a negative charge water soluble protein with 60,000-70,000 molecule weight²⁵. On the other hand, in the hybrid hydrogel, the pKa of sulfonic group on VSA is -2.8 that means very strong negative charge in an aqueous environment¹⁸. Several interactions, including hydrophobic interaction, hydrogen bonding and electrostatic interaction, simultaneously take part in the protein release / adsorption behavior. The information should be important in apprehending the behavior of GMA-chitosan hydrogel with sulfonic groups in physiological environment when it is used as protein drug carrier³.

The release profile of GMA-chitosan with negative charge didn't show significant difference with pure GMA-chitosan hydrogel in the first 7 days when the concentration of albumin remained in the hydrogel is higher than 40% of its original amount. The electrical repulsion between the sulfonic groups of GMA-chitosan/VSA and BSA is not able to be the driving force to accelerate the release of BSA because the inner space between hydrogel molecules are much larger than the size of BSA in PBS ($15 \times 3.8 \times 3.8 \text{ nm}$). However, the sulfonic groups creates a structure prevent the albumin adsorption. When the albumin content in the hydrogels is lower than 40% of its original weight, the GMA-chitosan/VSA achieved higher release speed of BSA and almost release all of BSA loaded in 12 days. Whereas the GMA-chitosan hydrogel still can reserve about 12% BSA in PBS solution which shows its interface is more favorable for protein adsorption. The GMA-chitosan/VSA hydrogel achieved higher release rate after 7 days release (BSA content $< 40\%$ original amount at this time) than the GMA-chitosan hydrogels whose protein release driving force is only by diffusion without sulfonic groups. It could be useful for some drug release process which requires more sustained the release rate because for most hydrogels when the protein concentration decreased to some extent, the residue protein will attach to the hydrogel molecules and slow down the release speed from it. In some protein drug release application, such as growth factors, the protein concentration in the hydrogel is very low, from ng/ml to pg/ml²⁶, if the hydrogel is not able to create a surface preventing the protein absorption, the release rate of protein drug will be slow down by the hydrogel absorption. Moreover, the mechanism of many polysaccharides containing sulfonic groups such as heparin and HS can prevent proteins attachment, including globulin or fibrinogen attachment is the repulsion of their negative charge to proteins⁷. Because protein adsorption is involved in many physical processes such as blood coagulation, cell attachment, by adding VSA in GMA-chitosan can be used as

an approach to control the anti-biofouling properties of GMA-chitosan as well ³. In other BSA release study from other chitosan base hydrogels, Bhattarai et al. developed one BSA preloaded PEG-grafted chitosan hydrogel crosslinked by genipin ²⁷. The burst release from PEG-grafted chitosan hydrogel (crosslinked by genipin for 10min) in the first 24 hours is about 12% preloaded BSA and 42% of BSA was released in 7 days. By adjusting the genipin treatment time, the PEG-grafted-chitosan can achieve longer BSA release time up to 40 days. The BSA release profile of GMA-chitosan / VSA hybrid hydrogel is about 10% more cumulative release than PEG-grafted chitosan hydrogel (crosslinked by genipin for 10min) at the same release time. Sun et al. reported BSA release from one positive charged dextran-allylisocyanate ethylamine (Dex-AE) / PEGDA hydrogel ²⁸. The cationic free amine groups of Dex-AE component effectively decreased the burst release of BSA and a longer-last sustained BSA release period (in 11-30 days by tuning the feed ratio of Dex-AE / PEGDA) than the release profile of GMA-chitosan /VSA hydrogel. One synthetic polymer hydrogel with mild cationic charge (poly (*N*-isopropylacrylamide) hydrogels) have larger adsorption to BSA. Zhang et al. reported the BSA release study from poly (*N*-isopropylacrylamide) hydrogels ²⁹. After 100 hours release in aqueous environment, poly (*N*-isopropylacrylamide) based hydrogel release about 50% of loaded BSA and the cumulative release of BSA is almost no change after 50 hours release which means the release rate is very slow approaching 0. The possible reason of BSA adsorption in poly (*N*-isopropylacrylamide) based hydrogel maybe attributed to two reasons: (a) BSA was entrapped in the hydrogel network; (b) low BSA loading concentration leads to weak release driving force. Compared with synthetic polymer based hydrogel, GMA-chitosan /VSA hydrogel is able to achieve a more thoroughly albumin release than synthetic polymer hydrogels. Low protein adsorption of GMA-chitosan /VSA

hydrogel is a useful feature for the some types of protein drug release which is loaded in hydrogel with comparatively low concentration.

4.5 Conclusions

This chapter describes the synthesis and characterization of the GMA-chitosan/VSA hybrid hydrogel. Unsaturated methacrylate groups were incorporated onto the hydroxyl groups of chitosan. Under 365nm UV radiation and presence of photo-initiator, the methacrylate groups of GMA-chitosan are able to react with the vinyl groups of VSA molecule to form crosslinked hybrid hydrogel.

By varying the feed ratio of VSA to GMA-chitosan, the negative charge density in the hybrid hydrogel could be controlled. The hydrogel of GMA-chitosan/VSA has porous structure and high capacity of water absorption. The incorporation of VSA in the hybrid hydrogel decreased the compression modulus of the hydrogel due to the reduced hydrogen bond interaction between GMA-chitosan molecules. The presence of negative charge sulfonic groups attributes the hybrid hydrogel the ionic strength responsive swelling behavior. GMA-chitosan/VSA and GMA-chitosan achieve their larger swelling ratio in lower ionic strength environment. The reason of swelling ratio change is related to the balance of osmotic pressure of the hydrogel interior and exterior solution environment. The photo-crosslinked negatively charged GMA-chitosan / VSA can be used as protein drug carrier. The protein drug is incorporated in the hydrogel precursor solution to be preloaded into the hydrogel. The 3D porous structure and negatively charged interior of GMA-chitosan /VSA hybrid hydrogel achieved higher release rate at low protein concentration than that of GMA-chitosan hydrogel without VSA and a more thoroughly release of the preloaded BSA protein drug model in 11 days.

Reference:

- 1 Gandhi NS, Mancera RL, The structure of glycosaminoglycans and their interactions with proteins, 2008, Chem Biol Drug Des, 72, 455-482
- 2 Kisilevsky R., Ancsin J.B., Szarek W.A., Petanceska S. (2007) Heparan sulfate as a therapeutic target in amyloidogenesis: prospects and possible complications. Amyloid; 14:21–32.
- 3 Fromm J.R., Hileman R.E., Caldwell E.E.O., Weiler J.M., Linhardt R.J. (1997) Pattern and spacing of basic amino acids in heparin binding sites. Arch Biochem Biophys; 343:92–100.
- 4 Hileman R.E., Fromm J.R., Weiler J.M., Linhardt R.J. (1998) Glycosaminoglycan–protein interactions: definition of consensus sites in glycosaminoglycan binding proteins. BioEssays; 20:156–167
- 5 Voravee P. Hoven et al, Surface-charged chitosan: Preparation and protein adsorption, Carbohydrate polymers, 2007, 68, 44-53
- 6 Ram Sasisekharan,, Zachary Shriver, Ganesh Venkataraman and Uma Narayanasami, Roles of heparan-sulphate glycosaminoglycans in cancer, nature reviews, 2002, 2, 521
- 7 Neha S. Ganhi, Ricardo L. Mancera, The structure of glycosaminoglycans and their interactions with proteins, Chem Biol Drug Des 2008, 72, 455-482
- 8 Benesch, J., & Tengvall, P, Blood protein adsorption onto chitosan. Biomaterials, 2002, 23(12), 2561–2568
- 9 Okamoto, Y., Yano, R., Miyatake, K., Tomohiro, I., Shigemasa, Y., Minami, S. Effects of chitin and chitosan on blood coagulation. Carbohydrate Polymers, 2003, 53(3), 337–342.
- 10 Amiji, M. M. Synthesis of anionic poly (ethylene glycol) derivative for chitosan surface modification in blood-contacting applications. Carbohydrate Polymers, 1997, 32(3–4), 193–199.

- 11 Phithupha Chansaia, Anuvat Sirivat, Sumonman Niamlanga, Datchanee Chotpattananontb, Kwanchanok Viravaidya-Pasuwatc, Controlled transdermal iontophoresis of sulfosalicylic acid from polypyrrole/poly(acrylic acid) hydrogel, *International Journal of Pharmaceutics*, 2009, 381, 25–33
- 12 Ji-Won Rhim, Ho Bum Park, Choong-Sub Lee, Ji-Hyun Jun, Dae Sik Kim, Young Moo Lee, Crosslinked poly(vinyl alcohol) membranes containing sulfonic acid group: proton and methanol transport through membranes, *Journal of Membrane Science*, 2004, 238, 143–151
- 13 Tuncer Caykara, Ugur bozkaya, Omer Kantoglu, Network structure and swelling behavior of poly(acrylamide/crotonic acid) hydrogels in aqueous salt solutions, *Journal of Polymer Science: Part B: Polymer Physics*, 2003, 41, 1656–1664
- 14 Joanny, J. F.; Leibler, L. *J. Phys. (Paris)*, 1990, 51, 545
- 15 Ferenc Horkay, Ichiji Tasaki, Peter J. Basser, Osmotic swelling of polyacrylate hydrogels in physiological salt solutions, *Biomacromolecules*, 2000, 1, 84-90
- 16 M.K. Yoo, Y.K. Sung, Y.M. Lee, C.S. Cho, Effect of polyelectrolyte on the lower critical solution temperature of poly(*N*-isopropyl acrylamide) in the poly(NIPAAm-*co*-acrylic acid) hydrogel, *Polymer*, 2000, 5713-5719
- 17 Jin Ho Lee, Se Heang Oh, MMA/MPEOMA/VSA copolymer as a novel blood-compatible material: Effect of PEO and negatively charged side chains on protein adsorption and platelet adhesion, *J Biomed Mater Res*, 2002, 60, 44-52
- 18 Bryan D. Smith, Matthew B. Soellner, Ronald T. Raines, Potent Inhibition of Ribonuclease A by Oligo(vinylsulfonic Acid), *THE JOURNAL OF BIOLOGICAL CHEMISTRY*, 2008, 278, 23, 20934-20938
- 19 F.L. Mi, Y.C. Tan, H.F. Liang, H.W. Sung, 2002, In vivo biocompatibility and degradability of a novel injectable-chitosan-based implant, *Biomaterials* 23, 181–191.

- 20 Guoming Sun, Chih-Chang Chu, Synthesis, characterization of biodegradable dextran-allyl isocyanate-ethylamine/polyethylene glycol-diacrylate hydrogels and their in vitro release of albumin, *Carbohydrate Polymers*, 2006, 65, 273-287
- 21 Sun Namkung, Chih-Chang Chu, Effect of solvent mixture on the properties of temperature and pH sensitive polysaccharide –based hydrogel, *J Biomater Sci Polymer Edn*, 2006, 17, 5, 519-546
- 22 J. K. Francis Suh, Howard W.T. Matthew, Applications of chitosan-based polysaccharide biomaterials in cartilage tissue engineering: a review, *Biomaterials*, 2000, 21, 2589-2598
- 23 Chao Zhong, Jun Wu, C.A. Reinhart-King, C.C. Chu, Synthesis, characterization and cytotoxicity of photo-crosslinked maleic chitosan–polyethylene glycol diacrylate hybrid hydrogels, *Acta Biomaterialia*, 2010, 6, 3908-3918
- 24 Jing Shang, Zhengzhong Shao, Xin Chen, Chitosan-based electroactive hydrogel, *Polymer*, 2008, 49, 5520-5525
- 25 Z.G. Peng, K. Hidajat, M. S. Uddin, Adsorption of bovine serum albumin on nanosized magnetic particles, *Journal of Colloid and Interface Science*, 2004, 271, 277-283
- 26 M. J. Whitaker, R. A. Quirk, S. M. Howdle and K. M. Shakesheff, Growth factor release from tissue engineering Scaffolds, *Journal of Pharmacy and Pharmacology*, 2001, 53, 1427-1437
- 27 Narayan Bhattarai, Hassna R. Ramay, Jonathan Gunn, Frederick A. Matsen, Miqin Zhang, PEG-grafted chitosan as an injectable thermosensitive hydrogel for sustained protein release, 2005, 103, 3 609-624
- 28 Guoming Sun, Chih-Chang Chu, Synthesis, characterization of biodegradable dextran-allyl isocyanate-ethylamine/polyethylene glycol-diacrylate hydrogels and their in vitro release of albumin, *Carbohydrate Polymers*, 2006, 65, 273-287

29 Xianzheng Zhang, Da-qing Wu, Chih-Chang Chu, Synthesis, characterization and controlled drug release of thermosensitive IPN-PNIPAAm hydrogels, *Biomaterials*, 2004, 25, 3793-3805

CHAPTER FIVE:
SYNTHESIS, CHARACTERIZATION OF CATIONIC ARGININE BASED
POLYESTER AMIDE / GLYCIDYL METHACRYLATE CHITOSAN HYBRID
HYDROGEL AND ALBUMIN RELEASE STUDY

5.1 Abstract

A new family of biodegradable cationic hybrid hydrogels was designed and fabricated from an unsaturated arginine (Arg) based functional poly(ester amide) (Arg-UPEA) and glycidyl methacrylate chitosan (GMA-chitosan) precursors by UV photocrosslinking in an aqueous medium. The hybrid hydrogels were characterized for their chemical structures by fourier transform infrared spectroscopy (FTIR), and elemental analysis. MTT assay of the Arg-UPEA/GMA-chitosan mixed aqueous solution showed virtually non-cytotoxicity toward porcine aortic valve smooth muscle cells at polymer concentration up to 6 mg/mL. These hybrid hydrogels were further characterized in terms of their equilibrium swelling ratio (Q_{eq}), compressive modulus by dynamic mechanical analysis (DMA), and interior morphology by scanning electron microscope (SEM). By varying the feed ratio of Arg-UPEA to GMA-chitosan and the methylene group length (x) of the diol building block of Arg-UPEA, the swelling (from 297.8% to 3318.2%, depending on pH), mechanical (compressive modulus, 17.649 ± 0.78 KPa \sim 18.103 ± 1.30 KPa) and morphological properties of this hybrid hydrogel system could be adjusted. The enzymatic biodegradation of Arg-UPEA/GMA-chitosan hybrid hydrogels by lysozyme *in vitro* was studied. Lysozyme effectively accelerated the biodegradation rate of the hybrid hydrogels at 37 °C. Bovine serum albumin (BSA) was used as a model protein to study the protein drug release from this cationic hybrid hydrogel. A sustained release of BSA can be achieved from Arg-UPEA/GMA-chitosan hybrid hydrogels in 11 days *in vitro* with a lower burst and more sustained BSA release than a pure GMA-chitosan hydrogel. This new family of biodegradable cationic Arg-UPEA/GMA-chitosan hybrid hydrogels may have the potential as the protein delivery vehicles as well as scaffolds for tissue engineering.

5.2 Introduction:

5.2.1 Arginine metabolism

Arginine (2-amino-5-guanidinovaleric acid) is one nonessential amino acid which presents in animal protein ¹. Arginine is of particular interest in the regard as it was demonstrated to have many fundamental roles in nitrogen metabolism, creatine and polyamine synthesis and the production of nitric oxide (NO). One major function of arginine within the mammal body is as an intermediate in the urea cycle. Arginase-I removes the guanidino group from arginine to produce urea and ornithine (Figure 5.1). In the protein synthesis, which is another major function of arginine, arginine can be converted into proline, glutamate and glutamine (Figure 5.1). Synthesis of these three amino acids begins with ornithine which is converted from arginine. The process of arginine metabolism generates several essential nitrogen-containing compounds, including creatine, polyamines, agmatine and nitric oxide ².

There are two identified pathways of arginine metabolism. First, the "arginase" pathway: arginine is converted to urea and ornithine, generates polyamines, including: putrescine, spermine, spermidine, by the action of ornithine decarboxylase. polyamines, such as spermine, play a key role in cell proliferation, cell division, DNA replication, and regulation of cell cycle. Second, arginine is the sole substrate for NO synthesis in biological systems. NO is synthesized from arginine by the activity of nitric oxide synthase (NOS) resulting in the formation of nitric oxide and citrulline. The metabolism of NO is critically depends on the metabolism of L-arginine, because arginine is the sole source of produced NO ^{3,4}. The rate of cellular NO synthesis is limited by the rate of arginine uptake.

Arginine could be converted into NO by three NO synthase (NOS) isoforms, neuronal NOS (nNOS), endothelial NOS (eNOS), and inducible NOS (iNOS).

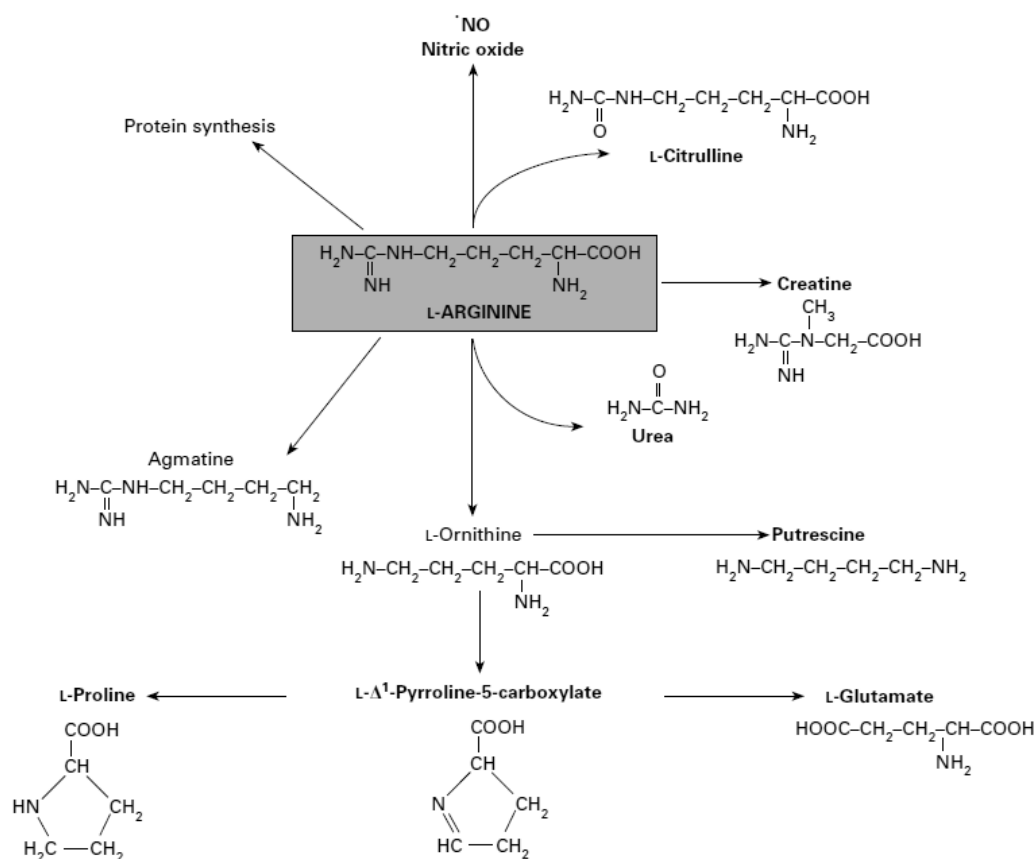


Figure 5.1 Metabolic fates of arginine in mammalian cells ²

nNOS and eNOS are constitutive isoforms which are permanently active generating low concentration of NO. The enzymatic activities are regulated by intracellular calcium fluxes or exogenous calmodulin. Compared to the amount of NO generated by the constitutive isoforms, iNOS could release high levels of NO and the expression, transcription and function are induced by a variety of cytokines, growth factors and inflammatory stimuli on target cells ³. During wound healing, burn injury, endotoxin exposure, arthritis and inflammatory bowel diseases, iNOS releases high amounts of NO.

Many studies demonstrated vascular dysfunctions, septic shock, cerebral infarction, diabetes mellitus are associated with the impaired production of NO⁴⁻⁷. However, the NO overproduction is associated with neurodegenerative disorders. The rate of NO production depends on the availability of intracellular arginine. On the other hand, arginine can also be consumed via arginase in wound. In some cases, arginase can decrease NO production by decreasing intracellular arginine concentration. Arginase exists in two known isoforms, liver-type arginase I and nonhepatic type arginase II. Arginase I is located in the cytosol, and arginase II is located in the mitochondrial matrix⁴. Through the action of arginase, ornithine is formed which is a precursor for proline and polyamines. This is one possible significant pathway for wound healing because proline serves as one substrate for collagen synthesis, whereas polyamines are involved in cell proliferation¹. The activities of iNOS and arginase are regulated reciprocally in cells by cytokines. Because arginine is one of the regulating factors of NO synthesis, it is theoretically feasible to regulate NO production by controlling the availability of arginine for NOS reaction.

5.2.2 NO physiological functions

NO works as a messenger molecule functioning in vascular regulation, immunity, neurotransmission, wound healing etc⁴. In wound healing, NO production is critical to wound collagen accumulation and acquisition of mechanical strength⁸. Inflammatory and mesenchymal cells both have been shown to synthesize large amount of NO in response to lipopolysaccharide (LPS) and cytokines^{9, 10}. With the development of analysis technology of NOS, the time course of NO was well elucidated. In rat models of healing, iNOS expression is highest in the first 5 days after injury (Figure 5.2)^{3, 11}. During the early phase of healing, the majority of NO synthesis is due to the present of

inflammatory cells, particularly, macrophages. Fibroblasts, keratinocytes and endothelial cells contributed to NO synthesis as well but in a lower level.

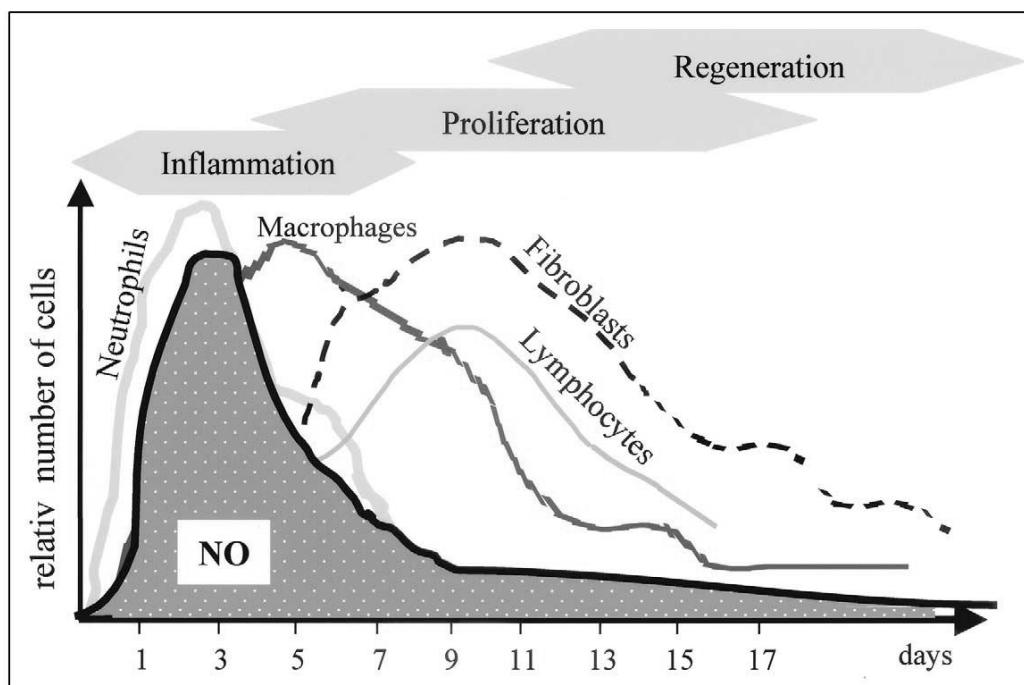


Figure 5.2. Phases of wound healing and the generation of wound NO³

The up-regulation of iNOS in wounded tissue is probably related to the anti-microbial function of NO. As the number of inflammatory cells decreasing, the NO generation during wound healing shows a decreasing curve over time. NO acts to cells in multiple and different mechanism. Some of its effects are due to its chemical reaction to produce reactive radical species. NO influences the cell proliferation, cellular differentiation, gene expression. The regulations to cells by NO probably occur indirectly and are not completely understood³.

In wound healing process, NO plays a functional role. Many studies provided evidences: (1) arginine-free nutrition inhibits LPS-induced NO synthesis in several organs not only at the wound site; (2) NO mediates inflammation-induced edema formation and inhibits cell infiltration into granulomas; (3) The healing process of

eNOS knock-out mice was impaired demonstrates: iNOS-mediation is not the only way to control NO generation; (4) The group of injured animals which are treated with high concentration iNOS inhibitors show high lethality. Some studies showed collagen synthesis during wound healing correlates with NO synthesis. iNOS inhibition impairs matrix synthesis whereas iNOS transfection enhance collagen synthesis^{8, 12}. Wound contraction which is a major contributor to closure of open wounds is delayed by iNOS inhibition¹³. In vitro studies also showed that NO induces keratinocyte in a locomotory phenotype which is involved in the closure of open wound¹⁴. And also, the lack of iNOS gene expression alters wound cytokine expression. The loss of functional iNOS impaired expression vascular endothelial growth factor (VEGF) and Interleukin-4 (IL-4) that partially explained the delay of wound healing of iNOS knock-out animals³. Several studies have demonstrated diabetes decrease the formation of NO metabolites in the wound environment^{15, 16}. Arginine and NO donors can partially reverse the impaired healing of diabetes.

5.2.3 The role of arginine in wound healing

Wound healing is a complex biological process which could be divided into four phases, haemostasis, inflammation, proliferation and tissue remodeling. In haemostasis, platelets play a crucial role in wound healing process. Not only they are essential for clot formation, but also produce multiple growth factors and cytokines which continue to regulate the healing cascade. The key aim of inflammation stage of wound healing is to prevent infection. Neutrophils which are highly motile cells infiltrate the wound within an hour of the insult and migrate in sustained levels for the first 48 hours. Various chemical signaling mechanisms mediated neutrophils migration, including interleukin activation and transforming growth factor- β (TGF- β). When the neutrophils completed ingesting and destroying foreign particles and bacteria, they undergo apoptosis or are phagocytosed by macrophages. Macrophages are much larger

phagocytic cells which reach peak concentration in a wound at 48-72 hours after injury. Macrophages harbor a large amount of growth factors, such as TGF- β and epidermal growth factor (EGF), which is important in regulating the inflammatory response, stimulating angiogenesis and enhancing the formation of granulation tissue. Lymphocytes appear in the wound after 72 hours and are thought to be important in the production of an extracellular matrix scaffold and collagen remodeling. The inflammatory stage will persist until all excessive bacteria and debris are cleared from the wound. After haemostasis has been achieved, the inflammatory response is balanced, the proliferation stage can begin to repair the defect. This complex process incorporates angiogenesis, the formation of granulation tissue, collagen deposition, epithelialization and wound retraction which occur simultaneously. The final stage of wound healing can take up to 2 years and results in the development of normal epithelium and scar tissue. Eventually they will regain a similar structure to the unwounded tissue. However, wounds never achieve the same level of tissue strength and scar tissue has lower vascularity than unwounded tissue¹⁷. In many experimental wound model studies, activated macrophages avidly consume or deplete arginine from culture medium via the action of iNOS and arginase^{18,19}. The uptake of arginine into macrophage is mediated by cationic amino acid transporters (CAT)^{20, 21}. Inflammatory macrophages convert arginine to citrulline and NO through NOS pathway and produce ornithine and urea from arginine by the activity of arginase. In the early stage of inflammation (< 3 days), activated macrophages show increased NO-production for their anti-bacterial function. The sustained expression of NOS is critical to the accumulation of collagen and the acquisition of mechanical strength in wound. This NO production is subsequently down-regulated by arginase through substrate competition²².

Macrophages have both arginase I and arginase II. Arginase II which is localized

in mitochondria and is inducible by LPS and cytokines seems to play an important role in the metabolism process from arginine. Ornithine produced by arginase I may be preferentially used for polyamine synthesis which is the possible mechanism whereby arginine augments lymphocyte mitogenesis, whereas ornithine produced by arginase II may be preferentially used for synthesis of proline or glutamate¹⁹. Arginase could be brought to the wound by macrophages. The polyamines which are synthesized through arginase metabolism pathway are required for the proliferation and differentiation of mammalian cells. And arginase metabolism pathway was demonstrated as the predominant pathway of arginine metabolism in maturing wounds. And in healing wound, the degradation of extracellular arginine is mainly caused by arginase activity²³. However, arginase was expressed by macrophages only after cell lysis and no arginase was released by viable macrophages in vitro. Thus, the extracellular arginase of wounds may derive from dead macrophages within the injured tissue²⁴. Some study proposed that arginine depletion occurs in inflammatory sites is through the action of release arginase²⁵.

5.2.4 The effect of arginine dietary supplement on wound healing, diabetic ulcer and tumor

Under normal conditions, arginine is not required for normal growth and development and in human, adequate arginine can be produced from citrulline. However, trauma and severe sepsis could lead to depletion of arginine in plasma. In an inflammatory milieu, the activity of macrophage derived arginase depletes the extracellular fluid of arginine. Moreover, some study reported arginine free diet suppressed nitric oxide production in wounds²⁶. Arginine supplementation has been reported to be beneficial to wound healing²⁷. Supplemental arginine is associated with increased lymphocyte and monocyte proliferation, enhanced T-helper cell production, activation of macrophage cytotoxicity, reinforcement of natural killer cell activity and

increased phagocytosis through the mediation of NO production ²⁸. Heffernan et al. demonstrated that continuous supplemental arginine infusion produced significant and sustained increases in wound fluid NO production without significant difference in concentrations of ornithine, citrulline, or proline. Their result also showed sustained NO production maybe inhibit arginase function, there by limits polyamines and ornithine synthesis which are also crucial to wound healing. In their conclusion, early supplemental arginine may disturb the reciprocal regulation of iNOS and arginase, leading to the preferential iNOS metabolism pathway of arginine to produce excess NO rather than ornithine which is produced in arginase metabolism pathway, with consequent reductions in angiogenesis and granulation tissue formation. Diabetic patients usually suffer diabetic foot. If the diabetic foot is not properly treated, diabetic foot will produce amputation of the damaged lower limb ²⁹. Diabetic ulcer healing is impaired, but the mechanisms are not completely understood. High blood glucose decreased cell proliferation and affect collagen synthesis. Production of growth factors and the mediators of collagen synthesis are reduced in the wound milieu. And reduction of phagocytosis and increased apoptosis were observed which is potentially reduced granulation tissue formation ³⁰. Arginine dietary supplement was studied as a treatment to diabetic wound healing. In diabetes, NO synthesis is reduced in the wound milieu. The NO deficiency could occur because of a decreased inflammatory reaction with less iNOS activity in the diabetic wounds. And also, wound fluid of diabetic animals shows lower arginase activity and ornithine concentration. Animal studies demonstrated arginine dietary supplement restored diabetic NO levels toward normal values and improves diabetic rats wound healing (increasing breaking strength of the healing wound, collagen content of implanted sponges in diabetic healing) ³⁰. Clinical research demonstrated dietary arginine supplement in elderly population that result in increased T-cell activity and increased protein and collagen deposition in

experimental wound³¹. However, in the animal study, arginase activity in wound fluid is unaffected by dietary arginine treatment. Only the NO synthesis in the diabetic wound milieu was partially be reversed which was helpful to restore impaired healing in the acute wound. But the function of NO in diabetes is not simple. NO is the mediator of autoimmune disease in diabetic onset and development as well. Elevated systemic NO in diabetes are usually observed with the NO synthesis level is lower than normal NO level at the wound. The possible reason brought by some studies is decreased insulin levels lead to a down-regulation of transforming growth factor beta (TGF- β). The lack of the inhibition function of TGF- β to NOS elevated systemic NO in diabetes³². Some researchers suggest that the wound site and the plasma reflect two distinct compartments of arginine metabolism³⁰. In the clinical studies, arginine dietary supplement did not significantly change the size of diabetic ulcer²⁹.

The metabolism of arginine has a complex and paradoxical action on tumor growth which is tightly related with the behavior of tumor-associated macrophages. And also the role of tumor-associated macrophages in tumor growth is controversial and is still not completely understood. But one thing has been recognized that macrophage can inhibit tumor by achieving tumor cytotoxicity, or promote tumor growth. Both actions are exerted via arginine metabolism.

Macrophages are able to infiltrate tumors. Actually, in animal models, the mass of infiltrated macrophages in a tumor varies greatly from 0 to more than 80% of the total cellular tumor mass³³. Activated macrophages are able to recognize bind and subsequently kill tumor cells including those that are resistant to cytostatic drug and activated macrophages can distinguish between tumorigenic and non-tumorigenic cells. However, the role of tumor-associated macrophages in tumor angiogenesis seems to be influenced by the stage of the tumor growth. In the early stages, the presence of tumor-associated macrophages will delay tumor cell proliferation. When the tumor

grows beyond a size of 1 cm³, angiogenesis is thought to be necessary to provide sufficient blood supply to tumor. At this time, tumor-associated macrophages may support tumor growth by secretion of angiogenic factors. In addition, the tumor may be able to produce substances to prevent macrophages from being tumor cytotoxic. Moreover, tumors sometimes produce factors that are likely to be responsible for accumulation of macrophages in the tumors ³³.

Macrophages produce NO enzymatically from arginine by NOS. The toxic effect of NO and its oxidative end products on target cells are due to three mechanisms. First, NO mediates loss of iron from cells thereby inactivating iron-sulfur cluster-containing enzymes of the mitochondria electron transport. Second, NO is capable of inducing zinc release from zinc-containing proteins there by inducing disulfide formation. Disulfide formation inhibits DNA-binding activity of zinc finger type transcription factors. Third, NO is capable of influencing the activity of iron channels thereby destroying the mitochondrial membrane potential ^{33, 34}. Although the anti-tumor role of NO in the anti-tumor effect of rodent macrophages is established, the anti-tumor cytotoxicity of NO in humans is still controversial. NO or NO metabolite secretion in human cells was substantially lower than in rodent macrophages ³⁵. Experimental studies have shown that NO has a complex and paradoxical action on tumor growth, depending on the local concentration of the molecule: high concentration of NO may inhibit tumor growth by induction of apoptosis in susceptible cells ³⁶, whereas low concentration of NO protects tumor cells from apoptosis ³⁷. Low levels of NO may stimulate tumor neovascularization through the modulation of angiogenesis inducers and may be responsible for maintaining the expanded blood vessel in and around the tumor ³⁸.

The other arginine metabolism pathway which is co-expressed in macrophage is to produce ornithine and polyamines by arginase. The synthesis of polyamines via

arginase I and arginase II isoforms is essential for human tumor cell proliferation^{39,40}. Experimental studies observed tumor associated macrophages from the mid and late tumor-bearing stages had an enhanced arginase activity compared with the early tumor associated macrophages or normal macrophages. Tumor associated macrophages might gradually switched over from NOS metabolism pathway of the early tumor-bearing stages to the arginase metabolism pathway during the course of progressive tumor growth⁴¹.

Both of arginine depletion and arginine supplementation were considered as anti-cancer treatment. Arginine depletion is not feasible because normal cells are able to synthesize arginine through arginosuccinase synthase. Some studies show arginine supplementation augments both specific and nonspecific anti-tumor mechanisms, retards tumor growth and prolongs survival in some animal tumor models⁴². But the supplement of arginine without regulation of its metabolism pathway is still a risky strategy to inhibit tumor growth.

5.2.5 The effect of chitosan on arginine metabolism in macrophage

Chitosan is a linear polymer of N-acetyl-D-glucosamine and deacetylated glucosamine which could be utilized as wound-healing accelerator in clinical and veterinary medicine. Chitosan is able to enhance the functions of many kinds of inflammatory cells, such as polymorphonuclear leukocyte, macrophages and fibroblasts⁴³⁻⁴⁶. Some study observed the chitosan oligosaccharides could activate the production of interleukin-12 (IL-12) of macrophage. The stimulation is relied on the acetylated residue of chitosan⁴⁷. However, the binding of N-acetyl-D-glucosamine to the specific receptors of macrophages is a prerequisite for enhancing macrophage activation. The mechanism of chitosan induced macrophage activation involves mannose receptor-mediated phagocytosis. High affinity binding to mannose receptor requires the cooperation of multiple carbohydrate recognition domains. During

inflammation, the mannose receptor is highly regulated on local macrophages, increasing the possibility to interact with suitable ligand, like chitosan. Chitosan signaling through the up-regulated mannose and other possible receptors together with the inhibition of NO production is one possible mechanism of the enhancement of the arginase pathway in chitosan treated inflammatory cells.

The effects of low molecular weight (LMW) chitosan (50k Da) and high molecular weight (HMW) chitosan (~1,000k Da) on inflammatory macrophage were studied. LMW chitosan strongly enhanced the arginase activity of inflammatory macrophages. HMW chitosan shows no effect on the arginine metabolism pathway⁴⁸. Even though the over-expression of arginase in macrophages enhances tumor cell growth by providing polyamines, no evidence was reported that chitosan can help tumor cell growth. Particularly, HMW chitosan has little effect to improve arginase activity. Different targeted cells and different dosages, sources and preparation methods of chitosan and its derivatives may achieve different cell proliferation effect.

5.2.6 The rationale of the design of glycidyl methacrylate Arg-UPEA/GMA-chitosan hybrid hydrogel and its possible application in wound healing study and tumor study

Even though the metabolism of arginine is well established, the treatment to arginine related disease is not largely improved. In most animal and clinical studies, arginine supplement is provided in diet. Despite free arginine supplement in diet is safe and easy, the medical effect is not satisfying. In normal wound healing, dietary arginine supplement disturbs the reciprocal regulation of iNOS and arginase. Sustained NO production is excessively improved might be inhibit arginase function, there by limits polyamines and ornithine synthesis. Even though NO production is crucial in the first several days after injury, the inhibition of iNOS metabolism pathway lead to low production of polyamine and ornithine which are important in the later stage of wound healing. In diabetic wound studies, arginine dietary supplement

does not obviously reduce the ulcer area or show obvious improvement to the impaired wound healing due to the difference of metabolism of arginine at the wound site and in systemic plasma. Moreover, free arginine which is easily dissolved in plasma is not able to form a concentrated area around the wound site. Whereas the arginase released from dead macrophages are mainly acquire arginine from the local extracellular microenvironment.

Arginine rich degradable hydrogel is one ideal device that it can sustainably improve the local arginine concentration around the wound milieu. The hydrophilic and soft, flexible nature of hydrogel is also suitable for the treatment of wound healing. One series of novel unsaturated arginine based polyester amide (Arg-UPEA) with photocrosslinkable unsaturated double bonds on the polymer chain was developed which is degradable through hydrolysis of ester bond. However, Arg-UPEA is water soluble and could not be able crosslinked by itself due to the low activity of the double bonds on the backbone of the polymer and space hindrance of the guanidino group of arginine. Arg-UPEA could be incorporated can chemically bonded in other photocrosslinkable water soluble materials to form a hydrogel in aqueous solution, such as polyethylene glycol diacrylate (PEGDA), by a UV-photocrosslinking technology ⁴⁹. To achieve improved polyamine and ornithine production, chitosan which is able to improve arginase activity was used as the starting material to synthesize a new type of photocrosslinkable material as another composition of hydrogel. By utilizing the reaction between the epoxy groups of glycidyl methacrylate and reactive amine and hydroxyl groups of chitosan, methacrylate chitosan (GMA-chitosan) was successfully developed. It could be combined with Arg-UPEA to form UV-photocrosslinked hydrogel in aqueous solution. Lysozyme which exists in the human body is able to accelerate the hydrolysis of chitosan ⁵⁰.

In this chapter, the chemical structure of GMA-chitosan and Arg-UPEA was characterized by nuclear magnetic resonance (NMR), Fourier transform infrared spectroscopy (FTIR), carbon and nitrogen elemental analysis. Scanning electron microscopy (SEM) and dynamic mechanical test were employed to characterize the morphology and mechanical properties GMA-chitosan and Arg-UPEA hybrid hydrogel. The enzymatic degradation process of GMA-chitosan hydrogel by lysozyme in vitro was studied. And bovine serum albumin is used as model drug to study the protein drug release from this hybrid hydrogel.

5.3 Experimental

5.3.1 Materials

L-Arginine (L-Arg), fumaryl chloride, ethylene glycol, 1,4-butanediol were purchased from Alfa Aesar (Ward Hill, MA). *p*-toluene sulfonic acid monohydrate (TsOH·H₂O), *p*-nitrophenol (J. T. Baker, Philipsburg, NJ) and triethylamine (Avantor Performance Materials, Center Valley, PA) were used without further purification. Solvents including toluene, isopropyl alcohol, and *N, N*-dimethylacetamide (DMAc), DMSO, were purchased from VWR Scientific (West Chester, PA), ethyl acetate, acetone were purchased from Mallinckrodt incorporation (St.Louis, MO). All solvents were ACS grade and used without further purification. Chitosan (75-85% deacetylated) of molecular weight (MW) 50,000-190,000 Da and bovine serum albumin (BSA) of molecular weight ~66,000 Da. were purchased from Sigma Chemical Company (St.Louis, MO). Glycidyl methacrylate (GMA, 97%), 4-(*N, N*-dimethylamino) pyridine (DMAP, 99%), 0.05 M buffer solutions (pH 3, pH 7.4, pH 10) and lysozyme (from Chicken egg) were purchased from VWR Scientific (West Chester, PA). Irgacure 2959 was donated by Ciba Specialty Chemicals Corp.

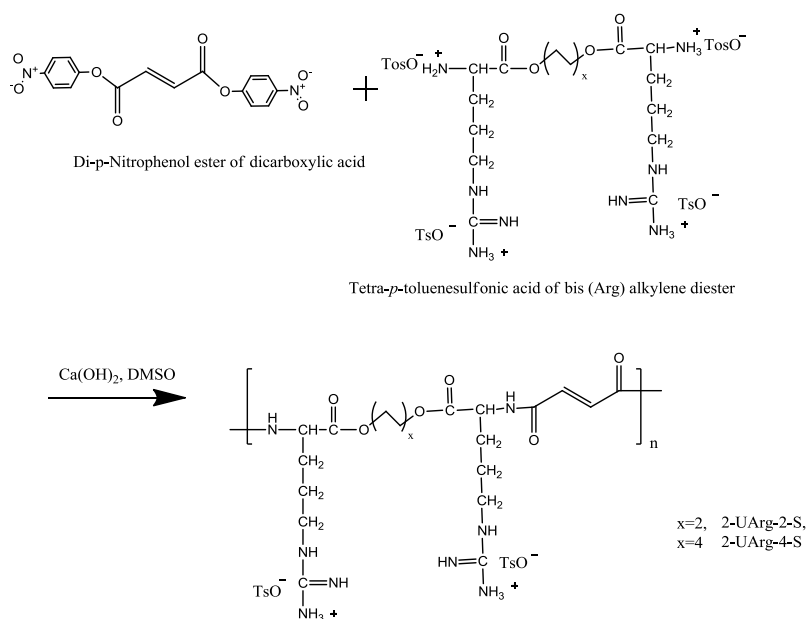
5.3.2 Methods

5.3.2.1 Synthesis of unsaturated Di-*p*-nitrophenyl ester of dicarboxylic acid (monomer 1)

Unsaturated Di-*p*-nitrophenyl ester of dicarboxylic acid was prepared by reaction by fumaroyl dichloride (0.03mol) with *p*-nitrophenol (0.063mol) in acetone in the presence of triethylamine (0.063mol). A dry ice/isopropyl alcohol mixture was prepared to keep *p*-nitrophenol and triethylamine mixed acetone solution (100mL) at -78 °C. Fumaroyl dichloride was diluted in 50mL of acetone before dropped to the above chilled solution with stirring for 2h at -78 °C and keep overnight at room temperature. The resulting di-*p*-nitrophenyl ester of succinic acid was precipitated in distilled water, dried in *vacuo* at room temperature before final recrystallization from ethyl acetate three times. Figure 5.3 A shows the chemical process of this reaction.

5.3.2.2 Synthesis of tetra-*p*-toluene sulfonic acid salt of bis (L-arginine) alkylene diesters (monomer 2).

L-Arginine (0.02 mol) and ethylene glycol or 1, 4-butanediol (0.01 mol) were directly condensed in refluxed toluene (b.p. 110 degree) (80mL) with the presence of *p*-toluene sulfonic acid monohydrate (0.04 mol). The heterogeneous solid-liquid reaction mixture was heated to 120 °C and reflux for 24 hours after 1.08 mL (0.06 mol) of water generated and collected by a dean-stark apparatus. The reaction mixture was then cooled to room temperature. Toluene was decanted. The dried resulted mixture was then purified by repeated precipitation in isopropyl alcohol three times. The dried resulted mixture was put in a 500mL round bottom flask filled with sufficient amount of isopropyl alcohol to completely dissolve the reaction mixture with refluxing at 100 °C. The clear solution was then cooled down to room temperature naturally, and left still for overnight before transferred to freezer (-20 °C) to promote further precipitation. Isopropyl alcohol was decanted afterwards, and the



C

Figure 5.3 (A) synthesis of di-*p*-nitrophenyl ester of dicarboxylic acid (monomer 1), (B) synthesis of tetra-*p*-toluene sulfonic acid salt of bis (L-arginine) alkylene diesters (monomer 2), (C) Synthesis of 2-UArg-4-S polyester amide.

to obtain a uniform mixture. Triethylamine (0.31 mL, 2.2mmol) was added dropwise to the mixture while heating up to 70 °C with vigorous stirring until the complete dissolution of the monomers. The reaction was then kept for 48 hours at 70 °C with stirring. The resulting solution was precipitated in cold ethyl acetate, decanted, dried re-dissolved in methanol and re-precipitate in cold ethyl acetate to further purify. Repeat purification for 2 times before final drying in *vacuo* at room temperature.

5.3.2.4 Cytotoxicity of Arg-UPEA/ GMA-chitosan hybrid hydrogel precursor in the aqueous solution

Porcine aortic valve smooth muscle cells (PAVSMC) were maintained in minimum essential medium (MEM) supplemented with 10% fetal bovine serum (FBS) and 1% each of penicillin-streptomycin. The cells were incubated in CO₂ incubator at 37 °C with 5% CO₂. After reaching confluence, the cells were detached from the flask

with Trypsin-EDTA (Invitrogen, Carlsbad, CA). The cell suspension was centrifuged at 3,000 rpm for 3 min and then re-suspended in the growth medium for further study. PAVSMCs were used between passages 4 and 7.

Evaluation of the cytotoxicity of Arg-UPEA/GMA-chitosan hydrogel precursor was performed using the MTT assay. 20 mL Arg-UPEA/GMA-chitosan (DS 37)-33/67 sample solution (total 3 wt %) was obtained by dissolving 400 mg GMA-chitosan and 200 mg Arg-UPEA in PBS (0.05M, pH 7.4). 6 different total concentrations of Arg-UPEA/ GMA-chitosan-33/67 (0.1 mg/mL, 0.3 mg/mL, 0.6 mg/mL, 1 mg/mL, 3 mg/mL and 6 mg/mL) were prepared by diluting 3 wt % Arg-UPEA/ GMA-chitosan-33/67 PBS solution with MEM media and sterilized after filtration through a 0.45 μ m filter. Cultured PAVSMCs at an appropriate cell density (2,000 cells well⁻¹) were seeded into 96-well plates and incubated overnight. After 24 h, the cells were treated with 100 μ L freshly prepared Arg-UPEA/GMA-chitosan-33/67 in MEM media at 6 different concentrations. The cells treated only with normal cell culture media were used as the control. After 24 h treatment and incubation, 10 μ L of MTT solution (5 mg/mL thiazolyl blue tetrazolium bromide in deionized water after filtration by 0.22 μ m filter) was added into each wells and incubated for another 4 h at 37 $^{\circ}$ C under a 5 % CO₂ atmosphere to allow the formation of formazan crystals. After that, the cell culture medium including Arg-UPEA/ GMA-chitosan - 33/67 was then carefully removed and 100 μ L of acidic isopropyl alcohol (contains 10% Triton-X 100 with 0.1M HCl) was added into each well and gently shaken at room temperature for 1 h to ensure that the purple crystals have been completely dissolved. The optical density of the solution was measured at a wavelength of 570 nm and 690 nm (Spectramax plus 384, Molecular Devices, USA). The cell viability (%) was calculated according to the following equation: Viability (%) = [OD570 (sample) - OD690 (sample)]/[OD570 (control) - OD690 (control)] \times 100%, where the OD570

(control) represents the measurement from the wells treated with medium only, and the OD570 (sample) from the wells treated with various polymers. 8 samples were analyzed for each experiment. Differences between group means were assessed using one-way ANOVA followed by parametric multiple comparison tests. A value of $p < 0.05$ was considered statistically significant.

5.3.2.5 Fabrication of Arg-UPEA/ GMA-chitosan hybrid hydrogel

Although almost all Arg-UPEAs have water solubility at room temperature, the methylene chain length (x) in the diol part between the two adjacent ester groups is one crucial material parameter of Arg-UPEA which can largely influence the polymer solubility in water.⁵¹ Only the Arg-UPEA with $x = 2$ and 4 were used in the fabrication of Arg-UPEA/GMA-chitosan hybrid hydrogel, because the water solubility of Arg-UPEA with $x > 4$ is too low to form water soluble hydrogel precursor solution with some other water-soluble polymer precursors, such as GMA-chitosan. In a typical Arg-UPEA/GMA-chitosan hybrid hydrogel fabrication process, 0.3 g GMA-chitosan (DS 37) and desired amounts of Arg-UPEA (2-UArg-4-S or 2-UArg-2-S, 43mg~150mg), were added into a glass vial and dissolved in deionized water (6.0 mL) to form a clear homogeneous solution with light yellow color. 10 mg Irgacure 2959 photo-initiator was added into the precursors' solution and dissolved completely. In order to keep the structure integrity of the hybrid hydrogels, the weight feed ratio of Arg-UPEA to GMA-chitosan could not be higher than 33 to 67.

Every 400 μ L of this aqueous solution mixture was transferred onto a custom-made 20 well Teflon mold (11 mm diameter, 6 mm depth) using a micropipette and then irradiated by a long wavelength UV light (100 watts, 365nm, mercury spot lamp, Blak-ray[®]) at room temperature for about 30 min until disk-shaped solid hydrogels were formed. The resultant hydrogels were immersed into deionized water for 16 h at room temperature to leach residues and to reach the swelling equilibrium. The swollen

Arg-UPEA/GMA-chitosan hydrogel samples were then dehydrated on a Teflon plate in the ambient air at room temperature until the dry weight was constant for further studies, such as FTIR, equilibrium swelling ratio. Pure GMA-chitosan hydrogels were fabricated from 6wt% GMA-chitosan water solution. In the further study (swelling test, morphology, compressive mechanical study, enzymatic degradation etc.), pure GMA-chitosan hydrogels served as the control sample.

5.3.2.6 Characterization of 2-UArg-4-S PEA and its hybrid hydrogel with GMA-chitosan

Dehydrated Arg-UPEA/GMA-chitosan hybrid hydrogels were analyzed by FTIR, and elemental analysis. FTIR spectra of Arg-UPEA/GMA-chitosan hybrid hydrogel samples were recorded on a PerkinElmer (Madison, WI) Nicolet Magna 560 FTIR spectrophotometer with Omnic software for data acquisition and analysis. Elemental analysis of Arg-UPEA and Arg-UPEA/GMA-chitosan hybrid hydrogels was performed with a Thermo Scientific ConFlo III elemental analyzer by Stable Isotope Laboratory of Cornell University.

5.3.2.7 Equilibrium swelling ratio (Q_{eq}) test under different pH environment at room temperature

The Q_{eq} of Arg-UPEA/GMA-chitosan hybrid hydrogel and the pure GMA-chitosan hydrogel (as control) were performed at room temperature (25 °C) by immersing dehydrated hydrogels individually in glass vials containing 15 mL 0.05M buffers (pH 3, 7.4, 10). After 16 h, the Arg-UPEA/GMA-chitosan hybrid hydrogels reached their swelling equilibrium. The swollen hydrogels were then removed, the excess surface water was wiped and the hydrogels were weighed until a constant weight was obtained. The swelling ratios of the hydrogels were calculated from the swollen and dry weights of the hydrogels according to the following equation.

$$Q_{eq} (\%) = (W_r - W_0) / W_0 \times 100$$

W_i is the weight of the hydrogel at swelling equilibrium

W_0 is the initial dry weight of the hydrogel before immersion.

The reproducibility of the swelling profiles of a hydrogel was determined in triplicate.

5.3.2.8 Morphological study of 2-UArg-4-S/GMA-chitosan hydrogels

Scanning electron microscope (SEM) was employed to analyze the interior microstructure of two hybrid hydrogels having different Arg-UPEA to GMA-chitosan feed ratios: 2-UArg-4-S/GMA-chitosan-12.5/87.5 and 2-UArg-4-S/GMA-chitosan-33/67 hybrid hydrogels. A pure GMA-chitosan hydrogel was examined for comparison. Individual hydrogels were soaked in deionized water at room temperature to reach their swelling equilibrium. Then, the hydrogels were transferred into liquid nitrogen immediately to freeze and retain the swollen structure. The samples were subsequently freeze-dried for 72 h in a Labconco (Kansas City, MO) Freezone 2.5 Freeze drier under vacuum at $-50\text{ }^{\circ}\text{C}$, and finally glued onto aluminum stubs and coated with gold for 30s for SEM observation by Leica Microsystems GmbH (Wetzlar, Germany) 440 SEM.

5.3.2.9 Compression mechanical properties of 2-UArg-4-S/GMA-chitosan hydrogels

The mechanical testing of the GMA-chitosan and Arg-UPEA/GMA-chitosan hybrid hydrogel was performed on a DMA Q800 Dynamic Mechanical Analyzer (TA Instrument Inc., New Castle, DE) in a “controlled force” compression mode. A pure GMA-chitosan hydrogel was tested for comparison. The compressive mechanical properties of Arg-UPEA/GMA-chitosan hybrid hydrogels and GMA-chitosan hydrogel in circular disc shape after reached their equilibrium swelling in deionized water were measured at room temperature ($25\text{ }^{\circ}\text{C}$). The hydrogels were mounted between the movable compression probe (diameter 15mm) and the fluid cup without any liquid media. A compression force from 0.01 to 4 N at a rate of 0.5 N/min was applied on the swollen hydrogel samples at room temperature until fragment of the

hydrogels was produced. TA Universal Analysis software was used for mechanical data analysis. Initial compressive modulus and compressive strain at break were used to examine the hydrogel mechanical property. The initial compressive modulus was calculated from the slope of the initial linear portion of the curve. For each type of hydrogel, five samples were used, and their mean value was calculated with a standard deviation.

5.3.2.10 Enzymatic degradation of 2-UArg-4-S/GMA-chitosan-33/67 hybrid hydrogels

The enzymatic biodegradation of the circular disk shaped GMA-chitosan and 2-UArg-4-S/GMA-chitosan-33/67 hybrid hydrogel was evaluated by their weight loss at 37 °C in 15mL lysozyme (1mg/mL) in 0.05M pH 7.4 PBS over a period of 10 days. A 15 mL PBS of pH 7.4 served as the control. The weight of each dry GMA-chitosan or 2-UArg-4-S/GMA-chitosan-33/67 hydrogels was measured before immersion. At various immersion intervals, three GMA-chitosan hydrogel and 2-UArg-4-S/GMA-chitosan hybrid hydrogel samples were removed from the immersion solution and dried under vacuum at room temperature till constant weights. The weight loss was calculated according to the following equation: $\% \text{ Weight loss} = (W_o - W_t) / W_o \times 100\%$, where W_o was the average initial ($t=0$) dry weight of hydrogel in the biodegradation test, and W_t was the dry weight of the hydrogel tested after incubation at time t . Mean value of experimental value was calculated as the weight loss at time t with a standard deviation.

5.3.2.11 Release study of bovine serum albumin from 2-UArg-4-S/GMA-chitosan-33/67 hydrogel

BSA was selected as the model protein to investigate the release behaviors of 2-UArg-4-S/GMA-chitosan hybrid hydrogels. In order to load proteins, 100 μ L 15 mg/mL BSA aqueous solution was added to a solution of GMA-chitosan (150 mg, DS

37) and 2-UArg-4-S (75 mg or 21 mg) and in 2.5mL deionized water and mix well. 5 mg Irgacure 2959 was dissolved in 400 μ L deionized water and was then added into the BSA-loaded Arg-UPEA/GMA-chitosan hybrid hydrogel precursor solution. A 400 μ L BSA loaded hybrid hydrogel precursor solution was then transferred onto a Teflon mold (11 mm diameter, 6 mm depth) and irradiated by a long wavelength (100 watts, 365nm, mercury spot lamp, Blak-ray[®]) UV light at room temperature for about 30 min until disk-shaped solid hydrogel was obtained. GMA-chitosan hydrogel precursor with BSA loaded (6 wt% GMA-chitosan with 500 μ g /mL BSA) was used to fabricate pure GMA-chitosan hydrogel in the BSA release study.

In the BSA control release study, each Arg-UPEA/GMA-chitosan hybrid hydrogel or pure GMA-chitosan hydrogel sample (11 mm diameter, 6 mm thickness circular disk-shaped hydrogel with 200 μ g BSA loaded) was placed in glass vials individually and filled with 5 mL 0.05 M PBS (pH 7.4) supplemented with 0.02 w/v% sodium azide, and then incubated at 37°C. At each pre-determined time intervals, 200 μ L PBS bath solution was taken out from the vial and diluted with PBS to 1mL. 200 μ L fresh PBS was added back into the glass vial to compensate the amounts removed for the BSA release study.

MicroBCA kit was used to measure the BSA concentration of the diluted PBS bath solutions. PerkinElmer (Madison, WI) Lambda 35 UV-Vis spectrophotometer was used to determine the absorption of sample solutions at 278 nm wavelength. Pure GMA-chitosan hydrogel samples with the same amounts BSA loaded were used as the control to evaluate the effect of Arg-UPEA co-precursor on the BSA release behavior. The standard curve was prepared by plotting the average Blank-corrected 278nm reading for each BSA standard which is provided in the kit vs. its concentration in μ g/mL. The standard curve was used to determine the BSA concentration of each sample at each time point. The release kinetics were calculated as C_t/C_0 where C_t was

the amounts of BSA in the release medium at a given time and C_0 is the initial amounts of the BSA loaded in each hydrogel sample (200 μg).

5.4 Results

5.4.1 ^1H NMR spectroscopy of Arg-UPEA monomers

The chemical structure of monomer 2 (tetra-*p*-toluenesulfonic acid salts of bis(L-arginine butandiol diester monomer) were confirmed by ^1H NMR in Figure 5.4. ^1H NMR (DMSO-*d*₆, ppm, δ): 1.52 [4H, -OC(O)-CH(NH₃⁺)-CH₂-CH₂-CH₂-NH-], 1.65 [4H, -(O)C-O-CH₂-CH₂-], 1.80 [4H, -OC(O)-CH(NH₃⁺)-CH₂-CH₂-CH₂], 2.29 [6H, H₃C-Ph-SO₃⁻], 3.10 [4H, -CH₂-CH₂-CH₂-NH], 4.04 [2H, ⁺H₃N-CH(R)-C(O)-O-], 4.14 [4H, -(O)C-O-CH₂-CH₂], 7.18, 7.53 [16H, Ph]. The ratio of integration of peak area of benzene group to that of peak 10 is about 8. It demonstrated the monomer has

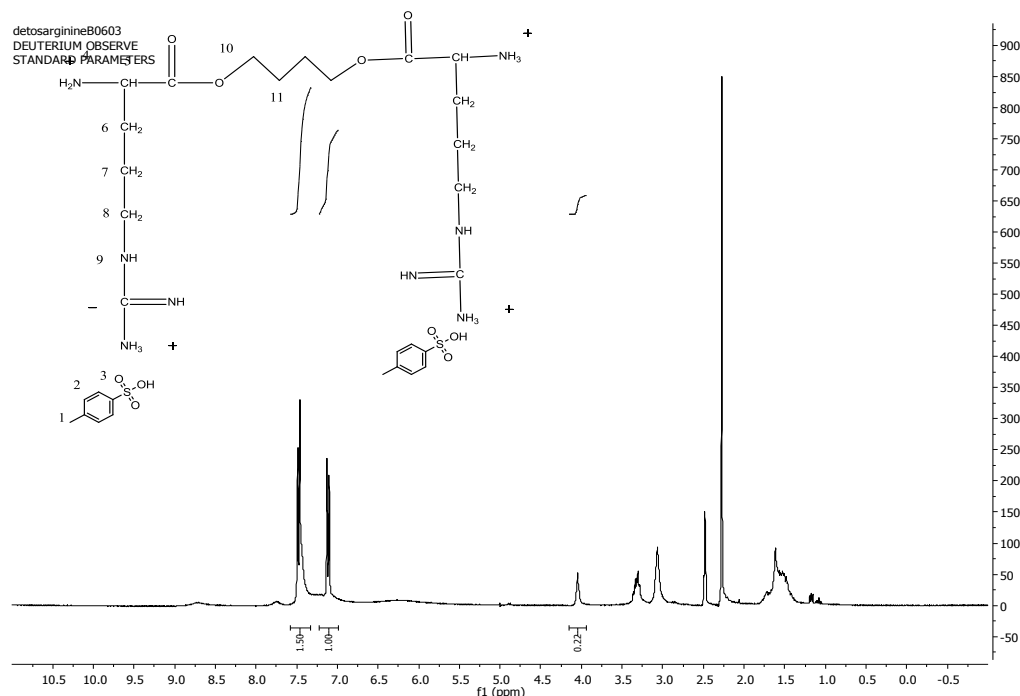


Figure 5.4 H-NMR of bis (L-Arginine) alkylene diester toluene sulfonic acid salt (Arg-4) in DMSO-*d*₆

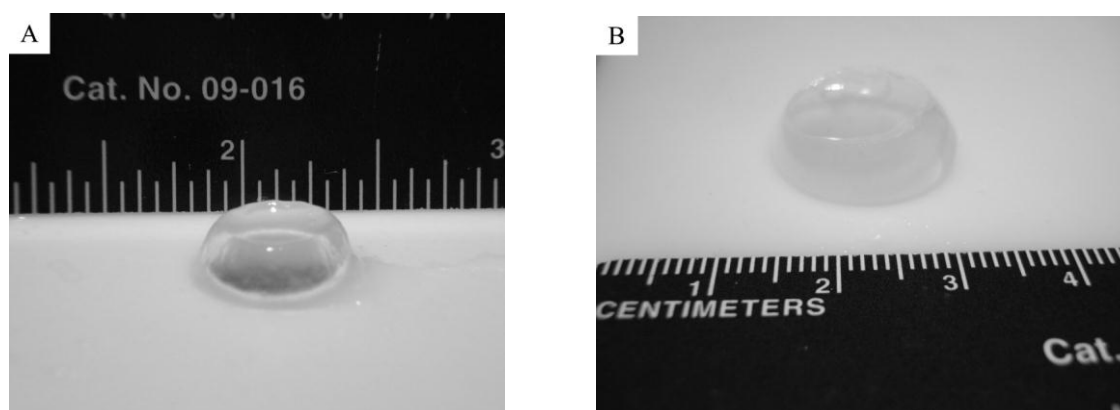
4 *p*-toluene sulfonic acid molecules attached on one diester of arginine-butenediol molecule. The peak 10 ($\delta=4.04$ ppm) also demonstrated the formation of ester bond of the diester of arginine-butenediol.

5.4.2 Fabrication of Arg-UPEA/ GMA-chitosan Hybrid Hydrogel.

2-UArg-4-S/GMA-chitosan-33/67 hybrid hydrogel was used as a representative hybrid hydrogel sample. The optical images of 2-UArg-4-S/GMA-chitosan (DS 37)-33/67 hybrid hydrogel after photocrosslinking before (Figure 5.5 A) and after (Figure 5.5 B) swelling in deionized water showed that this hybrid hydrogel had good transparency with the light yellow color came from the 2-UArg-4-S. A representative chemical network structure of the photocrosslinked Arg-UPEA/GMA-chitosan hybrid hydrogel is shown in Figure 5.5 C.

5.4.3 FTIR spectroscopy

Figure 5.6 shows the FTIR spectra of the 2-UArg-4-S PEA and GMA-chitosan and their hybrid hydrogels after dehydration in the air after 2 days. The carbonyl bands of ester bonds at $1738-1742\text{ cm}^{-1}$ were shown on 2-UArg-4-S PEA. The ester bond of GMA on GMA-chitosan is about 1725 cm^{-1} . The characteristic absorption bands of the



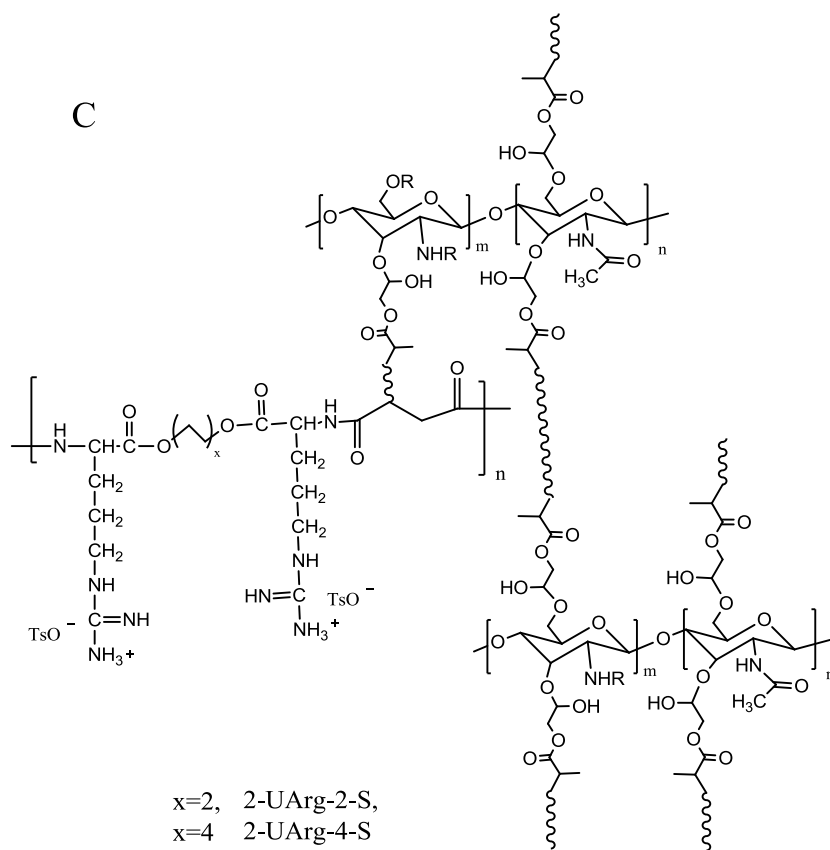


Figure 5.5 Images of 2-UArg-4-S/GMA-chitosan-33/67 hybrid hydrogel (A) 2-UArg-4-S/GMA-chitosan-33/67 hybrid hydrogel after photocrosslinking, (B) 2-UArg-4-S/GMA-chitosan-33/67 hybrid hydrogel after 16 h swelling in deionized water. (C) One representative chemical structure of Arg-UPEA/GMA-chitosan hybrid hydrogel. The degree of GMA substitution in GMA-chitosan is 37, the swelling ratio of 2-UArg-4-S/GMA-chitosan-33/67 hybrid hydrogel is 3,826.1% in deionized water.

unsaturated C=C bond ($\sim 3030\text{ cm}^{-1}$) in 2-UArg-4-S disappeared in the 2-UArg-4-S/GMA-chitosan hybrid hydrogel. 2-UArg-4-S PEA and 2-UArg-4-S/GMA-chitosan also shows amide (I) band and amide (II) band at $1648\sim 1650\text{ cm}^{-1}$ and $1538\sim 1542\text{ cm}^{-1}$. And -C-O-C structure of GMA-chitosan repeat unit shows absorption at 1150 cm^{-1} which is absent at 2-UArg-4-S PEA spectra. 2-UArg-4-S/GMA-chitosan has absorption at 1150 cm^{-1} which shows the feature of chitosan repeat unit. All of the samples have NH linkage, they showed NH vibration at 3290 cm^{-1} . The FT-IR spectra

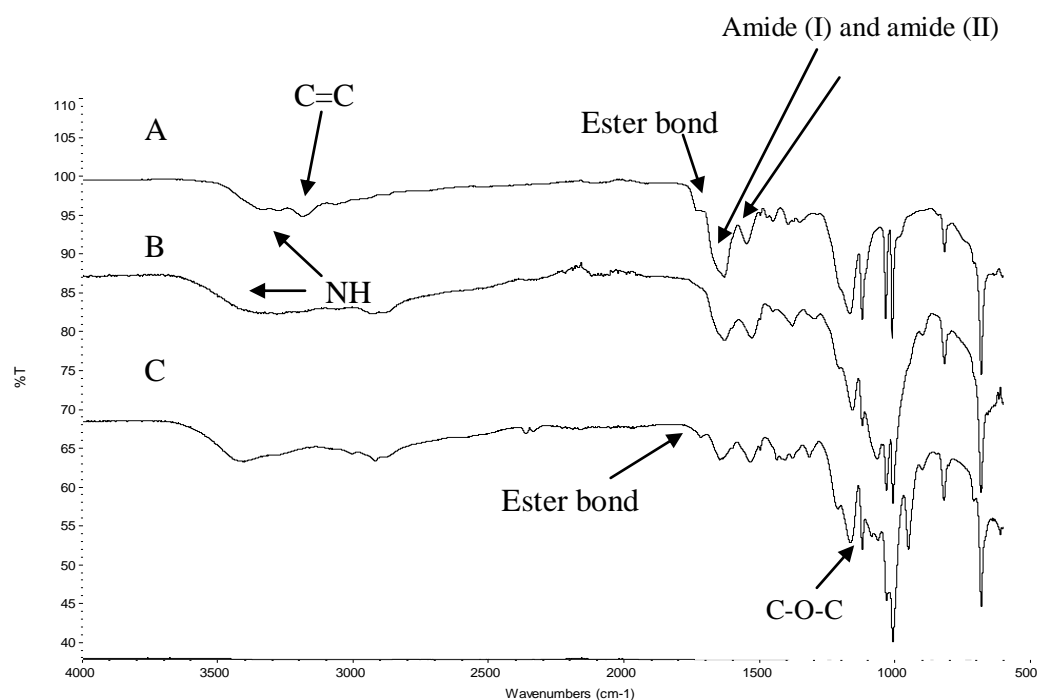


Figure 5.6 FTIR spectra of 2-UArg-4-S, GMA-chitosan and 2-UArg-4-S/GMA-chitosan-33/67 hybrid hydrogel. (A) 2-UArg-4-S; (B) 2-UArg-4-S/GMA-chitosan-33/67 hybrid hydrogel; (C) GMA-chitosan. The degree of GMA substitution in GMA-chitosan is 37.

demonstrated the presence of chitosan and 2-UArg-4-S in the dried hydrogel. The water soluble 2-UArg-4-S was chemically bonded with the GMA-chitosan hydrogel network.

5.4.4 Elemental analysis of Arg-UPEA/GMA-chitosan hybrid hydrogel

Carbon and nitrogen elemental analysis was also used to characterize the chemistry composition of GMA-chitosan and Arg PEA. 2-UArg-4-S PEA has much higher nitrogen composition than GMA-chitosan. The result is shown in Table 5.1. The nitrogen content of 2-UArg-4-S/GMA-chitosan hydrogels which are made with different ratio of two components is in 5.4%-7.8% range. This value is between that of GMA-chitosan and 2-UArg-4-S PEA nitrogen content. It is another proof that GMA-chitosan and 2-UArg-4-S are bonded together in the hydrogel. The theoretical data was calculated with the assumption that 100% of the two components are bonded together. On the other hand: the difference of carbon content and nitrogen content of 2-UArg-4-S/GMA-chitosan between the calculated data and the data acquired from elemental analysis shows a little portion of unsaturated arginine PEA is not covalently linked to the GMA-chitosan matrix.

5.4.5 Cytotoxicity of 2-UArg-4-S/GMA-chitosan-33/67 hybrid hydrogel

Figure 5.7 shows MTT assay data for PAVSMCs after 24 h treatment in six different concentrations of the aqueous mixture of 2-UArg-4-S/GMA-chitosan at the feed ratio of 33 to 67 in MEM media (0.1, 0.3, 0.6, 1, 3, 6 mg/mL). PAVSMCs cultured onto the 24 well cell culture plate without 2-UArg-4-S and GMA-chitosan treatment were used as the blank control. The MTT data indicated no significant difference in cytotoxicity in all of the concentrations of 2-UArg-4-S/GMA-chitosan-33/67 aqueous solution when compared with a blank control. It is evident from the results that at least 85% PAVSMCs were viable when these cells were incubated with up to 6 mg/mL 2-UArg-4-S and GMA-chitosan aqueous mixture at the 33 to 67 mixed

ratio for 24 h. These results indicated that the 2-UArg-4-S/GMA-chitosan-33/67 mixed solutions up to 6 mg/mL had virtually no cytotoxicity to PAVSMC cells.

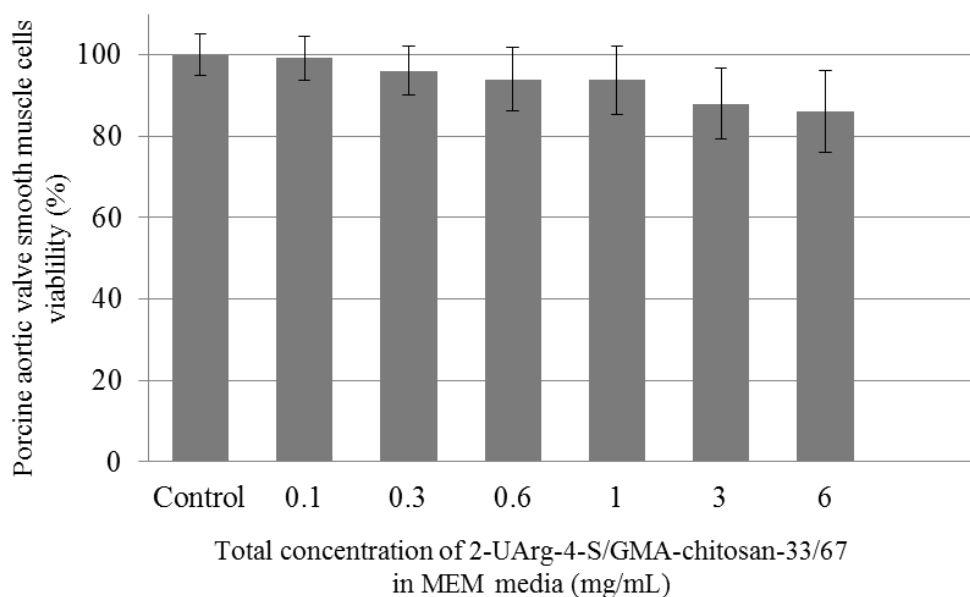


Figure 5.7 Porcine aortic valve smooth muscle cell viability test by MTT assay of 2-UArg-4-S/GMA-chitosan-33/67 mixed solution at 0.1, 0.3, 0.6, 1, 3, 6 mg/mL total concentration. 24 h culture and culture medium without the polymers as the control.

Arg-UPEA was reported to be non-cytotoxic to rat vascular smooth muscle cells, Detroit 539 human fibroblast cells and bovine aortic endothelial cells.^{20,35} Arg-UPEA also had a special function to improve the cell attachment, proliferation and cell viability in the Arg-UPEA/Pluronic acid (F127) hybrid hydrogels, probably due to its cationic property.²⁰ In the current study, the aqueous solution mixture of Arg-UPEA and a new chitosan based derivative (GMA-chitosan) also showed good biocompatibility to PAVSMCs based on the MTT assay. The combination of 2-UArg-4-S and GMA-chitosan components in their hybrid hydrogel could provide a cell-

friendly environment that may make the Arg-UPEA/GMA-chitosan hybrid hydrogels suitable as scaffolds for cell seeding in tissue engineering applications.

5.4.6 Equilibrium swelling ratio (Q_{eq}) test of Arg-UPEA/GMA-chitosan hybrid hydrogels under different pH environment at room temperature

Figure 5.8 shows the effect of pH environment on the swelling behavior of Arg-UPEA/GMA-chitosan hybrid hydrogels at the same ionic strength (0.05M). The swelling results demonstrated that the Arg-UPEA/GMA-chitosan hybrid hydrogels changed their ability to swell significantly when the environmental pH was altered, i.e., a lower swelling at a higher pH. For example, 2-UArg-4-S/GMA-chitosan-33/67 hybrid hydrogel achieved 2,779%, 1,558% and 298% Q_{eq} in pH 3, 7.4 and 10 buffers, respectively. The Q_{eq} of a pure GMA-chitosan hydrogel also significantly decreased as the pH increased. The Q_{eq} of GMA-chitosan were 5,914%, 3,668%, 914% at pH 3, 7.4 and 10. The data in Figure 5.7 also demonstrate that the incorporation of the Arg-UPEA precursor into GMA-chitosan reduced the swelling of GMA-chitosan over the pH range studied.

Apparently, the swelling ratio decreased as the pH increased from 3 to 10 for all GMA-chitosan hydrogels and Arg-UPEA/GMA-chitosan hybrid hydrogels. It is known that the swelling ratios of polymer network structure at various pH environments depend upon the available free volume of the expanded polymer matrix, polymer chain relaxation and availability of ionizable functional groups, such as amine groups, guanidine groups. A reduction in swelling ratios from pH 3 to 10 in the Arg-UPEA/GMA-chitosan hybrid hydrogels is because the pKa of guanidine groups in the Arg-UPEA is about 12.5,⁵¹ and the pKa of the amine groups of GMA-chitosan is about 6.5. Both of the primary amine groups and guanidine groups of hydrogels tended to be ionized at an acid pH. The osmotic pressure inside the hydrogels decreases with the increasing pH from 3-10, that led to swelling decreasing.

At all pH environments, the contents of Arg-UPEA also influenced the hybrid hydrogel swelling. The Q_{eq} of the hybrid hydrogels at pH 3, 7.4 and 10, generally decreased with an increase in the Arg-UPEA contents. For example, the Q_{eq} of 2-UArg-4-S/GMA-chitosan-12.5/87.5 hybrid hydrogel were 3,318%, 2,708%, 429% at pH 3, 7.4 and 10, respectively, while the Q_{eq} of 2-UArg-4-S/GMA-chitosan-33/67 (more Arg contents) were 2,779%, 1,558% and 298% at pH 3, 7.4 and 10. The reason is probably related to the difference of molecular weight (MW) of these two polymers. The MW of chitosan used in the synthesis of GMA-chitosan is from 50 to 190 kg/mol, and after the grafting methacrylate (MA) groups, the MW of GMA-chitosan molecules

Table 5.1 Carbon and nitrogen content analysis of GMA-chitosan* and Arg-UPEA hybrid hydrogel.

	Carbon content (%, experimental)	Carbon content (%, theoretical data)	Nitrogen content (%, experimental)	Nitrogen (%, theoretical data)
GMA-chitosan	44.4	45.3	6.1	6.4
2-UArg-4-S	47.3	49.3	13.1	13.5
2-UArg-2-S	47.7	48.0	14.2	14.0
2-UArg-4-S/GMA-chitosan - 20/80	43.7	46.1	6.4	7.8
2-UArg-4-S/GMA-chitosan - 33/67	44.3	46.6	7.5	8.8
2-UArg-2-S/GMA-chitosan - 33/67	44.4	46.2	7.8	8.9

* The degree of GMA substitution in GMA-chitosan is 37.

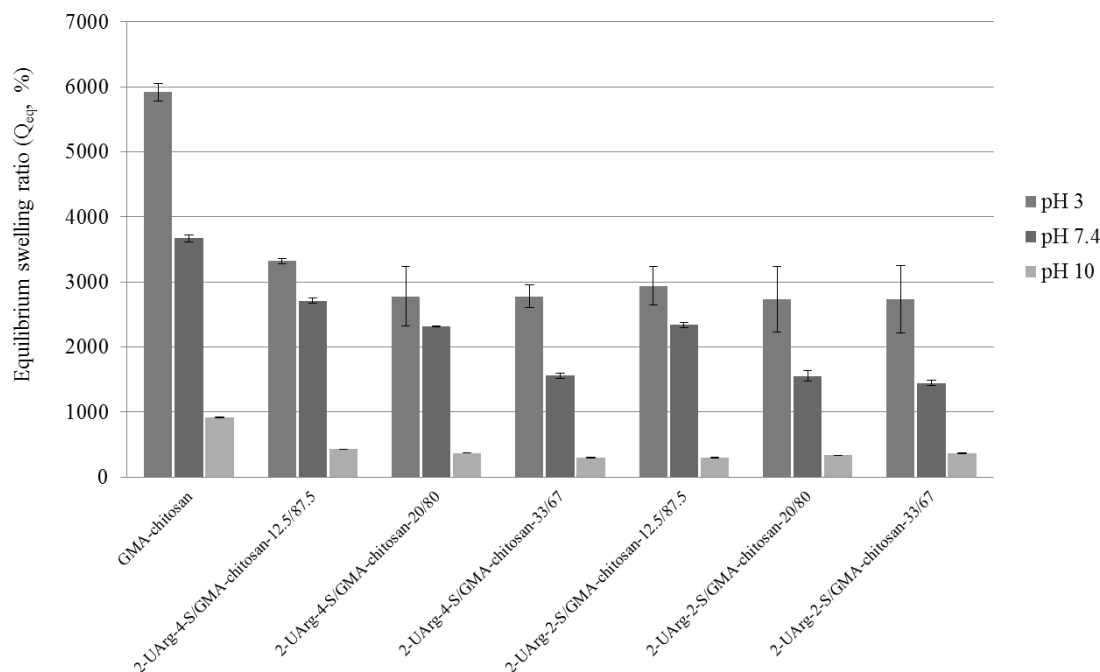


Figure 5.8 The influence of pH environment to the equilibrium swelling ratio Q_{eq} of Arg-UPEA/GMA-chitosan hybrid hydrogels of different Arg-UPEA to GMA-chitosan feed ratio in an ionic strength 0.05M aqueous buffer at room temperature.

with DS 37 theoretically was from 76 to 289 kg/mol. While the MW of Arg-UPEA synthesized by polycondensation in solution ranged from 12.93 to 15.71 kg/mol.⁵¹

That suggests that the polymer chains of GMA-chitosan precursor were much longer than that of Arg-UPEA precursor. Thus, an increase in the Arg-UPEA contents in the hybrid hydrogels would make the resulting hydrogel network structure tighter, i.e., more compact and lower swelling. The swelling data in Figure 5.8 also indicate that the methylene chain length (x) in the Arg alkylene diester repeating unit of the Arg-UPEA precursor didn't show much influence on the Q_{eq} of hybrid hydrogels at all pH environments. For example, at the same Arg-UPEA/GMA-chitosan weight feed ratio (33/67), the Q_{eq} of 2-UArg-4-S/GMA-chitosan hybrid hydrogels ($x=4$) at pH 3,

7.4 and 10 were 2778.7%, 1558.3% and 297.8%. The Q_{eq} of 2-UArg-2-S/GMA-chitosan hybrid hydrogels ($x=2$) were 2735.8%, 1445.9% and 363.4%.

The pH effect on the swelling property of other chitosan-based hybrid hydrogels had also been reported.⁵² In the Zhong et al. study of maleic-chitosan/PEGDA hydrogels, they also discovered pH-dependent swelling; but contrary to the findings of the current Arg-UPEA/GMA-chitosan hybrid system, the maleic-chitosan/PEGDA hybrid hydrogel achieved a higher swelling ratio at an alkaline pH than at an acidic condition.⁵² This is because the ionizable groups in maleic-chitosan/PEGDA is mainly carboxyl group (pKa 1.8-2.4) that are easier to be ionized (deprotonized) in such an alkaline condition, while the current Arg-UPEA/GMA-chitosan hybrid system doesn't have such carboxyl group. Only the ionized groups localized within the hydrogel could create osmotic pressure between the hydrogel interior and the surrounding buffer solution. So, the osmotic pressure inside the maleic-chitosan/PEGDA hybrid hydrogel was higher at an alkaline condition, which led to a higher Q_{eq} .

5.4.7 Morphology of 2-UArg-4-S/GMA-chitosan hybrid hydrogel

The cross-sectional interior morphology of the 2-UArg-4-S/GMA-chitosan hybrid hydrogels at 2 different precursor weight feed ratios (i.e. 12.5/87.5 and 33/67) were examined and shown in Figure 5.9. No obvious phase separation of the 2-UArg-4-S/GMA-chitosan hybrid hydrogel was observed, probably due to the good miscibility between the two components. Compared with a pure GMA-chitosan hydrogel (Figure 5.9 A), 2-UArg-4-S/GMA-chitosan-12.5/87.5 hybrid hydrogel (Figure 5.9 B) and 2-UArg-4-S/GMA-chitosan-33/67 hybrid hydrogel (Figure 5.9 C) had three-dimensional porous network structures, and an increase in the 2-UArg-4-S to GMA-chitosan feed ratio led to a smaller pore size and compact network structure

(Figure 5.9 B vs. 5.9 C). For example, GMA-chitosan hydrogel and 2-UArg-4-S/GMA-chitosan-12.5/87.5 hybrid hydrogel

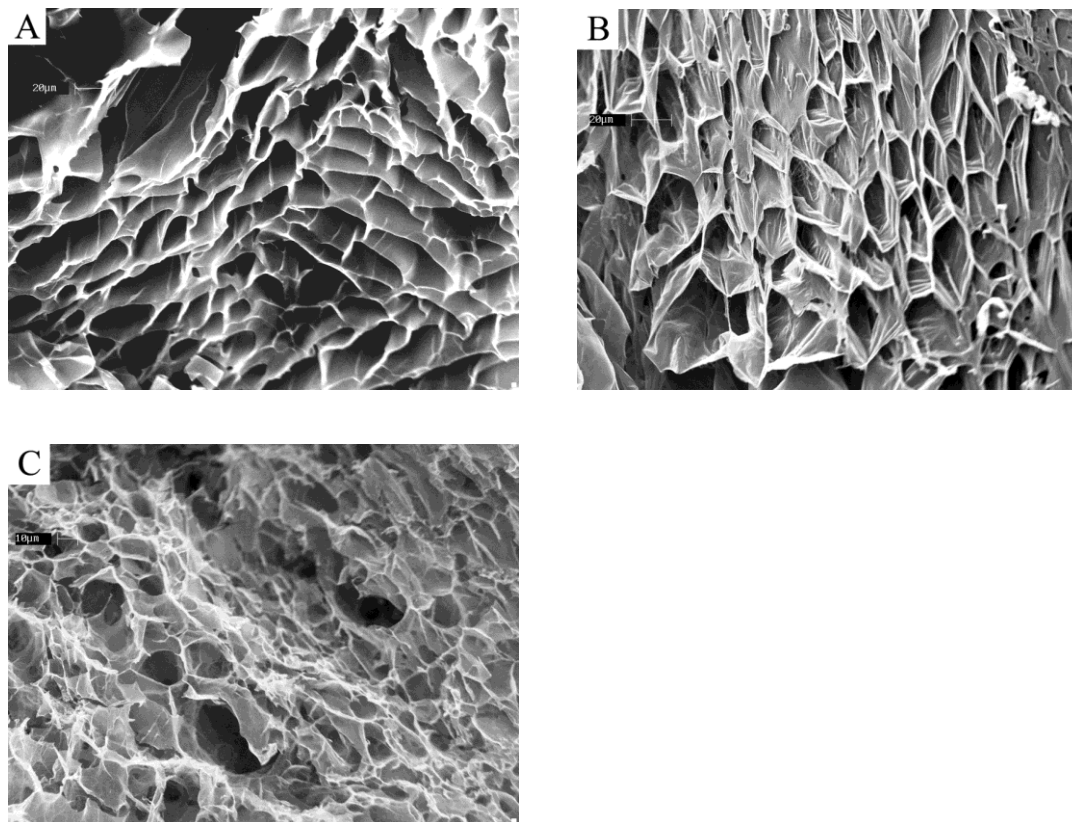


Figure 5.9 SEM images of the interior morphology of 2-UArg-4-S/GMA-chitosan hybrid hydrogels of different Arg-UPEA to GMA-chitosan precursors' feed ratios, at 500 X. A, GMA-Chitosan hydrogel; B, 2-UArg-4-S/GMA-chitosan-12.5/87.5 hybrid hydrogel; C, 2-UArg-4-S/GMA-chitosan-33/67 hybrid hydrogel

showed the most pores with a diameter of 20-40 μm , whereas 2-UArg-4-S/GMA-chitosan-33/67 had relatively smaller 10-18 μm pores. This micro-morphological change was also reflected in the swelling data in which, as the 2-UArg-4-S to GMA-chitosan feed ratio increased, the Q_{eq} of the hybrid hydrogel became lower at all pH (Figure 5.8).

Wu et al reported the hybrid hydrogels made from Arg-UPEA and the Pluronic diacrylate (F127-DA) had a porous structure with 10-15 μm diameter average pore size,⁵¹ which was in the same range of the current 2-UArg-4-S/GMA-chitosan-33/67 hybrid hydrogel (i.e. 10-18 μm). The swelling data of these two different types of hybrid hydrogels were also similar, 1,700% for the 2-UArg-4-S /F127-DA-20/80⁵¹ vs. 1,558% for the 2-UArg-4-S/GMA-chitosan-33/67(However, this similarity disappeared when the Arg-UPEA contents dropped in the 2-UArg-4-S/GMA-chitosan-12.5/87.5 hybrid in the current study which showed a larger Q_{eq} (i.e. 2,779%) and larger pore size (i.e. 20-40 μm) than those of 2-UArg-4-S / F127-DA hybrid hydrogel reported by Wu et al.⁵¹

5.4.8 Mechanical properties of 2-UArg-4-S/GMA-chitosan hybrid hydrogel

The compressive moduli of the Arg-UPEA/GMA-chitosan hybrid hydrogels and the pure GMA-chitosan hydrogel are shown in Table 5.2. Arg-UPEA/GMA-chitosan hybrid hydrogels showed slightly higher compressive initial moduli (ranging from 17.649 to 18.103 KPa) and smaller compressive strain at break (~20%) than a pure GMA-chitosan hydrogel (i.e. 17.640 KPa, 31% strain). Increasing the contents of Arg-UPEA slightly increased the rigidity of the hybrid hydrogels (17.783 vs. 18.103 KPa).

The data in Table 5.2 also show that the molecular structure (x value) of Arg-UPEA didn't significantly influence the compressive modulus and strain at break as shown before that x didn't significantly change the interior morphology of the hybrid hydrogels (Figure 5.9) either. For example, at a fixed feed weight ratio of Arg-UPEA to GMA-chitosan of 33/67, 2-UArg-2-S/GMA-chitosan and 2-UArg-4-S/GMA-chitosan hydrogels had the same compressive strain at break (~20%). The compressive modulus of these two hybrid hydrogels were also very close (i.e. 17.649 ± 0.78 KPa for 2-UArg-2-S/GMA-chitosan vs. 18.103 ± 1.30 KPa for 2-UArg-4-S/GMA-chitosan).

These compressive modulus data of the 2-UArg-2-S/GMA-chitosan hybrid hydrogels are significantly higher than the data reported by Wu et al. in their study of Arg-UPEA/F127DA hybrid hydrogel system which had compressive modulus ranging

Table 5.2 Mechanical property of Arg-UPEA/GMA-chitosan hybrid hydrogel*

	Initial modulus (KPa)	Compression strain at break (%)
GMA-chitosan hydrogel	17.640±0.75	31±4
2-UArg-4-S/GMA-chitosan -12.5/87.5	17.783±0.90	20±3
2-UArg-4-S/GMA-chitosan -33/67	18.103±1.30	21±5
2-UArg-2-S/GMA-chitosan -33/67	17.649±0.78	19±4

*The DS of GMA-chitosan is 37.

from 2.58±0.25 to 4.85±0.41 KPa.⁵¹ The compressive modulus of the Arg-UPEA/F127DA hybrid hydrogel was found to decrease with an increase in the Arg-UPEA contents, while the Arg-UPEA/GMA-chitosan hybrid hydrogel system did not show significant change in compressive modulus as the Arg-UPEA contents or types of Arg-UPEA varied. That was probably because of the different network structures between Arg-UPEA/GMA-chitosan and Arg-UPEA/F127DA hybrid hydrogels due to not only the molecular structure difference between GMA-chitosan and F127DA, but also their location of the double bonds. In the GMA-chitosan precursor, multiple unsaturated methacrylate groups were grafted on the chitosan backbone as the side

groups, while in the F127DA precursor, there were only 2 acrylate end groups that can be used for photo-crosslinking with Arg-UPEA precursor. Therefore, in the crosslinking process, the backbones of GMA-chitosan and Arg-UPEA polymers were interconnected through the GMA pendant group that was not largely influenced by the feed ratio of these two polymers. In the case of Arg-UPEA/F127DA, the unsaturated acrylate groups of F127DA were at the two ends of F127, and hence it acted as a crosslinker. In the crosslinking process, the end groups F127-DA must be close to the double bonds on the Arg-UPEA polymer backbones for the photo-crosslinking to occur. When the contents of F127DA in the mixed precursor decreased (contents of Arg-UPEA increasing), the possibility of F127DA effectively formed network structure with Arg-UPEA was reduced. So, the crosslinking density of Arg-UPEA/F127DA hybrid hydrogel was significantly influenced by the precursors' feed ratio, and that further changed the elastic modulus of the Arg-UPEA/F127DA hybrid hydrogels.

5.4.9 Enzymatic degradation of 2-UArg-4-S/GMA-chitosan hybrid hydrogel

The biodegradation behavior of 2-UArg-4-S/GMA-chitosan-33/67 hybrid hydrogels were evaluated in terms of their weight loss in both pure PBS buffer control and lysozyme solution of pH 7.4 at 37 °C over a period of 10 days. Figure 5.10 shows 2-UArg-4-S/GMA-chitosan-33/67 hybrid hydrogel was degraded faster than a pure GMA-chitosan hydrogel in the presence of either 1 mg/mL lysozyme or PBS buffer. Pure GMA-chitosan hydrogel specimens lost 32.8% of original weight in PBS but 41.0% in 1mg/mL lysozyme solution after 10 days incubation at 37°C. 2-UArg-4-S/GMA-chitosan-33/67 hybrid hydrogels had weight lost 41% and 55% in PBS or in 1 mg/mL lysozyme, respectively after 9 days. Thus, lysozyme accelerated the biodegradation in both the pure GMA-chitosan and Arg-UPEA/GMA-chitosan hybrids.

It is also noted that, most of the weight loss of the pure GMA-chitosan hydrogels occurred during the first 4-6 days, and after that the weight loss rates of pure GMA-chitosan hydrogel in both PBS and lysozyme became near zero, i.e., no change of weight with time. For example, the pure GMA-chitosan hydrogel lost 23.2% and 36.5% of original weight in the first 4 days degradation in PBS and lysozyme media, respectively. During the next 4 days, however, the pure GMA-chitosan hydrogel had only 8.8% and 5% more weight loss in PBS and lysozyme, respectively.

The weight loss profiles of the Arg-UPEA/GMA-chitosan hybrid hydrogels are quite different from the pure GMA-chitosan, particularly at the late stage (after 4-6 days). For example, 2-UArg-4-S/GMA-chitosan-33/67 hybrid hydrogels showed continuously faster weight loss after the first 4 days degradation. In the first 4 days, 2-UArg-4-S/GMA-chitosan-33/67 hybrid hydrogel lost about 26.8% and 36% original weight in PBS and lysozyme solution, respectively. These values were similar to that of the pure GMA-chitosan hydrogel, but the difference was after this period as 2-UArg-4-S/GMA-chitosan-33/67 hybrid hydrogels had additional 11% and 16.2% weight loss in PBS and lysozyme, respectively, i.e., more than triple of the weight loss of a pure GMA-chitosan hydrogel during the same period.

The hydrolytic degradation of hydrogels mainly follows a bulk erosion model: the degradation happened both at the surface and interior.⁵³ The biodegradation mechanism of enzyme-mediated polymer hydrogel degradation is likely to be complex. Lysozyme could biodegrade many natural and synthetic polymers, including chitosan,⁵⁴ dextran, poly-(HEMA),⁵⁵ polyester etc. The degradation of a pure GMA-chitosan hydrogel can be attributed to two reasons: (1) the ester bonds of methacrylate group can be degraded by pure hydrolysis, and (2) lysozyme is able to cleave GMA-chitosan backbone structure at the β (1, 4) linked glucosamine unit and N-acetyl-D-glucosamine unit.⁵⁴ The observed accelerated degradation of a pure GMA-chitosan in

the first 4 days in the presence of lysozyme than in PBS is due to the cleavage of chitosan backbone chain by lysozyme. However, the weight loss data in Figure 5.10 show no meaningful weight loss after the initial 4-6 days in both lysozyme and PBS control media. The possible reasons could be attributed to the unique chitosan backbone structure. Since chitosan is the partially deacetylated derivative of chitin, and hence has 2 major units in its backbone: N-acetyl-D-glucosamine and D-glucosamine, and these 2 units are linked via β , 1-4 glucosidic linkage. The ratio of these 2 units would depend on the deacetylation level.

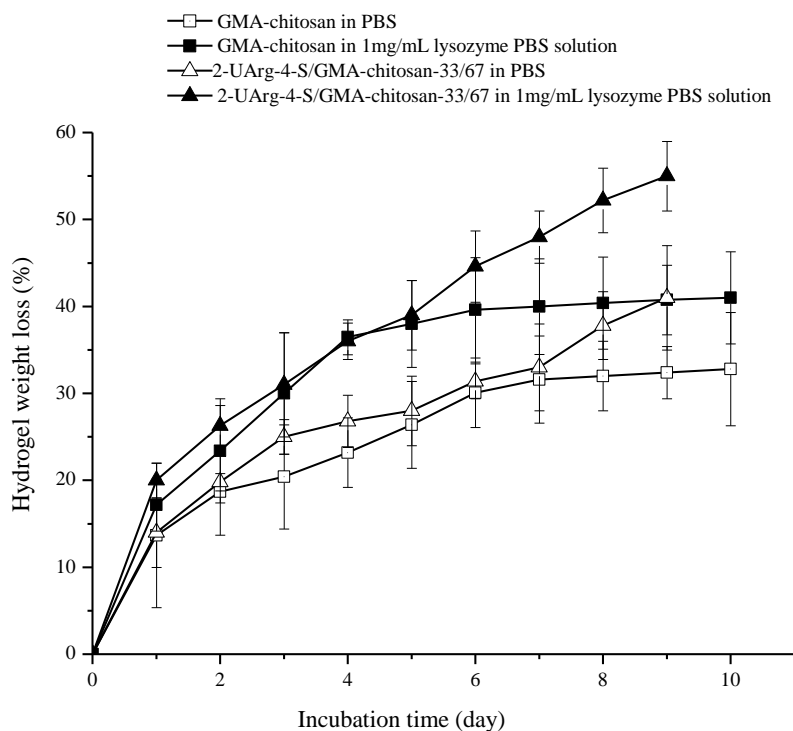


Figure 5.10 *In vitro* enzymatic degradation of GMA-chitosan hydrogel and 2-UArg-4-S /GMA-chitosan-33/67 hybrid hydrogel at 37°C, pH 7.4, 0.05M PBS. The solid symbol: degradation of hydrogels with the presence of 1 mg/mL lysozyme; open symbol: degradation of hydrogel control samples in PBS. The DS of GMA-chitosan composition is 37.

In the current study, the chitosan used was 75-85% deacetylated, i.e., 75-85% of D-glucosamine unit to 15-25% N-acetyl-D-glucosamine unit. Since N-acetyl-D-glucosamine unit is the one that be targeted by lysozyme, the weight loss of GMA-chitosan during the first 4-6 days in Figure 5.10 may already reflect the complete or near complete fragmentation of the N-acetyl-D-glucosamine units in the GMA-chitosan hydrogels. Since the grafted GMA could be biodegraded by lysozyme, thus, no meaningful weight loss of the pure GMA-chitosan hydrogel was observed beyond the first 4 days in lysozyme medium.

In the reported study of enzyme-catalyzed biodegradation of chitosan, Hirano et al. suggested that the accessibility of the enzyme to polysaccharide based hydrogel is one key factor to influence the biodegradation rate.⁵⁴ In the case of 2-UArg-4-S/GMA-chitosan hybrid hydrogel, both the diester bonds in the Arg-UPEA moiety and the ester bond in the methacrylate groups of GMA-chitosan can be hydrolyzed, which would create more open space for lysozyme to approach the N-acetyl-D-glucosamine unit of the GMA-chitosan macromolecular chains for additional biodegradation. This may be one of the reasons for the hybrid hydrogels to show continue weight loss after the initial 4-6 days than a pure GMA-chitosan hydrogel which showed very little weight loss after that initial period. According to Wu's study of Arg-UPEA/Pluronic acid hybrid hydrogels,⁵¹ the M_n of Arg-UPEA synthesized by a solution polycondensation was from 12.93 to 15.71 kg/mol which is close to the MW of lysozyme.^{51,56} During the degradation process of 2-UArg-4-S/GMA-chitosan-33/67 hybrid hydrogels, 2-UArg-4-S was degraded via the scission of the diester bonds, and dissolved in water. The resulting additional open space in the hydrogel network could facilitate more lysozyme access to GMA-chitosan to form enzyme-substrate complex, and hence degrade the hybrid hydrogel faster than a pure GMA-chitosan hydrogel. Another possible reason of the faster degradation of 2-UArg-4-S/GMA-chitosan

hybrid hydrogel than a pure GMA-chitosan hydrogel is the hybrid hydrogel combined 2 polymer compositions with different molecular weight and different degradable building blocks. 2-UArg-4-S segment hydrolyzed faster than GMA-chitosan in terms of weight loss, because the Arg-UPEA has much lower MW than GMA-chitosan, and hence would take a shorter time to be hydrolyzed to an extent that the water soluble degradation-product can be eliminated from the hydrogel network to create more open space for lysozyme to diffuse into the network for additional biodegradation.

5.4.10 Cumulative Release of Bovine Serum Albumin (BSA) from 2-UArg-4-S/GMA-chitosan Hybrid Hydrogel at 37 °C, pH 7.4.

2-UArg-4-S/GMA-chitosan hybrid hydrogels at the two precursor weight feed ratios of 12.5/87.5 and 33/67 were used for the BSA release study. Figure 5.11 shows the percent BSA cumulative release profiles of the hybrid hydrogel matrices, and a pure GMA-chitosan hydrogel with the same amounts BSA loaded was used as the control to examine the effect of 2-UArg-4-S contents on BSA release behavior. The data in Figure 5.11 show that the pure GMA-chitosan hydrogels had the fastest and highest amounts of BSA release among the 3 testing hydrogels, and showed a near 40% burst release in the first h, but the 2-UArg-4-S/GMA-chitosan hybrid hydrogels showed much lower burst releases of BSA in the first h (14% for 2-UArg-4-S/GMA-chitosan-12.5/87.5 hydrogel and 11% for the 2-UArg-4-S/GMA-chitosan -33/67 hydrogel). A burst release of impregnated drugs from hydrogels is a very common phenomenon as those incorporated agents like BSA near a hydrogel surface could be released immediately upon immersion. Both 2-UArg-4-S and GMA-chitosan are cationic polyelectrolytes⁵¹ and the isoelectric point of bovine serum albumin (60,000-70,000 molecule weight) is about 4.7.⁵⁷ In a pH 7.4 PBS buffer, BSA is a hydrophilic biomacromolecule with negative charge. The interaction between the negatively charged BSA and cationic guanidine groups of Arg and the amine groups of GMA-

chitosan exists, and the intensity is influenced by the feed ratio of Arg-UPEA to GMA-chitosan because the Arg-UPEA possesses stronger positive charge than GMA-chitosan. Thus, the feed ratio of Arg-UPEA to GMA-chitosan in the hybrid hydrogel influenced the BSA release profile as observed in Figure 5.11. So the Arg-UPEA/GMA-chitosan hybrid hydrogels could retard some of this common BSA initial burst release

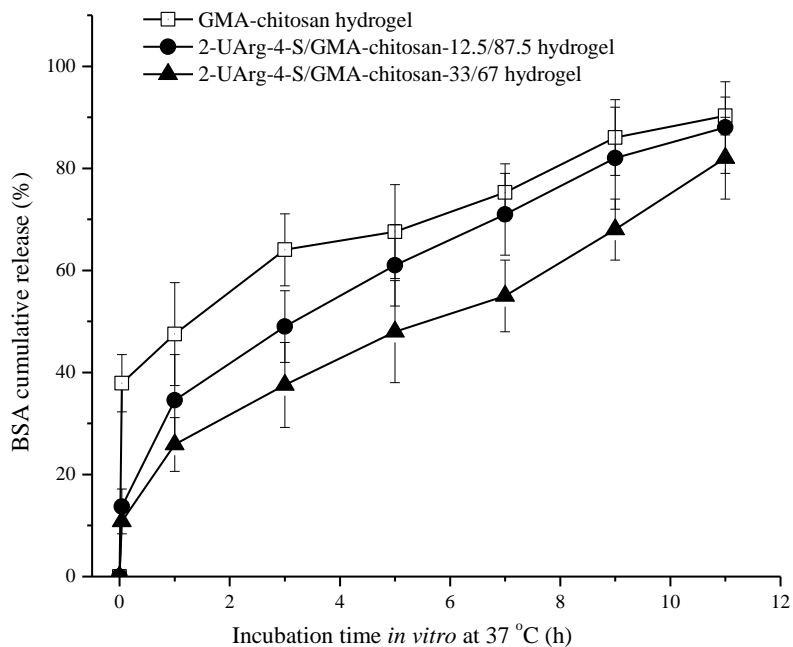


Figure 5.11 Cumulative BSA release profile from 2-UArg-4-S /GMA-chitosan hybrid hydrogels in PBS (0.05M, pH 7.4) at 37°C. A pure GMA-chitosan hydrogel as control. The DS of GMA-chitosan is 37.

because the electrostatic interaction retains the anionic BSA, particularly the one near the hybrid hydrogel surface to reduce its rapid dissolution in water.

This retardation effect extended over the entire study period and increased with an increase in the Arg-UPEA contents in the hybrid hydrogels. For example, the BSA

release from 2-UArg-4-S/GMA-chitosan-33/67 was about 10 % lower than that of 2-UArg-4-S/GMA-chitosan-12.5/87.5 at each of the time point during the 11 days of study. At the last day of the release study (day 11), a pure GMA-chitosan hydrogel showed more than 85% cumulative BSA release, while the release of 2-UArg-4-S/GMA-chitosan-12.5/87.5 and 2-UArg-4-S/GMA-chitosan-33/67 were ~80% and ~76%, respectively.

Release of a protein through a hydrogel matrix can be controlled by many factors such as swelling or release mechanisms. The property of hydrogels, such as hydrophilicity, surface area to volume ratio and ionic interactions between the protein and the hydrogel also influence the protein release behavior.⁵⁷ The diffusion of BSA and the degradation of GMA-chitosan and 2-UArg-4-S/GMA-chitosan hybrid hydrogel are two main release mechanisms. For 2-UArg-4-S/GMA-chitosan hybrid hydrogel, the presence of the 2-UArg-4-S reduced the BSA diffusion and further reduced the BSA release by the electrostatic interaction. It is worth to note the hydrogel degradation could also release the trapped BSA by destroying the crosslinked network structure. 2-UArg-4-S/GMA-chitosan hybrid hydrogel experienced faster degradation than a pure GMA-chitosan hydrogel in PBS (Figure 5.10). But the influence of charge interaction to BSA diffusion played a dominate role that it slowed down the release rate in these two competing BSA release mechanisms from 2-UArg-4-S/GMA-chitosan hybrid hydrogel. By tuning the 2-UArg-4 contents in the hybrid hydrogels, the BSA release profile from the 2-UArg-4-S/GMA-chitosan hybrid hydrogels could be adjusted.

5.5 Conclusions and recommendation for future work

A new family of cationic biodegradable Arg-UPEA/GMA-chitosan hybrid hydrogels was successfully designed and fabricated in an aqueous medium via UV photocrosslinking of both Arg-UPEA and GMA-chitosan precursors. The

physicochemical, swelling, mechanical and morphology properties of the resulting hybrid hydrogels were investigated. By varying the feed ratio of Arg-UPEA to GMA-chitosan and the methylene group length (x) of the diol building block of Arg-UPEA, the swelling (from 297.8% to 3318.2% , depending on pH), mechanical (compressive modulus, $17.649 \pm 0.78 \sim 18.103 \pm 1.30$ KPa) and morphological properties of this hybrid hydrogel system could be adjusted. Cell culture studies indicated that the Arg-UPEA and GMA-chitosan mixed aqueous solutions as hybrid hydrogel precursors had no significant cytotoxicity to porcine aortic valve smooth muscle cells. Lysozyme was able to effectively accelerate the Arg-UPEA/GMA-chitosan hybrid hydrogel biodegradation in aqueous media. A sustained release of BSA can be achieved from Arg-UPEA/GMA-chitosan hybrid hydrogels in 11 days in vitro. The negatively charged protein (BSA) release behavior was able to be adjusted by the presence of cationic Arg-UPEA moiety and by changing its contents in the hybrid hydrogel system. This newly developed cationic biodegradable Arg-UPEA/GMA-chitosan hybrid hydrogel system offers the advantage in terms of water soluble precursors for pre-loading therapeutic protein, flexible mechanical property, biodegradable by enzyme, natural Arg content which is crucial in the amino acid metabolism process of many diseases.

In the future works, the 3T3 cell attachment and proliferation on the hybrid hydrogel could demonstrate the potential of the hydrogel application as a tissue culture scaffold. The macrophage cell (RAW) culture on the Arg-UPEA/GMA-chitosan hybrid hydrogel in vitro could verify the effect of the hybrid hydrogel on the wound healing for the future studies. The TNF- α production of RAW cells could be used test the inflammatory response to the hybrid hydrogel. The NO production and Arginase activity analysis for RAW cells cultured on Arg-UPEA/GMA-chitosan hybrid

hydrogels could determine the effect of Arg-UPEA component in the hybrid hydrogel on the Arg metabolism.

Acknowledgement

The authors would like to thank the support of Vincent V.C. Woo Fellowship to this study. The authors also wish to thank to Cornell Nanobiotechnology Center (NBTC) who provided cell culture facility and Dr. Duan Bin who provided the PAVSMC cells in our study.

References:

- 1 Carmelo Nieves Jr, Bobbi Langkamp-Henken, Arginine and immunity: a unique perspective, *Biomed Pharmacother*, 2002, 56, 471-482
- 2 Guoyao Wu and Sidney M. Morris, JR, Arginine metabolism: nitric oxide and beyond, *Biochem. J.*, 1998, 336, 1-17
- 3 Maria B. Witte, Adrian Barbul, Role of nitric oxide in wound repair, *The American Journal of Surgery*, 2002, 183, 406-412
- 4 Masataka Mori, Tomomi Gotoh, Regulation of nitric oxide production by arginine metabolic enzymes, *Biochemical and Biophysical Research Communications*, 2000, 275, 715-719
- 5 Carl Nathan, Inducible nitric oxide synthase: what difference does it make?, *J. Clin. Invest*, 1997, 100, 2417-2423
- 6 David G. Harrison, Cellular and molecular mechanisms of endothelial cell dysfunction, *J. Clin. Invest*, 1997, 100, 2153-2157
- 7 Karen S. Christopherson, David S. Bredt, Nitric oxide in excitable tissues: physiological roles and disease, *J. Clin. Invest*, 1997, 2424-2429
- 8 Michael R. Schaffer, Udaya Tantry, Stevens S. Gross, Hannah L. Wasserkrug, Adrian Barbul, Nitric Oxide Regulates Wound Healing, *Journal of surgical research*, 1996, 63, 237-240

- 9 Robert B. Lorsbach, Willam J. Murphy, Charles J. Lowenstein, Solomon H. Snyder, Stephen W. Russel, Expression of the nitric oxide synthase gene in mouse macrophages activated for tumor cell killing, *The journal of biological chemistry*, 1993, Vol. 268, No. 3, 25, 1908-1913
- 10 Karen P. Beckerman, Howard W. Rogers, John A. Corbett, Robert D. Schreiber, Michael L. McDaniel, Emil R. Unanue, Release of nitric oxide during the T cell-independent pathway of macrophage activation, 1993, Vol 150, No.3, 888-895
- 11 Stefan Frank, Marianne Madlener, Josef Pfeilschifter, Sabine Werner, Induction of inducible nitric oxide synthase and its corresponding tetrahydrobiopterin- cofactor-synthesizing enzyme GTP-cyclohydrolase I during cutaneous wound repair. *J Invest Dermatol* 1998;111:1058–64.
- 12 Frank J. Thornton, FRCSI, Michael R. Schaffer, Maria B Witte, Lyle L. Moldawer, Sally L. D. Mackay, Amer Abouhamze, Cynthia L. Tannahill, Adrian Barbul, Enhancece collagen accumuation following direct transfection of the inducible nitric oxide synthase gene in cutaneous wounds, 1998, *Biochemical and Biophysical Research Communications*, 246, 654-659
- 13 Stallmeyer B, Kampfer H, Kolb N, et al. The function of nitric oxide in wound repair: inhibition of inducible nitric oxide-synthase severely impairs wound reepithelialization. *J Invest Dermatol* 1999;113:1090–8.
- 14 Noiri E, Peresleni T, Srivastava N, et al. Nitric oxide is necessary for a switch from stationary to locomoting phenotype in epithelial cells. *Am J Physiol* 1996; 270: c794–802.
- 15 Schaffer MR, Tantry U, Efron PA, et al. Diabetes-impaired healing and reduced wound nitric oxide synthesis: A possible pathophysiologic correlation. *Surgery* 1997; 121: 513–9.
- 16 Witte MB, Thornton FJ, Tandry U, et al. L-arginine enhances diabetic

- wound healing. *Wound Rep Reg* 1999;7: A326.
- 17 Alistair Young, Clare-Ellen McNaught, *The physiology of wound healing*, Surgery, 2011, Vol 29, 10, 475-479
- 18 M. Jalkanen, H. Larjava, J. Heino et al., Arginine depletion in macrophage medium inhibits collagen synthesis by fibroblasts, *Immunology letter*, 1982, 4, 259-261
- 19 Morris, Sidney M., Jr., Diane Kepka-Lenhart, Li-Chun Chen, Differential regulation of arginases and inducible nitric oxide synthase in murine macrophage cells, *Am. J. Physiol.*, 1998, 275, E740-E747
- 20 E.I. Closs, CATs, a family of three distinct mammalian cationic amino acid transporters, *Amino Acids* 11 (1996) 193–208.
- 21 D.K. Kakuda, M.J. Sweet, C.L. MacLeod, D.A. Hume, D. Markovich, CAT2-mediated L-arginine transport and nitric oxide production in activated macrophages, *Biochem. J.* 340 (1999) 549–553.
- 22 I.B.J.G. Debats, T.G.A.M Wolfs, T.Gotoh, et al., Role of arginine in superficial wound healing in man, *Nitric Oxide*, 2009, 21, 175-183
- 23 J.S. Reichner, A.J. Meszaros, C.A. Louis, W.L. Henry Jr., B. Mastrofrancesco, B.A. Martin, J.E. Albina, Molecular and metabolic evidence for the restricted expression of inducible nitric oxide synthase in healing wounds, *Am. J. Pathol.* 1999, 154, 1097–1104.
- 24 Jorge E. Albina, Charles D. Mills, Adrian Barbul et al., Arginine metabolism in wounds, *American Journal of Physiology Endocrinology and metabolism*, 1988, Vol 254, No. 4, E459-E467
- 25 G. A. Currie, L. Gyure, L. Cifuentes, Microenvironmental arginine depletion by macrophages in vivo, *Br J Cancer*, 1979, 39, (6), 613-620
- 26 Jeffrey P. Bulgrin, Mohammad Shabani, Daniel J. Smith, Arginine-free diet suppresses nitric oxide production in wounds, *J. Nutr. Biochem*, 1993, Vol. 4, 588-593

- 27 Xiao-jun Zhang, David L. Chinkes, Robert R. Wolfe, The anabolic effect of arginine on proteins in skin wound and muscle is independent of nitric oxide production, *Clinical Nutrition* (2008) 27, 649-656
- 28 Heys SD, Walker LG, Smith I. Enteral nutrition supplementation with key nutrients in patients with critical illness and cancer: A meta-analysis of randomized controlled clinical trials. *Ann Surg* 1999;229:467.
- 29 Victor Arana, Yolanda Paz, Angelica Gonzalez, Healing of diabetic foot ulcers in arginine treated patients, *Biomedicine & Pharmacotherapy*, 2004, 58, 588-597
- 30 Maria B. Witte, Frank J. Thornton, Udaya Tantry, Adrian Barbul, L-Arginine supplementation enhances diabetic wound healing: involvement of the nitric oxide synthase and arginase pathways, 2002, *Metabolism*, Vol 51, No 10, 1269-1273
- 31 Lee RH, Efron DT, Tantry U, et al: Nitric oxide in the healing wound: A time-course study. *J Surg Res* 101:104-108, 2001
- 32 Stevens RB, Sutherland DE, Ansite JD, et al: Insulin downregulates the inducible nitric oxide synthase pathway: Nitric oxide as cause and effect of diabetes? *J Immunol* 159:5329-5335, 1997
- 33 A.H. Klimp, E.G.E. de Vries, G.L. Scherphof, T. Daemen, A potential role of macrophage activation in the treatment of cancer, *Critical Reviews in Oncology/Hematology*, 2002, 44, 143-161
- 34 Kroncke KD, Fehsel K, Kolb Bachofen V. Inducible nitric oxide synthase and its product nitric oxide, a small molecule with complex biological activities. *Biol Chem Hoppe Seyler* 1995;376:327
- 35 Albina JE, On the expression of nitric oxide synthase by human macrophages. Why no NO?, *J Leukoc Biol*, 1995,58, 643-649
- 36 Nicotera P, Bonfoco E, Brune B. Mechanisms for nitric oxide-induced cell death: involvement of apoptosis. *Adv Neuroimmunol* 1997;5: 411- 420.

- 37 Dimmeler S, Haendler J, Nehls M, Zeiher AM. Suppression of apoptosis by nitric oxide via inhibition of interleukin-1 β -converting enzyme (ICE)-like and cysteine protease protein (CPP)-32-like proteases. *J Exp Med* 1997;185:601-607.
- 38 Daniela Massi, Chiara Marconi, Alessandro Franchi et al., Arginine metabolism in tumor-associated macrophages in cutaneous malignant melanoma: evidence from human and experimental tumors, *Human Pathology*, 2007, 38, 1516-1525
- 39 Rajan Singh, Shehla Pervin, Ardeshir Karimi, Arginase activity in human breast cancer cell lines: N-Hydroxy-L-arginine selectively inhibits cell proliferation and induced apoptosis in MDA-MB-468 Cells, *Cancer Res*, 2000, 60, 3305-3312
- 40 Lilia Elena Davel, Maria Adela Jasniz, Eulalia de la Torre et al, Arginine metabolic pathways involved in the modulation of tumor-induced angiogenesis by macrophages, *FEBS letters*, 2002, 532, 216-220
- 41 Prahlad Parajuli, Sukh Mahendra Singh, Alteration in IL-1 and arginase activity of tumor-associated macrophages: a role in the promotion of tumor growth, *Cancer Letter*, 1996, 107, 249-256
- 42 D. Scott Lind, Arginine and Cancer, *the journal of nutrition*, 2004, Vol 134, No 10, 28375-28415
- 43 Y. Usami, Y. Okamoto, T. Takayama, Y. Shigemasa, S. Minami, Chitin and chitosan stimulate canine polymorphonuclear cells to release leukotriene B₄ and prostaglandin E₂, *J. Biomed. Mater. Res.* 1998, 42, 517–522.
- 44 G. Peluso, O. Petillo, M. Ranieri, M. Santin, L. Ambrosio, D. Calabro, B. Avallone, G. Balsamo, Chitosan-mediated stimulation of macrophage function, *Biomaterials*, 1994, 15, 1215–1220.
- 45 I.D. Bianco, J. Balsinde, D.M. Beltramo, L.F. Castagna, C.A. Landa, E.A. Dennis, Chitosan-induced phospholipase A₂ activation and arachidonic acid mobilization in P388D1 in macrophages, *FEBS Lett.* 2000, 466, 292–294.

- 46 T. Mori, M. Okumura, M. Matsuura, K. Ueno, S. Tokura, Y. Okamoto, S. Minami, T. Fujinaga, Effects of chitin and its derivatives on the proliferation and cytokine production of fibroblasts in vitro, *Biomaterials*, 1997, 18, 947–951.
- 47 Y. Shibata, W.J. Metzger, Q.N. Myrvik, Chitin particle-induced cell-mediated immunity is inhibited by soluble mannan: mannose receptor-mediated phagocytosis initiates IL-12 production, *J. Immunol.* 159 (1997) 2462–2467.
- 48 Carina Porporatto, Ismael D. Bianco, Clelia M. Riera, Silvia G. Correa, Chitosan induces different L-arginine metabolic pathways in resting and inflammatory macrophages, *Biochemical and Biophysical Research Communications*, 2003, 304, 266-272
- 49 Dai Yamanouchi, Jun Wu, Andrew N. Lazar, K. Craig Kent, Chih-Chang Chu, Bo Liu, Biodegradable arginine-based poly(ester-amide)s as non-viral gene delivery reagents, *Biomaterials*, 2008, 29, 22, 3269-3277
- 50 Singh DK, Ray AR, Biomedical applications of chitin, chitosan, and their derivatives, *J Macromol Sci Rev, Macromol Chem Phys*, 2000; C40:69–83.
- 51 Jun Wu, Dequn Wu, Martha A. Mutschler, C. C. Chu, Cationic Hybrid Hydrogels from Amino Acid-Based Poly (ester amide):Fabrication, Characterization, and Biological Property, *Advanced functional materials*, 2012, 22, 18, 3815-3823
- 52 Chao Zhong, Jun Wu, C. A. Reinhart-King, C.C. Chu, Synthesis, characterization and cytotoxicity of photo-crosslinked maleic chitosan–polyethylene glycol diacrylate hybrid hydrogels, *Acta Biomaterialia*, 2010, 6, 3908-3918
- 53 Friederike von Burkersroda, Luise Schedl, Achim G.opperich, Why degradable polymers undergo surface erosion or bulk erosion, *Biomaterials*, 2002, 23, 4221-4231
- 54 Shigehiro Hirano, Hisaya Tsuchida, Norio Nagao, N-acetylation in chitosan and the rate of its enzymic hydrolysis, 1989, 10 (8), 574-576

55 Lord MS, Stenzel MH, Simmons A, Milthorpe BK. Lysozyme interaction with poly(HEMA)-based hydrogel. *Biomaterials*, 2006 ,27(8):1341-1345.

56 K.J.Palmer, M. Ballantyne, J.A. Galvin, The molecular weight of lysozyme determined by the X-ray diffraction method, *J. Am. Chem. Soc*, 1948, 70, 906-908

57 Michael B. Mellott, Katherine Searcy, Michael V. Pishko, Release of protein from highly cross-linked hydrogels of poly(ethylene glycol) diacrylate fabricated by UV polymerization, *Biomaterials*, 2001, 22, 929-941

CHAPTER SIX:
A NEW FAMILY OF FUNCTIONAL BIODEGRADABLE ARGININE-BASED
POLYESTER UREA URETHANES: SYNTHESIS, CHARACTERIZATION AND
BIODEGRADATION

6.1 Abstract

A new family of biodegradable functional cationic L-Arginine (L-Arg) poly (ester urea urethane) (Arg-PEUU) polymers was synthesized by the solution polycondensation of three monomers: L-Arg hydrochloride alkylene diester (Arg-*x*-Cl), hexamethylene diisocyanate (HDI) and glycerol α -monoallyl ether (GAE). Chemical structures of Arg-*x*-Cl and the Arg-PEUU polymers were characterized by H-NMR, FTIR, and carbon/nitrogen elemental analysis. The molecular weight of Arg-PEUU ranged from 23.930 to 29.350 Kg/mol. The glass transition temperature (T_g) of Arg-PEUU ranged from -20.80 °C to 4.23 °C, depending on the feed ratio of the 3 monomers. The water contact angle of Arg-PEUU ranged from $26.7 \pm 4.3^\circ$ to $61.3 \pm 5.2^\circ$. The Arg-PEUU had no cytotoxicity toward porcine aortic valve smooth muscle cells at low concentrations (0.1 – 0.2 mg/mL). Arg-PEUUs can be photo-crosslinked into elastic gels with compressive modulus ranged from 54.2 ± 9.1 to 120.7 ± 5.4 KPa. The biodegradation data (weight loss) of the Arg-PEUU in a lipase media suggested that the crosslinking density as well as the Arg-*x*-Cl contents in the functional Arg-PEUU had a profound impact on the biodegradation rate.

6.2 Introduction:

6.2.1 Polyurethane

To develop biocompatible polyurethanes and poly (urethane-urea) is of interest in biomedical research field, because they offer to mimic the soft nature of different tissues. Polyurethanes (PU) are considered one of the most promising materials in biomedical applications due to their structure/property diversity. Blood bags, bladders of the left ventricular assist device, the total artificial heart and small caliber vascular grafts for vascular access and arterial reconstruction or bypass which are made of PU were developed and successfully used clinically¹. Polyurethane can be divided as thermoplastics or thermosets by composition. The thermoplastic PU are block

copolymers composed of hard segment (A) and soft segment (B) blocks arranged in $(AB)_n$ structure. The hard segment block is composed of diisocyanate and the chain extender, usually low molecular weight diol or diamine. The soft segment is usually a polyol comprising a chain having a low glass transition temperature, either hydroxyl or amine-terminated polyester, polyether, polycarbonate, etc. Thermoset PUs are chemically crosslinked, either in the hard segment or the soft segment. The crosslinking improves the strength and durability of resultant polymer. In the synthesis of PU, the stoichiometry between the isocyanate and the active-hydrogen-containing-end-groups must be maintained as close as possible to a 1:1 ratio in order to achieve the high molecular weight needed for the optimal physical mechanical properties. The character of PU material can be determined by the hard or soft segment content. On hard segment content, the polyurethane can be soft, rubbery elastomer (hard segment content of 15-40 weight percent), tough elastomer (hard segment content between 40-65 weight percent), or hard and strong engineering polymer (with hard segment over 65 weight percent). The synthesis of anionomer type polyurethane is produced in two steps: (A) formation of a prepolymer of diisocyanate, polyols; (B) conversion of the prepolymer to high molecular weight polyurethane by adding a suitable chain extender². However, the diisocyanate and chain extenders which are typically used in the segment of conventional PUs are not biocompatible, such as 4, 4'-diphenylmethane diisocyanate (MDI) or toluene diisocyanate (TDI). The degradation products of these diisocyanates include toxic and carcinogenic compounds such as aromatic diamines. Aliphatic diisocyanates are preferred over conventional aromatic diisocyanates. However, the aliphatic diisocyanates have lower reactivities than aromatic ones and a catalyst is needed. Stannous 2-ethylhexanoate is one type of catalyst which is accepted by FDA as catalyst in the formulation of polymeric coating in contact with food³.

6.2.2 Degradation of polyurethane

Several sources were found to contribute to the PUs degradation. For example, the ester linkage in polyester-urethanes is known can be degraded by hydrolysis. And also, oxidative degradation is another contributing mechanism of PU degradation. An oxidative environment may be present in vivo due to attack from the immune system via macrophages, phagocytes, foreign body giant cells⁴⁻⁶. Inflammatory cells play an important role in the biodegradation of polyurethanes. Neutrophils are considered as the key factor which is the primary source of HOCl in vivo⁵. But neutrophils are not the sole source of oxidants. Monocyte derived macrophages are believed to be involved in the degradation of PUs⁷. And also, nitric oxide based oxidants have been used to study the degradation of polyurethanes⁵. Even though the enzymes are designed for highly specific interactions with particular biological substrates, some enzymes appear capable act upon PU substrates. Polyurethanes with polyether, polyester and polycarbonate soft segments have shown degradation in the presence of several hydrolytic and inflammatory cell derived enzymes⁸⁻¹⁰. All of the degradation mechanism is related to the surface organization of PUs. In PU-based materials, a microphase segregation process leads to the formation of a two-microphase structure with regions enriched in either hard or soft segments. Because of the mobility of the soft segments, the surface composition of segmented PUs varies in order to minimize the interfacial free energy. So, PUs will have a higher proportion of polar hard segments on the surface when the environment is polar (aqueous environment) and more non-polar hard segments at the interface when the environment is non-polar (air)

11.

6.2.3 Enzymatic degradation of polyurethane

The enzymatic degradation of segmented polyurethane and polyurethane urea has been studied by several groups in the field of biomedical materials. The enzymes mainly used are chymotrypsin, papain, cholesterol esterase and lipase¹². Lipase and esterases attack specifically carboxylic linkages and endopeptidases (including chymotrypsin) are able to cleave amide bond. α -Chymotrypsin is a proteolytic enzyme that degrades the peptide linkages at the carboxylic sites of aromatic amino acids, e.g. tyrosine and phenylalanine. Phenylalanine based polyurethanes have shown α -chymotrypsin mediated degradation in vitro^{13, 14}. The presence of specific sites, e.g. hydrophobic aromatic side chains, enhances the tendency toward enzymatic degradation of phenylalanine based polyurethanes. Chymotrypsin cleaved the ester bond adjacent to the phenylalanine in the PU chain extender. But it also can degrade urethane linkage of PU. Papain which is one type of thiol protease can mediate the hydrolysis of PUs. The mechanical stability and tensile strength of poly ester urethane are decreased after incubation with papain¹⁵. Cholesterol esterase is a characteristic hydrolytic activity in monocyte derived macrophages and has been shown to degrade both polyester and polyether urethanes. However, probably more enzyme was required for poly (ether-urethane) than the amount needed for polyester¹⁶. Cholesterol esterase cleaves poly (ether-urethanes) at the urethane bonds¹⁷⁻¹⁹. Lipase is a pancreatic enzyme responsible for fat decomposition into fatty acids and glycerol by the cleaving of ester bonds. The degradation of poly (ester urethane)s and poly (carbonate urethane)s catalyzed by this enzyme has been studied^{20, 21}. Lipase always cleaves the ester or carbonate linkages.

The reaction mechanism is hydrolases uses three amino acids residues: aspartate, histidine and serine (shown in Figure 6.1). Aspartate interacts with the histidine

ring to form a hydrogen bond. The ring of histidine is oriented to interact with serine. Histidine acts as a base, deprotonating the serine to generate a very nucleophilic alkoxide group ($-O^-$). The alkoxide group is a stronger nucleophile than an alcohol group. It is the group attacks the ester bond leading to the formation of an alcohol end group and an acyl-enzyme complex. Subsequently, water attacks the acyl-enzyme bond to produce a carboxyl end group and the free enzyme²².

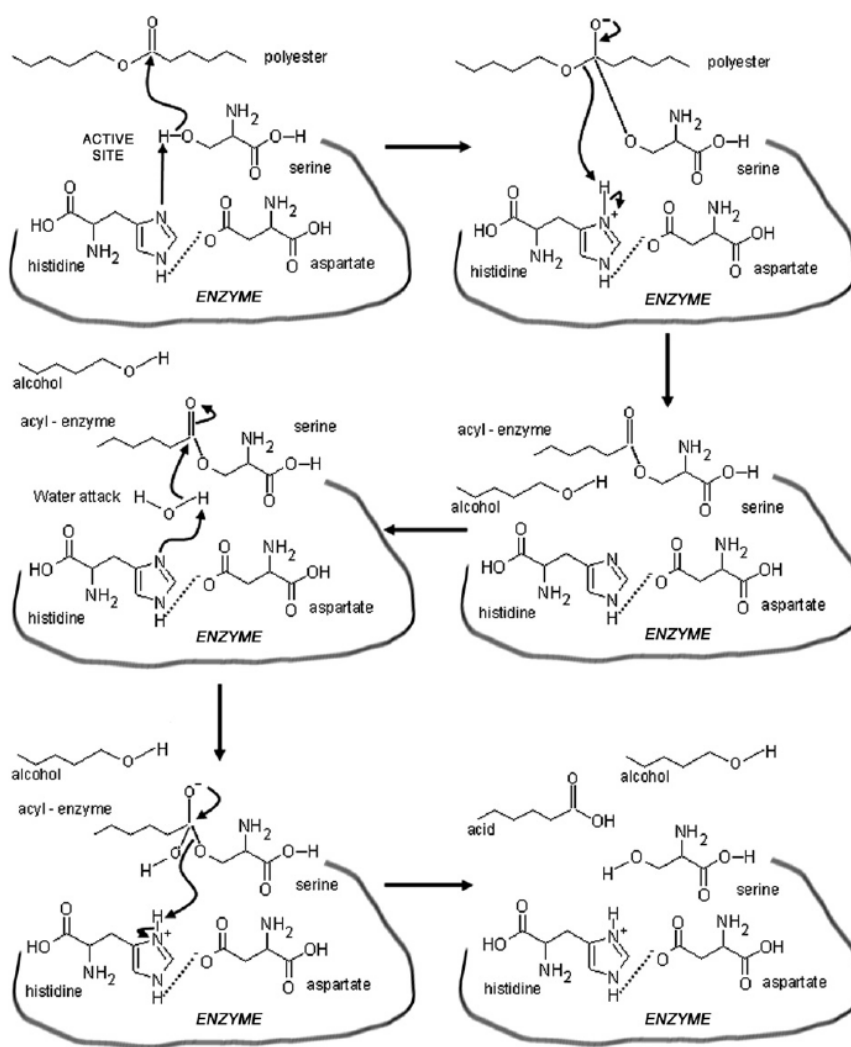


Figure 6.1 Representation of the catalytic site of depolymerase and the mechanism of action²²

6.2.4 Arginine based polymer

Arginine (2-amino-5-guanidinovaleric acid) is one nonessential amino acid which presents in animal protein which plays one significant role in nitrogen metabolism, polyamine synthesis and the production of nitric oxide. The metabolism of arginine through arginase and nitric oxide synthase are indispensable to different stages of wound healing^{23, 24}. And arginine metabolism also is involved in many diseases, such as diabetic foot, even tumor growth. Arginine based polymer is of interest in the development of new biomaterials due to its cationic property and special physiological functions of its metabolism. Moreover, arginine-riched peptides were also reported to possess cell-penetrating ability²⁵. Several types arginine based polymer has been studied. Polyarginine is composed of arginine residue with guanidino groups which can help cell uptake of nanoparticles²⁶. Some studies reported polymers of L-Arginine of 6 amino acids in length or greater were highly effectively in gaining intracellular access. Polymers of less than 6 amino acids were found to be ineffective in crossing cellular membranes²⁷. Polymer which was grafted with arginine also shows tissue penetrability²⁸. For the case of linear polymers, arginine based poly (ester amide) have been reported to display high transfection efficiency, meaning that the conjugated arginines still are able to deliver gene into cells even though they are not in oligo-peptides forms²⁹.

6.2.5 Design of biodegradable PUs for the in vivo environment

Recent works by many investigators has utilized the flexibility and diverse mechanical properties of PU materials to design degradable polymers for medical applications, for example, neural conduits, bone replacements^{30, 31}. To design degradable PU materials required a change in the choice of diisocyanates used in the synthesis. Conventional aromatic diisocyanate are more suitable for the non-degradable PUs. Particularly, because of the carcinogenic nature of aromatic diisocyanates, degradable PUs are mainly made from linear diisocyanates, such as

lysine-diisocyanate (LDI), hexamethylene diisocyanate (HDI), 1, 4 diisocyanatobutane which degraded as more likely non-toxic products. Glycerol and sucrose were chosen as the soft segment in newly developed biodegradable PUs³²⁻³⁴. Both these two types of PU show good biocompatibility and mechanical properties. The degradation of the PU made from LDI and glycerol was linear at 37 °C and glycerol and lysine are degradation products.

Enzyme sensitive hard segment of PU was designed by Woodhouse et al^{35,36}. Not like the hydrolysis mechanism of most common degradable PU, PUs containing a phenylalanine diester chain extender shows enzyme-mediated degradation. Chymotrypsin cleaved the ester bonds adjacent to the phenylalanine in the novel chain extender. Arginine based biodegradable PU has not been reported before. It is believed to be one promising biomaterial due to the physiological function of arginine, cationic property of the surface and good mechanical properties. In this chapter, we report the design, synthesis, characterization, and some unique properties of the functional cationic Arg based PEUU (Arg-PEUU) without the tedious protection and deprotection process because of the unique chemical structure of Arg and its biological role in many important biological functions. A novel family of biocompatible Arg-PEUU incorporating di-hydrochloride acid salt of bis (L-Arg) alkylene diester as a chain extender was developed for biomedical applications. Arg alkylene diester building block was incorporated into the PEUU via the urea linkage. This new family of biodegradable functional cationic Arg-PEUU biomaterials is believed to be a promising new biomaterial due to the integration of the unique physiological function and cationic character of Arg with the good mechanical property of traditional PU as well as the additional pendant double bond functionality. This new family of Arg-PEUU biomaterials may lead to new therapy to accelerate

wound healing or diabetic ulcer which is not be able to cure by simple free Arg supplement (dietary supply or infusion).

6.3 Experimental

6.3.1 Materials

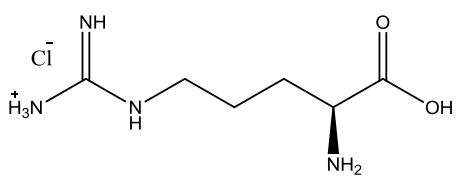
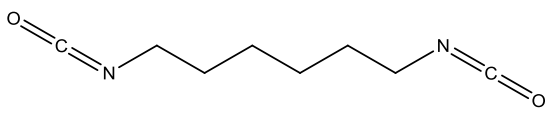
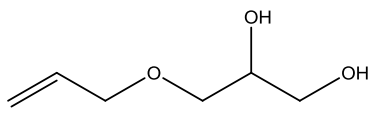
L-Arginine hydrochloride (L-Arg-Cl) (Alfa Aesar, Ward Hill, MA), ethylene glycol (Mallinckrodt, St. Louis, MO), 1,4-butanediol (Alfa Aesar, Ward Hill, MA) 1, 6-hexanediol (Avocado Research Chemicals Ltd, Morecambe, Lancaster, UK), *p*-toluene sulfonic acid monohydrate (TsOH H₂O) (JT Baker, Philipsburg, NJ), glycerol α -monoallyl ether (GAE, TCI, Portland, OR), hexamethylene diisocyanate (HDI) (Acros organics, Geel, Belgium), triethylamine (99%, EMD Chemical, Darmstadt, Germany) were used without further purification. 2, 6 di-*tert*-butyl-4-methyl phenol was purchased from Alfa Aesar (Ward Hill, MA) and stannous 2-ethyl-hexanoate was purchased from Sigma (St. Louis, MO). Solvents like toluene (VWR Science, West Chester, PA), dimethyl sulfoxide (DMSO) and *N, N*-dimethyl formamide (DMF) (Mallinckrodt incorporated, St. Louis, MO), isopropyl alcohol (ACS, 99.5%, Macron Chemicals, Philipsburg, NJ) and ethyl acetate (BDH, London, UK) were used without further purification. Irgacure 2959 was donated by Ciba Specialty Chemicals Corp. Lipase was purchased from VWR Science (West Chester, PA). The chemical structures of L-arginine hydrochloride, hexamethylene diisocyanate, glycerol α -monoallyl ether were shown in Table 6.1.

6.3.2 Methods

6.3.2.1 Synthesis of di-hydrochloride acid salt of bis (L-Arg) alkylene diester monomers (Arg-*x*-Cl)

The synthesis of di-hydrochloride acid salt of bis (L-Arg) alkylene diester monomers (Arg-*x*-Cl, *x* is the number of methylene groups of diol) of Arg-PEUU is similar to those used for the Arg-PEA synthesis³⁷⁻³⁹ but with minor modification so

Table 6.1 The chemical structures of raw materials of Arg-PEUU

Chemical name:	Chemical structures:
L-Arginine hydrochloride	
hexamethylene diisocyanate	
glycerol α -monoallyl ether	

that the resulting new Arg-*x*-Cl monomer would have 2 free amino groups that the prior reported synthesis method didn't have. L-Arg hydrochloride (0.04 mol) and ethylene glycol (0.02 mol) (or 1, 4 butanediol, 1, 6-hexanediol) were directly condensed in refluxed toluene (b.p. 110 °C) (80mL) with the presence of TsOH H₂O (0.05 mol). The heterogeneous solid-liquid reaction mixture was heated to 120 °C and reflux for 48 h after 1.62 mL (0.09 mol) of water generated and collected by a dean-stark apparatus. The reaction mixture was then cooled to room temperature in about 1 h. Toluene was decanted. The reaction mixture was placed in a 500 mL round bottom flask filled with sufficient amounts of isopropyl alcohol to completely dissolve the reaction mixture with refluxing at 100 °C. Because the solubility of Arg alkylene diester monomer in isopropyl alcohol at 100 °C is much larger than that at lower temperature, the clear reaction mixture solution was then cooled down to room temperature to facilitate the precipitation of the Arg alkylene diester monomer from the oversaturated isopropyl alcohol solution in the cooling process. This solution was left for overnight in a freezer (-20 °C) to promote further precipitation. This step was

repeated to purify the monomer by recrystallization in isopropyl alcohol. The precipitant was dried at 30 °C in a vacuum oven overnight, and the resulting white powder product was di-*p*-toluene sulfonic acid di-hydrochloride acid salt of bis (L-Arg) alkylene diester.

The di-*p*-toluene sulfonic acid di-hydrochloride acid salt of bis (L-Arg) alkylene diester was then thoroughly dissolve in deionized water at room temperature and its pH was adjusted to 9.5 by adding oversaturated calcium hydroxide aqueous solution dropwise under magnetic stirring to remove the TsO⁻ counter ion attached to the 2 amino groups of the Arg alkylene diester which have pKa 9. Because the pKa of guanidino group of Arg is about 12.48, the chloride counter ions attached to the guanidino group was not able to be removed in this step.

After the pH of Arg-*x*-Cl aqueous solution was adjusted to 9.5, extra calcium hydroxide was removed immediately by bubbling carbon dioxide into the solution for 10 min to convert calcium hydroxide to water insoluble calcium carbonate. The pH of the Arg-*x*-Cl solution quickly became neutral or mild acidic pH (4.5~6). Arg-*x*-Cl aqueous solution only experienced pH > 7 for about 15 seconds or less at room temperature to prevent the hydrolysis of ester bond. Similar approach was reported by Skarja et al to used K₂CO₃ to convert the tosylate salt of Phe alkylene diester to the free diamine form^{14,35} for further polyurethane synthesis. Because Phe alkylene diester in diamine form was not soluble in water, the monomer was able to be collected soon to prevent hydrolysis caused by the alkaline environment. However Arg-*x*-Cl with free diamine groups in the current study is still water soluble, an excess K₂CO₃/Na₂CO₃ may cause undesirable hydrolysis of the diester bonds in Arg-*x*-Cl monomer. Therefore, in the current study, a mild calcium hydroxide was used instead of K₂CO₃/Na₂CO₃, the excess base could be easily removed by converting it into water-insoluble calcium carbonate. The lack of any significant ester hydrolysis of the

resulting pH adjusted Arg diester monomer was further demonstrated from its H-NMR spectrum that the integral ratio of ester linkage in the Arg diester monomer having 2 free amine group (i.e., free of TsO^- counter ions) was not different from the Arg diester before pH adjustment (i.e., with TsO^- counter ion). The resulting Arg alkylene diester aqueous solution was then vacuum dried at room temperature overnight after the calcium carbonate precipitation was filtered out. This reaction scheme is shown in Figure 6.2. This extra step of pH adjustment to the Arg diester monomer distinguished it from all the prior reported Arg diester monomer synthesis.

Three types of Arg- x -Cl were synthesized by changing the types of diol reactant, where x is the number of methylene groups of diol: di-hydrochloride acid salt of bis (L-Arg) ethane diester (Arg-2-Cl with $x = 2$); di-hydrochloride acid salt of bis (L-Arg) butane diester (Arg-4-Cl with $x = 4$); di-hydrochloride acid salt of bis (L-Arg) hexane diester (Arg-6-Cl with $x = 6$) (Table 6.2).

6.3.2.2 Synthesis of Arg-PEUU

The Arg-PEUU was synthesized using a two-step solution polymerization. In the step 1, HDI and GAE formed prepolymer through the reaction between isocyanate group in HDI and hydroxyl group in GAE. In the step 2, the Arg- x -Cl monomer with two free amine end groups (i.e. Arg-2-Cl, Arg-4-Cl, Arg-6-Cl) extended the prepolymer chain synthesized in step 1 above for improving the molecular weight of the resulting polymers.

The synthesis was carried out in a 250 mL three-necked round bottomed flask under a dry nitrogen atmosphere. The three stoichiometry of the HDI, GAE, Arg- x -Cl monomers were 2/1/1, 5/1/4, and 5/4/1. The sum of the molar amounts of GAE and Arg- x -Cl must be equal to the molar amounts of HDI. For example, in the first

Table 6.2 List of L-Arg alkylene diester monomers used in the synthesis of Arg-PEUU

Reactants	Number of methylene groups of diester	Product after removing toluene sulfonic acid	bis (L-Arg) alkylene diester Monomer
L-Arg hydrochloride + ethylene glycol	2	di-hydrochloride acid salt of bis (L-Arg) ethane diester	Arg-2-Cl
L-Arg hydrochloride + 1, 4 butanediol	4	di-hydrochloride acid salt of bis (L-Arg) butane diester	Arg-4-Cl
L-Arg hydrochloride + 1, 6 hexanediol	6	di-hydrochloride acid salt of bis (L-Arg) hexane diester	Arg-6-Cl

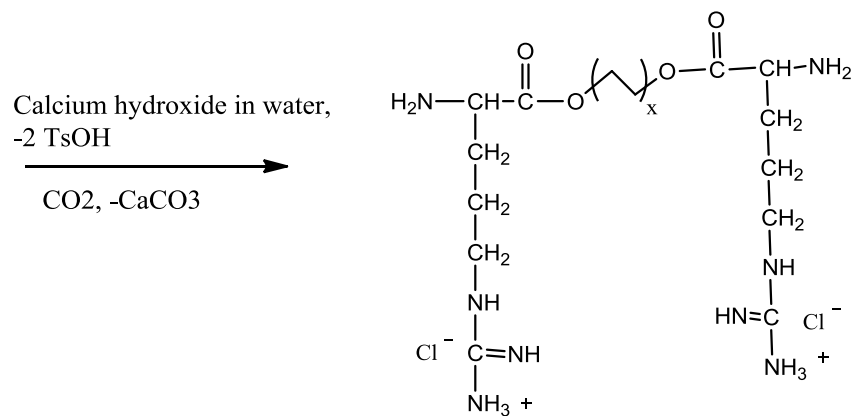
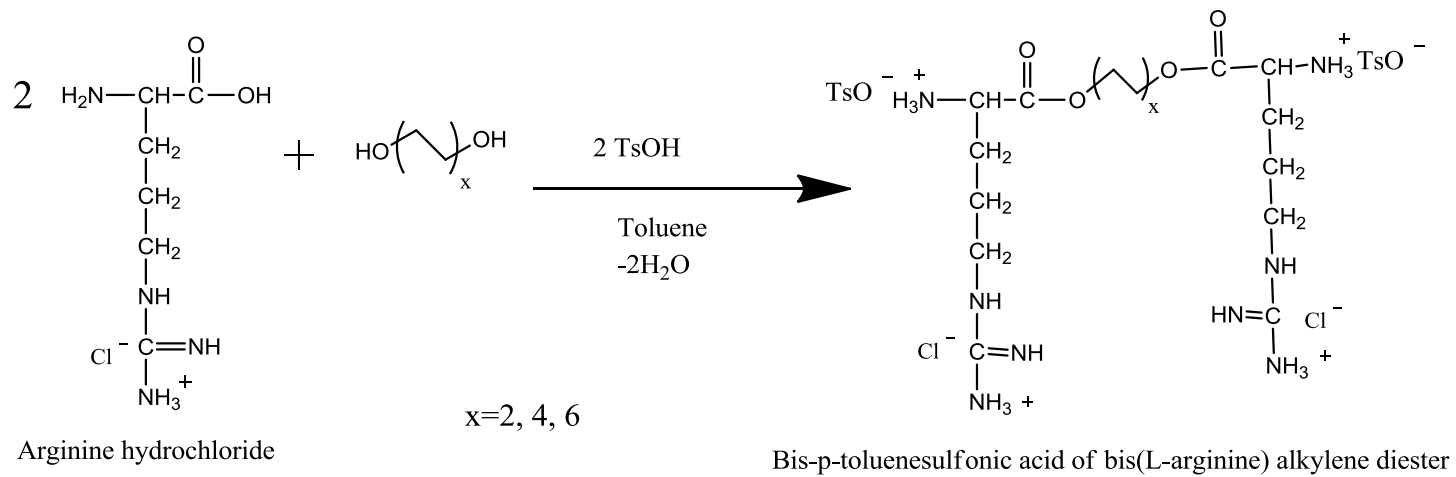


Figure 6.2 Synthesis of di-hydrochloride acid salt of bis(L-Arg) alkylene diester monomers (Arg-*x*-Cl)

polymerization step of 6-Arg-2-PEUU A/G-1/1 (where A/G-m/n is the molar ratio of Arg alkylene diester building blocks to GAE building blocks in Arg-PEUU), 8.41 gram HDI (0.05 mol) in 30 mL DMSO was stirred continuously with 3.30 gram GAE (0.025 mol) in 20 mL DMSO. Stannous 2-ethyl-hexanoate catalyst (2 wt % of total mass of reactants), which is the most common polyurethane synthesis catalyst, and 2, 6 di-tert-butyl-4-methyl phenol (1 wt % of total mass of reactants) were added into the HDI / GAE mixture. 2, 6 di-tert-butyl-4-methyl phenol acted as an antioxidant to protect the double bond of GAE. The mixture was allowed to react at 60 °C for a period of 5 h under dry nitrogen atmosphere. A DMSO solution of calculated molar amounts (0.025 mol) of Arg-*x*-Cl monomer (in the case of 6-Arg-2 PEUU A/G-1/1 synthesis described above, 20.75 gram of Arg-2-Cl was dissolved in 80 mL DMSO) was then added to the prepolymer solution, and the reaction was continued at 60 °C for 18 h under dry nitrogen atmosphere and then cooled down to room temperature. The polymer product was precipitated out from the solution by adding ethyl acetate first to remove residual chemicals like stannous 2-ethyl-hexanoate, 2, 6 di-tert-butyl-4-methyl phenol, DMSO and unreacted monomers. Then, the precipitant was vacuum dried at room temperature first, and then dissolve in equal weight of DMF again. The Arg-PEUU polymer in DMF solution was precipitated out in deionized water, and repeated purification in water two times before final drying in *vacuo* at room temperature.

The Arg-PEUU polymers have two types of repeating building blocks: the m block contains urea linkage and Arg alkylene diester, and the n block contains urethane linkage and pendant double bond from GAE. The ratio of these two building blocks (m/n) is equal to the feed ratio of Arg-*x*-Cl to GAE. In the polymerization reaction, if the Arg-*x*-Cl monomer to GAE molar ratio is 4 to 1, the m/n is also assumed as 4/1. The generic synthesis route of the Arg-PEUU is shown in Figure 6.3. Table 6.3 summarizes the types of Arg-PEUU synthesized by changing the molar feed ratios of HDI, Arg-*x*-Cl and GAE

Table 6.3 Arg-PEUU series synthesized from different di-hydrochloride acid salt of bis (L-Arg) alkylene diester (Arg-*x*-Cl) monomer and the feed ratios to hexamethylene diisocyanate and glycerol α -monoallyl ether monomers (GAE)*.

Reactants	Molar feed ratio (HDI: Arg- <i>x</i> -Cl : glycerol α -monoallyl ether)	Molar ratio of Arg alkylene diester building block to glycerol α -monoallyl ether (m/n)	Polymer Abbreviation
HDI : GAE	1:0:1	0	Allyl PU
HDI: Arg-2-Cl : GAE	5:4:1	4:1	6-Arg-2 PEUU A/G-4/1
HDI: Arg-2-Cl : GAE	2:1:1	1:1	6-Arg-2 PEUU A/G-1/1
HDI: Arg-2-Cl : GAE	5:1:4	1:4	6-Arg-2 PEUU A/G-1/4
HDI: Arg-4-Cl: GAE	2:1:1	1:1	6-Arg-4 PEUU A/G-1/1
HDI: Arg-6-Cl: GAE	5:4:1	4:1	6-Arg-6 PEUU A/G-4/1
HDI: Arg-6-Cl: GAE	2:1:1	1:1	6-Arg-6 PEUU A/G-1/1
HDI: Arg-6-Cl: GAE	5:1:4	1:4	6-Arg-6 PEUU A/G-1/4

*The sample labels for the Arg-PEUU polymers are ascribed as 6-Arg-*x* A/G=m/n, where 6 is the number of methylene groups in the hexamethylene diisocyanate (HDI), A/G-m/n is the molar ratio of Arg alkylene diester monomer (A) to glycerol α -monoallyl ether monomer (G)

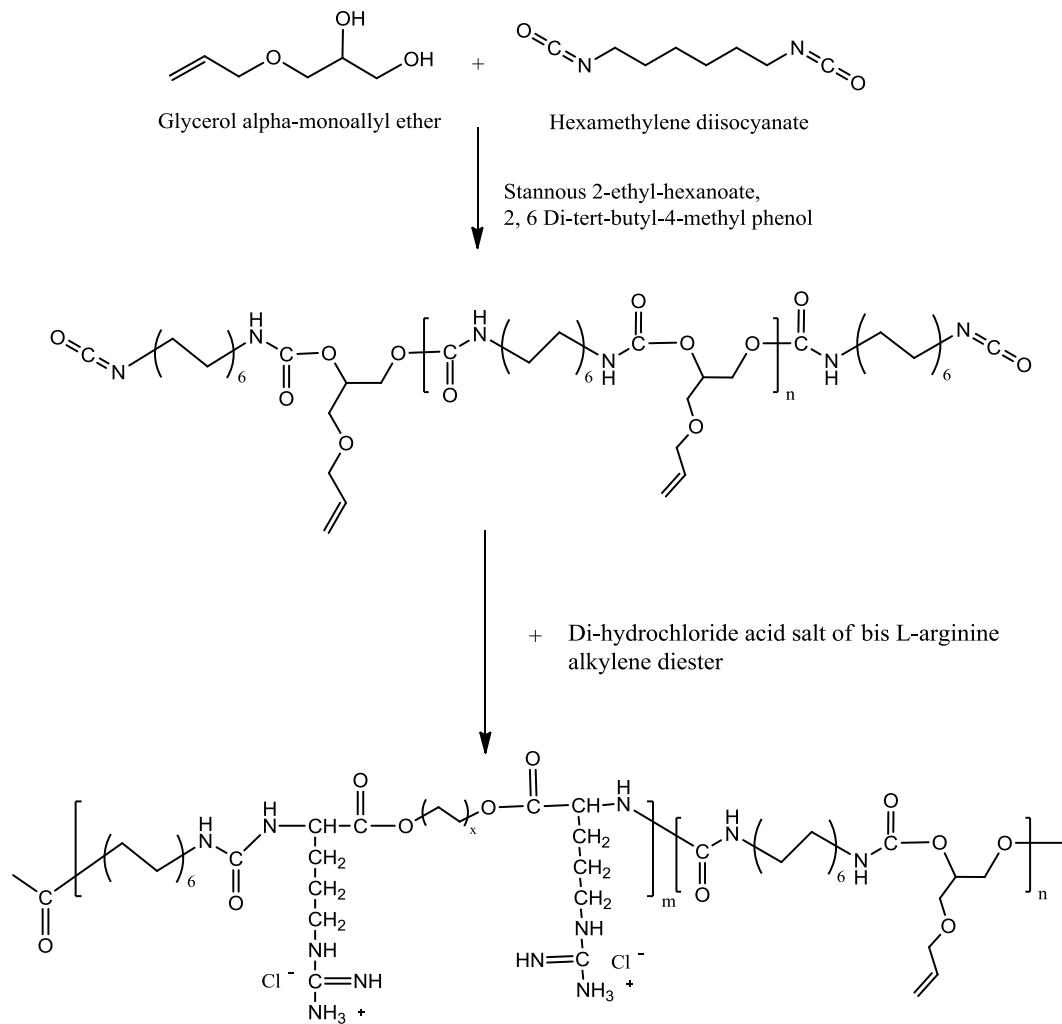


Figure 6.3 Synthetic pathway for the preparation of Arg-PEUU having pendant carbon-carbon double bond

in the reaction. As a control sample to study the effect of Arg alkylene diester building block content on polymer properties, allyl polyurethane (allyl PU) was synthesized from HDI and GAE without Arg-*x*-Cl monomer by using the identical reaction conditions (60 °C, 23h, dry nitrogen atmosphere, 2 wt% stannous 2-ethyl-hexanoate, 1 wt% 2, 6 di-tert-butyl-4-methyl phenol).

6.3.2.3 Characterization of Arg-*x*-Cl monomer and Arg-PEUU

The new Arg-*x*-Cl monomers were analyzed by proton nuclear magnetic resonance (¹H NMR). ¹H NMR spectra were recorded on a Varian (Palo Alto, CA) Mercury spectrophotometer at 400MHz. Deuterated dimethyl sulfoxide (DMSO-*d*₆, Cambridge Isotope Laboratories) was used as the solvent. The Arg-*x*-Cl monomers concentration in DMSO-*d*₆ were about 2 % (w/v). All of the chemical shifts were reported in parts per million (ppm).

Fourier transform infrared (FTIR) spectra of Arg-PEUU were recorded on a PerkinElmer (Madison, WI) Nicolet Magna 560 FTIR spectrophotometer with Omnic software for data acquisition and analysis. Elemental analysis of Arg-PEUU was performed with a Thermo Scientific ConFlo III elemental analyzer by Stable Isotope Laboratory of Cornell University.

6.3.2.4 Molecular weight determination of Arg-PEUU

Gel permeation chromatography (GPC) of Arg-PEUU was performed on an Agilent GPC equipped with a RI detector. PSS SDV gel columns (30 x 8 mm, 5 μm particle size) with 500 Å pore sizes were used. DMF was used as an eluent (flow rate 0.5 mL/min) at temperature of 25 °C. The injection volume was 100 μL and a WATERS 510 HPLC pump was used. Polystyrene standards were used for calibration.

6.3.2.5 Thermal properties of Arg-PEUU

The thermal property of the synthesized Arg-PEUU was characterized by a differential scanning calorimetry (DSC) TA Q2000 under a nitrogen gas flow 50 mL/min. The measurements were carried out from -60 °C to 150 °C at a scanning rate of 15

°C/min. TA Universal Analysis software was used for thermal data analysis. The glass transition temperature (T_g) was determined at the onset of the step.

6.3.2.6 Water contact angle test of Arg-PEUU

The hydrophilicity of all types of Arg-PEUU was measured by Imass CAA2 contact angle analyzer at room temperature. To make the specimens for water contact angle test, one droplet of 80% (w/v) solution of all types of Arg-PEUU in DMF were placed onto the center of micro cover glass (12mm Circle, VWR, West Chester, PA). Another piece of cover glass was placed onto the prior cover glass to squeeze the polymer solution droplet evenly spread over the whole glass wafer to form one thin layer of the Arg-PEUU coating and then the upper cover glass was removed to expose the Arg-PEUU coating layer. This coated micro cover glass were dried in a fume hood for 24 h and further dried under vacuum in a vacuum oven for another 24 h at room temperature. In the water contact angle tests, a drop of deionized water was generated on the tip of the needle of a syringe. The needle was lowered carefully until the water droplet touched the coated micro cover glass on the specimen stage until the droplet came off the needle. The height and 1/2 of the droplet width was measured in the center of the field of view, and contact angle, ϕ , was calculated according to the following equation.

$$\text{Cos}\phi = \frac{x^2 - y^2}{x^2 + y^2}$$

where: x = 1/2 drop width, y = drop height, ϕ = contact angle

Five samples of each type of Arg-PEUU were used for proper statistical average, and mean value was calculated with a standard deviation.

6.3.2.7 Cytotoxicity test of 6-Arg-2 PEUU suspension (MTT assay)

Porcine aortic valve smooth muscle cells (PAVSMC) were maintained in minimum essential medium (MEM) supplemented with 10% fetal bovine serum (FBS) and 1% each of penicillin-streptomycin. The cells were incubated in CO₂ incubator at 37 °C with 5% CO₂. After reaching confluence, the cells were detached from the flask with

trypsin-EDTA (Invitrogen, Carlsbad, CA). The cell suspension was centrifuged at 3,000 rpm for 3 min and then re-suspended in the growth medium for further study. PAVSMCs were used between passages 4 and 7.

Although all Arg-PEUU are insoluble in water at room temperature, the hydrophilic Arg alkylene diester building block attributes amphiphilicity to this polymer. All Arg-PEUU showed improved solubility in water at 60~70 °C. 6-Arg-2 PEUU A/G-1/1 and 6-Arg-2 PEUU A/G-4/1 achieved higher than 25 mg/mL solubility in deionized water at 70 °C. When these Arg-PEUU aqueous solutions were cooled down to room temperature, polymer did not precipitated out from its aqueous solution but formed homogenous suspension in water (supplemental picture). This polymer suspension was further diluted with MEM to evaluate the cytotoxicity of 6-Arg-2 PEUU from a MTT assay for PAVSMC cells. The Arg-PEUU stock suspension was prepared by dissolving 50 mg 6-Arg-2 PEUU A/G-1/1 or 6-Arg-2 PEUU A/G-4/1 in 5mL 0.05M phosphate buffered saline (PBS, pH 7.4) at 70 °C with magnetic stirring for 15 min, cooled down to room temperature, and then was sterilized by 30 min UV radiation. The sterilized stock suspension was diluted with sterilized minimum essential medium (MEM) supplemented with 10% fetal bovine serum (FBS) to 2, 1.5, 1, 0.5, 0.2, and 0.1 mg/mL of the polymer solutions.

PAVSMC were seeded on a 96 well plate with a density of 2,000 cells / well. The cells were washed with PBS buffer, and each of the 6 concentrations of 6-Arg-2 PEUU A/G-1/1 and 6-Arg-2 PEUU A/G-4/1 were added and incubated along with tissue cultured wells for 24 h. The cells treated only with normal cell culture media were used as the control. Afterward, the cells were incubated with 10 µL of MTT solution (5 mg/mL thiazolyl blue tetrazolium bromide in deionized water after filtration by 0.22 µm filter) for 4 h to form formazan crystals by mitochondrial dehydrogenases. About 100 µL of acidic isopropyl alcohol (contains 10% Triton-X 100 with 0.1M HCl,) was added into each well and incubated at room temperature for 1 h to dissolve the formazan crystals.

The optical density of the solution was measured at a wavelength of 570 nm and 690 nm (Spectramax plus 384, Molecular Devices, USA). The cell viability (%) was calculated according to the following equation:

$$\text{Viability (\%)} = \frac{[\text{OD570 (sample)} - \text{OD690 (sample)}]}{[\text{OD570 (control)} - \text{OD690 (control)}]} \times 100\%$$

where the OD570 (control) represents the measurement from the wells treated with medium only, and the OD570 (sample) from the wells treated with various polymers. 8 samples of each type of the Arg-PEUU were analyzed. Differences between group means were assessed using one-way ANOVA followed by parametric multiple comparison tests. A value of $p < 0.05$ was considered statistically significant.

6.3.2.8 Fabrication of Arg-PEUU gel via UV-crosslinking

In order to demonstrate the reactivity of the pendant double bonds in the Arg-PEUU, 0.3g of Arg-PEUU and 2 mg Irgacure 2959 were dissolved in 1 g DMF at room temperature under magnetic stirring. Every 400 μL of the above DMF mixture solution was transferred onto a custom-made 20 well Teflon mold and irradiated by a long wavelength (100 watts, 365nm) UV light at room temperature for about 25 min. Disk-shaped gels were obtained in the molds (11 mm diameter, 6 mm thickness). The gels were then soaked in 300 mL deionized water for 16 h at room temperature under a magnetic stirring to remove residual DMF solvent and unreacted precursor from the gels. The Arg-PEUU gels were then dried in vacuum oven at room temperature for about 4 h. Allyl PU gels was prepared by using the identical protocol as a control for the study of the effect of Arg alkylene diester building block incorporation on mechanical properties.

6.3.2.9 Compressive mechanical property of Arg-PEUU gels

The compressive mechanical property of all types of Arg-PEUU gels and allyl PU gels were measured by a TA Dynamic mechanical thermal analysis (DMA) Q800 (TA instruments) at room temperature (25 $^{\circ}\text{C}$) under a compression mode. Each dry gel sample was tested at a constant compression strain rate of 10 % /min until 40%

compressive strain was reached. TA Universal Analysis software was used for mechanical data analysis. Initial compressive modulus (calculated from the corresponding stress/strain curve) was used to represent the gel mechanical property. For each type of gels, three samples were used for calculating mean value with a standard deviation.

6.3.2.10 Enzymatic biodegradation of Arg-PEUU films *in vitro*

The effects of Arg alkylene diester building block contents of Arg-PEUU and photo-crosslinking on the enzymatic biodegradation of Arg-PEUU was studied in terms of weight loss over specific periods. Every 2 mL 60% (w/v) solution of uncrosslinked 6-Arg-2 PEUU in DMF were casted evenly onto a disk shaped Teflon[®] mold (about 27 cm²) and dried in a fume hood for 24 h at room temperature. The film samples were soaked in deionized water at room temperature for 3 h and dried under vacuum in a vacuum oven for another 24 h at room temperature. The same method was used to fabricate crosslinked 6-Arg-2 PEUU films. Every 2 mL 60% (w/v) solution of uncrosslinked 6-Arg-2 PEUU with 2 mg Irgacure 2959 initiator in DMF was casted evenly onto a Teflon[®] mold (about 27 cm²), and then irradiated by a long wavelength UV light (100 watts, 365nm) at room temperature for 20 min. The crosslinked 6-Arg-2 PEUU films were dried in a fume hood for 24 h at room temperature, soaked in deionized water at room temperature for 3 h and further dried in a vacuum at room temperature for another 24 h. The crosslinked and uncrosslinked Arg-PEUU films of 350 μm ~ 400 μm thickness were cut into 2cm \times 2cm (4 cm², ~150 mg) film specimens.

The enzymatic biodegradation of the crosslinked and uncrosslinked 6-Arg-2 PEUU films were carried out in glass vials containing the film specimen and lipase enzyme PBS solutions (1 and 3 mg/mL concentrations) with a constant reciprocal shaking (100 rpm). The original dry weight of each film sample was measured and recorded as W_0 . The biodegradation was evaluated by the specimen weight loss at 37 °C in 10 mL lipase PBS (pH 7.4, 0.05M) solutions. The enzyme PBS solutions were

refreshed daily in order to maintain enzymatic activity. The crosslinked and uncrosslinked 6-Arg-2 PEUU films in 10 mL PBS at 37 °C served as controls. Three replicated samples of each type of 6-Arg-2 PEUU were tested.

At predetermined intervals, 3 samples of each type of 6-Arg-2 PEUU films were removed from the immersion media (lipase PBS, and pure PBS control) rinsed in deionized water and dried under vacuum at room temperature till a constant weight achieved (about 12 h). The weight loss was calculated according to the following equation:

$$\% \text{ Weight loss} = (W_o - W_t) / W_o \times 100\%$$

where W_o was the initial dry weight of each film sample at $t=0$, and W_t was the dry weight of each film sample after t incubation. A mean value of three specimens was calculated as the weight loss at time t with a standard deviation.

6.4 Results and discussion

6.4.1 ^1H NMR spectroscopy of Arg- x -Cl monomers

The chemical structure of di-*p*-toluene sulfonic acid di-hydrochloride acid salt of bis (L-Arginine) alkylene diester and di-hydrochloride acid salt of bis (L-Arginine) alkylene diester monomers were confirmed by ^1H NMR (as shown in Figure 6.4).

Three types of Arg- x -Cl monomers due to different diols were prepared in this study: di-hydrochloride acid salt of bis (L-Arg) ethane diester Arg-2-Cl ($x=2$); di-hydrochloride acid salt of bis (L-Arg) butane diester Arg-4-Cl ($x=4$); di-hydrochloride acid salt of bis (L-Arg) hexane diester Arg-6-Cl ($x=6$) (Table 6.2). x indicates the number of methylene group in the diol segment of the Arg alkylene diester. The MW of these 3 Arg- x -Cl monomers are 0.446 Kg/mol for Arg-2-Cl, 0.474 Kg/mol for Arg-4-Cl, and 0.502 Kg/mol for Arg-6-Cl. The chemical structures of Arg- x -Cl monomers were confirmed by ^1H NMR.

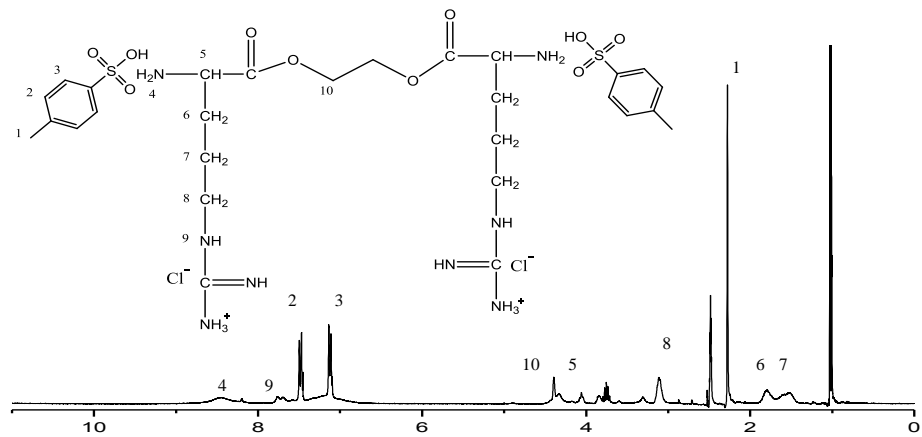
di-hydrochloride acid salt of bis (L-Arg) ethane diester (Arg-2-Cl): ^1H NMR (DMSO- d_6 , ppm, δ): 1.62 [4H, -OC(O)-CH(NH $_3^+$)-CH $_2$ -CH $_2$ -NH-], 1.80 [4H, -

OC(O)-CH(NH₃⁺)-CH₂-CH₂-CH₂], 2.29 [6H, H₃C-Ph-SO₃⁻], 3.10 [4H, -CH₂-CH₂-CH₂-NH], 4.04 [2H, ⁺H₃N-CH(R)-C(O)-O-], 4.39 [4H, -(O)C-O-CH₂-CH₂], 7.69, bump between 6.70~7.53 [10H, -CH₂-NH(NH₂⁺)-NH₂], 8.42 [6H, ⁺H₃N-CH(R)-C(O)-O-]

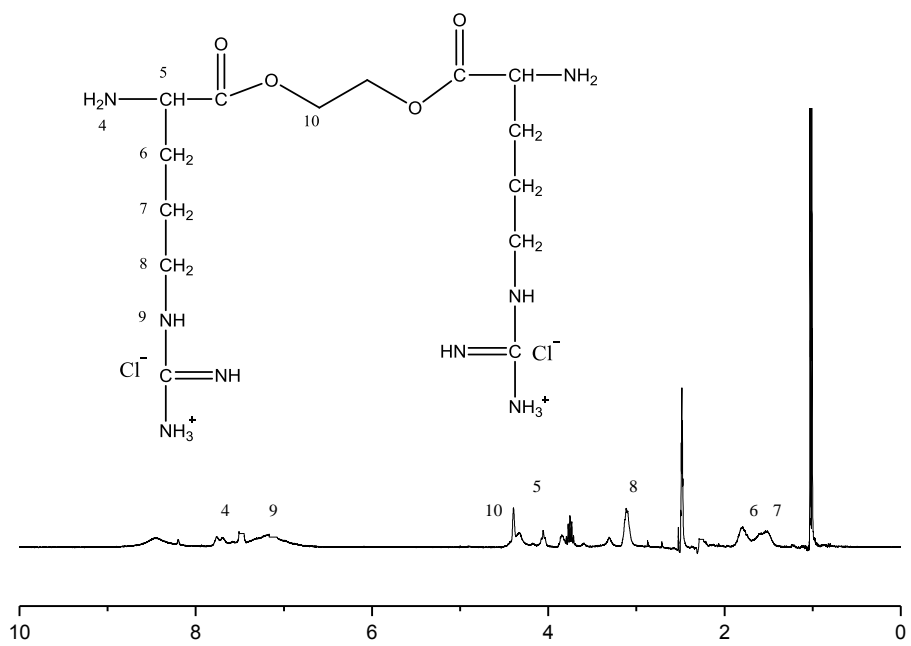
di-hydrochloride acid salt of bis (L-Arg) butane diester (Arg-4-Cl): ¹H NMR (DMSO-*d*₆, ppm, δ): 1.53 [4H, -CH₂-CH₂-CH₂-NH-], 1.65 [4H, -(O)CO-O-CH₂-CH₂-], 1.80 [4H, -OC(O)-CH(NH₃⁺)-CH₂-CH₂-CH₂-NH-], 2.29 [6H, H₃C-Ph-SO₃⁻], 3.10 [4H, -(CH₂)₂-CH₂-NH-], 4.04 [2H, ⁺H₃N-CH(R)-C(O)-O-], 4.14 [4H, -(O)C-O-CH₂-CH₂-], bump between 6.77~7.53 [10H, -CH₂-NH(NH₂⁺)-NH₂], 8.40 [6H, ⁺H₃N-CH(R)-C(O)-O-]

di-hydrochloride acid salt of bis (L-Arg) hexane diester (Arg-6-Cl): ¹H NMR (DMSO-*d*₆, ppm, δ): 1.59 [4H, -CH₂-CH₂-CH₂-NH-], 1.61 [4H, -(O)C-O-CH₂-CH₂-CH₂-] 1.78 [4H, -OC(O)-CH(NH₃⁺)-CH₂-CH₂-CH₂-NH-], 1.99 [2H, -(O)C-O-CH₂-CH₂-], 2.29 [6H, H₃C-Ph-SO₃⁻], 3.12 [4H, -(CH₂)₂-CH₂-NH-], 4.03 [2H, ⁺H₃N-CH(R)-C(O)-O-], 4.25 [4H, -(O)C-O-CH₂-CH₂-], bump between 6.75~7.50 [10H, -CH₂-NH(NH₂⁺)-NH₂], 8.26 [6H, ⁺H₃N-CH(R)-C(O)-O-]

The absence of protons of benzene group (7.1~7.2 ppm and 7.50~7.55 ppm) and methyl group (2.29 ppm) on the ¹H NMR of Arg-2-Cl and Arg-6-Cl demonstrated the toluene sulfonic acid group was removed from the amine group of arginine. The ¹H NMR spectra of Arg-PEUU are shown in Figure. 6.5 All of the ¹H NMR spectra showed proton on nitrogen and aliphatic signals.



A



B

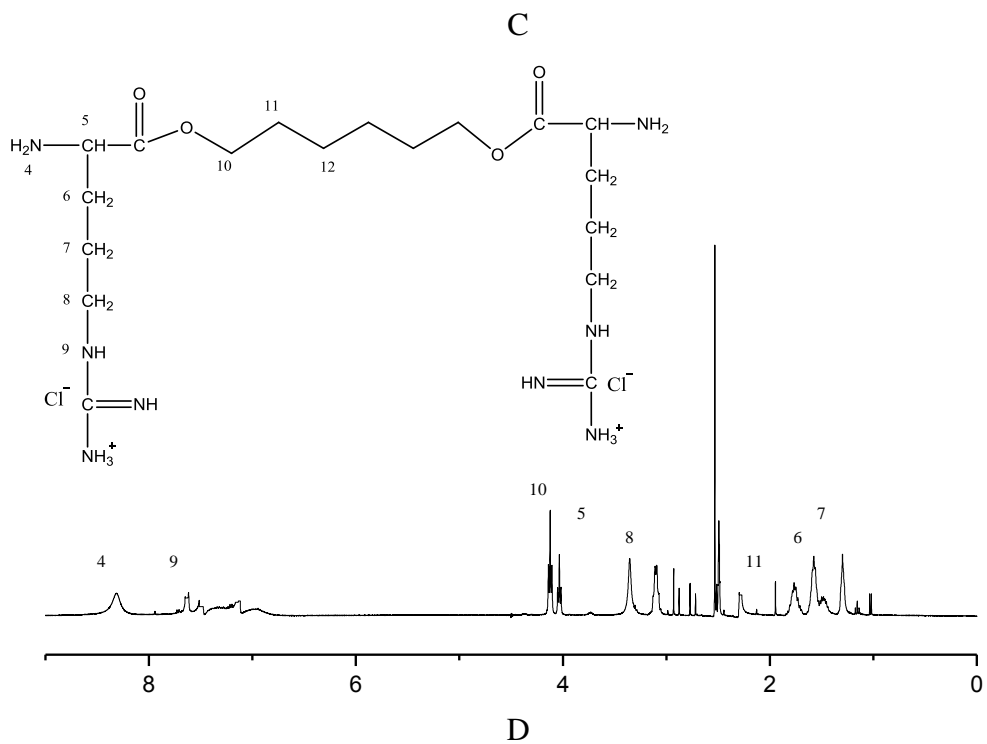
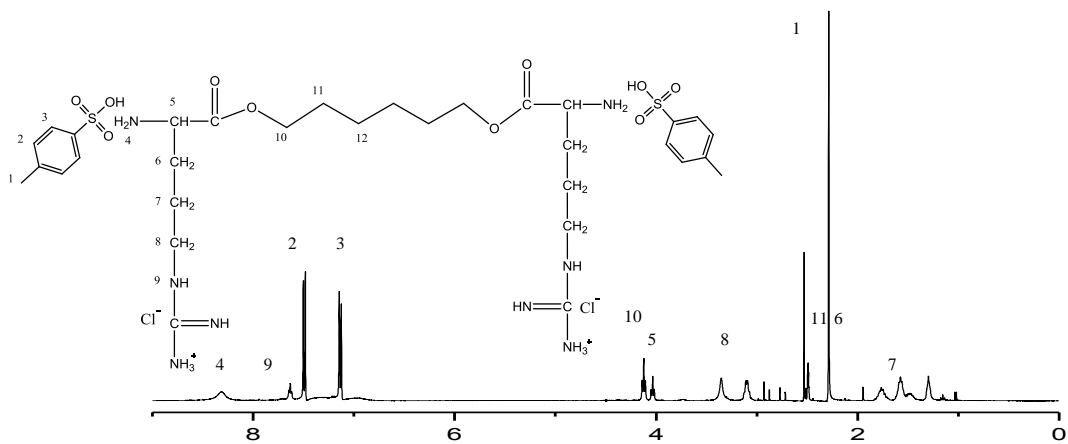
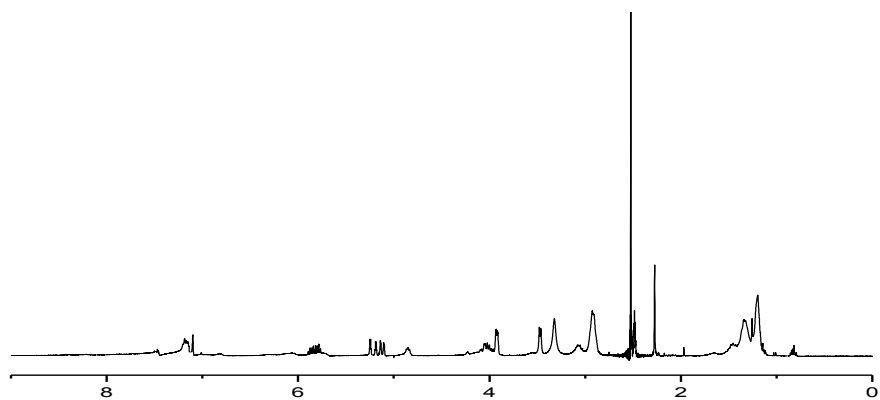
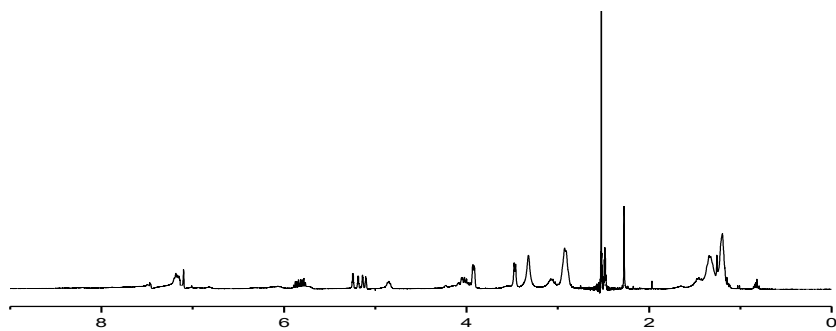


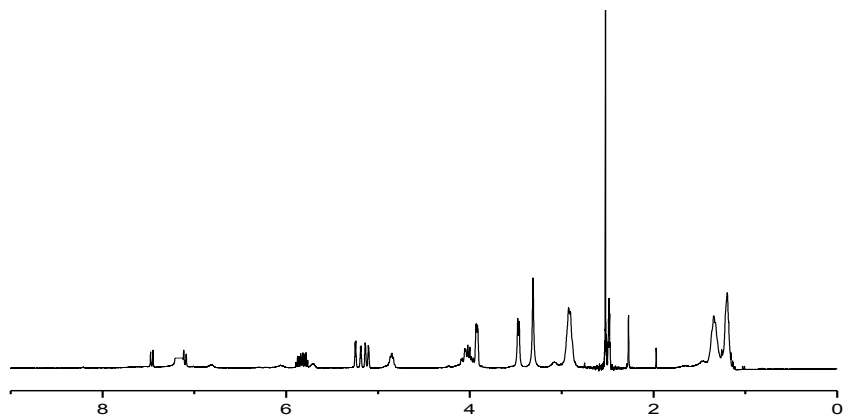
Figure 6.4 ^1H NMR spectroscopy of Arg diester monomers. (A) Di-*p*-toluene sulfonic acid dihydrochloride acid salt of bis (L-Arginine) ethane diester; (B) Di-hydrochloride acid salt of bis (L-Arginine) ethane diester (Arg-2-Cl); (C) Di-*p*-toluene sulfonic acid dihydrochloride acid salt of bis (L-Arginine) hexane diester; (D) Di-hydrochloride acid salt of bis (L-Arginine) hexane diester (Arg-6-Cl)



A



B



C

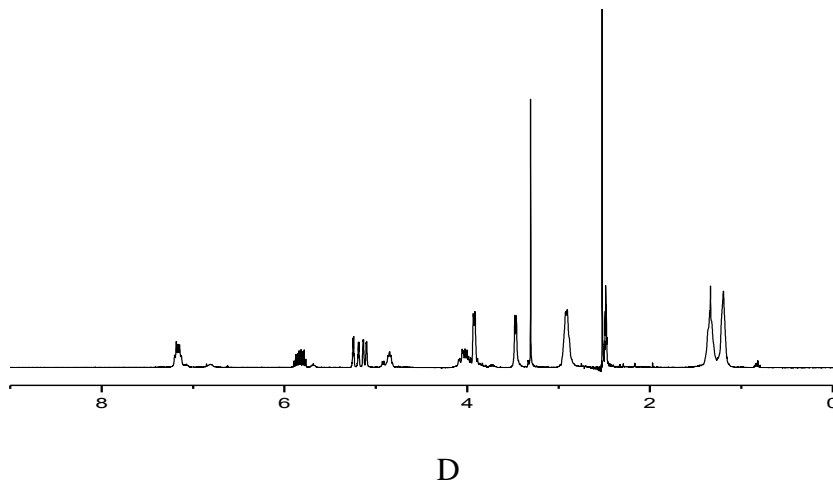


Figure 6.5. ^1H NMR spectroscopy of Arg-PEUU. (A) 6-Arg-2 PEUU A/G-4/1; (B) 6-Arg-2 PEUU A/G-1/1; (C) 6-Arg-6 PEUU A/G-4/1; (D) 6-Arg-6 PEUU A/G-1/1

6.4.2 Arg-PEUU synthesis and characterization

In order to verify the chemical composition of Arg-PEUU, their FTIR spectra and carbon / nitrogen content data were obtained. The FTIR spectra of Arg-PEUU is mainly influenced by the monomers feed ratio in the synthesis, and an example of the FTIR spectra of 6-Arg-2 PEUU of three different feed ratios and an allyl PU control without Arg component are shown in Figure 6.6. The absorption band at 3310 cm^{-1} is the characteristic of N-H group of urethane which is presented on all 6-Arg-2 PEUU spectra and allyl PU ³⁴. The absorption at 2859 cm^{-1} and 2950 cm^{-1} are attributed to $-\text{CH}_2$ symmetric and anti-symmetric stretching vibrations. 6-Arg-2 PEUU A/G-4/1 and 6-Arg-2 PEUU A/G-1/1 spectra shows absorption peak at 1725 cm^{-1} which is the carbonyl band of the Arg alkylene diester building block (Figure 6.6 A & B). 6-Arg-2 PEUU A/G-1/4 didn't show the obvious carbonyl absorption peak at 1725 cm^{-1} which is similar with allyl PU (Figure 6.6 C & D). The possible reason is the 6-Arg-2 PEUU A/G-1/4 contains less Arg alkylene diester building block contents than that of 6-Arg-2 PEUU A/G-4/1 and 6-Arg-2 PEUU A/G-1/1 due to the low feed ratio of Arg- x -Cl monomers to HDI and

glycerol monoallyl ether. Allyl PU shows trace amounts of absorption at 2270 cm^{-1} which is the characteristic peak of isocyanate group³⁴. However, the isocyanate peak did not present on any 6-Arg-2 PEUU which indicates HDI monomers were depleted in the chain extension reaction.

The carbon and nitrogen contents (Table 6.4) from the elemental analysis were consistent with the calculated composition based on the chemical formula of Arg-PEUU. Arg is the most nitrogen rich amino acid among all natural amino acids found in eukaryotes which has 32% nitrogen content. Another source of nitrogen in the polymer is from HDI. The calculated nitrogen content of allyl PU is 9.77%, while all Arg-PEUU have much higher nitrogen contents (12.82 to 21.18%) than allyl PU 9.77%. The Arg-PEUU having more Arg alkylene diester building block contents has higher nitrogen contents, e.g., from 12.82% at A/G 1/4, 18.69% at A/G 1/1 to 21.18 at A/G 4/1.

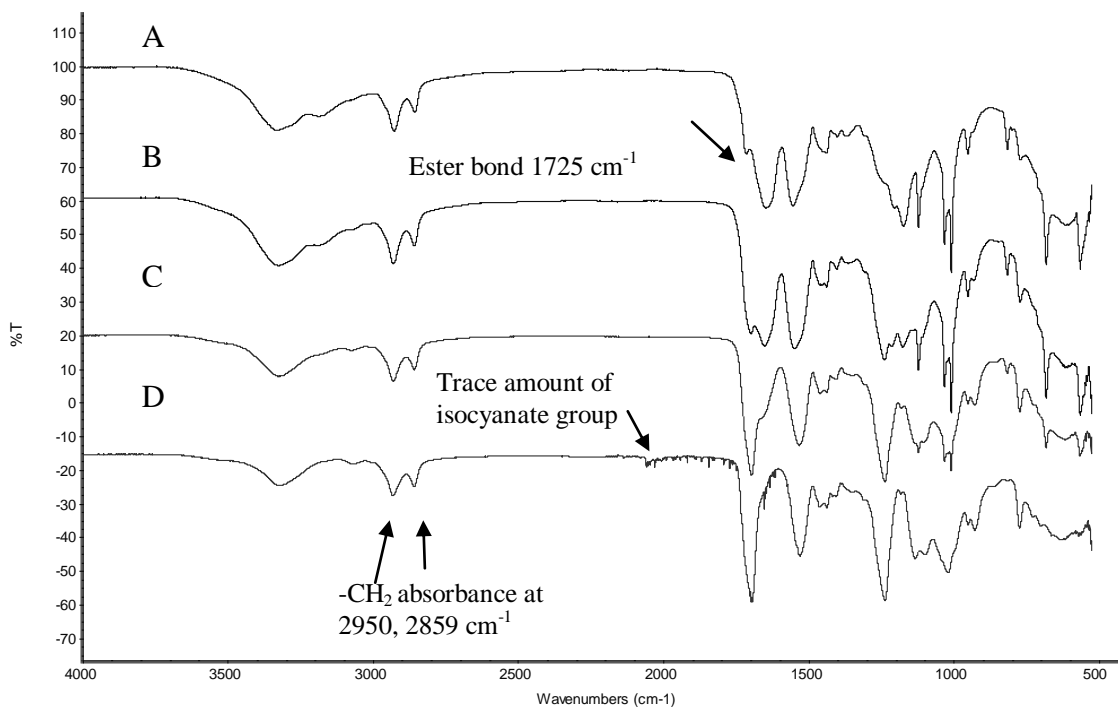


Figure 6.6 FTIR of 6-Arg-2 PEUU synthesized with different monomer feed ratio and allyl PU. (A) 6-Arg-2 PEUU A/G-4/1; (B) 6-Arg-2 PEUU A/G-1/1; (C) 6-Arg-2 PEUU A/G-1/4; (D) allyl PU

The molecular weights of Arg-PEUU as determined by GPC are shown in Table 6.5. The M_n (number average molecular weight) of Arg-PEUU ranged from 23.930 to 29.350 Kg/mol with M_w/M_n (MWD) 1.224~1.587. When comparing the molecular weight distribution (MWD) data of Arg-PEUU to other amino acid incorporated polyurethanes, like the Phe-PU reported by Skarja et al.³⁵ and Lys-PEUU reported by Guan et al.³⁴ which reported M_w/M_n about or higher than 2, the MWD of the Arg-PEUU was lower. The M_n of Phe-PU and Lys-PEUU ranged from 25.400 to 69.300 Kg/mol for the Phe-PU and from 28.300 to 92.900 Kg/mol for the Lys-PEUU. The comparatively higher MW of Phe-PU and Lys-PEUU than the current Arg-PEUU was because both of them contained PCL or polyethylene oxide (PEO) diol segments in the PU block had MW ranging from 0.530 to 2 Kg/mol, while the diol segment in the PU block of the Arg-PEUU is GAE which has the MW merely 0.132 Kg/mol.

This relatively narrow MWD of Arg-PEUU is also consistent with the Wu et al. reported water soluble Arg based poly (ester amide)s (Arg-PEA) which had MWD ranging from 1.07 - 1.10, but the Wu et al. Arg-PEAs synthesized by a solution polycondensation had a comparatively lower molecular weight than Arg-PEUU. For example, Wu et al reported the M_n of their Arg-PEAs ranged from 12.8 to 14.4 Kg/mol. The similar narrow MWD findings were also reported in another Wu et al. study of unsaturated Arg-UPEAs³⁷. The possible reason is in the polycondensation step of Arg-PEA in which the amino group of Arg- x -Cl reacted with nitrophenol diester monomer. In that synthesis, the ester bond of nitrophenol diester must be cleaved for forming amide bond with Arg- x -Cl monomer. The reaction time of Arg-PEA polymerization was about 24 h to 48 h. In the current study of the synthesis of Arg-PEUU, the polymerization step is the reaction between the free amine group of Arg- x -Cl monomer and HDI-based prepolymer. The reactivity of these 2 reactants of Arg-PEUU is higher than that of Arg-PEA synthesis as the polymerization time of Arg-PEUU was about 10-12 h which was about half of the time for the Wu et al.'s Arg-PEA synthesis. Based on the molecular

Table 6.4 Carbon and Nitrogen contents of Arg-PEUU and allyl PU from elemental analysis

Arg-PEUU samples	Formula	Calculated carbon content (%)	Carbon content (%)	Calculated nitrogen content (%)	Nitrogen content (%)
6-Arg-2 PEUU	(C ₂₂ H ₄₄ Cl ₂ N ₁₀ O ₆) ₁	53.95	53.50	14.52	12.82
A/G-1/4	(C ₁₄ H ₂₄ N ₂ O ₅) ₄				
6-Arg-2 PEUU	(C ₂₂ H ₄₄ Cl ₂ N ₁₀ O ₆) ₁	48.27	50.69	18.77	18.69
A/G-1/1	(C ₁₄ H ₂₄ N ₂ O ₅) ₁				
6-Arg-2 PEUU	(C ₂₂ H ₄₄ Cl ₂ N ₁₀ O ₆) ₄	44.67	45.34	21.46	21.18
A/G-4/1	(C ₁₄ H ₂₄ N ₂ O ₅) ₁				
6-Arg-6 PEUU	(C ₂₆ H ₅₂ Cl ₂ N ₁₀ O ₆) ₁	54.94	54.68	14.07	13.77
A/G-1/4	(C ₁₄ H ₂₄ N ₂ O ₅) ₄				
6-Arg-6 PEUU	(C ₂₆ H ₅₂ Cl ₂ N ₁₀ O ₆) ₁	50.47	51.67	17.67	17.89
A/G-1/1	(C ₁₄ H ₂₄ N ₂ O ₅) ₁				
6-Arg-6 PEUU	(C ₂₆ H ₅₂ Cl ₂ N ₁₀ O ₆) ₄	47.77	46.81	19.84	19.07
A/G-4/1	(C ₁₄ H ₂₄ N ₂ O ₅) ₁				
Allyl PU	C ₁₄ H ₂₄ N ₂ O ₅	60.00	58.60	10.00	9.77

weight, FTIR and carbon and nitrogen content data, Arg-PEUU should possess the chemical structure shown in Figure 6.3.

In addition to the MW and MWD differences, both Phe-PU from the Skarja et al.³⁵ and Lys-PEUU from the Guan et al.³⁴ didn't have pendant charge functional groups, while the current Arg-PEUU has positively charged guanidino side groups as well as the pendant photo-reactive vinyl group. In the Guan et al. Lys-PEUU, the free carboxyl groups of Lys were protected by ethyl ester³⁴ that can't be deprotected without adversely affecting the molecular weight of the Lys-PEUU.

6.4.3 Structure difference of Arg-PEUU with other published polyurethane materials with amino acids building blocks

Even though many types of polyurethane materials having ester bonds on the polymer backbone have been developed by others, most of them used aromatic multi-isocyanates as monomers which are considered cytotoxic and possible carcinogen³³. In the studies of polyurethane materials for biomedical application, Wagner and Woodhouse's groups developed linear degradable polyester urethane-urea with protected lysine as one of the building blocks³⁷ or polyester urea urethane with phenylalanine diester as one of the building block³⁵. Table 6.6 summarizes the difference of our present Arg-PEUU from both Wagner and Woodhouse groups' PEUU^{35, 37} in terms of raw materials and final product structure.

In the Wagner's study, polycaprolactone diols (M_w 1,250 and M_w 2,000) were used to react with 1, 4-diisocyanatobutane to form a poly (ester urethane) prepolymer having the urethane linkage adjacent to the ester bonds of the polycaprolactone segments, then a protected lysine ethyl ester was added to form a urea linkage between the amine groups of the protected lysine ethyl ester and the 2 diisocyanate ends of the poly (ester urethane) prepolymer. The result Lys-based PEUU polymer has the linkage sequence ester-urethane-urea. The protected -COOH in Lys was not deprotected because the deprotection procedure of lysine ethyl ester is able to cleave both the ester bonds of

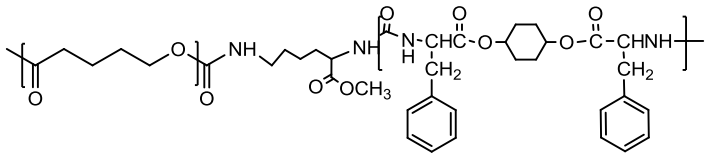
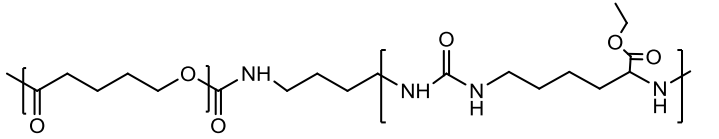
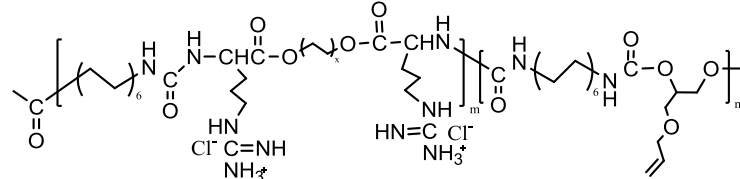
Table 6.5 Molecular weight and molecular weight distribution of Arg-PEUU

Sample	M_n (kg/mol)	M_w (kg/mol)	M_w/M_n
6-Arg-2 PEUU A/G-4/1	27.000	33.050	1.224
6-Arg-2 PEUU A/G-1/1	29.350	41.175	1.403
6-Arg-2 PEUU A/G-1/4	28.100	44.600	1.587
6-Arg-4 PEUU A/G-1/1	26.670	34.510	1.394
6-Arg-6 PEUU A/G-4/1	28.225	38.825	1.376
6-Arg-6 PEUU A/G-1/1	23.930	36.475	1.524
6-Arg-6 PEUU A/G-1/4	24.420	33.800	1.384

lysine carboxyl group and the ester bonds of polycaprolactone diols on the polymer backbone which could lead to the fragmentation of the polymer. So, the lysine carboxyl group could not be recovered, the only pendant groups on the polymer is methyl ester (Table 6.6)

The Woodhouse's Phe-based polyester urea urethane shares more structure similarity with our Arg-PEUU. The incorporation of phenylalanine diester segment permits the Phe-based PEUU enzymatic degradable, and the backbone linkage sequence is ester-urea-urethane which is the same linkage as our Arg-PEUU backbone.

Table 6.6 Comparison of Arg-PEUU with published amino acid contained polyurethane ^{35, 37}

Author	Publication	Monomers in polymerization	Chemical structure of final product
G.A.Skarja and K.A. Woodhouse	J. Biomater. Sci. Polymer Edn, 2001, 12, 851-873	Polycaprolactone diol, 2,6 diisocyanato methylcaproate, L-phenylalanine diester,	
Jianjun Guan, William Wagner	Journal of biomedical materials research, 2002, 61, 493-503	Polycaprolactone diol, 1,4-diisocyanatobutane, lysine ethyl ester	
Mingyu He, C.C.Chu	Polymer, 2013, pending	L-Arg diester, 1,6 diisocyanatohexane, Glycerol α -monoallyl ether	

However, both the Woodhouse et al. Phe-based PEUU and the Wagner et al. Lys-based PEUU are lack of pendant reactive or functional groups, while our Arg-PEUU has both pendant double bonds in the urea-urethane block and positively charged guanidino pendant groups in the Arg diester block. Moreover, Arginine possesses unique physiological functions in many cell activities.

6.4.4 Thermal properties of Arg-PEUU

The DSC thermograms of the Arg-PEUU are presented in Figure 6.7. T_g and T_m of all the Arg-PEUU from the DSC thermograms are summarized in Table 6.6. T_g of all Arg-PEUU and allyl PU ranged from -26.80 °C to 4.23 °C, depending on the 3 monomers feed ratio and x (number of methylene group in the diol segment of Arg alkylene diester). The allyl PU without Arg component had the lowest T_g (-26.80 °C) among all the polymer samples tested in this study. An increase in the Arg alkylene diester building blocks contents in the Arg-PEUU from 1/5 (i.e. 6-Arg-2 PEUU A/G-1/4) to 4/5 (i.e. 6-Arg-2 PEUU A/G-4/1) led to an increase in T_g from -9.66 °C to 4.23 °C. This relationship could be attributed to the fact that more Arg contents in the Arg-PEUU would have more bulky guanidino side groups to the Arg-PEUU which could reduce polymer segmental mobility and hence higher T_g . In addition, all Arg-PEUU synthesized have far more nitrogen contents than allyl PU (Table 6.6), as a result, Arg-PEUU should have more intermolecular hydrogen bonding than allyl PU which could lead to higher T_g . For example, the guanidino side groups could form strong intermolecular hydrogen bonding when guanidino groups approach the urethane/urea groups of Arg-PEUU, as Song et al. indicated in their study of Arg-PEA³⁹. The intermolecular force could further decrease the segmental mobility of polymer chain and also increase the T_g further.

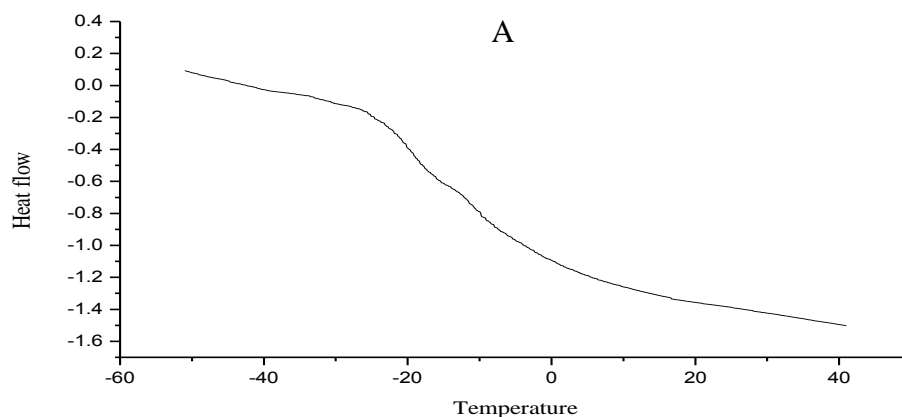
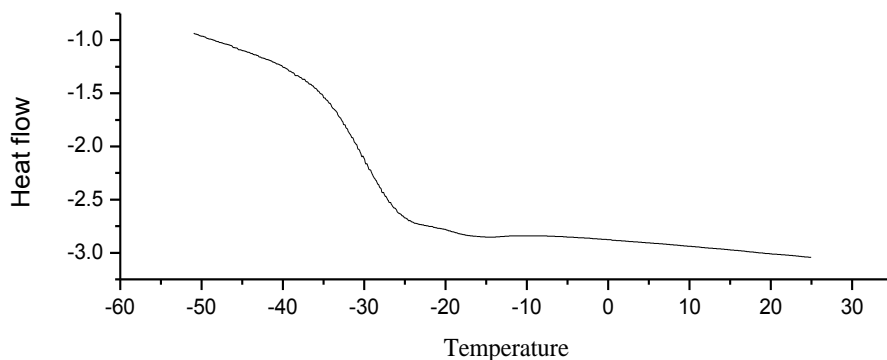
As the Arg alkylene diester building block contents decreased, more GAE was incorporated into the polymer. GAE is able to impart additional chain flexibility by increasing free volume from pendant double bonds which acts as an internal plasticizer. Thus, increasing GAE component in Arg-PEUU resulted in a lower T_g as observed.

This reduction in T_g with an increasing pendant double bonds in the Arg-PEUU polymer is consistent with the finding from the reported Pang et al. study of functional AA-PEAs having pendant double bonds^{38,40}. For example, Pang et al. reported that an increase in the pendant double bond in bis-DL-2-allylglycine esters (i.e., increasing AG contents in the Phe-PEA polymers) from 25% (8-Phe-4-AG-4-25) to 50% (8-Phe-4-AG-4-50) led to a reduction in T_g from 30 °C to 26 °C⁴⁰.

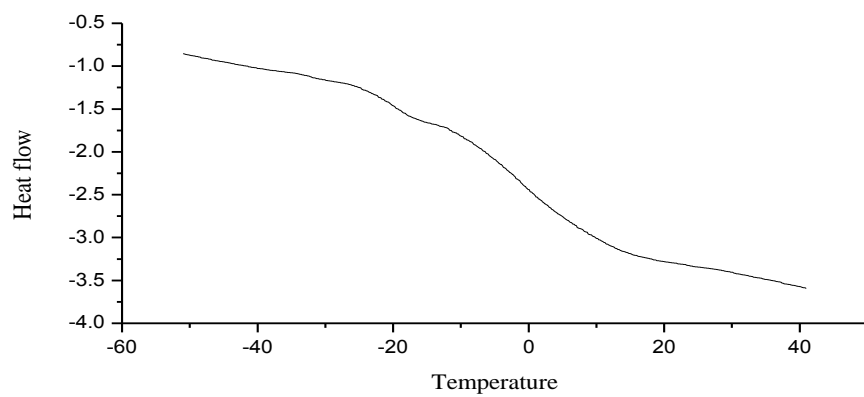
Furthermore, the change in methylene group length (x) in the diol segment of Arg alkylene diester also affected the T_g of the corresponding Arg-PEUU. For example, as the x increased from 2 to 6 in the Arg alkylene diester building block at the identical molar feed ratio of Arg- x -Cl to 2 other monomers (HDI and GAE), the T_g of the resulting Arg-PEUU was reduced from 1.90 °C of the 6-Arg-2 PEUU A/G-1/1 to -8.69 °C of the 6-Arg-6 PEUU A/G-1/1. The effect of x on T_g was attributed to the higher Arg-PEUU polymer chain flexibility as the methylene group length increased. The similar relationship between T_g and the number of methylene group length in AA-PEA polymer backbone was found and reported^{37, 38,40,43,45}.

When comparing with other amino acid incorporated PEUU such as Guan et al. reported Lys-PEUU which had Lys ethyl ester and PCL building block³⁴ the T_g of the new Arg-PEUU are relatively higher than the Guan et al.'s Lys-PEUU. For example, the T_g of the Guan et al. Lys-PEUU ranged from -36.5 °C to -54.3 °C, depending on monomer feed ratios and molecular weight of PCL diol segment, while the lowest T_g in our current Arg-PEUU was -20.80 °C. Similarly, Skarja et al. developed a polyurethane which has Phe and PCL as building blocks, and its T_g ranged from -6.2 °C to -51.9 °C¹⁴. The relatively higher T_g in our Arg-PEUU than other reported amino acid contained PU and PEUU could be attributed to the Arg alkyl diester of our Arg-PEUU as the Arg moiety can provide more rigidity to the molecule chain polymer due to the bulky guanidino side groups and the possible intermolecular interaction described earlier.

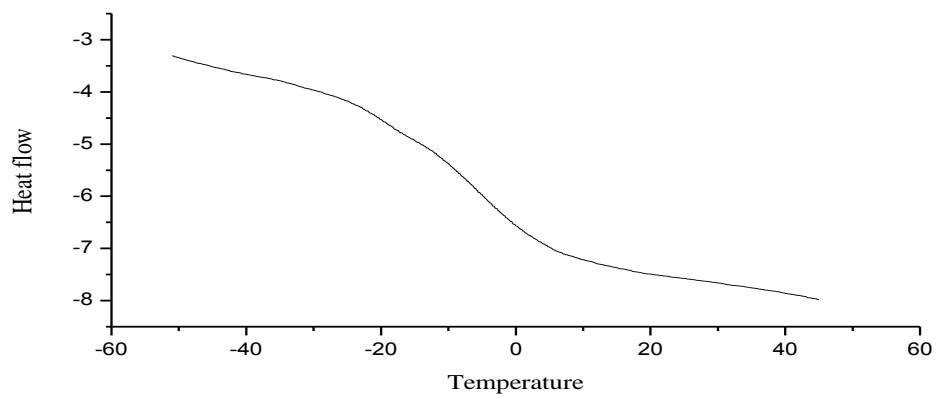
Table 6.7 showed the dependence of T_m on weight fraction of GAE segments, and the effect of x in Arg alkylene diester building blocks. Typical melting endotherms (T_m) are shown on the DSC spectra of 6-Arg-2 PEUU A/G-1/4, 6-Arg-2 PEUU A/G-1/1 and allyl PU samples. But no evident crystalline melting point could be detected for the Arg-PEUU having the feed ratio of Arg- x -Cl to GAE segments greater than 1 : 1 or the methylene group length (x) of Arg alkylene diester building block was higher than 2. 6-Arg-2 PEUU showed a decrease in the melting point from 141.3 °C (6-Arg-2 PEUU A/G-1/4) to 129 °C (6-Arg-2 PEUU A/G-1/1) as the fraction of GAE segments decreasing from A/G-1/4 to A/G-1/1.



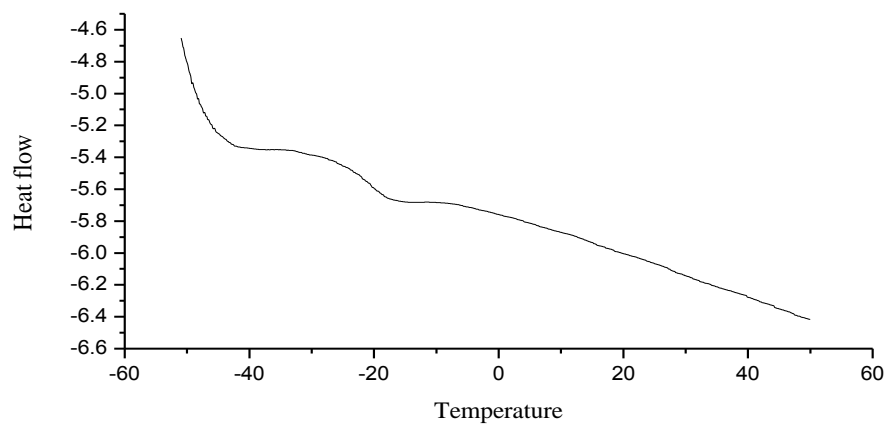
B



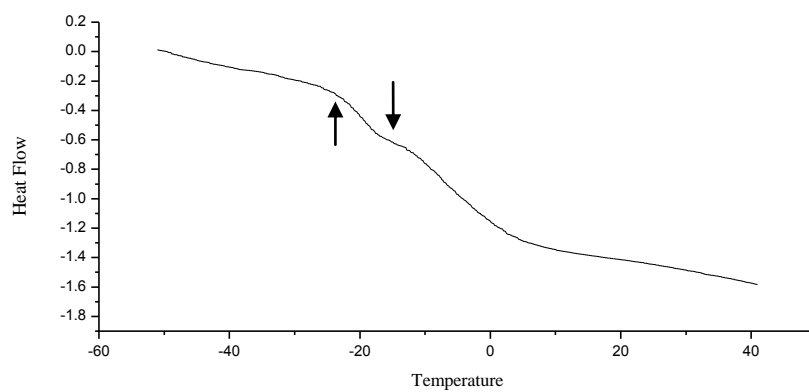
C



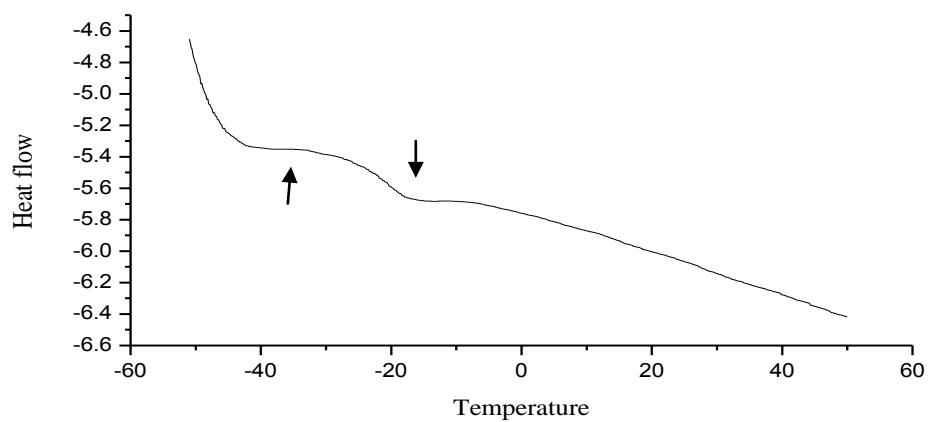
D



E



F



G

Figure 6.7 DSC of Arg-PEUU. (A) Allyl PU; (B) 6-Arg-2 PEUU A/G-1/4; (C) 6-Arg-2 PEUU A/G-1/1; (D) 6-Arg-2 PEUU A/G-4/1; (E) 6-Arg-6 PEUU A/G-1/4; (F) 6-Arg-6 PEUU A/G-1/1; (G) 6-Arg-6 PEUU A/G-4/1

Table 6.7 T_g and T_m of Arg-PEUU

PEUU	T_g (°C)	T_m (°C)
Allyl PU	-26.8	141.8
6-Arg-2 PEUU A/G-1/4	-9.66	141.3
6-Arg-2 PEUU A/G-1/1	1.90	129.0
6-Arg-2 PEUU A/G-4/1	4.23	N/A
6-Arg-6 PEUU A/G-1/4	-20.80	N/A
6-Arg-6 PEUU A/G-1/1	-8.69	N/A
6-Arg-6 PEUU A/G-4/1	-2.24	N/A

6.4.5 Water contact angle of Arg-PEUU

The water contact angle was used to characterize the hydrophilicity level of the Arg-PEUU as shown in Table 6.8. Allyl PU was used as the control to exam the effect of the incorporation of hydrophilic Arg alkylene diester building blocks. Allyl PU showed the highest water contact angle ($75.4 \pm 0.7^\circ$) than all Arg-PEUU (from $26.7 \pm 4.3^\circ$ to $61.3 \pm 5.2^\circ$). This highest contact angle of allyl PU is within the reported contact angles of linear polyurethane with PCL and PEG segments (from $65 \pm 2^\circ$ to $73 \pm 2^\circ$)³¹. The contact angle values of this new family of Arg-PEUU biomaterials are in general lower than the Guo et al. reported pure Phe-PEAs⁴⁴ and Deng et al. reported Ser-PEAs⁴⁵ which had values close to allyl PU.

Arg alkylene diester monomer has been demonstrated to be highly hydrophilic in the reported studies of Arg-PEA and Arg-UPEA due to the presence of the pendant toluene sulfonic acid salt of guanidino groups³⁷. Therefore, the molar ratio of Arg alkylene diester to GAE (A/G) could also affect hydrophilicity of the resulting Arg-PEUU. The data in Table 6.8 show that as the contents of the Arg alkylene diester increases, the water contact angle of the Arg-PEUU becomes lower, i.e., more

hydrophilic. For example, as the 6-Arg-2 PEUU of A/G ratio increased from 1/4, 1/1 to 4/1, the water contact angle decreased from 44.2 to 32.7 and 26.7° correspondingly. The methylene group length in the diol segment of Arg alkylene diester (x) is another important material parameter that could influence the hydrophilicity of Arg-PEUU. At the identical molar ratio of Arg alkylene diester to GAE building blocks, for example 1:1, 6-Arg-6 PEUU ($x=6$) showed a higher hydrophobicity ($47.4 \pm 2.0^\circ$) than 6-Arg-2 PEUU ($x=2$) ($32.7 \pm 1.8^\circ$) due to the more hydrophobicity of a longer methylene chain length in Arg alkylene diester segment. The same relationship was also found at other A to G feed ratios. To adjust the hydrophilicity by changing the methylene group length in AA-PEAs was also reported in the Wu et al. study of Arg-PEAs³⁷ and Guo et al study of Phe-PEA⁴⁴.

Table 6.8 Water contact angle of Arg-PEUU

PEUU	Water contact angle (°)
Allyl PU	75.4 ± 0.7
6-Arg-2 PEUU A/G-1/4	44.2 ± 1.9
6-Arg-2 PEUU A/G-1/1	32.7 ± 1.8
6-Arg-2 PEUU A/G-4/1	26.7 ± 4.3
6-Arg-6 PEUU A/G-1/1	47.4 ± 2.0
6-Arg-6 PEUU A/G-4/1	34.2 ± 5.0

6.4.6 Solubility of Arg-PEUU in common solvents at room temperature

Table 6.9 summarized the solubility of allyl PU and Arg-PEUUs in several common organic solvents and water. Allyl PU is soluble in most common organic solvents like DMSO, DMF, THF, chloroform, except ethanol, whereas the Arg-PEUU could only be dissolved in DMF and DMSO. Allyl PU and the Arg-PEUU are not soluble in water at room temperature due to the hydrophobicity of urethane and ester.

Table 6.9 Solubility of Arg-PEUU in common solvents at room temperature

PEUU/solvents	H ₂ O	DMF	DMSO	Ethanol	Chloroform	THF	Ethyl acetate	Acetone
Allyl PU	-	+	+	-	+	+	+	+
6-Arg-2 PEUU A/G-1/4	-	+	+	-	-	-	-	-
6-Arg-2 PEUU A/G-1/1	-	+	+	-	-	-	-	-
6-Arg-2 PEUU A/G-4/1	-	+	+	-	-	-	-	-
6-Arg-6 PEUU A/G-1/4	-	+	+	-	-	-	-	-
6-Arg-6 PEUU A/G-1/1	-	+	+	-	-	-	-	-
6-Arg-6 PEUU A/G-4/1	-	+	+	-	-	-	-	-

Soluble: +; Insoluble: - .

6.4.7 Cytotoxicity of 6-Arg-2 PEUU A/G-1/1 and 6-Arg-2 PEUU A/G-4/1

Cytotoxicity of PAVSMC was conducted by incubating the cells with either the MEM media alone (control) or 6-Arg-2 PEUU suspension mixed with MEM media. Cell viability was determined from a MTT assay after treated by the 6-Arg-2 PEUU suspension and incubated for 24 h (Figure 6.8). Compared to the control, both 6-Arg-2 PEUU A/G-1/1 (Figure 6.8 A) and 6-Arg-2 PEUU A/G-4/1 (Figure 6.8 B) didn't show obvious cell viability change at low concentrations (0.1 - 0.2 mg/mL). While at concentration from 1-2 mg/mL, 6-Arg-2 PEUU A/G-1/1 shows significantly high cytotoxicity towards PAVSMC (Figure 6.8 A). At the same concentration, Arg-PEUU having higher Arg alkylene diester building block (e.g., 6-Arg-2 PEUU A/G-4/1) showed significantly higher cell viability than those Arg-PEUU having lower Arg alkylene diester contents like 6-Arg-2 PEUU A/G-1/1. This relationship between cell viability and the Arg diester contents in Arg-PEUU holds over the whole concentration range (0.1 – 2 mg/mL). For example, at 2 mg/mL, the PAVSMC viability cultured with 6-Arg-2 PEUU A/G-4/1 and 6-Arg-2 PEUU A/G-1/1 and exhibited 67.7 and 55.9%, respectively. Therefore, Arg-PEUU biomaterials are PAVSMC biocompatible as long as the polymer concentration is low and the Arg diester contents are high.

A similar relationship between Arg contents in other AA-PEA polymers and cell viability was also observed in the prior studies of pure Arg-PEAs^{29,37}. For example, Yamanouchi et al.²⁹ and Wu et al.³⁷ reported the cytotoxicity of Arg-PEA/ DNA complex to vascular smooth muscle cells. Arg-PEA didn't significantly reduce the smooth muscle cell viability from the control, and the lowest cell viability of all tested pure Arg-PEAs was about 70%-80% which are similar with our current Arg-PEUU having higher Arg diester contents like 6-Arg-2 PEUU A/G-4/1. In the Wu et al.'s cytotoxicity data, 2-Arg-6-S which had the lowest Arg contents in the polymer showed a lower cell viability (~70%) than other Arg-PEA tested (75%~95%) at the identical

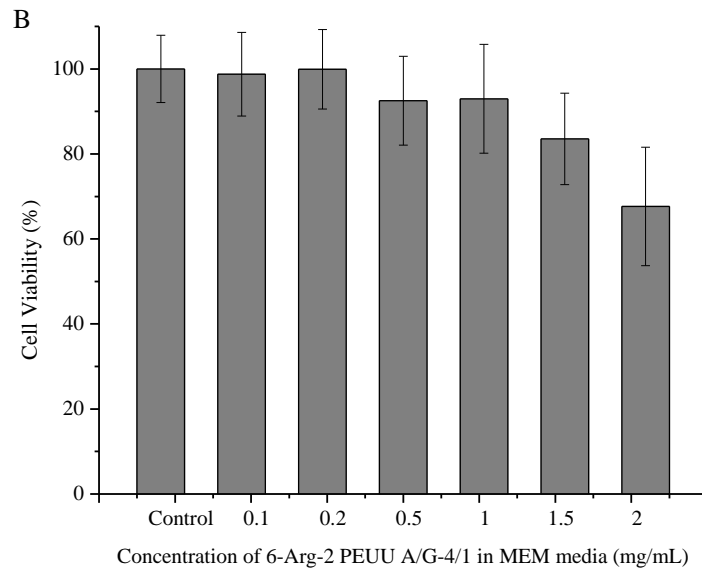
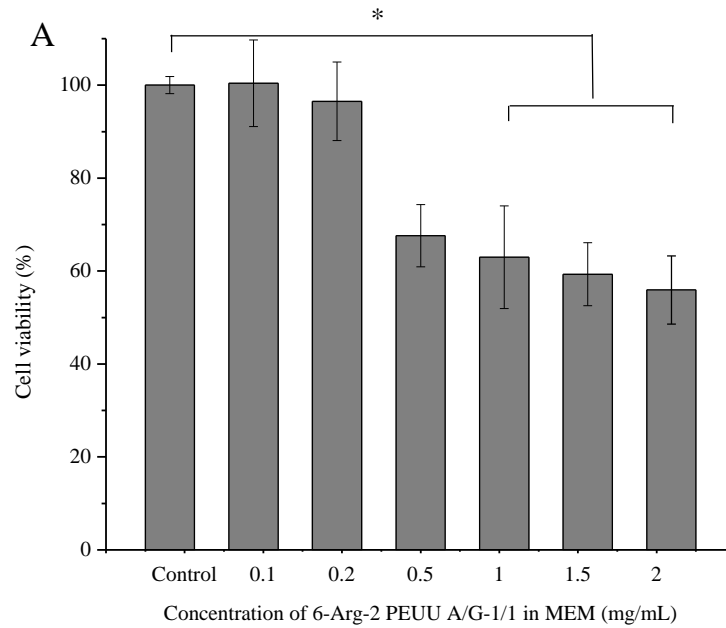


Figure 6.8 MTT Assay for porcine aortic valve smooth muscle cells (PAVSMC) after 24 h culture with 6-Arg-2 PEUU at 0.1, 0.2, 0.5, 1, 1.5, and 2 mg/mL concentrations. (A) 6-Arg-2 PEUU A/G-1/1; (B) 6-Arg-2 PEUU A/G-4/1. * $P < 0.05$ vs. control group

condition. Therefore, both our current Arg-PEUU and others prior studies demonstrate that there is a relationship between the cellular biocompatibility and the composition of Arg in Arg-PEA or Arg-PEUU, that increasing the Arg content can improve the biocompatibility of the polymers as well.

6.4.8 Photo-crosslinked Arg-PEUU and the interior morphology

GAE was used for the synthesis of Arg-PEUU because it introduced pendant functional double bonds which can be further converted into other functional groups or be crosslinked for the potential biomedical applications. Arg-PEUU synthesized with the A/G ratio no more than 1/1 (i.e., Arg alkylene diester/ GAE @ 1/4 and 1/1) could be photo-crosslinked in a DMF solution with Irgacure 2959 initiator (Table 6.9). Figure 6.9 A showed the images of the photo-crosslinked 6-Arg-2 PEUU A/G-1/4 gel as a representative example. Photo-crosslinked 6-Arg-2 PEUU A/G-1/4 was transparent yellow color elastic gel with good mechanical strength. Upon a 2 Kg weight applied onto the 6-Arg-2 PEUU A/G-1/4 disk-shaped gel sample (12mm diameter, 6mm thickness) (Figure 6.9 B), the force could not break the material. The 6-Arg-2 PEUU A/G-1/4 gel is also elastic.

Unlike Arg-PEUU which can form gels by itself upon UV irradiation, Arg-UPEA having unsaturated double bonds, however, could not be photo-crosslinked by themselves because of the steric hindrance of a large pendant guanidino group of Arg on the polymer. But Arg-UPEAs could be crosslinked with the help of other photo-reactive crosslinkable polymer co-precursors like polyethylene glycol diacrylate (PEGDA) and Pluronic diacrylate (Pluronic-DA)³⁷. Similarly, the Pang et al. Arg-AG PEA polymers could also not form hydrogels by themselves, even though the Arg-AG-PEAs had pendant photo-reactive double bonds in the AG unit (i.e., DL-2-Allylglycine) as Arg-PEUU does. Like Arg-UPEAs, the Pang et al. Arg-AG-PEA can form hybrid hydrogels with the assistance of another photo-reactive polymeric co-precursor⁴³.

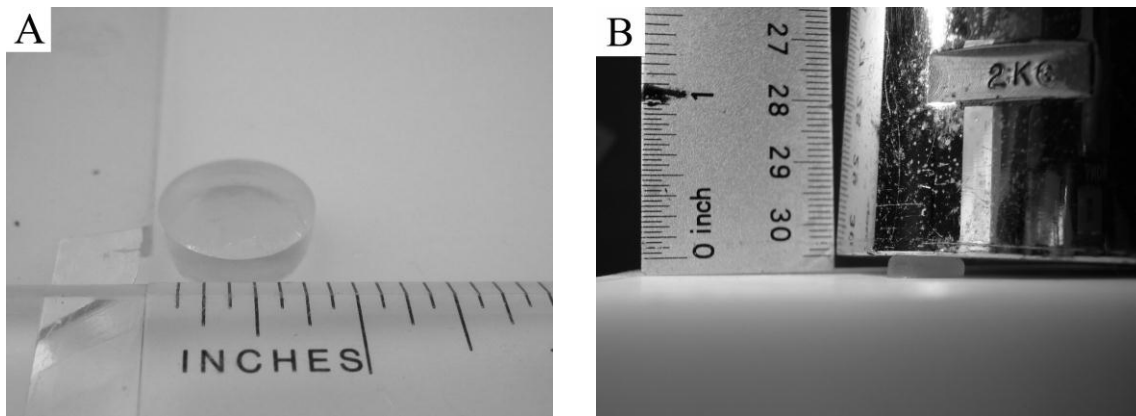


Figure 6.9 Images of photo-crosslinked Arg-PEUU gels; (A) photo-crosslinked 6-Arg-2 PEUU A/G-1/4 gel formed after removing DMF solvent; (B) photo-crosslinked 6-Arg-2 PEUU A/G-1/4 gel under 2 kg weight load

In the current Arg-PEUU study, the choice of GAE as one of the 3 monomers for synthesizing Arg-PEUU is due to its reactive vinyl group with a long spacer (4 methylene groups) which could minimize the adverse steric hindrance effect of the Arg moiety from photo-induced crosslinking reaction. However, if the Arg alkylene diester building block content versus GAE (A/G) was higher than 1/1, the resulting Arg-PEUU could not be photo-crosslinked as shown in Table 6.10. This suggests that even GAE has a long spacer for exposing its pendant reactive vinyl group to react, if the Arg contents in Arg-PEUU would be too high to block the pendant reactive group in GAE, Arg-PEUU could not form gels by itself

Table 6.10 Compression mechanical data of allyl PU gel and Arg-PEUU gels

Samples	Gel formation by photo-crosslinking	Compressive modulus (KPa)	Compressive strength at break (KPa)	Compressive strain at break (%)
Allyl PU	Y	39.8 ± 4.4	> 350	> 60
6-Arg-2 PEUU A/G-1/4	Y	120.7 ± 5.4	> 350	> 55
6-Arg-2 PEUU A/G-1/1	Y	76.2 ± 8.1	150 ± 34.8	17 ± 5.2
6-Arg-2 PEUU A/G-4/1	N	n/a	n/a	n/a
6-Arg-6 PEUU A/G-1/4	Y	105.7 ± 7.2	> 170	> 55
6-Arg-6 PEUU A/G-1/1	Y	54.2 ± 9.1	165 ± 29.2	19 ± 4.4
6-Arg-6 PEUU A/G-4/1	N	n/a	n/a	n/a

Y: able to be photocrosslinked; N: unable to be crosslinked

Figure 6.10 shows the SEM images of photo-crosslinked 6-Arg-2 PEUU A/G-1/4 gel. The SEM morphological data showed smooth surface without visible porous network structure as normally observed in all AA-PEA based hydrogel networks. Although Arg-PEUU polymer chain formed interconnected 3D network, the hydrophobicity of urethane linkage on the polymer backbone makes it difficult to expand in water.

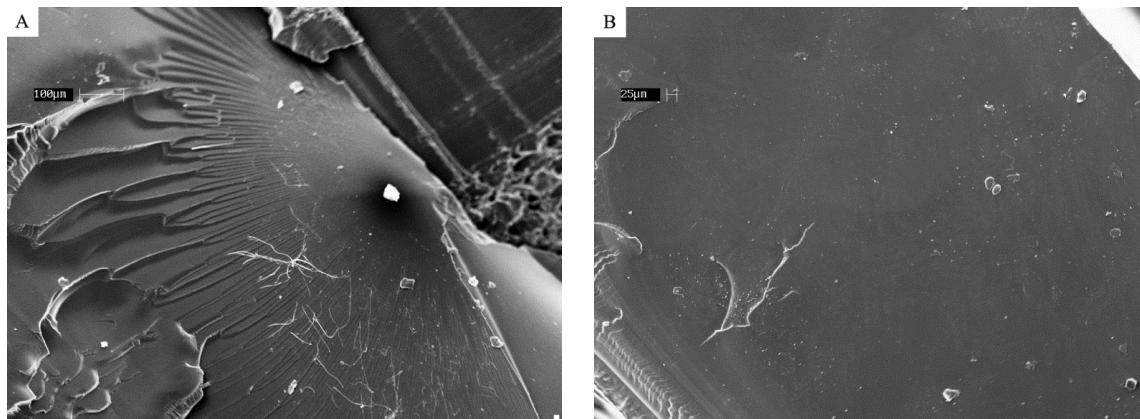


Figure 6.10 SEM images of cross section of photocrosslinked Arg-PEUU (6-Arg-2 PEUU A/G-1/4) gels; (A) 100X; (B) 200X

6.4.9 Compressive mechanical properties of photo-crosslinked Arg-PEUU gels

The effect of Arg-PEUU chemical structure on the mechanical response of the photo-crosslinked Arg-PEUU gels is shown in Table 6.11. Comparing with the published data (8~62 KPa) of linear polyurethane elastomers made from HDI and PEG ⁴⁶, allyl PU's gel initial modulus (39.8 ± 4.4 KPa) is a typical PU based elastomers. When the Arg alkylene diester building block was incorporated into the allyl PU, the compressive modulus of the resulting Arg-PEUU is higher than allyl PU and other linear polyurethane elastomers. For example, the compressive modulus of 6-Arg-2 PEUU A/G-1/4 gel is ~120.7 KPa which is 3 times higher than allyl PU gel. However, as the contents of the Arg alkylene diester building block increased further e.g., from A/G feed ratio of 1/4 to 1/1, the compressive modulus of the crosslinked copolymer gel decreased. This is because the GAE contents decreased, i.e., smaller available copolymer segments

responsible for photo-crosslinking and hence lower crosslinking density in 6-Arg-2 PEUU A/G-1/1 than 6-Arg-2 PEUU A/G-1/4. This lower crosslinking density was subsequently reflected in a reduction in compressive modulus. For example, 6-Arg-2 PEUU A/G-1/4 had 120.7 ± 5.4 KPa, whereas 6-Arg-2 PEUU A/G-1/1 had 76.2 ± 8.1 KPa, a 37% reduction. Similar findings were also reported by Pang et al. in their study of Phe-based PEA having pendant double bonds in the allylglycine (AG) unit ⁴³. The compressive modulus of Phe-AG hydrogel increased with increasing the AG contents that provided more crosslinking in the Phe-AG PEA.

The change in another Arg-PEUU material parameter, x , also affected the compressive modulus of the corresponding Arg-PEUU. For example, as the x increased from 2 to 6 in the Arg alkylene diester building block at the same molar feed ratio (A/G-1/4), the compressive modulus of the resulting Arg-PEUU was reduced from 120.7 ± 5.4 KPa of the 6-Arg-2 PEUU A/G-1/4 to 105.7 ± 7.2 KPa of the 6-Arg-6 PEUU A/G-1/4. This is mainly because a longer methylene chain length of the Arg alkylene diester building block attributed to the higher Arg-PEUU polymer chain flexibility in the crosslinked structure that led to lower compressive modulus. In addition, a higher x also reduced the density of the pendant double bonds which could lead to a lower modulus.

The Pang et al.'s study of crosslinked allylglycine based PEA copolymers demonstrated that an increase in crosslinking density can improve the compressive modulus of the crosslinked AA-PEA copolymer gel ⁴³. Moreover, the crosslinking density is tightly related to the robustness of the gel. In the current study of the Arg-PEUU, the higher GAE contents (e.g., 6-Arg-2 PEUU A/G-1/4) were able to withstand higher than 55% deformation and recover to the original dimension without breaking. Whereas 6-Arg-2 PEUU A/G-1/1 had a lower crosslinking density and lesser soft GAE contents, the largest compressive deformation was about 17%. The crosslinked structure and flexible polymer chain attribute elasticity to the network material.

A similar relationship between compressive breaking strength and Arg diester contents of the Arg-PEUU gels was also observed, i.e., increasing Arg diester contents reduced compressive breaking strength. The compressive breaking strength of the Arg-PEUU gels (150~350 KPa) was also much larger than some reported crosslinked linear PU copolymers which had compressive breaking strength no larger than 100 KPa ³⁶. These data suggested that the mechanical property of the Arg-PEUU gel could be tuned by simply changing the feed ratio of Arg-*x*-Cl to GAE monomers.

The mechanical strength of Arg-PEUU was significantly larger than other reported photocrosslinked Arg-based PEA hydrogels, such as Arg-UPEA/Pluronic-DA F-127 hydrogel ³⁷. The compressive modulus of Arg-UPEA/Pluronic-DA F-127 hybrid hydrogel was in the range of 0.77~4.85 KPa, depending on the ratio of Arg-UPEA to Pluronic-DA F-127 ratio ³⁷. The compressive modulus of a pure Pluronic-DA F-127 hydrogel was 12.27 KPa. Contrary to our current Arg-PEUU gels, the incorporation of Arg based PEA into F127 pluronic acid decreased the mechanical strength of hybrid hydrogels from the pure F127 hydrogel because the unsaturated double bonds in the Arg-based PEA was on the backbone of the polymer and the positive charge, space hindrance of guanidino groups decreased the crosslinking density of the hybrid hydrogel.

6.4.10 In vitro enzymatic biodegradation of Arg-PEUU and photo-crosslinked Arg-PEUU films

In the enzymatic biodegradation study of the crosslinked and uncrosslinked 6-Arg-2 PEUU, two concentrations of lipase (1 mg/mL and 3 mg/mL) were used. The weight loss of crosslinked and uncrosslinked 6-Arg-2 PEUU having different monomer feed ratios (6-Arg-2 PEUU A/G-1/4, 6-Arg-2 PEUU A/G-1/1) were recorded in the first 30 days in vitro degradation (Figure 6.11). Generally, 6-Arg-2 PEUU were degraded faster in the lipase than in the PBS at 37 °C. The biodegradation rate of the uncrosslinked 6-Arg-2 PEUU increased with an increase in lipase concentration as shown in Figure 6.11. For example, in the day 5, 6-Arg-2 PEUU A/G-1/4 had 10% weight loss in a lipase

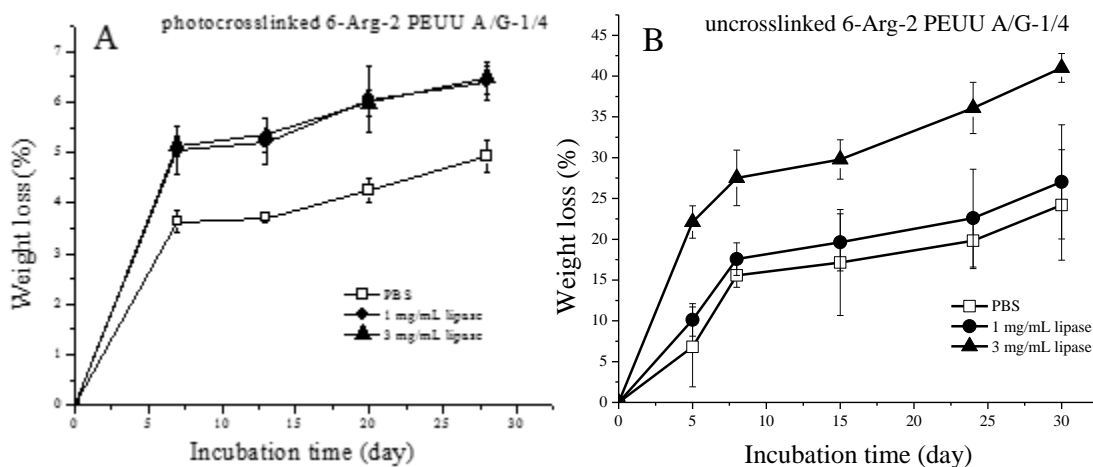
solution (1 mg/mL), while its weight loss increased to 22% in a 3 mg/mL lipase solution (Figure 6.11). After 10-day incubation, the weight loss of 6-Arg-2 PEUU A/G-1/4 ranged from 19.6% (in 1 mg/mL lipase solution) to 29.8% (in 3 mg/mL lipase solution) as shown in Figure 6.11 B.

The crosslinked 6-Arg-2 PEUU biodegradation showed a much slower rate than the uncrosslinked ones as shown by comparing the degradation profiles of Figure 6.11 A vs. Figure 6.11 B, and Figure 6.11 C vs. Figure 6.11 D. For example, crosslinked 6-Arg-2 PEUU A/G-1/4 film in 1mg/mL lipase lost 4.05~5.14 % of its original weight after 15 days degradation (Figure 6.11 A), while uncrosslinked 6-Arg-2 PEUU A/G-1/4 films had ~19.6 % mass losses in the same medium (Figure 6.11 B). It is widely recognized that an enzyme must adsorb onto the polymer surface in its native active form in order for it to biodegrade certain bonds at the polymer surface. The crosslinked 6-Arg-2 PEUU forms an interconnected very tight molecular network structure which could make lipase difficult to diffuse and adapt to the molecular architecture of the substrate.

Irrespective of crosslinked or uncrosslinked, Arg-PEUU having a higher Arg alkylene diester contents biodegraded more in an enzyme medium than those having a lower Arg alkylene diester content. For example, the uncrosslinked 6-Arg-2 PEUU A/G-1/1 which had a higher Arg alkylene diester contents showed a faster enzymatic biodegradation than the uncrosslinked 6-Arg-2 PEUU A/G-1/4 which had a lower Arg alkylene diester contents (Figure 6.11 B vs. Figure 6.11 D). According to the reported poly (ester-urea) enzymatic biodegradation model, the biodegradation sites most possibly happened at the ester portion of the polymer rather than the NH-C=O portion of the urethane linkage¹³. Hence, an increase in ester contents that reside in the Arg alkylene diester block of the uncrosslinked Arg-PEUU would create more target sites for lipase to cleave. And in Tshitlanadze et al. studies about enzymatic biodegradation of AA-PEA polymers, they reported that lipase could adsorb onto the AA-PEA polymer film surface and cleaved the ester bond of the copolymer⁴⁷⁻⁴⁹. The 6-Arg-2 PEUU A/G-1/1 should be

able to absorb more enzymes on its film surface due to the better hydrophilicity and positive charge of Arg.

Similarly, increasing Arg alkylene diester contents also accelerated the degradation rate of photo-crosslinked 6-Arg-2 PEUU film. The crosslinked 6-Arg-2 PEUU A/G-1/1 film (Figure 6.11 C) showed a faster enzymatic biodegradation rate than the crosslinked 6-Arg-2 PEUU A/G-1/4 (Figure 6.11 A) during the first 15 days biodegradation in the presence of the identical lipase concentration (3 mg/mL), i.e., 13% weight loss for the A/G-1/1 vs 5.1 % for the A/G-1/4. In addition to the Arg diester contents which provide the degradable ester linkages, the level of crosslinking density which is controlled by the GAE contents in the PU block is another important factor. Arg-PEUU having low GAE contents (relatively high Arg diester contents) led to a lower crosslinking density, and hence faster enzymatic biodegradation rate.



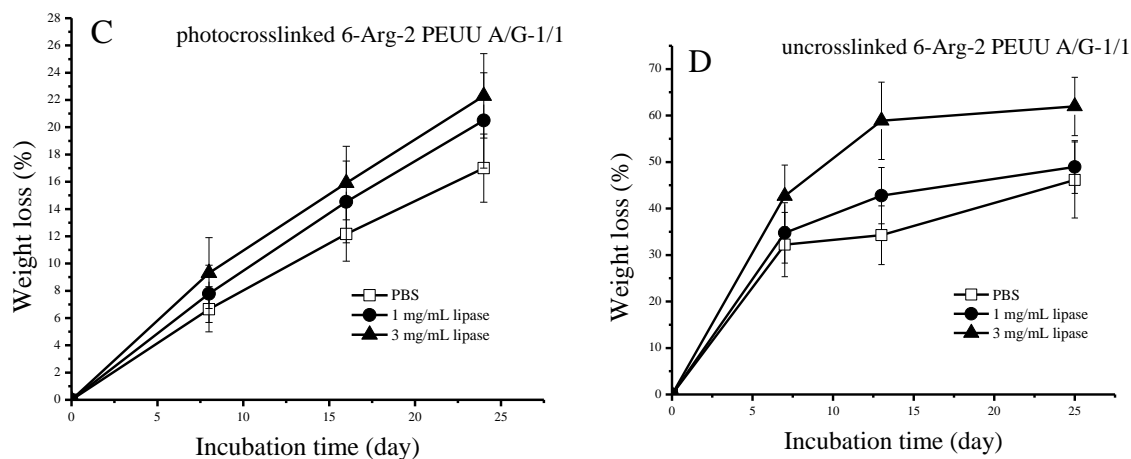


Figure 6.11 Effect of lipase concentration on the biodegradation rate of the 6-Arg-2 PEUU film having different Arg alkylene diester to glycerol α -monoallyl ether feed ratios at pH 7.4 and 37 °C. A. photo-crosslinked 6-Arg-2 PEUU A/G-1/4 film; B. uncrosslinked 6-Arg-2 PEUU A/G-1/4 film; C. photo-crosslinked 6-Arg-2 PEUU A/G-1/1 film; D. uncrosslinked 6-Arg-2 PEUU A/G-1/1 film.

6.5 Conclusion and recommendation for future work

A new family of cationic biodegradable and functional Arg based poly(ester urea urethane)s (Arg-PEUU) having functional pendant carbon-carbon double bonds were synthesized by a 2-step solution co-polycondensation of Arg- x -Cl, GAE and HDI monomers. The FTIR, elemental analysis and GPC data confirmed the chemical structures and molecular weight of the new functional Arg-PEUU. The M_n of Arg-PEUU ranged from 23.93 to 29.35 Kg/mol with a relatively narrow MWD (1.224 ~1.587) for polymers synthesized by polycondensation method.

The contents of the Arg and functional pendant double bond could be adjusted by tuning the feed ratio of the 3 monomers and hence influence the thermal properties (T_g ranging from -20.80°C to 4.23 °C) and hydrophilicity of the materials (water contact angle ranging from $26.7 \pm 4.3^\circ$ to $61.3 \pm 5.2^\circ$). As the contents of the Arg alkylene diester building block increased, the T_g of the corresponding Arg-PEUU increased and the water contact angle decreased. Another important materials parameter is the methylene group

length (x) in the diol segment of the Arg alkylene diester building block. Increasing x , led to a lower T_g and higher water contact angle (more hydrophobic).

MTT assays for porcine aortic valve smooth muscle cell were used to evaluate the cytotoxicity of 6-Arg-2 PEUU. The feed ratio of monomers as well as the concentration of the polymers influenced the biocompatibility, and Arg-PEUU having higher Arg diester contents showed far better cytotoxicity than those having lower Arg diester contents. All Arg-PEUU showed the same level of cell viability as the blank medium control when the polymer concentrations were at and below 0.1- 0.2 mg/mL. The effects of the Arg-PEUU chemical structures on their biodegradation property (in terms of weight loss) were investigated in a lipase media at different concentrations for 30 days. The *in vitro* biodegradation data suggested that the crosslinking density as well as the Arg alkylene diester building block contents in the functional Arg-PEUU had a profound impact on their rate and extent of biodegradation. The utility of the incorporated pendant carbon-carbon double bond in the Arg-PEUU was demonstrated by photo-crosslinking to form elastic gels with a wide range of mechanical property, e.g., compressive modulus ranged from 54.2 ± 9.1 to 120.7 ± 5.4 KPa by adjusting the monomer feed ratio and x parameter.

In the further study, the 3T3 cell attachment and morphology on the Arg-PEUU materials needs to be characterized for the further study by live/dead assay and F-actin staining. The TNF- α production of RAW cells culture on the Arg-PEUU coating or film could be used test the inflammatory response to the Arg-PEUU. The NO production and Arginase activity analysis for macrophages (RAW) treated by Arg-PEUU suspension could be used to exam the effect of Arg-PEUU suspension on the Arginine metabolism.

Acknowledgement

The authors would like to thank the support of Vincent V.C. Woo Fellowship to this study. The author also wish to thank to Cornell Nanobiotechnology Center (NBTC) who

provided cell culture facility, Lin Chen who helped in the GPC test and Dr. Duan Bin who provided the PAVSMC cells in our study.

References:

1 Richard J. Zdrahala, Ivanka J. Zdrahala, Promises, present realities, and a vibrant future, *J Biomater Appl*, 1999, 14: 67-90

2 Wenshou Wang, Yanlin Guo, Joshua U. Otaigbe, Synthesis and characterization of novel biodegradable and biocompatible poly (ester-urethane) thin films prepared by homogeneous solution polymerization, *Polymer*, 2008, 49, 4393-4398

3 FDA (Food and Drugs Administration). Resinous and polymeric coatings. In: Title 21, Chapter I, Part 175, Subpart C, Sec. 175,300. USA; 2002.

4 Elizabeth M. Christenson, Mahrokh Dadsetan, Michael Wiggins, James M. Anderson, Anne Hiltner, Poly-(carbonate urethane) and poly(ether urethane) biodegradation: in vivo studies, *J Biomed Mater Res* 2004;69A:407-416

5 Sutherland K, Mahoney II JR, Coury AJ, Eaton JW. Degradation of biomaterials by phagocyte-derived oxidants, *J Clin Invest*, 1993; 92: 2360-2367

6 Hu W-J, Eaton JW, Tang L. Molecular basis of biomaterial-mediated foreign body reactions. *Blood* 2001;98:1231-1238

7 Marchant R, Hiltner A, HamLin C, Rabinovitch A, Slocobodkin R, Anderson JM. In vivo biocompatibility studies. I. The cage implant system and a biodegradable hydrogel. *J Biomed Mater Res* 1983;17:301-325.

8 Ratner BD, Gladhill KW, Horbett TA. Analysis of in vitro enzymatic and oxidative degradation of polyurethanes. *J Biomed Mater Res* 1998; 22: 509-527

9 Christenson EM, Patel S, Anderson JM, Hiltner A. Enzymatic degradation of poly(ether urethane) and poly(carbonate urethane) by cholesterol esterase. *Biomaterials* 2006;27:3920-3926.

- 10 Santerre JP, Labow RS, Duguay DG, Erfle DJ, Adams GA. Biodegradation evaluation of polyether and polyester-urethanes with oxidative and hydrolytic enzymes. *J Biomed Mater Res* 1994;28:1187-1199
- 11 J.P. Santerre, K. Woodhouse, G. Laroche, R.S. Labow, Understanding the biodegradation of polyurethanes: From classical implants to tissue engineering materials, *Biomaterials*, 2005, 26, 7457-7470
- 12 Cristina Ferris, M. Violante de Paz, Francisca Zamora, Juan A. Galbis, Dithiothreitol-based polyurethanes. Synthesis and degradation studies, 2010, 95, 1480-1487
- 13 Huang SJ, Bansleben DA, Knox JR. Biodegradable polymers: chymotrypsin degradation of low molecular weight poly(ester-urea) containing phenylalanine. *J Appl Polym Sci*, 1979, 23, 429-437.
- 14 Skarja GA, Woodhouse KA. In vitro degradation and erosion of degradable, segmented polyurethanes containing an amino acid-based chain extender. *J Biomater Sci Polym Ed* 2001;12(8):851-873.
- 15 Kao WJ, Hiltner A, Anderson JM, Lodoen GA. Theoretical analysis of in vivo macrophage adhesion and foreign body giant cell formation on strained poly(etherurethane urea) elastomers. *J Biomed Mater Res*, 1994, 28, 515–522.
- 16 Santerre JP, Labow RS. The effect of hard segment size in determining the hydrolytic stability of polyether-urea-urethanes exposed to cholesterol esterase. *J Biomed Mater Res* 1997;33: 223–32.
- 17 Labow RS, Tang Y, McCloskey CB, Santerre JP. The effect of oxidation on the enzyme-catalyzed hydrolytic biodegradation of poly (urethane)s. *J Biomater Sci Polym Edn* 2002;13:651-665.
- 18 Tang YW, Labow RS, Revenko J, Santerre JP. Influence of surface morphology and chemistry on the enzyme catalyzed biodegradation of polycarbonateurethanes. *J Biomater Sci Polym Edn* 2002;13:463-483.
- 19 Christenson EM, Patel S, Anderson JM, Hiltner A. Enzymatic degradation of

- poly(ether urethane) and poly(carbonate urethane) by cholesterol esterase. *Biomaterials* 2006;27:3920-3926.
- 20 Soeda Y, Toshima K, Matsumura S. Synthesis and chemical recycling of novel poly(ester-urethane)s using an enzyme. *Macromol Biosci*, 2005, 5, 277-288.
- 21 Matsumura S, Soeda Y, Toshima K. Perspectives for synthesis and production of polyurethanes and related polymers by enzymes directed toward green and sustainable chemistry. *Appl Microbiol Biotechnol* 2006, 70, 12-20.
- 22 Nathalie Lucas et al, Polymer biodegradation: Mechanisms and estimation techniques, *Chemosphere*, 2008, 73, 429-442
- 23 Carmelo Nieves Jr, Bobbi Langkamp-Henken, Arginine and immunity: a unique perspective, *Biomed Pharmacother*, 2002, 56, 471-482
- 24 I.B.J.G. Debats, T.G.A.M Wolfs, T.Gotoh, et al., Role of arginine in superficial wound healing in man, *Nitric Oxide*, 2009, 21, 175-183
- 25 Tung C-H, Weissleder R. Arginine containing peptides as delivery vectors. *Adv Drug Deliv Rev*, 2003, 55, 281-294.
- 26 Huayu Tian, Zhaohui Tang, Xiuli Zhuang, Xuesi Chen, Xiabin Jing, Biodegradable synthetic polymers: preparation, functionalization and biomedical application, *Progress in Polymer Science*, 2011
- 27 Murray H. Kown, Maarten A. Lijkwan, Christina L. Jahncke, Seiichiro Murata, MD, Jonathan B. Rothbard, Robert C. Robbins, L-arginine polymers enhance coronary flow and reduce oxidative stress following cardiac transplantation in rats, *J Thorac Cardiovasc Surg* 2003;126:1065-1070
- 28 Jagadish Beloor, et al, Arginine-engrafted biodegradable polymer for the systemic delivery of therapeutic siRNA, *Biomaterials*, 2012, 33, 1640-1650
- 29 Yamanouchi D, Wu J, Lazar AN, Craig Kent K, Chu CC, Liu B. Biodegradable arginine-based poly(ester-amide)s as non-viral gene delivery reagents. *Biomaterials* 2008;29:3269–3277.

- 30 Borkerhagen M, Stoll RC, Neuenschwander P, Suter UW. Aebischer. In vivo performance of a new biodegradable polyester urethane system used as a nerve guidance channel, *Biomaterials* 1998, 19, 2155-2165
- 31 Saad B, Hirt TD, Welti M, Uhlschmid GK, Neuenschwander P, Suter UW. Development of degradable polyesterurethanes for medical applications. *J Biomed Mater Res* 1997, 36, 65–74.
- 32 Zhang JY, Beckman EJ, Hu J, Piesco NP, Agarwal S. A new peptide-based urethane polymer:synthesis degradation and potential to support cell growth in vitro, *Biomaterials* 2000; 21, 1247-1258.
- 33 J.P. Santerre et al, Understanding the biodegradation of polyurethanes: From classical implants to tissue engineering materials, *Biomaterials*, 2005, 26, 7457-7470
- 34 Jianjun Guan, Michael S. Sacks, Eric Beckman, William R. Wagner, Synthesis, characterization, and cytocompatibility of elastomeric, biodegradable poly(ester-urethane) ureas based on poly(caprolactone) and putrescine, *Journal of biomedical materials research*, 2002, 61, 493-503
- 35 Skarja GA, Woodhouse KA. Structure-property relationships of degradable polyurethane elastomers containing an amino acid based chain extender. *J Appl Polym Sci* 2000;75:1522–34.
- 36 Ji Hye Hong, Hyun Jeong Jeon, Jae Heung Yoo, Woong-Ryeol Yu, Ji Ho Youk, Synthesis and characterization of biodegradable poly(3-caprolactone-co-b-butyrolactone)-based polyurethane, *Polymer Degradation and Stability*, 2007, 92, 1186-1192
- 37 Jun Wu, Dequn Wu, Martha A. Mutschler, C. C. Chu, Cationic Hybrid Hydrogels from Amino Acid-Based Poly (ester amide):Fabrication, Characterization, and Biological Property, *Advanced functional materials*, 2012, accepted manuscript, DOI: 10.1002/adfm.201103147

- 38 Xuan Pang et al., Synthesis and characterization of functionalized water soluble cationic poly(ester amide)s, *Journal of Polymer Science Part A: Polymer Chemistry*, 2010, 28, 3758-3766
- 39 Hua Song, C. C. Chu. Synthesis and Characterization of A New Family of Cationic Poly(ester amide)s and Their Biological Properties. *J. Appl. Polym. Sci.* 2012; 124 (5): 3840–3853.
- 40 Xuan Pang, Chih-Chang Chu, Synthesis, characterization and biodegradation of functionalized amino acid-based poly(ester amide)s, *Biomaterials*, 31, 14, 3745-3754
- 41 L. Rueda-Larraz, Synthesis and microstructure–mechanical property relationships of segmented polyurethanes based on a PCL–PTHF–PCL block copolymer as soft segment, *European Polymer Journal*, 2009, 45, 7, 2096-2109
- 42 P. Ferreira, António F. M. Silva, M. I. Pinto and M. H. Gil, Development of a biodegradable bioadhesive containing urethane groups, *Journal of Materials Science :Materials in medicine*, 2008, 19, 111-120
- 43 Xuan Pang, Chih-Chang Chu, Synthesis, characterization and biodegradation of poly(ester amide)s based hydrogels, *Polymer*, 51, 18, 4200-4210
- 44 Kai Guo, Chih-Chang Chu, Synthesis and Characterization of Novel Biodegradable Unsaturated Poly(ester amide)/Poly(ethylene glycol) Diacrylate Hydrogels, *Journal of polymer science Part A: Polymer Chemistry*, 2005, 43, 3932-3944
- 45 Mingxiao Deng, Jun Wu, Cynthia A. Reinhart-King, and C. C. Chu. Biodegradable Functional Poly(ester amide)s with Pendant Hydroxyl Functional Groups: Synthesis, Characterization, Fabrication and *In Vitro* Cellular Response. *Acta. Biomater.* 2011; 7:1504–1515.
- 46 S.H. Baek, B.K. Kim, Synthesis of polyacrylamide/polyurethane hydrogels by latex IPN and AB crosslinked polymers, *Colloids and Surfaces A: Physicochem. Eng. Aspects*, 2003, 220, 191-198

47 Liu Jingjiang, Liu Wenzhong, Zhou Huarong, Hou Chunrong, Ni Shaoru, Morphology and dynamic mechanical properties of AB crosslinked polymers based on polyurethanes, *Polymer*, 1991, 32, 9, 1361-1368

48 Zhang JY, Beckman EJ, Hu J, Yang GG, Agarwal S, Hollinger JO. Synthesis, biodegradability, and biocompatibility of lysine diisocyanate-glucose polymers. *Tissue Eng* 2002;8:771-785.

49 Fromstein JD, Woodhouse KA. Elastomeric biodegradable polyurethane blends for soft tissue application. *J Biomater Sci Polym Ed* 2002;13:391-406.

CHAPTER SEVEN:

A NEW FAMILY OF FUNCTIONAL BIODEGRADABLE ARGININE-BASED POLYETHER ESTER UREA URETHANES: SYNTHESIS, CHARACTERIZATION, BIODEGRADATION AND GEL OR MICROSPHERE FABRICATION

7.1 Abstract

A new family of biodegradable functional cationic L-Arginine (L-Arg) poly (ether ester urea urethane) (Arg-PEEUU) were designed and synthesized by the solution polycondensation of three monomers: L-Arg hydrochloride oligoethylene glycol diester (Arg-*x*EG-Cl) monomers, hexamethylene diisocyanate (HDI) and glycerol α -monoallyl ether (GAE). These new cationic amino acid containing PEEUU has functional pendant unsaturated double bonds located in the GAE moiety, and the double bond contents could be adjusted by tuning the feed ratio of the GAE to other 2 monomers. Chemical structures of this new functional cationic Arg-PEEUU family were characterized by ^1H nuclear magnetic resonance (H-NMR), fourier transform infrared spectroscopy (FTIR), and carbon/nitrogen elemental analysis. The molecular weight of Arg-PEEUU ranged from 21.800 to 60.225 Kg/mol with molecular weight distribution 1.298~1.460. The glass transition temperature (T_g) of Arg-PEEUU ranged from $-23.38\text{ }^\circ\text{C}$ to $-2.35\text{ }^\circ\text{C}$, depending on the feed ratio of the 3 monomers. The hydrophilicity of Arg-PEEUU was characterized by water contact angle ranging from $24.3 \pm 3.3^\circ$ to $56.7 \pm 3.9^\circ$. Arg-PEEUU is not water soluble at room temperature, at $40\text{ }^\circ\text{C}$ and $70\text{ }^\circ\text{C}$, Arg-PEEUU with A/G-1/1 and A/G-4/1 showed increased water solubility up to 55 mg/mL, depending on the Arg oligoethylene glycol (OEG) building block content. Cytotoxicity from the MTT assays of porcine aortic valve smooth muscle cells showed that 6-Arg-2EG PEEUU A/G-4/1 and 6-Arg-4EG PEEUU A/G-4/1 had no cytotoxicity at low concentrations (0.1 – 0.5 mg/mL). By utilizing the amphiphilicity of Arg-PEEUU, microsphere with average hydrodynamic diameter from $123.2 \pm 3.7\text{ nm}$ to $217.8 \pm 12.2\text{ nm}$ with strong positive ζ -potential ranging from 48.1 ± 0.7 to $52.3 \pm 1.7\text{ mV}$ was fabricated in water. Due to the presence of pendant unsaturated double bond, Arg-PEEUUs having adequate GAE contents were able to be photo-crosslinked into elastic gels in DMF solvent. The compressive modulus of Arg-PEEUU gels ranged from 80.4 ± 10.28 to $184.5 \pm 9.0\text{ KPa}$ by adjusting the 3 monomers' feed ratio and OEG group length in the Arg-*x*EG-Cl

monomer. The biodegradation data (weight loss) of the Arg-PEEUU in lipase media of different concentrations suggested that the crosslinking density as well as the Arg OEG diester building block contents in the functional Arg-PEEUU had a profound impact on the degradation rate and extent of biodegradation.

7.2 Introduction:

The development of biodegradable and biocompatible synthetic polymers suitable for a variety of biomedical applications, including tissue engineering, drug-delivery vehicles or temporary barrier to tissue adhesion is of great interest in the last two decades^{1,2}. Aliphatic polyester derivatives are one type widely accepted absorbable polymers, but they usually are lack of functionality, tunable physicochemical, biological and mechanical properties¹. In the effort to design new biodegradable polymers, amino-acid based biodegradable polymers attracted many research interests, because of the abundant availability of amino acid from natural resources, potential biodegradability under certain enzymatic catalyzed conditions, and the biological or physiological functions of amino acid²⁻¹⁶, L-phenylalanine (Phe)²⁻⁷, L-leucine (Leu), L-valine (Val), DL-methionine⁵, L-Arginine (Arg)⁸⁻¹⁴ and Lysine (Lys)^{15,16} were successfully used to develop amino acid based polymers.

Among all natural amino acids, Arg is of particular interest due to its strong cationic property and fundamental roles in nitrogen metabolism¹⁷⁻¹⁹. L-Arg is the sole substrate for nitric oxide (NO) synthesis in biological systems. NO is synthesized from Arg by the activity of nitric oxide synthase (NOS)¹⁹. Moreover, through the action of arginase, Arg is converted to urea and ornithine, generates polyamines²⁰. Ornithine is a precursor for proline which serves as the substrate for collagen synthesis, whereas polyamines are involved in cell proliferation²¹. The metabolism of Arg is tightly related to many diseases including: wound healing, diabetic ulcer, even tumor^{20,22-26}. Very recently, Wu et al. and Song et al. have reported the incorporation of Arg into the design and synthesis of synthetic biodegradable amino acid-based poly(ester amide)s (AA-PEA)

⁸⁻¹³. Wu et al. reported that those Arg-based PEAs have some very unique biological property, such as improving cell attachment and proliferation and capable of capture DNA as non-viral gene transfection vectors ^{9,10}. Among the Arg-PEAs reported, one particular series of novel cationic Arg based polyester amide (Arg-UPEA) has photocrosslinkable unsaturated double bonds on the polymer backbone ^{8,10}. Arg-UPEA is able to be used as a co-precursor to fabricate photo-crosslinked hybrid hydrogels with pluronic acid (F127) with good biocompatibility and biodegradability for biomedical applications.

Biodegradable elastomers are expected to be suited for the applications requiring the use of a flexible, elastic material such as soft tissue engineering. Segmented polyurethanes (PU) are considered one of the most promising materials in biomedical applications due to their structure/property diversity. Flexibility and diverse mechanical properties of polyurethane materials has been utilized to design degradable polymer for medical applications, i.e., neural conduits, bone replacement ^{27,28}. Degradable polyurethanes were produced through the introduction of hydrolysable linkages into the backbone in a variety of ways. PU which contains phenylalanine (Phe) diester moiety was designed by Skarja et al ^{2,4}. Not like the hydrolysis mechanism of most common degradable PU, this Phe-containing PU polymer shows enzyme-mediated biodegradation. Another lysine moiety contained polyester urea urethane (PEUU) synthesized from polycaprolactone and 1, 4-diisocyanatobutane (BDI) was reported by Guan et al ¹⁵. Lysine ethyl ester was used as chain extender (two amine groups of Lys were reacted to form urea linkage with BDI, the carboxyl groups were protected with ester linkage).

Poly(ethylene glycol) (PEG) shows biocompatibility, less toxicity and hydrophilicity and has been studied for a number of years in applications such as coating to improve the biocompatibility of implanted sensors and for use in modifying protein-based drugs to increase efficacy in vivo ^{29,30}. In this study, we reported the synthesis, characterization and in vitro biological evaluation of a new family of block copolymers

of Arg based poly(ether ester urea urethane)s (Arg-PEEUU) on the polymer backbone using Arg diester, glycerol α -monoallyl ether (GAE) and HDI. By varying the molecular weight of OEG in Arg diester, feed ratio of monomers, it was possible to alter the subsequent Arg-PEEUU physicochemical properties.

7.3 Materials and methods

7.3.1 Materials

L-Arginine hydrochloride (L-Arg-Cl) (Alfa Aesar, Ward Hill, MA), diethylene glycol (Alfa Aesar, Ward Hill, MA), tetraethylene glycol (Alfa Aesar, Ward Hill, MA), *p*-toluene sulfonic acid monohydrate (TsOH H₂O) (JT Baker, Philipsburg, NJ), glycerol α -monoallyl ether (TCI, Portland, OR), hexamethylene diisocyanate (HDI) (Acros organics, Geel, Belgium), triethylamine (99%, EMD Chemical, Darmstadt, Germany) were used without further purification. 2, 6 di-*tert*-butyl-4-methyl phenol was purchased from Alfa Aesar (Ward Hill, MA) and stannous 2-ethyl-hexanoate was purchased from Sigma (St. Louis, MO). Solvents like toluene (VWR Science, West Chester, PA), dimethyl sulfoxide (DMSO) (Mallinckrodt incorporated, St. Louis, MO), isopropyl alcohol (ACS, 99.5%, Macron Chemicals, Philipsburg, NJ) and ethyl acetate (BDH, London, UK) were used without further purification. Irgacure 2959 was donated by Ciba Specialty Chemicals Corp. Lipase was purchased from VWR Science, (West Chester, PA).

7.3.2 Synthesis of di-hydrochloride acid salt of bis (L-Arg) oligoethylene glycol diester monomers (Arg-*x*EG-Cl)

The synthesis of di-hydrochloride acid salt of bis (L-Arg) diester monomers (Arg-*x*EG-Cl, *x* is the number of ethylene glycol unit of the diol) of Arg-PEEUU is similar to those used for the Phe-PEEA, Arg-PEA and Arg-PEUU synthesis^{7,8,31}. The reactants of Arg-*x*EG-Cl are L-Arg hydrochloride and diethylene glycol (or tetraethylene glycol). Under the catalysis of TsOH, a Fischer esterification reaction between the carboxyl function of 2 mol L-Arg hydrochloride and 1 mol of diethylene glycol (or tetraethylene

glycol) was carried out in refluxing toluene. The method is reported in detail elsewhere^{8,31}. The tosylate salt of the Arg-*x*EG-Cl was converted to a diamine, diester form by reaction with calcium hydroxide. The extra calcium hydroxide was converted to water insoluble calcium carbonate and filtered out. This reaction scheme is shown in Figure 7.1.

Two types of Arg-*x*EG-Cl were synthesized by changing the types of OEG reactant, where *x* is the number of ethylene glycol unit of diol: di-hydrochloride acid salt of bis (L-Arg) diethylene glycol diester (Arg-2EG-Cl with *x* = 2); di-hydrochloride acid salt of bis (L-Arg) tetraethylene glycol diester (Arg-4EG-Cl with *x* = 4).

7.3.3 Synthesis of Arg based poly(ether ester urea urethane)s (Arg-PEEU)

The Arg-PEEU was synthesized using a two-step solution polymerization. In the step 1, HDI and GAE formed prepolymer through the reaction between isocyanate group in HDI and hydroxyl group in GAE. In the step 2, the Arg-*x*EG-Cl monomer with two free amine end groups (i.e. Arg-2EG-Cl, Arg-4EG-Cl) extended the prepolymer chain synthesized in step 1 above for improving the molecular weight of the resulting polymers. The method is reported in detail in prior study of Arg-PEEU³¹.

The Arg-PEEU polymers have two types of repeating building blocks: the *m* block contains urea linkage and Arg OEG diester, and the *n* block contains urethane linkage and pendant double bond from GAE. The ratio of these two building blocks (*m/n*) is equal to the feed ratio of Arg-*x*EG-Cl to GAE. In the polymerization reaction, if the Arg-*x*EG-Cl monomer to GAE molar ratio is 4 to 1, the *m/n* is also 4/1. The generic synthesis route of the Arg-PEEU is shown in Figure 7.2. Table 7.1. summarizes the types of Arg-PEEU synthesized by changing the molar feed ratios of HDI, Arg-*x*EG-Cl and GAE in the reaction. Allyl polyurethane (PU) Glycerol which was used as a comparison for Arg-PEEU was synthesized from GAE and HDI with 1/1 molar feed ratio³¹.

7.3.4 Characterization of Arg-*x*EG-Cl monomer and Arg-PEEU

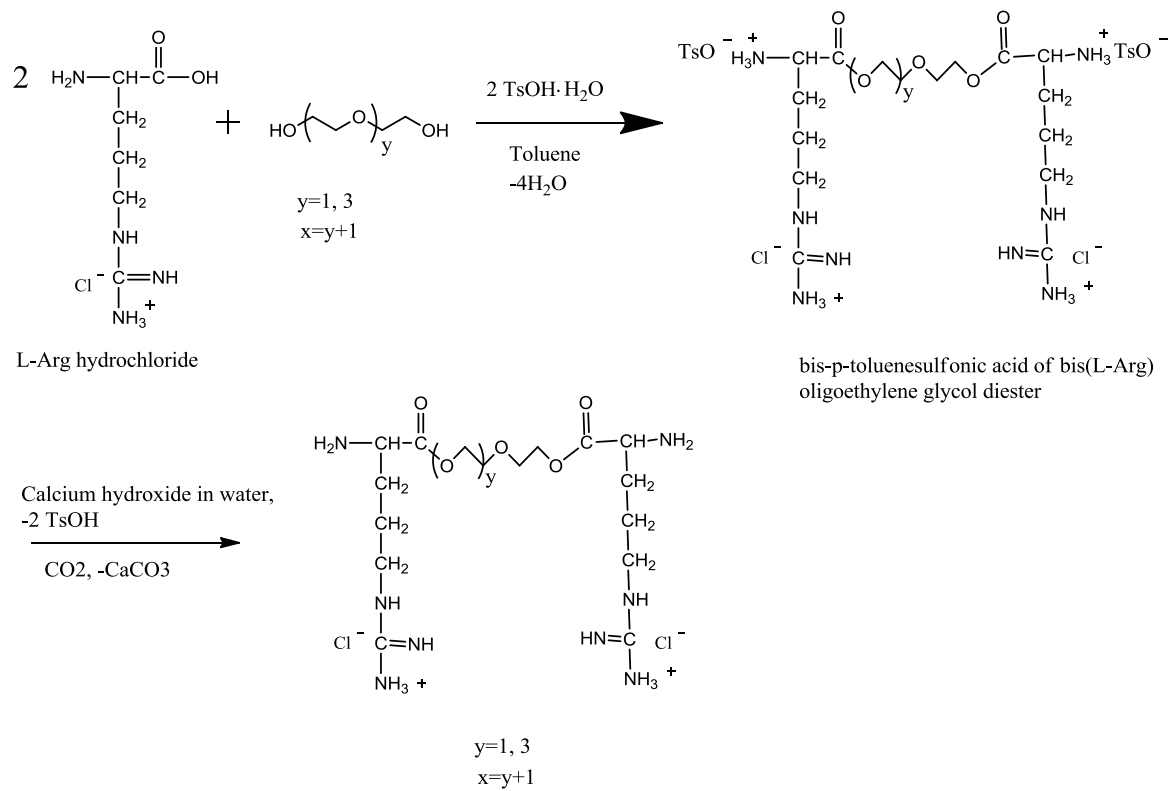


Figure 7.1 Synthesis of di-hydrochloride acid salt of bis(L-Arg) oligoethylene glycol diesters (Arg- x EG-Cl). x is the number of ethylene glycol unit of diol; $x=y+1$

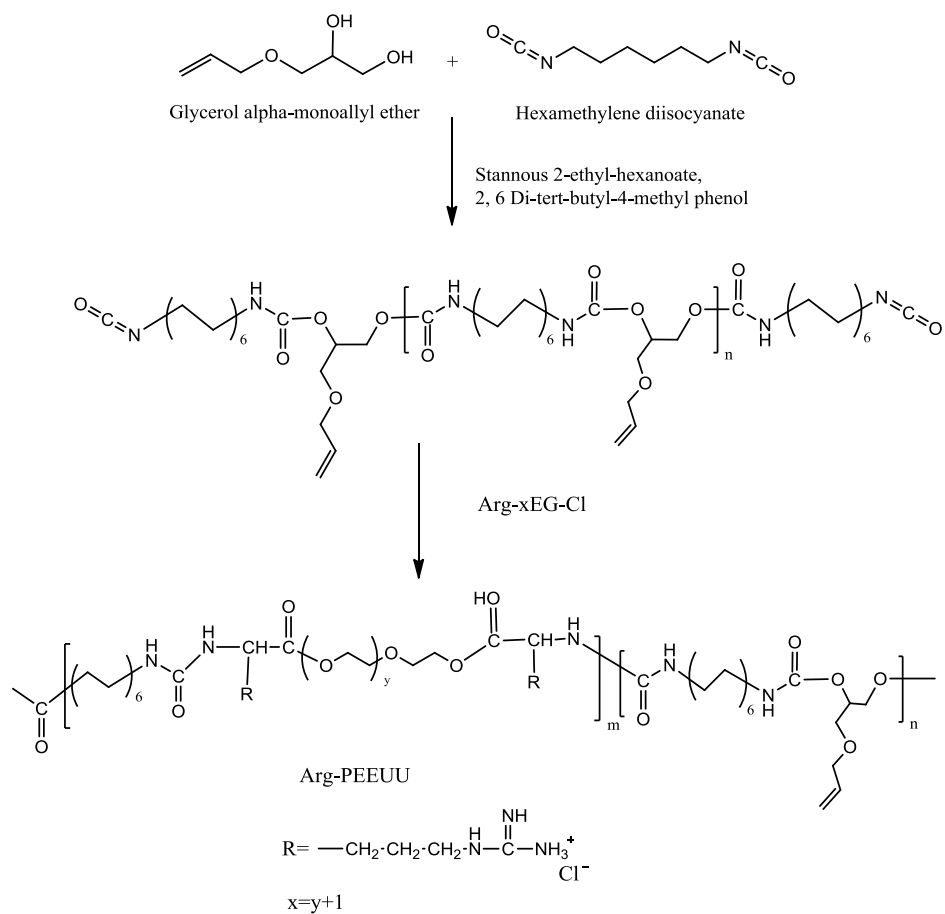


Figure 7.2. Synthetic pathway for the preparation of Arg-PEEUU having pendant carbon-carbon double bond

Table 7.1 Arg-PEEUU series synthesized from different di-hydrochloride acid salt of bis (L-Arg) oligoethylene glycol diester (Arg-*x*EG-Cl) monomer and the feed ratios to hexamethylene diisocyanate and glycerol α -monoallyl ether monomers*.

Reactants	Molar feed ratio (HDI: Arg- <i>x</i> EG-Cl : glycerol α -monoallyl ether)	Molar ratio of Arg alkylene diester building block to glycerol α -monoallyl ether (m/n)	Polymer Labels
HDI : Arg-2EG-Cl : Glycerol α -monoallyl ether	5:4:1	4:1	6-Arg-2EG PEEUU A/G-4/1
HDI: Arg-2EG-Cl : Glycerol α -monoallyl ether	2:1:1	1:1	6-Arg-2EG PEEUU A/G-1/1
HDI: Arg-2EG-Cl : Glycerol α -monoallyl ether	5:1:4	1:4	6-Arg-2EG PEEUU A/G-1/4
HDI, : Arg-4EG-Cl: Glycerol α -monoallyl ether	5:4:1	4:1	6-Arg-4EG PEEUU A/G-4/1
HDI, Arg-4EG-Cl, Glycerol α -monoallyl ether	2:1:1	1:1	6-Arg-4EG PEEUU A/G-1/1
HDI, Arg-4EG-Cl, Glycerol α -monoallyl ether	5:1:4	1:4	6-Arg-4EG PEEUU A/G-1/4
HDI, Glycerol α -monoallyl ether	1:0:1	N/A	Allyl PU

The new Arg-*x*EG-Cl monomers were analyzed by proton nuclear magnetic resonance (¹H NMR). ¹H NMR spectra were recorded on a Varian (Palo Alto, CA) Mercury spectrophotometer at 400MHz. Deuterated dimethyl sulfoxide (DMSO-*d*₆, Cambridge Isotope Laboratories) was used as the solvent. The Arg-*x*EG-Cl monomers and Arg-PEEUU sample concentration in deuterated DMSO were about 1 % (w/v). All of the chemical shifts were reported in parts per million (ppm).

Fourier transform infrared (FTIR) spectra of Arg-PEEUU were recorded on a PerkinElmer (Madison, WI) Nicolet Magna 560 FTIR spectrophotometer with Omnic software for data acquisition and analysis. Elemental analysis of Arg-PEEUU was performed with a Thermo Scientific ConFlo III elemental analyzer by Stable Isotope Laboratory of Cornell University.

7.3.5 Molecular weight determination of Arg-PEEUU

Gel permeation chromatography (GPC) of Arg-PEEUU was performed on an Agilent Associates liquid chromatograph equipped with a RI detector. PSS SDV gel columns (30 x 8 mm, 5 μm particle size) with 500 Å pore sizes were used. DMF was used as an eluent (flow rate 0.5 mL/min) at temperature of 25 °C. The injection volume was 100 μL and a WATERS 510 HPLC pump was used. Polystyrene standards were used for calibration.

7.3.6 Thermal properties of Arg-PEEUU

The thermal property of the synthesized Arg-PEEUU was characterized by a differential scanning calorimetry (DSC) TA Q2000 under a nitrogen gas flow 50 mL/min. The measurements were carried out from -60 °C to 150 °C at a scanning rate of 15 °C/min. TA Universal Analysis software was used for thermal data analysis. The glass transition temperature (*T*_g) was determined at the onset of the step.

7.3.7 Water contact angle test of Arg-PEEUU

The hydrophilicity of all types of Arg-PEEUU was measured by Imass CAA2 contact angle analyzer at room temperature. To make the specimens for water contact

angle test, one droplet of 80% (w/v) solution of all types of Arg-PEEUU in DMF were placed onto the center of micro cover glass (12mm Circle, VWR, West Chester, PA). Another piece of cover glass was placed onto the prior cover glass to squeeze the polymer solution droplet evenly spread over the whole glass wafer to form one thin layer of the Arg-PEEUU coating and then the upper cover glass was removed to expose the Arg-PEEUU coating layer. This coated micro cover glass were dried in a fume hood for 24 h and further dried under vacuum in a vacuum oven for another 24 h at room temperature. In the water contact angle tests, a drop of deionized water as spreading liquid was generated on the tip of the needle of a syringe. The needle was lowered carefully until the water droplet touched the coated micro cover glass on the specimen stage until the droplet came off the needle. The height and 1/2 of the droplet width was measured in the center of the field of view, and contact angle, ϕ , was calculated according to the following equation.

$$\text{Cos}\phi = \frac{w^2 - h^2}{w^2 + h^2}$$

where: w = 1/2 drop width, h = drop height, ϕ = contact angle

Five samples of each type of Arg-PEEUU were used for proper statistical average, and mean value was calculated with a standard deviation.

7.3.8 The water solubility change of Arg-PEEUU at different temperature

The solubility of Arg-PEEUU in deionized water was assessed at room temperature (25 °C), 50 °C and 70 °C (Julabo, thermostated water bath). All Arg-PEEUU was grounded into small grains. Arg-PEEUU was added continuously (25 mg in each time) until Arg-PEEUU could not be completely dissolved in 50 mL water under magnetic stirring).

7.3.9 Cytotoxicity test of 6-Arg-2EG PEEUU A/G-4/1 and 6-Arg-4EG PEEUU A/G-4/1 (MTT assay)

Porcine aortic valve smooth muscle cells (PAVSMC) were maintained in minimum essential medium (MEM) supplemented with 10% fetal bovine serum (FBS) and 1% each of penicillin-streptomycin. The cells were incubated in CO₂ incubator at 37 °C with 5% CO₂. After reaching confluence, the cells were detached from the flask with trypsin-EDTA (Invitrogen, Carlsbad, CA). The cell suspension was centrifuged at 3,000 rpm for 3 min and then re-suspended in the growth medium for further study. PAVSMCs were used between passages 4 and 7.

Although Arg-PEEUUs are mainly insoluble in water at room temperature. 6-Arg-2EG PEEUU A/G-4/1 and 6-Arg-4EG PEEUU A/G-4/1 achieved 30 mg/mL solubility and 55 mg/mL in deionized water at 70 °C. When these Arg-PEEUU aqueous solution were cooled down to room temperature, Arg-PEEUU formed homogenous suspension in water. The Arg-PEEUU suspension was further diluted with MEM to evaluate the cytotoxicity of Arg-PEEUU from a MTT assay for PAVSMC cells. The Arg-PEEUU stock suspension was prepared by dissolving 60 mg 6-Arg-2EG PEEUU A/G-4/1 or 6-Arg-2EG PEEUU A/G-4/1 in 10 mL 0.05M phosphate buffered saline (PBS, pH 7.4) at 70 °C with magnetic stirring for 15 min, cooled down to room temperature, and then was sterilized by 30 min UV radiation. The sterilized stock suspension was diluted with sterilized minimum essential medium (MEM) supplemented with 10% fetal bovine serum (FBS) to 2, 1, 0.5, 0.2, and 0.1 mg/mL of the polymer solutions.

PAVSMC were seeded on a 96 well plate with a density of 2,000 cells / well. The cells were washed with PBS buffer, and each of the 5 concentrations of 6-Arg-2EG PEEUU A/G-4/1 and 6-Arg-4EG PEEUU A/G-4/1 were added and incubated along with tissue cultured wells for 24 h. The cells treated only with normal cell culture media were used as the control. Afterward, the cells were incubated with 10 µL of MTT solution (5 mg/mL thiazolyl blue tetrazolium bromide in deionized water after filtration by 0.22 µm filter) for 4 h to form formazan crystals. About 100 µL of acidic isopropyl alcohol (contains 10% Triton-X 100 with 0.1M HCl,) was added into each well and incubated at

room temperature for 1 h to dissolve the formazan crystals. The optical density of the solution was measured at a wavelength of 570 nm and 690 nm (Spectramax plus 384, Molecular Devices, USA). The cell viability (%) was calculated according to the following equation 2:

$$\text{Viability (\%)} = \frac{[\text{OD570 (sample)} - \text{OD690 (sample)}]}{[\text{OD570 (control)} - \text{OD690 (control)}]} \times 100\%$$

where the OD570 (control) represents the measurement from the wells treated with medium only, and the OD570 (sample) from the wells treated with various polymers. Eight samples of each type of the Arg-PEEUU were analyzed. Differences between group means were assessed using one-way ANOVA followed by parametric multiple comparison tests. A value of $p < 0.05$ was considered statistically significant.

7.3.10 Fabrication, size and ζ -potential characterization of Arg-PEEUU microsphere in deionized water

A simple one-step procedure was used to prepare microsphere from Arg-PEEUU in water. 6-Arg-2EG PEEUU A/G-1/1 or 6-Arg-4EG PEEUU A/G-1/1 (10 mg) were first dissolved in 10 mL DMF and then poured rapidly into 200 mL deionized water with a magnetic stirring at 300 rpm for 5 min. Stable Arg-PEEUU microsphere suspension is light milky cloudy in water.

Scanning electron microscope (SEM) was employed to observe 6-Arg-2EG PEEUU A/G-1/1 microsphere as an example for all Arg-PEEUU. One drop of Arg-PEEUU microsphere suspension was dripped on the top of aluminum stubs and freeze-dried for 72 h in a Labconco (Kansas City, MO) Freezone 2.5 freeze drier under vacuum at $-50\text{ }^{\circ}\text{C}$. The Arg-PEEUU microspheres samples with SEM stubs were stored in refrigerator at $-20\text{ }^{\circ}\text{C}$. The Arg-PEEUU microspheres were coated with gold for 30s for SEM observation by Leica Microsystems GmbH (Wetzlar, Germany) 440 SEM.

ζ -potential and particle size of Arg-PEEUU microsphere were tested by using Zetasizer Nano-ZS (Malvern, Worcestershire, UK). Arg-PEEUU microsphere

suspensions in deionized water (0.05 mg/mL) solution prepared as described above and were loaded in the cuvette which can be applied in an alternating high-frequency electric field. Three replicated samples of each type of Arg-PEEUU microsphere were tested. The ζ -potential and particle size were calculated from the dynamic mobility with the standard zetasizer software.

7.3.11 Fabrication of Arg-PEEUU gel via UV-crosslinking

In order to demonstrate the reactivity of the pendant double bonds in the Arg-PEEUU, 300 mg of Arg-PEEUU and 2 mg Irgacure 2959 were dissolved in 1 g DMF at room temperature under magnetic stirring. Every 400 μ L of the above DMF mixture solution was transferred onto a custom-made 20 well Teflon mold and irradiated by a long wavelength (100 watts, 365nm) UV light at room temperature for about 25 min. Disk-shaped gels were obtained in the molds (11 mm diameter, 6 mm thickness). The gels were then soaked in 300 mL deionized water for 16 h at room temperature under a magnetic stirring to remove residual DMF solvent and unreacted precursor from the gels. The Arg-PEEUU gels were then dried in vacuum oven at room temperature for about 4 h. Allyl PU gels was prepared by using the identical protocol as a control for the study of the effect of Arg OEG diester building block incorporation on mechanical properties.

7.3.12 Compressive mechanical property of Arg-PEEUU gels

The compressive mechanical property of all types of dry Arg-PEEUU gels and allyl PU gels were measured by a TA Dynamic mechanical thermal analysis (DMA) Q800 (TA instruments) at room temperature (25 °C) under a compression mode. Each dry gel sample was tested at a constant compression strain rate of 10 % /min until 40% compressive strain was reached. TA Universal Analysis software was used for mechanical data analysis. Compressive initial modulus (calculated from the corresponding stress/strain curve) was used to represent the gel mechanical property. For each type of gels, three samples were used for calculating mean value with a standard deviation.

7.3.13 Enzymatic biodegradation of Arg-PEEUU films in vitro

The effects of Arg OEG diester building block contents of Arg-PEEUU and photo-crosslinking on the enzymatic biodegradation of Arg-PEEUU was studied in terms of weight loss over specific periods. Every 2 mL 60% (w/v) solution of uncrosslinked 6-Arg-4EG PEEUU in DMF were casted evenly onto a disk shaped Teflon[®] mold (about 27 cm²) and dried in a fume hood for 24 h at room temperature. The film samples were soaked in deionized water at room temperature for 3 h and dried under vacuum in a vacuum oven for another 24 h at room temperature. The similar method was used to fabricate crosslinked 6-Arg-4EG PEEUU films. Every 2 mL 60% (w/v) solution of uncrosslinked 6-Arg-4EG PEEUU with 2 mg Irgacure 2959 initiator in DMF was casted evenly onto a Teflon[®] mold (about 27 cm²), and then irradiated by a long wavelength UV light (100 watts, 365nm) at room temperature for 20 min. The crosslinked 6-Arg-4EG PEEUU films were dried in a fume hood for 24 h at room temperature, soaked in deionized water at room temperature for 3 h and further dried in a vacuum at room temperature for another 24 h. The crosslinked and uncrosslinked Arg-PEEUU films of 350 μm ~ 400 μm thickness were cut into 2cm \times 2cm (4 cm², ~150 mg) film specimens.

The enzymatic biodegradation of the crosslinked and uncrosslinked 6-Arg-4EG PEEUU films were carried out in glass vials containing the film specimen and lipase enzyme PBS solutions (1 mg/mL and 3 mg/mL). The original dry weight of each film sample was measured and recorded as W_o . The biodegradation was evaluated by the specimen weight loss at 37 °C in 10 mL lipase PBS (pH 7.4, 0.05M) solutions with a constant reciprocal shaking (100 rpm). The enzyme PBS solutions were refreshed daily in order to maintain enzymatic activity. The crosslinked and uncrosslinked 6-Arg-4EG PEEUU films in 10 mL PBS at 37 °C served as controls. Three replicated samples of each type of 6-Arg-4EG PEEUU were tested.

At predetermined intervals, 3 samples of each type of 6-Arg-4EG PEEUU films were removed from the immersion media (lipase PBS, and pure PBS control) rinsed in

deionized water and dried under vacuum at room temperature till a constant weight achieved (about 12 h). The weight loss was calculated according to the following equation:

$$\% \text{ Weight loss} = (W_o - W_t) / W_o \times 100\%$$

where W_o was the initial dry weight of each film sample at $t=0$, and W_t was the dry weight of each film sample after t incubation. A mean value of three specimens was calculated as the weight loss at time t with a standard deviation.

7.4 Results and discussion

7.4.1. Synthesis of Arg-*x*EG-Cl monomers

The Arg-*x*EG-Cl monomers were synthesized from L-Arg and OEG from a modified method that is different from the Wu et al. and Song et al. method⁸⁻¹³. In prior studies of Guo et al., the similar Phe OEG diester monomer synthesis method was also used in the study of Phe based Poly(ether ester amide) (Phe-PEEA)⁷. Before the polymerization reaction with and HDI, TsO⁻ counter ions attached to the two amino groups of Arg-*x*EG-Cl monomers were removed^{2,4,31,32}.

Two types of Arg-*x*EG-Cl monomers due to different diols were prepared in this study: di-hydrochloride acid salt of bis (L-Arg) diethylene glycol diester, Arg-2EG-Cl ($x=2$); di-hydrochloride acid salt of bis (L-Arg) tetraethylene glycol diester, Arg-4EG-Cl ($x=4$). x indicates the number of ethylene glycol repeat unit in the diol segment of Arg diester. The chemical structures of Arg-*x*EG-Cl monomers were confirmed by ¹H NMR.

di-hydrochloride acid salt of bis (L-Arg) diethylene glycol diester (Arg-2EG-Cl):
¹H NMR (DMSO-d₆, ppm, δ): 1.52 [4H, -OC(O)-CH(NH₂)-CH₂-CH₂-CH₂-NH-], 1.75 [4H, -OC(O)-CH(NH₂)-CH₂-CH₂-CH₂], 3.10 [4H, -CH₂-CH₂-CH₂-NH], 3.49 [4H, -(O)C-O-CH₂-CH₂-O-CH₂-], 3.60 [4H, -(O)C-O-CH₂-CH₂-O-CH₂-], 4.04 [2H, ⁺H₃N-CH(R)-C(O)-O-], 4.39 [4H, -(O)C-O-CH₂-CH₂-], 7.60, bump between 6.95~7.50 [10H, -CH₂-NH(NH₂⁺)-NH₂], 8.36 [6H, ⁺H₃N-CH(R)-C(O)-O-]

di-hydrochloride acid salt of bis (L-Arg) tetraethylene glycol diester (Arg-4EG-Cl): ^1H NMR (DMSO- d_6 , ppm, δ): 1.49 [4H, $-\text{OC}(\text{O})-\text{CH}(\text{NH}_3^+)-\text{CH}_2-\text{CH}_2-\text{CH}_2-\text{NH}-$], 1.67 [4H, $-\text{OC}(\text{O})-\text{CH}(\text{NH}_3^+)-\text{CH}_2-\text{CH}_2-\text{CH}_2-\text{NH}-$], 3.09 [4H, $-\text{CH}_2-\text{CH}_2-\text{CH}_2-\text{NH}$], 3.40 [4H, $-(\text{O})\text{C}-\text{O}-\text{CH}_2-\text{CH}_2-\text{O}-\text{CH}_2-$], 3.45 [4H, $-(\text{O})\text{C}-\text{O}-\text{CH}_2-\text{CH}_2-$], 3.47 [4H, $-(\text{O})\text{C}-\text{O}-\text{CH}_2-\text{CH}_2-\text{O}-\text{CH}_2-$], 3.49 [2H, $^+\text{H}_3\text{N}-\text{CH}(\text{R})-\text{C}(\text{O})-\text{O}-$], 3.83 [4H, $-(\text{O})\text{C}-\text{O}-\text{CH}_2-\text{CH}_2-$], bump between 7.07~7.53 [10H, $-\text{CH}_2-\text{NH}(\text{NH}_2^+)-\text{NH}_2$]

Figure 7.3 shows an example of the ^1H -NMR spectra of Arg-4EG-Cl monomer. The absence of protons of benzene group (7.13~7.15 ppm and 7.47~7.52 ppm) associated with TsOH and methyl group (2.29 ppm) on the ^1H NMR of Arg-4EG-Cl demonstrated the toluene sulfonic acid groups were removed from the amine group of Arg. A comparison of ^1H NMR spectra of Arg-4EG-Cl before (Figure 7.3A) and after (Figure 7.3B) clearly demonstrate the absence of the TsOH in Arg-4EG-Cl monomer. TsOH was removed from Arg-4EG-Cl monomer to expose the free amine groups for Arg-PEEU synthesis in the 2 steps polycondensation.

7.4.2 Arg-PEEU synthesis and characterization

Functional Arg-PEEU having pendant double bonds were synthesized using a two-step solution polymerization of Arg- x EG-Cl (Arg-2EG-Cl, Arg-4EG-Cl), HDI and GAE. To study the relationship between polymer structures and their chemical and physical properties, a control PU (allyl PU) synthesized using HDI/GAE and 6 Arg-PEEU of Arg-2EG-Cl or Arg-4EG-Cl chain extenders and feed ratio among the 3 monomers were synthesized and listed in Table 7.1.

In order to verify the chemical composition of Arg-PEEU, their FTIR spectra and carbon / nitrogen content data were obtained. The FTIR spectra of Arg-PEEU is mainly influenced by the monomers feed ratio in the synthesis, an example of the FTIR spectra of 6-Arg-2EG PEEU of three different feed ratios and allyl PU control without Arg component are shown in Figure 7.4. The absorption band at 3302 cm^{-1} ~ 3309 cm^{-1} is the characteristic of N-H group of urethane and urea which is presented on all 6-Arg-2EG

PEEUU spectra and allyl PU ^{15,31}. The absorption at 2859 cm⁻¹ and 2950 cm⁻¹ are attributed to -CH₂ symmetric and anti-symmetric stretching vibrations. 6-Arg-2EG PEEUU spectra shows absorption peak at 1725 cm⁻¹ which is the carbonyl band of the Arg-*x*EG-Cl building block (shown in Figure 7.4 A, B, C). A relatively broad shoulder is evident from 1630-1700 cm⁻¹ which result from both hydrogen bonded and free carbonyl stretching frequencies for urea and H-bonded urethane functionalities ². While allyl PU (Figure 7.4 D) only showed one narrower urethane peak than Arg-PEEUU at 1700 cm⁻¹. The absorption of ether group at 1125 cm⁻¹ was showed on all spectra of Arg-PEEUU and allyl PU due to the presence of C-O from OEG and GAE ⁷. Allyl PU showed trace amounts of absorption at 2270 cm⁻¹ which is the characteristic peak of isocyanate group ¹⁵. However, the isocyanate peak do not present on any 6-Arg-2EG PEEUU which indicates HDI monomers were depleted in the chain extension reaction.

The carbon and nitrogen contents (Table 7.2) from elemental analysis were consistent with the calculated composition based on the chemical formula of Arg-PEEUU. Arg is the most nitrogen rich amino acid among all natural amino acids which has 32% nitrogen content. Another source of nitrogen in the Arg-PEEUU is from HDI. The calculated nitrogen content of allyl PU is 9.77%, while all Arg-PEEUU have much higher nitrogen contents (14.03 to 22.34%) than allyl PU 9.77%. The Arg-PEEUU having more Arg diester building block contents has higher nitrogen contents, e.g., from 14.75% at A/G 1/4, 19.35% at A/G 1/1 to 22.34 at A/G 4/1.

The molecular weights of Arg-PEEUU as determined by GPC are shown in Table 7.3. The M_n (number average molecular weight) of Arg-PEEUU ranged from 20.425 to 60.225 Kg/mol with M_w/M_n (PDI) 1.298~1.460. In the synthesis of Phe based polyurethane which shared the similar chemistry structure with Arg-PEEUU also have the similar M_n ranging from 25.400 to 69.300 Kg/mol with PDI about 2 ⁴.

Guo et al. reported Phe-PEEA which possessed the same OEG building block on the polymer backbone ⁷. The MW of Phe-PEEA was from 2.6 to 27.3 Kg/mol. Most Phe-

PEEA had smaller MW than Arg-PEEUU. The possible reason is in the polycondensation step of Phe-PEEA in which the TsOH salt of Phe diester reacted with nitrophenol diester monomer. In that synthesis, the ester bond of nitrophenol diester must be cleaved for forming amide bond with the amine groups of Phe diester which also has TsO⁻ attached.

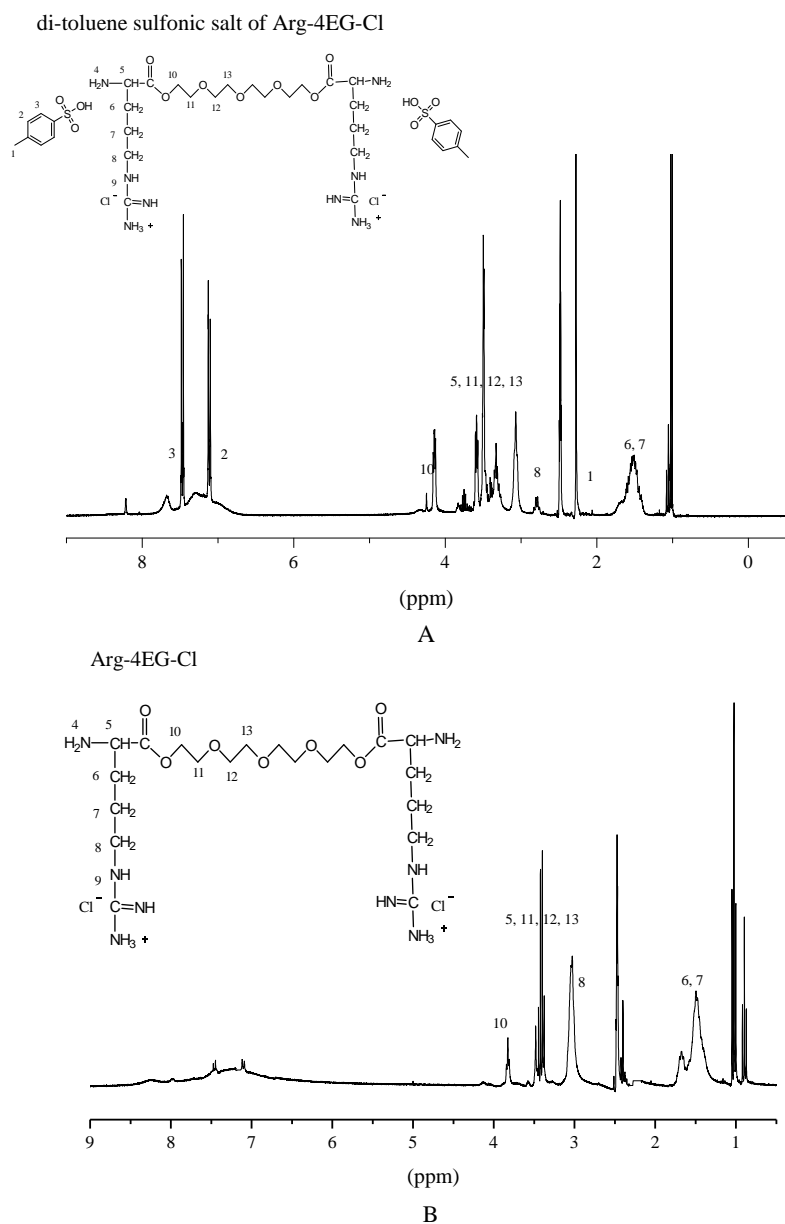


Figure 7.3 ¹H NMR spectroscopy of Arg oligoethylene glycol diester monomers before and after removing TsOH from the amine groups of Arg. (A) di-*p*-toluene sulfonic acid

di-hydrochloride acid salt of bis (L-Arg) tetraethylene glycol diesters; (B) di-hydrochloride acid salt of bis (L-Arg) tetraethylene glycol diester (Arg-4EG-Cl)

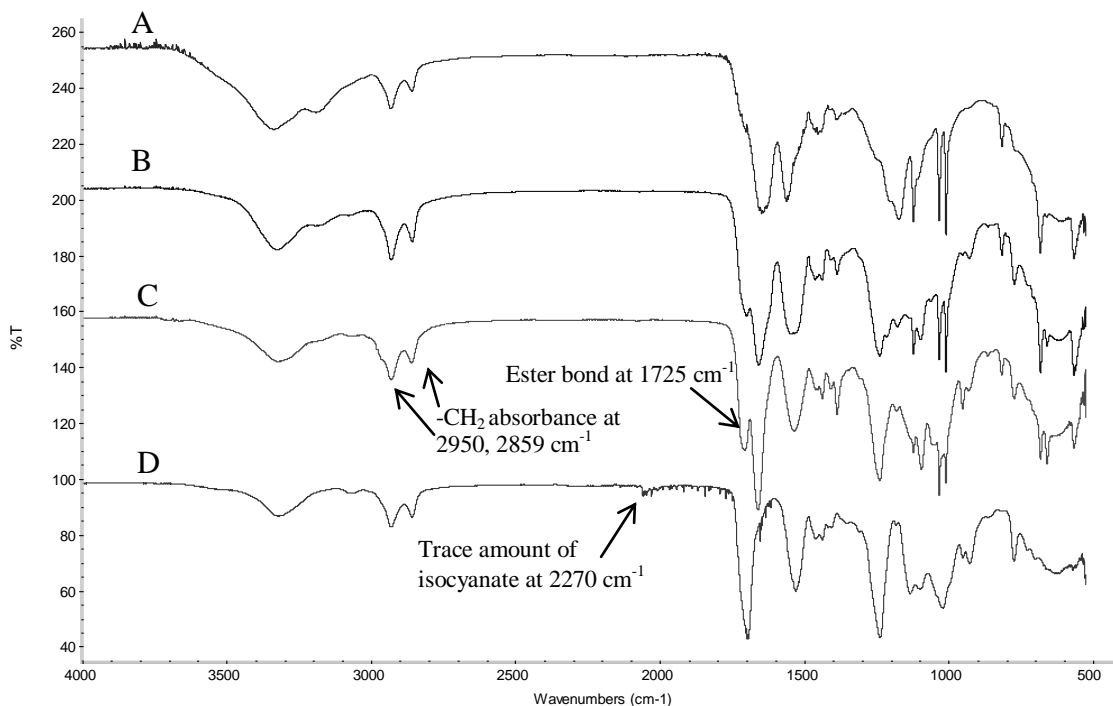


Figure 7.4 FTIR of 6-Arg-2EG PEEUU synthesized with different monomer feed ratio and allyl PU. (A) 6-Arg-2EG PEEUU A/G-4/1; (B) 6-Arg-2EG PEEUU A/G-1/1; (C) 6-Arg-2EG PEEUU A/G-1/4; (D) allyl PU

The reactivity of Phe-PEEA polycondensation is lower than the free amine group of Arg-*x*EG-Cl monomer and HDI-based prepolymer in the synthesis of Arg-PEEUA.

7.4.3 Thermo property of Arg-PEEUA

From differential scanning calorimetry (DSC) results, summarized in Table 7.4, T_g of all Arg-PEEUA ranged from -23.38 °C to -2.35 °C, depending on the 3 monomers feed ratio and *x* (number of OEG groups in the Arg diester building block).

With the same Arg-*x*EG-Cl chain extender, higher Arg-*x*EG-Cl contents in the Arg-PEEUA (i.e. T_g of 6-Arg-2EG PEEUA A/G-1/4 and 6-Arg-4EG PEEUA A/G-1/4 are

Table 7.2 C% and N% of Arg-PEEUU and allyl PU

Arg-PEEUU samples	Formula	Calculated carbon content (%)	Carbon content (%)	Calculated nitrogen content (%)	Nitrogen content (%)
6-Arg-2EG	(C ₂₄ H ₄₈ Cl ₂ N ₁₀ O ₇) ₁	56.20	55.60	14.75	14.16
PEEUU A/G-1/4	(C ₁₄ H ₂₄ N ₂ O ₅) ₄				
6-Arg-2EG	(C ₂₄ H ₄₈ Cl ₂ N ₁₀ O ₇) ₁	52.53	52.47	19.35	18.66
PEEUU A/G-1/1	(C ₁₄ H ₂₄ N ₂ O ₅) ₁				
6-Arg-2EG	(C ₂₄ H ₄₈ Cl ₂ N ₁₀ O ₇) ₄	50.15	49.81	22.34	22.07
PEEUU A/G-4/1	(C ₁₄ H ₂₄ N ₂ O ₅) ₁				
6-Arg-4EG	(C ₂₈ H ₅₆ Cl ₂ N ₁₀ O ₉) ₁	56.12	55.38	14.03	13.76
PEEUU A/G-1/4	(C ₁₄ H ₂₄ N ₂ O ₅) ₄				
6-Arg-4EG	(C ₂₈ H ₅₆ Cl ₂ N ₁₀ O ₉) ₁	52.72	52.20	17.57	17.37
PEEUU A/G-1/1	(C ₁₄ H ₂₄ N ₂ O ₅) ₁				
6-Arg-4EG	(C ₂₈ H ₅₆ Cl ₂ N ₁₀ O ₉) ₄	50.67	50.64	19.71	19.62
PEEUU A/G-4/1	(C ₁₄ H ₂₄ N ₂ O ₅) ₁				
Allyl PU	C ₁₄ H ₂₄ N ₂ O ₅	60.00	58.60	10.00	9.77

Table 7.3 Molecular weight of Arg-PEEUU

Sample	M_n (kg/mol)	M_w (kg/mol)	M_w/M_n
6-Arg-2EG PEEUU A/G-4/1	21.800	31.825	1.460
6-Arg-2EG PEEUU A/G-1/1	31.555	42.125	1.335
6-Arg-2EG PEEUU A/G-1/4	42.325	57.700	1.363
6-Arg-4EG PEEUU A/G-4/1	20.425	28.900	1.415
6-Arg-4EG PEEUU A/G-1/1	60.225	78.175	1.298
6-Arg-4EG PEEUU A/G-1/4	53.575	71.100	1.327

Table 7.4 T_g and water contact angle of Arg-PEEUU and allyl PU

PEEUU	T_g (°C)	Water contact angle (°)
Allyl PU	-26.80	75.4 ± 0.7
6-Arg-2EG PEEUU A/G-1/4	-20.43	49.8 ± 3.7
6-Arg-2EG PEEUU A/G-1/1	-14.90	31.3 ± 2.5
6-Arg-2EG PEEUU A/G-4/1	-2.35	24.3 ± 3.3
6-Arg-4EG PEEUU A/G-1/4	-23.38	56.7 ± 3.9
6-Arg-4EG PEEUU A/G-1/1	-18.87	31.4 ± 1.9
6-Arg-4EG PEEUU A/G-4/1	-6.47	29.2 ± 2.8

-20.43 °C and -23.38 °C, respectively) showed higher T_g (i.e. T_g of 6-Arg-4EG PEEUU A/G-4/1 and 6-Arg-4EG PEEUU A/G-4/1 are -2.35 °C and -6.47 °C). This relationship could be attributed to the fact that more Arg contents in the Arg-PEEUU would have more bulky guanidino side groups and to the Arg-PEEUU which could reduce polymer segmental mobility and hence higher T_g . In addition, guanidino side groups could form a strong intermolecular hydrogen bonding when guanidino groups approach the urethane/urea groups of Arg-PEEUU. The intermolecular force could further decrease the segmental mobility of polymer chain and also increase the T_g further^{8,31}. Moreover, as the Arg-*x*EG-Cl building block content decreased, more GAE was incorporated into the polymer. GAE is able to impart additional chain flexibility by increasing free volume from pendant double bonds which acts as an internal plasticizer. The increasing GAE component resulted in a lower T_g as well. This reduction in T_g with an increasing pendant double bonds in AA-PEA based polymers has also demonstrated by the reported Pang et al. study of functional AA-PEAs having pendant double bonds^{14,33}. For example, Pang et al. reported that an increase in the pendant double bond in bis-DL-2-allylglycine esters

(i.e., increasing AG contents in the Phe-PEA polymers) from 25% (8-Phe-4-AG-4-25) to 50% (8-Phe-4-AG-4-50) led to a reduction in T_g from 30 °C to 26 °C³³.

Except feed ratio effect, the presence of one or more OEG in the repeating units of PEEUU decreased the T_g , because the ether bond is well-known flexible bond for polymer free rotation⁷. Hence, the promoted Arg-PEEUU segmental movement leads to a lower T_g . For the same reason, with the same feed ratio of monomers, increasing the x parameter (number of ether bonds in Arg OEG repeating unit) led to lower T_g of Arg-PEEUU (i.e. at the same A/G ratio, all 6-Arg-2EG PEEUU showed higher than that of 6-Arg-4EG PEEUU). Compared to the T_g of Arg-PEUU synthesized with Arg alkylene ester chain extender in prior study³¹, at the same molar feed ratio of Arg diester / GAE, the Arg-PEEUU has lower T_g due to the flexibility brought by the incorporation of ether bond on the polymer backbone. For example, T_g of 6-Arg-2EG PEEUU A/G-1/1 and 6-Arg-4EG PEEUU A/G-1/1 are -14.90 °C and -18.87 °C, respectively while T_g of 6-Arg-2PEUU A/G-1/1 and 6-Arg-6PEUU A/G-1/1 are 1.90 °C and -8.69 °C³¹.

7.4.4 Water contact angle of Arg-PEEUU

The contact angle of Arg-PEEUU synthesized with different Arg- x EG-Cl chain extender and monomer feed ratio were measured and compared (Table 7.4). The water contact angle of Arg-PEEUU is from $24.3 \pm 3.3^\circ$ to $56.7 \pm 3.9^\circ$ by varying the feed ratio of monomers and the x parameter. Compared to the water contact angle of Phe based PU (i.e. from 30° to 80°)^{2,4} and Phe-PEEA (i.e. from $62 \pm 5^\circ$ to $88 \pm 5^\circ$)⁷ which share the most similar chemistry structure with Arg-PEEUU, the Arg-PEEUU is more hydrophilic due to the presence of the chloride salt of guanidino groups as side groups^{8,10}. The water contact angle of allyl PU ($75.4 \pm 0.7^\circ$) is higher than all Arg-PEEUU. It demonstrated the high hydrophilicity is related to the incorporation of Arg OEG diester building blocks. Allyl PU without Arg component showed similar water contact angle data with most reported linear block copolymer polyurethane with PCL and PEG segments synthesized for biomedical applications (from $65 \pm 2^\circ$ to $73 \pm 2^\circ$)²⁸. As the prior study about Arg-

PEUU ³¹, increasing the molar ratio of Arg alkylene diester to GAE (A/G) also effectively increase hydrophilicity of Arg-PEEUU, hence lower water contact angle value.

The number of OEG x in the diol of Arg diester building block also play a minor role to the hydrophilicity of Arg-PEEUU. With the same stoichiometry, higher x which means more ethylene glycol units incorporated between 2 Arg led to lower hydrophilicity / higher water contact angle. Table 7.4 shows the water contact angle of all 6-Arg-4EG PEEUU are about 0.1~6.9° higher than 6-Arg-2EG PEEUU with the same A/G ratio. It is because the hydrophilicity of Arg-PEEUU is mainly from the ionizable guanidino groups of Arg. Incorporating longer OEG chain between 2 Arg led to lower guanidino side group density of the resulting Arg-PEEUU. Although PEG has the better hydrophilicity (water contact angle about 63°) than most polyester/polyurethane, incorporating PEG segment usually decrease the water contact angle of the copolymer ², Arg-PEEUU with higher x presents slightly higher water contact angle due to the reduced ionizable side group density.

7.4.5 Water solubility of Arg-PEEUU at different temperature

Table 7.5 shows the effect of temperature on the water solubility of Arg-PEEUU. All Arg-PEEUUs are insoluble in water at room temperature. However, at 40 °C, 6-Arg-2EG PEEUU and 6-Arg-4EG PEEUU with A/G-4/1 shows about 5 mg/mL solubility. At 70 °C, all Arg-PEEUU shows water solubility depending on the Arg content up to 55 mg/mL. In prior Wu et al ^{9,10,13}, Song et al. ⁸ and Pang et al. ¹⁴ studies, Arg-PEA, Arg-UPEA and Arg-PEA-AG which have the Arg diester building blocks are all soluble in water at room temperature. While the urethane linkage of Arg-PEUU ³¹ and Arg-PEEUU is more hydrophobic than the amide linkage that makes these two types of polymer water insoluble at room temperature. Because of the presence of hydrophobic segment, large amount of Arg moieties with guanidino groups are trapped in the interior of the polymer

Table 7.5 Water solubility of Arg-PEEUU at different temperature

Arg-PEEUU	water solubility (mg/mL)		
	25 °C	40 °C	70 °C
6-Arg-2EG PEEUU A/G-1/4	n/a	n/a	5~10
6-Arg-2EG PEEUU A/G-1/1	n/a	n/a	20
6-Arg-2EG PEEUU A/G-4/1	n/a	5	30
6-Arg-4EG PEEUU A/G-1/4	n/a	n/a	5
6-Arg-4EG PEEUU A/G-1/1	n/a	~5	25
6-Arg-4EG PEEUU A/G-4/1	n/a	5	55

chain. It makes the dissolution of Arg-PEEUU in water even harder at room temperature. However, the Arg-PEEUU has one or three flexible ether bond in each Arg OEG diester repeating unit on the polymer backbones and hence low T_g (Table 7.4). The fast segmental mobility at temperature higher than room temperature makes more Arg moieties contact with water molecule and are ionized, hence the water solubility significantly increased. Incorporation more OEG unit in the Arg-PEEUU, the solubility at the same temperature increases (i.e. the water solubility of 6-Arg-2EG PEEUU A/G-4/1 and 6-Arg-4EG PEEUU A/G-4/1 are about 30 and 55 mg/mL, respectively.) The temperature responsive water solubility is one feature of Arg-PEEUU among all Arg based polymer.

7.4.6 Cytotoxicity of 6-Arg-2EG PEEUU A/G-4/1 and 6-Arg-4EG PEEUU A/G-4/1 (MTT assay)

Cytotoxicity of PAVSMC was conducted by incubating the cells with either the MEM media alone (control) or Arg-PEEUU (At the cell incubation temperature, both 6-Arg-2EG PEEUU A/G-4/1 or 6-Arg-4EG PEEUU A/G-4/1 suspension become water soluble at tested concentrations up to 2 mg/mL) mixed with MEM media. Cell viability was determined from a MTT assay after treated by 6-Arg-2EG PEEUU A/G-4/1 or 6-Arg-4EG PEEUU A/G-4/1 and incubated for 24 h (Figure 7.5). Compared to the control, both 6-Arg-2EG PEEUU A/G-4/1 (Figure 7.5 A) and 6-Arg-4EG PEEUU A/G-4/1 (Figure 7.5 B) didn't show obvious cell viability change at low concentrations (0.1 - 0.5 mg/mL). However, at 2 mg/mL the PAVSMC viability cultured with 6-Arg-2EG PEEUU A/G-4/1 and 6-Arg-4EG PEEUU A/G-4/1 decreased to 69.9% and 77.2%, respectively. The cell viability of 6-Arg-2EG PEEUU A/G-4/1 is significantly lower than the control group. Compared to the Arg-PEUU in prior study, at the same monomer feed ratio A/G-4/1 and same MTT test protocol, 6-Arg-2EG PEEUU and 6-Arg-4EG PEEUU have the similar or slightly higher PAVSMC cell viability than 6-Arg-2 PEUU (67.7%) which has the highest Arg moiety content among all Arg-PEUU³¹.

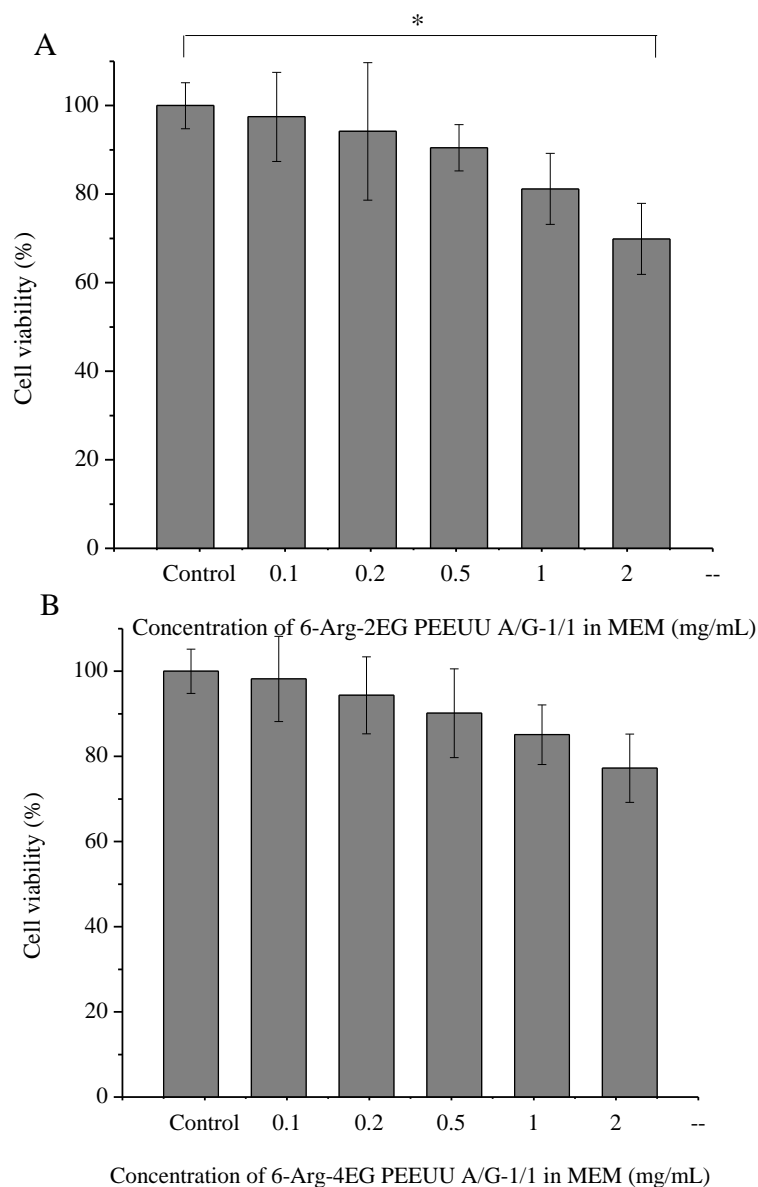


Figure 7.5 MTT Assay for porcine aortic valve smooth muscle cells (PAVSMC) after 24 h culture with Arg-PEEUU in 0.1, 0.2, 0.5, 1 and 2 mg/mL concentration. (A) 6-Arg-2EG PEEUU A/G-4/1; (B) 6-Arg-4EG PEEUU A/G-4/1. * $P < 0.05$ vs. control group

7.4.7 Characterization of Arg-PEEUU microsphere

Due to the presence of hydrophilic Arg OEG diester building blocks and hydrophobic urethane linkage on the Arg-PEEUU, the amphiphilicity can be utilized to prepare Arg-PEEUU microsphere by dripping its DMF solution (1 mg/mL) in water with fast stirring. The Arg-PEEUU microsphere dispersed in water and formed slight white

cloudy suspension that is stable for about 1 week. Based on the SEM images, the microspheres formed by 6-Arg-2EG PEEUU A/G-1/1 as a representative were generally spherical in shape with smooth surfaces as shown in Figure 7.6 A&B. The SEM images showed the diameter size of 6-Arg-2EG PEEUU A/G-1/1 microsphere is from less than 100 nm to 800~900 nm. The approximate hydrodynamic diameter distribution of suspended in deionized water was measured using dynamic light scattering (Nano-ZS zetasizer, Malvern, Worcestershire, UK) shown in Figure 7.6 C. Based on SEM and zetasizer result, 6-Arg-2EG PEEUU A/G-1/1 particles are sub-micron size and the size distribution of microsphere is unimodal. Table 7.6 summarized the hydrodynamic average diameter of all Arg-PEEUU synthesized with different monomer feed ratio and x parameter (ranging from 123.2 ± 3.7 to 217.8 ± 12.2 nm). Higher Arg OEG diester content is apt to form microsphere with slightly larger microsphere (the diameter of 6-Arg-2EG PEEUU A/G-4/1 microsphere is 17.9% larger than that of 6-Arg-2EG PEEUU A/G-1/4, the hydrodynamic diameter of 6-Arg-4EG PEEUU A/G-4/1 microsphere is 52.8% larger than that of 6-Arg-4EG PEEUU A/G-1/4) when suspended in deionized water, probably due to the increased hydrophilicity.

The strong positive ζ -potential of Arg-PEEUU was observed and summarized in Table 7.6 ($+48.1 \pm 0.7$ mV to $+52.3 \pm 1.7$ mV). Because the T_g of all Arg-PEEUU (Table 7.4) are lower than room temperature, the segment movement makes the hydrophilic Arg OEG diester building block is more concentrated on the water/polymer interface of the microspheres. The ionizable guanidino groups of Arg attribute this microsphere unique strong positive charge. The value of Arg-PEEUU microsphere is higher than the positive ζ -potential of polyarginine derivatives ($+15.6 \sim +35.3$ mV) or Arg grafted polymer (ranging from $+40 \sim +45$ mV) were observed in prior studies^{34,35}. The cationic Arg-PEEUU microsphere with 100~200 nm average diameter has potential application of delivery systems for small interfering RNA (siRNA) etc.^{34,35}

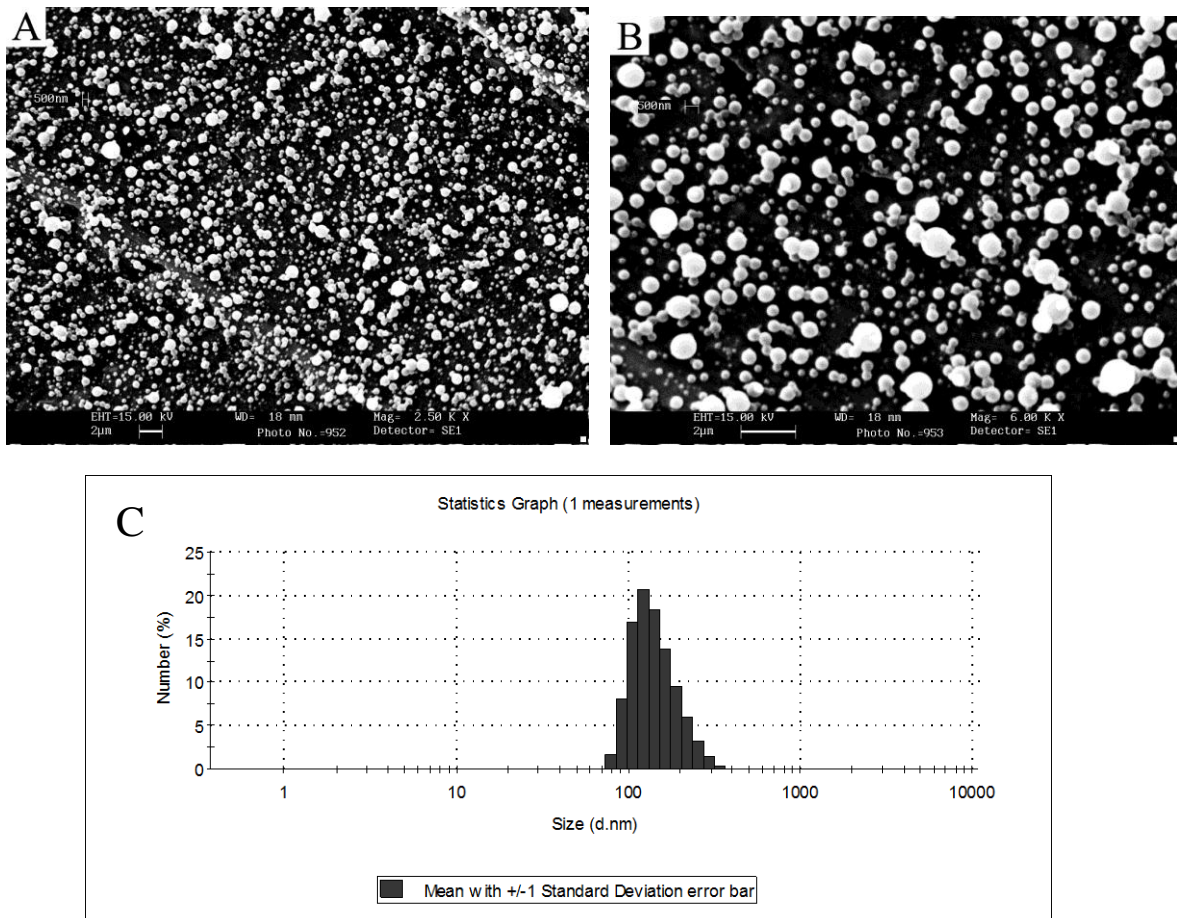


Figure 7.6 6-Arg-2EG PEEUU A/G-1/1 microsphere; (A) SEM images at 2,500X; (B) SEM images at 6,000X; (C) hydrodynamic diameter distribution of 6-Arg-2EG PEEUU A/G-1/1 microsphere

Table 7.6 ζ -potential and the average hydrodynamic diameter of Arg-PEEUU microsphere at 0.5 mg/mL concentration in deionized water at room temperature

Arg-PEEUU microsphere	ζ -potential (mV)	microsphere size (nm)
6-Arg-2EG PEEUU A/G-1/4	48.1 \pm 0.7	123.2 \pm 3.7
6-Arg-2EG PEEUU A/G-1/1	50.4 \pm 2.8	136.9 \pm 8.3
6-Arg-2EG PEEUU A/G-4/1	52.3 \pm 1.7	145.3 \pm 4.8
6-Arg-4EG PEEUU A/G-1/4	48.5 \pm 0.7	142.3 \pm 8.7
6-Arg-4EG PEEUU A/G-1/1	50.5 \pm 0.8	174.9 \pm 1.8
6-Arg-4EG PEEUU A/G-4/1	51.4 \pm 2.7	217.8 \pm 12.2

7.4.8 Photo-crosslinked Arg-PEEUU gel

Except the microsphere fabrication, Arg-PEEUU is able to be photo-crosslinked to form elastic gel. GAE introduced pendant functional double bonds in the synthesis of Arg-PEEUU. Arg-PEEUU synthesized with the A/G no more than 1/1 (i.e., Arg OEG diester/ GAE @ 1/4 and 1/1) could be photo-crosslinked in DMF solution with Irgacure 2959 initiator (Table. 7.7). Figure 7.7 showed the images of the photo-crosslinked 6-Arg-4EG PEEUU A/G-1/1 gel as a representative example. Similar with prior reported Arg-PEUU gel³¹, photo-crosslinked Arg-PEEUU was transparent yellow color. When the applied force was removed, this gel recovered its original dimension (supplemental video).

In the studies about Arg based polymers, Arg-UPEA or Arg-AG PEA are not able to be crosslinked by themselves, even though Arg-UPEA having unsaturated double bonds on the polymer backbone and Arg-AG-PEA have the pendant double bonds from allylglycine moiety^{9,14}. These two polymers could be used to fabricate hybrid hydrogels with another crosslinkable polymer co-precursor, like polyethylene glycol diacrylate

(PEGDA) or Pluronic diacrylate (Pluronic-DA). Due to the presence of Arg moiety, Arg-UPEA or Arg-AG PEA composition attributed the hybrid hydrogel cationic properties.

The reason of Arg-PEUU or Arg-PEEUU synthesized with GAE as one of the monomers is its reactive vinyl group with a long spacer (4 methylene groups) which could minimize the adverse steric hindrance effect of the Arg moiety from photo-induced crosslinking reaction ³¹.

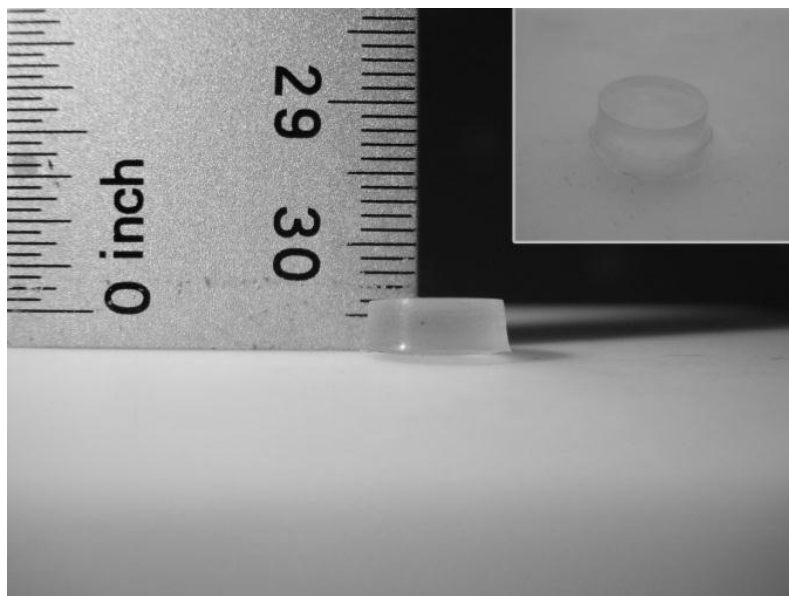


Figure 7.7 Images of photo-crosslinked 6-Arg-4EG PEEUU A/G-1/1 gel

7.4.9 Compressive mechanical property of photo-crosslinked Arg-PEEUU gels

Table 7.7 summarized the mechanical properties of photo-crosslinked Arg-PEEUU gels and photo-crosslinked allyl PU (control). The compressive initial modulus of Arg-PEEUU is from 80.4 ± 10.28 KPa to 184.5 ± 9.0 KPa, depending on the feed ratio

Table 7.7 Compression Mechanical Data of allyl PU gel and Arg-PEEUU gels

Samples	Gel formation by photo-crosslinking	Compressive modulus (KPa)	Compressive strength at break (KPa)	Compressive strain at break (%)
Allyl PU	Y	39.8 ± 4.4	> 350	> 60
6-Arg-2EG PEEUU A/G-1/4	Y	184.5 ± 9.0	> 350	> 60
6-Arg-2EG PEEUU A/G-1/1	Y	86.9 ± 5.5	187.7 ± 36.0	50.8 ± 6.5
6-Arg-2EG PEEUU A/G-4/1	N	n/a	n/a	n/a
6-Arg-4EG PEEUU A/G-1/4	Y	162.4 ± 12.1	> 350	> 60
6-Arg-4EG PEEUU A/G-1/1	Y	80.4 ± 10.28	162.1 ± 31.5	34.2 ± 4.5
6-Arg-4EG PEEUU A/G-4/1	N	n/a	n/a	n/a

and x parameter of Arg OEG diester in the Arg-PEEUU. While the compressive initial modulus of crosslinked allyl PU (39.8 ± 4.4 KPa) is lower than any Arg-PEEUU gel prepared. Using the Arg- x EG-Cl as the chain extender obviously increased the compressive initial modulus of crosslinked allyl PU due to the decreased polymer chain flexibility brought by bulky guanidino groups of Arg and the hydrogen bonding interaction. However, as the content of Arg OEG diester increased further, e.g., from A/G feed ratio of 1/4 to 1/1, the compressive modulus of the crosslinked copolymer gel decreased. For example, 6-Arg-2EG PEEUU A/G-1/4 had 184.5 ± 9.0 KPa, whereas 6-Arg-2EG PEEUU A/G-1/1 had 86.9 ± 5.5 KPa. This is because the GAE contents decreased, i.e., smaller available copolymer segments responsible for photo-crosslinking and hence lower crosslinking density in Arg-PEEUU with A/G-1/1 than Arg-PEEUU A/G-1/4. This lower crosslinking density was subsequently reflected in a reduction in compressive modulus.

Arg-PEUU gel which has Arg alkylene diester building blocks without the ether bonds brought by OEG repeating unit was fabricated in our prior study³¹. Due to the very similar chemical structure, Arg-PEUU shares many features of Arg-PEEUU (flexible, photo-crosslinkable, cationic, etc.). The Arg-PEEUU gel with the same A/G ratio showed higher compressive initial modulus than Arg-PEUU gels (i.e. 6-Arg-2EG PEEUU A/G-1/4, 184.5 ± 9.0 KPa > 6-Arg-2 PEUU A/G-1/4, 120.7 ± 5.4 KPa > 6-Arg-6 PEUU A/G-1/4, 105.7 ± 7.2 KPa) that is unexpected because the ether bonds of Arg OEG diester of Arg-PEEUU should be more flexible than Arg alkylene diester of Arg-PEUU. The reason is the ether bonds provide the segment of Arg-PEEUU free rotation mobility, not like the methylene groups on the backbone of Arg-PEUU is fixed in the planar space. The free rotation mobility largely increased the chance that the pendant double bonds of different Arg-PEEUU molecules contact and covalently bonded with each other among the co-existed bulky guanidino side groups, hence

increased the crosslinking density. In macroscopic, it is reflected from the increased compressive initial modulus. However, Arg-PEEUU gels are able to sustain even larger compressive deformation than Arg-PEUU gels (Table 7.7). It shows the gel flexibility change brought by ether group incorporation. For example, with the same A/G ratio, the compressive strain at break of 6-Arg-2EG PEEUU A/G-1/1 is 50.8 ± 6.5 , larger than that of 6-Arg-2 PEUU A/G-1/1 ($17 \pm 5.2\%$) and 6-Arg-6 PEUU A/G-1/1 ($19 \pm 4.4\%$)³¹.

Similar to Arg-PEUU gels³¹, the change in material parameter x which is the number of ether bonds in one Arg OEG diester repeating unit also affected the compressive modulus of the corresponding Arg-PEEUU gels. For example, as the x increased from 2 to 4 in the Arg OEG diester building block at the same molar feed ratio (A/G-1/4), the compressive modulus of the resulting Arg-PEEUU was reduced from 184.5 ± 9.0 KPa of the 6-Arg-2EG PEEUU A/G-1/4 to 162.4 ± 12.1 KPa of the 6-Arg-4EG PEEUU A/G-1/4. This is mainly because more OEG building block attributed to the higher polymer chain flexibility in the crosslinked structure that led to lower compressive modulus. The mechanical strength of Arg-PEEUU was significantly larger than other reported photo-crosslinked Arg-based PEA hydrogels, such as Arg-UPEA/Pluronic-DA F-127 hydrogel¹⁰.

7.4.10 In vitro enzymatic biodegradation of Arg-PEEUU and photo-crosslinked Arg-PEEUU films

Crosslinked and uncrosslinked 6-Arg-4EG PEEUU films (2cm×2cm) having different monomer feed ratios (6-Arg-4EG PEEUU A/G-1/4, 6-Arg-4EG PEEUU A/G-1/1) biodegradation data in terms of weight loss with two concentrations of lipase (1 mg/mL and 3 mg/mL) is shown in Figure 7.8. All 6-Arg-4EG PEEUU films showed higher degradation rate in the lipase than in the PBS at 37 °C. Increasing the

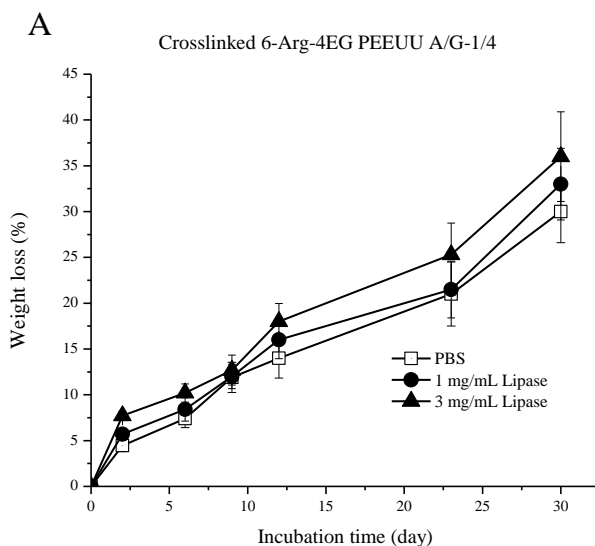
lipase concentration from 1 mg/mL to 3 mg/mL led to a faster degradation rate of all samples (the blue lines are above the red lines in Figure 7.8. A, B, C &D).

The crosslinked 6-Arg-4EG PEEUU biodegradation showed a much slower rate than the uncrosslinked ones as shown by comparing the degradation profiles of Figure 7.8A vs. Figure 7.8B, and Figure 7.8C vs. Figure 7.8D. For example, crosslinked 6-Arg-4EG PEEUU A/G-1/4 film in 1mg/mL lipase lost about 12 % of its original weight after 8 days degradation (Figure 7.8A), while uncrosslinked 6-Arg-4EG PEEUU A/G-1/4 films had ~39 % mass losses in the same medium (Figure 7.8B). Prior studies reported lipase must adsorb onto the polymer film surface and cleave the ester bond of the copolymer in the biodegradation process³⁷⁻⁴⁰. While the crosslinked 6-Arg-4EG PEEUU forms an interconnected molecular network structure which could make lipase difficult to diffuse and target the ester bonds to cleave.

Irrespective of crosslinked or uncrosslinked, Arg-PEEUU having a higher Arg OEG diester contents biodegraded more in a lipase medium at the same concentration than those having a lower Arg OEG diester content (Figure 7.8A vs. Figure 7.8 C and Figure 7. 8B vs. Figure 7.8D). For example, in the uncrosslinked groups at 1 mg/mL lipase, the weight loss of 6-Arg-4EG PEEUU A/G-1/1 film sample at day 4 is 74.3%. The degradation was stopped at day 4 because the film sample was deformed into one soft and sticky piece much smaller than the sample original size. While at the identical degradation condition, weight loss of 6-Arg-4EG PEEUU A/G-1/4 film is 20.8% at day 4. According to the reported poly (ester-urea) enzymatic biodegradation model, the biodegradation sites most possibly happened at the ester portion of the polymer rather than the NH-C=O portion of the urethane linkage³². An increase in ester contents that reside in the Arg OEG diester block of the crosslinked or uncrosslinked Arg-PEEUU would create more target sites for lipase to cleave. Another factor that accelerating the biodegradation is 6-Arg-4EG PEEUU with higher Arg OEG diester

content should be able to absorb more enzymes on its film surface due to the better hydrophilicity and positive charge of Arg.

Using the same 2 step polycondensation synthesis method, Arg-PEUU was synthesized and the biodegradation by lipase was studied ³¹. The only chemistry different is the segment of Arg-PEUU between two Arg is carbon-carbon, while Arg-PEEUU has carbon-oxygen linkage of ether group and the space between two Arg / two ester group is larger than Arg-PEUU. Comparing the lipase biodegradation data, 6-Arg-4EG PEEUU showed faster biodegradation than 6-Arg-2 PEUU at the same monomer feed ratio (A/G-1/1 or A/G-1/4). The biodegradation period of uncrosslinked 6-Arg-2 PEUU by lipase was about 20-30 days, while 6-Arg-4EG PEEUU biodegradation was only 4- 8 days. It is because the OEG segments of 6-Arg-4EG PEEUU provide the polymer chain more flexibility at the incubation temperature and longer space between two ester groups that makes lipase could target and degrade the polymer structure easier.



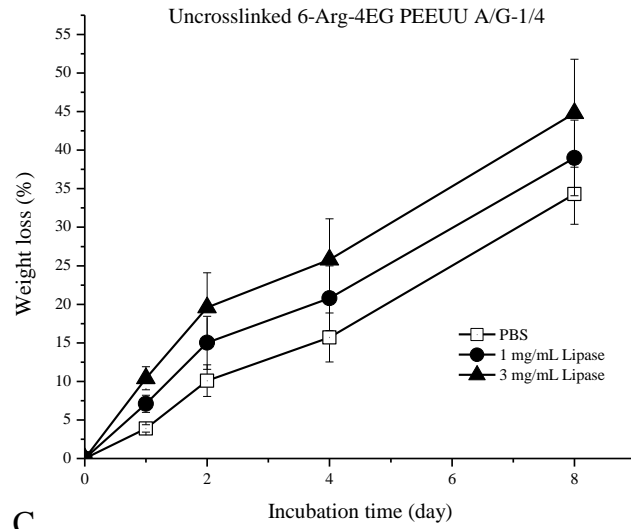
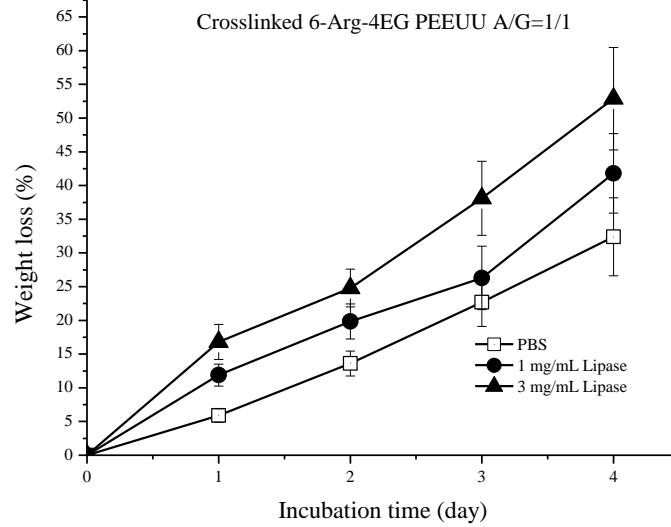
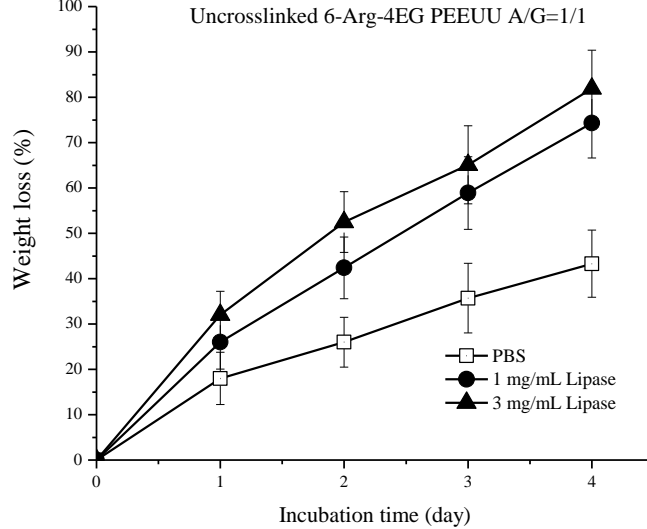
B**C****D**

Figure 7.8 Effect of lipase concentration on the biodegradation rate of the 6-Arg-4EG PEEUU film having different Arg oligoethylene glycol diester contents and Arg diester to glycerol α -monoallyl ether feed ratios at pH 7.4 and 37 °C. A. photo-crosslinked 6-Arg-4EG PEEUU A/G-1/4 film; B. uncrosslinked 6-Arg-4EG PEEUU A/G-1/4 film; C. photo-crosslinked 6-Arg-4EG PEEUU A/G-1/1 film; D. uncrosslinked 6-Arg-4EG PEEUU A/G-1/1 film.

7.5 Conclusions and recommendation for future work

A new family of cationic biodegradable and functional Arg based poly(ether ester urea urethane)s (Arg-PEEUU) having functional pendant carbon-carbon double bonds were synthesized by a 2-step solution co-polycondensation of Arg- x EG-Cl, GAE and HDI monomers. The FTIR, elemental analysis and GPC data confirmed the chemical structures and molecular weight of the new functional Arg-PEEUU. The M_n of Arg-PEEUU ranged from 20.425 to 60.225 Kg/mol with a relatively narrow MWD (1.298 ~1.460) for polymers synthesized by polycondensation method.

The contents of the Arg and functional pendant double bond could be adjusted by tuning the feed ratio of the 3 monomers and hence influence the thermal properties (T_g ranging from -23.38°C to -2.35 °C) and hydrophilicity of the materials (water contact angle ranging from $24.3 \pm 3.3^\circ$ to $56.7 \pm 3.9^\circ$). As the contents of the Arg OEG diester building block increased, the T_g of the corresponding Arg-PEEUU increased and the water contact angle decreased. Another important materials parameter is the number of ethylene glycol unit (x) in the Arg OEG diester building block. Increasing x , led to a lower T_g and higher water contact angle (more hydrophobic). Even though Arg-PEEUU is not water soluble at room temperature, at 40 °C and 70 °C, Arg-PEEUU with A/G-1/1 and A/G-4/1 showed increased water solubility up to 55 mg/mL.

MTT assays for porcine aortic valve smooth muscle cell were used to evaluate the cytotoxicity of 6-Arg-2EG PEEUU and 6-Arg-4EG PEEUU. Both Arg-PEEUU showed the same level of cell viability as the blank medium control when the polymer concentrations were at and below 0.1 – 0.5 mg/mL. By utilizing the amphiphilicity of Arg-PEEUU, microsphere with average hydrodynamic diameter from 123.2 ± 3.7 nm to 217.8 ± 12.2 nm was fabricated in water with strong positive ζ -potential ranging from 48.1 ± 0.7 to 52.3 ± 1.7 mV. The utility of the incorporated pendant carbon-carbon double bond in the Arg-PEEUU was demonstrated by photo-crosslinking to form elastic gels with a wide range of mechanical property, e.g., compressive modulus ranged from 80.4 ± 10.28 to 184.5 ± 9.0 KPa by adjusting the monomer feed ratio and x parameter.

The effects of the Arg-PEEUU chemical structures on their biodegradation property (in terms of weight loss) were investigated in a lipase media at different concentrations. The *in vitro* biodegradation data suggested that the crosslinking density as well as the Arg oligoethylene glycol diester building block contents in the functional Arg-PEEUU had a profound impact on their rate and extent of biodegradation. The elastic gel and microsphere made from Arg-PEEUU have the potential applications in the biomedical device study.

In the further study, the 3T3 cell attachment and morphology on the Arg-PEEUU materials needs to be characterized for the further study by live/dead assay and F-actin staining. The TNF- α production of RAW cells cultured on the Arg-PEEUU coated cover slip could be used test the inflammatory response to the Arg-PEEUU. The NO production and Arginase activity analysis for macrophages (RAW) treated by Arg-PEEUU suspension could be used to exam the effect of Arg-PEEUU suspension on the Arginine metabolism.

Acknowledgement

The authors would like to thank the support of Vincent V.C. Woo Fellowship to this study. The author also wish to thank to Cornell Nanobiotechnology Center (NBTC) who provided cell culture facility, Lin Chen who helped in the GPC test and Dr. Duan Bin who provided the PAVSMC cells in our study.

References:

- 1 Freed LE, Vunjak-Novakovic G, Biron RJ, Eagles DB, Lesnoy DC, Barlow SK et al. Biodegradable polymer scaffolds for tissue engineering. *Biotechnology* 1994;12:689–693.
- 2 Skarja GA, Woodhouse KA. Structure-property relationships of degradable polyurethane elastomers containing an amino acid based chain extender. *J Appl Polym Sci* 2000;75:1522–1534.
- 3 Guo K, Chu CC, Chkhaidze E, Katsarava R. Synthesis and characterization of novel biodegradable unsaturated poly(ester-amide)s. *J Polym Sci Polym Chem Ed* 2005;43:1463–1477.
- 4 Skarja GA, Woodhouse KA. In vitro degradation and erosion of degradable segmented polyurethanes containing an amino acid-based chain extender. *J Biomater Sci Polym* 2001; 12(8):851–873.
- 5 Katsarava, R.; Beridze, V.; Arabuli, N.; Kharadze, D.; Chu, C. C.; Won, C. Y. *J. Polym. Sci., Part A: Polym. Chem.* 1999; 37: 391–407.
- 6 Kai Guo, Chih-Chang Chu. Biodegradation of unsaturated poly(ester-amide)s and their hydrogels. *Biomaterials* 2007; 28: 3284–3294.
- 7 Kai Guo, C.C.Chu. Synthesis, characterization and biodegradation of novel poly(ether ester amide)s based on L-phenylalanine and oligoethylene glycol. *Biomacromolecules* 2007; 8 (9): 2851–2861.

- 8 H. Song, C. C. Chu. Synthesis and Characterization of A New Family of Cationic Poly(ester amide)s and Their Biological Properties. *J. Appl. Polym. Sci.* 2012; 124(5): 3840–3853.
- 9 Jun Wu, Dai Yamanouchi, Bo Liu, C.C.Chu. Biodegradable Arginine-based Poly(ether ester amide)s as Non-viral DNA delivery Vector and their Structure - Function Study. *J. Mater. Chem* 2012; 22: 18983–18991.
- 10 Jun Wu, Dequn Wu, Martha A. Mutschler, C. C. Chu. Cationic Hybrid Hydrogels from Amino Acid-Based Poly (ester amide):Fabrication, Characterization, and Biological Property. *Advanced functional materials* 2012; 22(18): 3815–3823.
- 11 Jun Wu, Chih-Chang Chu. Block Copolymer of Poly (ester amide) and Polyesters: Synthesis, Characterization, and in vitro Cellular Response. *Acta biomaterialia* 2012; 8: 4314–4323.
- 12 Jun Wu, C. C. Chu. Water insoluble cationic poly (ester amide)s: synthesis, characterization and applications. *J. Mater. Chem B.* 2013; (In press)
- 13 Jun Wu, Martha A. Mutschler, C. C. Chu. Synthesis and characterization of ionic charged water soluble arginine-based poly(ester amide). *J Mater Sci: Mater Med* 2011; 469–479.
- 14 Xuan Pang, J. Wu , C. A. Reinhart-King , C.C. Chu. Synthesis and characterization of functionalized water soluble cationic poly(ester amide)s. *Journal of Polymer Science Part A: Polymer Chemistry* 2010; 28: 3758–3766.
- 15 Jianjun Guan, Michael S. Sacks, Eric Beckman, William R. Wagner. Synthesis, characterization, and cytocompatibility of elastomeric, biodegradable poly(ester-urethane) ureas based on poly(caprolactone) and putrescine. *Journal of biomedical materials research* 2002; 61: 493–503.

- 16 M. Deng , J. Wu , C. A. Reinhart-King , C.C. Chu. Synthesis and Characterization of Biodegradable Poly(ester amide)s with Pendant Amine Functional Groups and In Vitro Cellular Response. *Biomacromolecules* 2009; 10: 3037–3047.
- 17 M. Jalkanen, H. Larjava, J. Heino, T. Vihersaari, J. Peltonen, R. Penttinen. Arginine depletion in macrophage medium inhibits collagen synthesis by fibroblasts, *Immunology letter* 1982; 4: 259–261.
- 18 Morris, Sidney M., Jr., Diane Kepka-Lenhardt, Li-Chun Chen. Differential regulation of arginases and inducible nitric oxide synthase in murine macrophage cells. *Am. J. Physio.* 1998; 275: E740–E747.
- 19 Guoyao Wu, Sidney M. Morris, JR. Arginine metabolism: nitric oxide and beyond. *Biochem. J.* 1998; 336: 1–17.
- 20 Masataka Mori, Tomomi Gotoh. Regulation of nitric oxide production by arginine metabolic enzymes. *Biochemical and Biophysical Research Communications* 2000; 275: 715–719.
- 21 Carmelo Nieves Jr, Bobbi Langkamp-Henken. Arginine and immunity: a unique perspective. *Biomed Pharmacother* 2002; 56: 471–482.
- 22 Carl Nathan. Inducible nitric oxide synthase: what difference does it make?. *J. Clin. Invest* 1997; 100: 2417–2423.
- 23 David G. Harrison. Cellular and molecular mechanisms of endothelial cell dysfunction. *J. Clin. Invest* 1997; 100: 2153–2157.
- 24 Karen S. Christopherson, David S. Brecht. Nitric oxide in excitable tissues: physiological roles and disease. *J. Clin. Invest* 1997; 2424–2429.
- 25 Michael R. Schaffer, Udaya Tantry, Stevens S. Gross, Hannah L. Wasserkrug, Adrian Barbul. Nitric Oxide Regulates Wound Healing. *Journal of surgical research* 1996; 63: 237–240.

- 26 Robert B. Lorsbach, Willam J. Murphy, Charles J. Lowenstein, Solomon H. Snyder, Stephen W. Russel. Expression of the nitric oxide synthase gene in mouse macrophages activated for tumor cell killing. *The journal of biological chemistry* 1993; Vol. 268, No. 3, 25: 1908–1913.
- 27 Borkerhagen M, Stoll RC, Neuenschwander P, Suter UW. Aebischer. In vivo performance of a new biodegradable polyester urethane system used as a nerve guidance channel. *Biomaterials* 1998; 19: 2155–2165.
- 28 Saad B, Hirt TD, Welti M, Uhlschmid GK, Neuenschwander P, Suter UW. Development of degradable polyesterurethanes for medical applications. *J Biomed Mater Res* 1997; 36: 65–74.
- 29 Michael B. Mellott, Katherine Searcy, Michael V. Pishko. Release of protein from highly cross-linked hydrogels of poly(ethylene glycol) diacrylate fabricated by UV polymerization. *Biomaterials* 2001; 22: 929–941.
- 30 Hiroaki Tanuma, Takashi Saito, Kenichi Nishikawa, Tungalag Dong, Koji Yazawa, Yoshio Inoue. Preparation and characterization of PEG-cross-linked chitosan hydrogel films with controllable swelling and enzymatic degradation behavior. *Carbohydrate Polymers* 2010; 80: 260–265.
- 31 Mingyu He, C.C.Chu. A new family of functional arginine based polyester urea urethanes: synthesis, characterization and biodegradation. *Biomaterials*; Pending
- 32 Huang SJ, Bansleben DA, Knox JR. Biodegradable polymers: chymotrypsin degradation of low molecular weight poly(ester-urea) containing phenylalanine. *J Appl Polym Sci* 1979; 23: 429–437.
- 33 Xuan Pang, Chih-Chang Chu. Synthesis, characterization and biodegradation of functionalized amino acid-based poly(ester amide)s. *Biomaterials* 2010; 31(14): 3745–3754

- 34 Jagadish Beloor, Choi CS, Nam HY, Park M, Kim SH, Jackson A et al. Arginine-
engrafted biodegradable polymer for the systemic delivery of therapeutic siRNA.
Biomaterials 2012; 33: 1640–1650.
- 35 Sang Myoung Noh, Myung Ok Park, Gayong Shim, Su Eun Han, Han Young Lee,
Jun Hyuk Huh et al. Pegylated poly-L-arginine derivatives of chitosan for effective
delivery of siRNA. Journal of Controlled Release 2010; 145: 159–164.
- 36 Xuan Pang, Chih-Chang Chu. Synthesis, characterization and biodegradation of
poly(ester amide)s based hydrogels. Polymer 2010; 51: 4200–4210.
- 37 Claire Sumner, Steffi Krause, Andrea Sabot, Katrina Turner. Biosensor based on
enzyme-catalysed degradation of thin polymer Films. Biosensors & Bioelectronics
2001; 16: 709–714.
- 38 G. Tsitlanadze, M. Machaidze, T. Kviria, R. Katsarava, C. C. Chu. *In vitro*
enzymatic biodegradation of amino acid based poly (ester amide)s biomaterials. J.
Mater. Sci. Mater. in Medicine 2004;15: 185–190.
- 39 G. Tsitlanadze, M. Machaidze, T. Kviria, N. Djavakhishvili, C. C. Chu, R.
Katsarava. Biodegradation of amino acid based poly(ester amide)s: In vitro weight
loss and preliminary *in vivo* study. J. Biomater. Sci. Polym. Ed. 2004; 15(1): 1–24.
- 40 D. Kharadze, L. Kirmelashvili, N. Medzmariashvili, V. Beridze, G. Tsitlanadze, D.
Tugushi et al. Amino acid based bioanalogous polymers: Synthesis and α -
chymotrypsinolysis study of regular poly(ester amides) based on phenylalanine, diols
and terephthalic acid. Polymer Science, Ser. A 1999; 41(9): 883–890.